
Schriftenreihe **IWAR**

274



TECHNISCHE
UNIVERSITÄT
DARMSTADT

IWAR

Mischa Jütte

Fundamental reaction mechanisms of chlorine dioxide during water treatment – Reactions with phenols and biomolecules during inactivation mechanisms

Herausgeber:

Verein zur Förderung des Instituts **IWAR** der TU Darmstadt e. V.



Fundamental reaction mechanisms of chlorine dioxide during water treatment – Reactions with phenols and biomolecules during inactivation mechanisms

Vom Fachbereich Bau- und Umweltingenieurwissenschaften
der Technischen Universität Darmstadt
zur Erlangung des akademischen Grades eines
Doktors (Dr. rer. nat.) genehmigte Dissertation

von

Mischa Jütte, M. Sc.
aus Düsseldorf

Erstgutachter: Prof. Dr. Holger V. Lutze
Zweitgutachter: Prof. Dr. Torsten C. Schmidt

Darmstadt 2023

D 17

Mischa Jütte

Fundamental reaction mechanisms of chlorine dioxide during water treatment – Reactions with phenols and biomolecules during inactivation mechanisms

Darmstadt, Technische Universität Darmstadt

Hrsg.: Verein zur Förderung des Instituts **IWAR** der TU Darmstadt e. V.
Darmstadt: Eigenverlag, 2023
(Schriftenreihe IWAR 274)

Jahr der Veröffentlichung der Dissertation auf TUprints: 2023

ISSN 0721-5282

ISBN 978-3-940897-75-6

Urheberrechtlich geschützt / In copyright

URI: <https://tuprints.ulb.tu-darmstadt.de/id/eprint/24197>

URN: urn:nbn:de:tuda-tuprints-241973

DOI:

Referent: Prof. Dr. Holger V. Lutze
Korreferent: Prof. Dr. Torsten C. Schmidt

Tag der schriftlichen Einreichung: 31.03.2023
Tag der mündlichen Prüfung: 23.06.2023

Alle Rechte vorbehalten. Wiedergabe nur mit Genehmigung des Vereins zur Förderung des Instituts **IWAR** der Technischen Universität Darmstadt e. V., c/o Institut IWAR, Franziska-Braun-Str. 7, 64287 Darmstadt.

Herstellung: Druckerei Lokay e.K.
Königsberger Str. 3
64354 Reinheim
IWAR

Vertrieb: Institut
TU Darmstadt
Franziska-Braun-Straße 7
64287 Darmstadt
Telefon: 06151 / 16 20301
Telefax: 06151 / 16 20305

„ Have no fear of perfection; you'll never reach it. “

–Dr. Marie Skłodowska Curie

Acknowledgment

First, I would like to thank Prof. Dr. Holger V. Lutze for offering me the possibility to pursue my Ph.D. in his working group. I can imagine that the choice for the first Ph.D. student in a newly founded chair is never easy. Therefore, I feel very honored that you choose me for this task and opportunity. I'm happy that I had the chance to be one of the founding members of the chair of 'Environmental Analytics and Pollutants' and could play my role in the strengthening the roots. I'm also very thankful that you gave me all the degrees of freedom that I needed to investigate the presented topic as good as I could from all different angles.

Every Ph.D. student has either a 'doctor father' or a 'doctor mother'. Beside this very important person, another person is playing a major role during your Ph.D., which I would like to call 'doctor uncle'. This person is very important for a successful thesis since he or she is giving you many advice during the time your boss is not available, or advices you how to transfer all the ideas from the 'doctor father' into feasible experiments in the lab. Additionally, this person is helping you to filter good ideas from the bad ones, motivates you when things are not running as planned, or simple enjoys a good cup of tea with you. In my case my 'doctor uncle' was Dr. Sajjad Abdi. I would really like to thank you for the all above mentioned things. I might haven't stayed till the end without this support.

Next I would like to thank my colleagues at the chair of environmental analytics and pollutants Amir Asadi and (now Prof.) Cheolyong Kim for the great working atmosphere I could experience during my time at this group. Thank you for the all the laughs and the good time. I would also like to thank my students Janine Große, Josephine Heyns, Rishab Puri, Catarina Ribeiro, Marcel Reusing, and Janis Wilbert. Thank you for your great contribution to this work. I am very glad that I could call myself your supervisor. Furthermore, I would like to thank the staff of the institute IWAR for their support and help especially during the beginning of my thesis.

No research is possible without collaboration. Therefore, I would like to thank the chair of hydrogeology leaded by Prof. Dr. Christoph Schüth at the Technical University of Darmstadt, for welcoming us in their laboratory. Thank you very much for your great hospitality and kindness. Additionally, I would like to thank the chair of molecular microbiology leaded by Prof. Dr. Torsten Waldminghaus at the Technical University of Darmstadt for the successful collaboration. I am very sure that many joint research projects will be based on our foundation.

Acknowledgment

My biggest gratitude goes to Hyerin Kim. Thank you very much for supporting me in the idea to go to Darmstadt and let me do my Ph. D. Within the last three years I went through many ups and downs. Your support lift me through the downs and made me enjoy the ups even more. My gratefulness is far beyond the words I am able to write here. Therefore, I will keep it very simple: Thank you for everything!

Finally, I would like to thank my family and friends to let me go to Darmstadt for such a long time. Their mental support contributed strongly to keep myself motivated and stay focused on the goal. Although many of you may not know what is going on in my thesis, your contribution to this success is not a minor.

Abstract

Two key elements of drinking water treatment are disinfection and pollution control. For this purpose, different chemical oxidants are used, for instance, chlorine (free available chlorine (FAC)), ozone (O₃), or chlorine dioxide (ClO₂). The presented work investigated the reaction mechanisms of ClO₂ during drinking water treatment. ClO₂ reacts mainly with activated aromatic compounds (e.g., phenols, anilines) and forms chlorite as major by-product (drinking water standard, 200 µg L⁻¹, Germany). It is increasingly implemented in drinking water treatment as a substitute for chlorination to avoid the formation of a halogenated disinfection by-product (DBP). However, recently it has been shown that FAC also forms in reactions of ClO₂ as a by-product. This results in a combined oxidation with ClO₂ and FAC, and both oxidants can work together synergistically in disinfection and pollutant degradation but may also form two sets of DBPs. The present study focuses on the intrinsic formation of FAC and other inorganic by-products (chloride, chlorite, and chlorate) in the ClO₂ reactions with phenols as representatives for reactive sites in natural organic matter (NOM) and biomolecules (amino acids). Furthermore, the contribution of FAC to disinfection in a ClO₂ water treatment model system has been investigated.

The reaction of ClO₂ with amino acids was studied in the context of disinfection mechanisms. Thereby amino acids may be an important reaction partner for reaction with microbial cells during the disinfection. Therefore, reactions of ClO₂ with tyrosine and tryptophan were investigated regarding reaction kinetics and the formation of different chlorine species (FAC, chlorite, chloride, chlorate). Tyrosine and tryptophan displayed a very high reactivity towards ClO₂ ($k_{app} = 3.16 \times 10^4 \text{ M}^{-1} \text{ s}^{-1}$ and $1.81 \times 10^4 \text{ M}^{-1} \text{ s}^{-1}$ at pH 7), and it seems likely that these represent a possible point of primary reaction of ClO₂ in microbial cells. Both investigated amino acids showed a significant formation of FAC (tyrosine $\approx 50 \%$, tryptophan $\approx 36 \%$ of dosed ClO₂ concentration). Thereby FAC may serve as an additional reactive species contributing to cell inactivation. Since amino acids are the building blocks of peptides and proteins, it is possible that the reaction of ClO₂ with cell proteins during disinfection is not only causing the inactivation of the corresponding proteins but also forms FAC, which can cause further cell damage and may enhance the total cell inactivation.

In ClO₂ based treatment ClO₂ is mainly consumed by NOM. The strong depletion can be explained by the different phenolic moieties, which show high reactivity towards ClO₂. Recently, it has been shown that the reaction of ClO₂ with NOM is forming 25 % FAC. Since phenol, the major reactive side in NOM, itself forms 50 % FAC in the reaction with ClO₂; it might be possible that the presence of different functional groups attached to the phenolic ring is causing a change in the reaction mechanism regarding the formation of inorganic chlorine species. Therefore, the yields of different chlorine species (chlorine balance) of different phenolic compounds with different substituents (e.g., alkyl, hydroxyl, or methoxy groups) in *ortho*-, *meta*-, and *para*-position were investigated. It could be shown that most substituents do not particularly affect the chlorine balance. However, *para*-substituted phenols seem to form *ortho*-benzoquinone, which is very reactive and causes a change in the chlorine balance over time (reduced FAC yields and increased chloride yields). This might explain the different reported yields of FAC in the literature. The substituents which strongly affect the chlorine balance of phenol are hydroxyl and amino groups in *ortho*- and *para*-position, which results in 100 % yields of chlorite and total hampering of FAC formation. The exact reason for this observation requires further investigation.

Glycine has been frequently used to determine intrinsic FAC in ClO₂ reactions with phenols which have a low reaction kinetics with FAC ($k_{app} = 10^2 \text{ M}^{-1} \text{ s}^{-1}$, at pH 7). Thus, FAC can be successfully scavenged by glycine, which reacts several orders of magnitude faster with FAC ($k_{app} = 1.5 \times 10^5 \text{ M}^{-1} \text{ s}^{-1}$ at pH 7). The ensuing product of this reaction (chloro-glycine) can be determined to quantify FAC formation. However, if the compound under study reacts fast with FAC (e.g., cysteine $k_{app} = 6.2 \times 10^7 \text{ M}^{-1} \text{ s}^{-1}$ at pH 7) glycine may not be able to quantitatively scavenge FAC resulting in an underestimation of intrinsic FAC. Examples of compounds with such high reaction kinetics with FAC are thiols (e.g., Glutathione (GSH)), which react fast with both oxidants ClO₂ and FAC ($k_{app} \geq 10^7 \text{ M}^{-1} \text{ s}^{-1}$). The reaction of GSH with FAC is two orders of magnitudes faster than the reaction of FAC with glycine. Therefore, a new method was developed using methionine as a selective scavenger. Methionine is a sulfide-containing amino acid, which reacts fast with FAC ($k_{app} = 6.8 \times 10^8 \text{ M}^{-1} \text{ s}^{-1}$ at pH 7) and forms chloride and methionine sulfoxide (MSO) in equal parts. The yields of chloride and MSO can be used to quantify the FAC yields. The reaction of methionine with ClO₂ was determined to be $k_{app} = 10^2 \text{ M}^{-1} \text{ s}^{-1}$ at pH 7. The method was successfully applied to qualitatively state that FAC is formed in the reaction of ClO₂ with the tripeptide GSH. However,

in some cases, MSO formation was observed from a yet unknown source, which requires further investigation.

Finally, the intrinsic FAC participation during ClO₂-based disinfection was investigated. First, a novel concept has been developed to determine different levels of microbial cell inactivation, which is based on the extension of the lag phase (initial growth phase preceding the exponential growth). Thereby an increase of the *Escherichia coli* inactivation results in a prolongation of the lag phase. Since the growth can be monitored online by an increase in optical density, this method is fast and enables the simultaneous measurement of several samples. With this method, it was possible to show that in ClO₂-based disinfection processes, the intrinsic formation of FAC may be very important. This was shown in experiments of *E. coli* elimination in the presence of NOM. The addition of methionine as a fast-reacting FAC-scavenger fully suppressed the inactivation of *E. coli*. This indicates that the observed *E. coli* inactivation on ClO₂-based processes with high loads of NOM may be mainly driven by FAC. Furthermore, it was shown that disinfection in the presence of NOM is pH-dependent (pH 6.5 > 7.5 > 8.5). This can be explained by the depletion of ClO₂, which is accelerated at higher pH values due to the dissociation of the phenolic moieties (pK_a: 10) of the NOM (note that the deprotonated phenolate species reacts more than five orders of magnitude faster with ClO₂ compared to protonated phenol). With an increasing consumption rate of ClO₂, less ClO₂ will be available for disinfection. Additionally, the speciation of FAC (HOCl) might be responsible for the observed stronger inactivation at lower pH since HOCl is a stronger disinfectant than OCl⁻ (pK_a: 7.54).

Kurzfassung

Zwei Hauptbestandteile der Trinkwasseraufbereitung sind die Desinfektion und der Abbau von Schadstoffen. Dazu können verschiedene chemische Oxidationsmittel, wie beispielsweise Chlor (frei verfügbares Chlor (FAC)), Ozon (O_3) oder Chlordioxid (ClO_2) verwendet werden. Die vorliegende Arbeit untersucht die Reaktionsmechanismen von ClO_2 in der Trinkwasseraufbereitung. ClO_2 reagiert hauptsächlich mit aktivierten aromatischen Verbindungen (z.B. Phenole, Aniline) und bildet Chlorit als Hauptnebenprodukt (Trinkwasserstandard in Deutschland $200 \mu g L^{-1}$). Um die Bildung von halogenierten Desinfektionsnebenprodukten (DBPs) zu vermeiden, wird ClO_2 zunehmend als Ersatz für die Chlorung eingesetzt. Allerdings wurde vor kurzem gezeigt, dass FAC auch bei bestimmten Reaktionen von ClO_2 als Nebenprodukt entstehen kann. Dies führt zu einer kombinierten Oxidation von ClO_2 und FAC, und beide Oxidationsmittel können bei der Desinfektion und dem Schadstoffabbau synergetische Effekte zeigen, aber auch unterschiedliche DBPs bilden. Die vorliegende Studie fokussiert sich auf die intrinsische Bildung von FAC und anderen anorganischen Nebenprodukten (Chlorid, Chlorit und Chlorat) die aus der Reaktion von ClO_2 entstehen können. Dabei dienen Phenole als Repräsentant für reaktive Stellen im natürlichen organischen Material (NOM) und Biomolekülen (Aminosäuren). Darüber hinaus, wurde in einem Wasseraufbereitungsmodellsystem untersucht, wie stark der Einfluss von intrinsisch gebildetem FAC auf die ClO_2 Desinfektion ist.

Die Reaktion von ClO_2 mit ausgewählten Aminosäuren wurde im Zusammenhang von Desinfektionsmechanismen untersucht. Dabei können Aminosäuren, als Bausteine von Peptiden und Proteinen, ein wichtiger Reaktionspartner während der Desinfektion sein. Daher wurde die Reaktion von ClO_2 mit Tyrosin und Tryptophan hinsichtlich der Reaktionskinetik und der Bildung verschiedener Chlorspezies (FAC, Chlorit, Chlorid, Chlorat) untersucht. Tyrosin und Tryptophan zeigten eine hohe Reaktivität gegenüber ClO_2 ($k_{app} = 3,16 \times 10^4 M^{-1} s^{-1}$ und $1,81 \times 10^4 M^{-1} s^{-1}$ bei pH 7), und es ist wahrscheinlich, dass diese Aminosäuren einen potentiellen primären Reaktionspartner von ClO_2 innerhalb mikrobiellen Zellen darstellen. Beide untersuchten Aminosäuren zeigten eine signifikante Bildung von FAC (Tyrosin $\approx 50 \%$, Tryptophan $\approx 36 \%$ der dosierten ClO_2 -Konzentration). Intrinsisch gebildetes FAC kann als zusätzliche reaktive Spezies dienen, die zur Zellinaktivierung beiträgt. Da Aminosäuren die Bausteine von Peptiden und Proteinen sind, ist es möglich, dass die Reaktion von ClO_2 mit Zellproteinen während der Desinfektion nicht nur die Inaktivierung der entsprechenden Proteine verursacht, sondern auch

FAC bildet, das dann weitere Zellschäden verursachen kann und somit die Zellinaktivierung verstärkt.

Bei der Anwendung von ClO_2 wird dieses hauptsächlich vom NOM verbraucht. Die starke Zehrung entsteht durch die phenolischen Einheiten des NOM, die eine hohe Reaktivität gegenüber ClO_2 aufweisen. Kürzlich konnte gezeigt werden, dass die Reaktion von ClO_2 mit NOM etwa 25 % FAC bildet. Da Phenol selbst 50 % FAC in der Reaktion mit ClO_2 bildet, ist es möglich, dass verschiedene funktionelle Gruppen, die an den Phenolring gebunden sind, eine Änderung des Reaktionsmechanismus bezüglich der Bildung von anorganischen Chlorspezies verursacht. Daher wurden die Ausbeuten verschiedener Chlorspezies (Chlorbilanz) unterschiedlicher phenolischer Verbindungen mit verschiedenen Substituenten (z. B. Alkyl-, Hydroxyl- oder Methoxygruppen) in *ortho*-, *meta*- und *para*-Position untersucht. Dabei konnte gezeigt werden, dass die meisten Substituenten die Chlorbilanz nicht stark beeinflussen. *para*-substituierte Phenole scheinen jedoch sehr reaktives *ortho*-Benzochinon zu bilden, das mit zunehmender Zeit eine Veränderung der Chlorbilanz verursacht (verringerte FAC-Ausbeuten und erhöhte Chlorid-Ausbeuten). Dies könnte die unterschiedlichen Ausbeuten an FAC in der Literatur erklären. Die Substituenten, die die Chlorbilanz von Phenol stark beeinflussen, sind Hydroxyl- und Aminogruppen in *ortho*- und *para*-Position, was zu einer Chlorit-Ausbeute von etwa 100 % und einer vollständigen Hinderung der FAC-Bildung führt. Der genaue Grund für diese Beobachtung bedarf weiterer Untersuchungen.

Glycin wurde häufig verwendet, um intrinsisch gebildetes FAC in ClO_2 Reaktionen mit Phenolen zu quantifizieren, da diese eine niedrige Reaktionskinetik mit FAC haben ($k_{app} = 10^2 \text{ M}^{-1} \text{ s}^{-1}$, bei pH 7). Somit kann FAC erfolgreich von Glycin abgefangen werden, das mehrere Größenordnungen schneller mit FAC reagiert als Phenol ($k_{app} = 1,5 \times 10^5 \text{ M}^{-1} \text{ s}^{-1}$ bei pH 7). Das resultierende Produkt dieser Reaktion (Chlor-Glycin) wird dabei gemessen, um die FAC-Bildung zu quantifizieren. Wenn die untersuchte Verbindung jedoch schnell mit FAC reagiert (z. B. Cystein $k_{app} = 6,2 \times 10^7 \text{ M}^{-1} \text{ s}^{-1}$ bei pH 7), ist Glycin möglicherweise nicht in der Lage, FAC vollständig abzufangen, was zu einer Unterschätzung der intrinsischen FAC führt. Beispiele für Verbindungen mit solch hoher Reaktionskinetik sind Thiole (z.B. Glutathion (GSH)), die schnell mit den beiden Oxidationsmitteln ClO_2 und FAC reagieren ($k_{app} \geq 10^7 \text{ M}^{-1} \text{ s}^{-1}$ at pH 7). Daher wurde eine neue Methode entwickelt, bei der Methionin als selektiver Scavenger verwendet wird. Methionin ist eine thioetherhaltige Aminosäure, die schnell mit FAC ($k_{app} = 6,8 \times 10^8 \text{ M}^{-1} \text{ s}^{-1}$ bei pH 7) reagiert und

zu gleichen Teilen Chlorid und Methioninsulfoxid (MSO) bildet. Die gemessenen Ausbeuten an Chlorid und MSO können zur Quantifizierung der FAC-Ausbeuten verwendet werden. Zusätzlich wurde die Reaktionsgeschwindigkeitskonstante von Methionin mit ClO_2 bestimmt ($k_{app} = 10^2 \text{ M}^{-1} \text{ s}^{-1}$ bei pH 7). Die Methode wurde erfolgreich angewendet, um qualitativ festzustellen, dass FAC bei der Reaktion von ClO_2 mit dem Tripeptid GSH gebildet wird. In einigen Fällen wurde jedoch die Bildung von MSO aus einer noch unbekanntem Quelle beobachtet, was weitere Untersuchungen erfordert.

Schlussendlich wurde die Beteiligung von intrinsisch gebildetem FAC während der ClO_2 -basierten Desinfektion untersucht. Zunächst wurde dafür ein neuartiges Konzept entwickelt, um verschiedene Grade der mikrobiellen Zellenaktivierung zu bestimmen. Dieses Konzept basiert auf der Verlängerung der Lag-Phase (anfängliche Wachstumsphase vor dem exponentiellen Wachstum. Dabei führt eine stärkere Inaktivierung von dem Modellobakterium *Escherichia coli* zu einer Verlängerung der Lag-Phase. Da das Wachstum online durch die Zunahme der optischen Dichte verfolgt werden kann, ist diese Methode schnell und ermöglicht die gleichzeitige Messung mehrerer Proben. Mit dieser Methode konnte gezeigt werden, dass bei ClO_2 -basierten Desinfektionsprozessen die intrinsische Bildung von FAC sehr wichtig sein kann. Dies wurde in Experimenten zur Inaktivierung von *E. coli* in Gegenwart von NOM gezeigt. Die Zugabe von Methionin als schnell reagierendem FAC-Scavenger führte zu einer vollständigen Unterbindung der Inaktivierung von *E. coli*. Dies deutet darauf hin, dass die beobachtete Inaktivierung von *E. coli* bei ClO_2 -basierten Prozessen mit hohen NOM-Belastungen hauptsächlich durch FAC verursacht wird. Weiterhin konnte gezeigt werden, dass die Desinfektion in Gegenwart von NOM pH-abhängig ist (pH 6,5 > 7,5 > 8,5). Dies kann durch die Zehrung von ClO_2 erklärt werden, die bei höheren pH-Werten aufgrund der Dissoziation der phenolischen Einheiten ($pK_s = 10$) des NOM beschleunigt wird (die deprotonierte Phenolatspezies reagiert mehr als fünf Größenordnungen schneller mit ClO_2 als die protonierte Spezies). Mit zunehmendem ClO_2 -Verbrauch steht weniger ClO_2 zur Desinfektion zur Verfügung. Darüber hinaus könnte die Spezierung von FAC (HOCl) für die beobachtete stärkere Inaktivierung bei niedrigerem pH-Wert verantwortlich sein, da HOCl ein stärkeres Desinfektionsmittel ist als OCl^- ($pK_s: 7,54$).

Abbreviation

Abbreviation

| | | | |
|-------------------------------|--|--------------------------------|---|
| ARB | Antibiotic resistant bacteria | k_{app} | Second-order reaction rate constant |
| ARG | Antibiotic resistant gene | k_{obs} | Pseudo-first order reaction rate constant |
| Br ⁻ | Bromide | MRG | Multi resistant gene |
| BrO ₃ ⁻ | Bromate | MS | Mass spectrometry |
| BQ | Benzoquinone | MSO | Methionine sulfoxide |
| CFU | Colony forming units | N _t /N ₀ | Number of bacteria |
| Cl ⁻ | Chloride | NAL | N-Acetyl-L |
| Cl-Gly | Chloro-glycine | NDMA | N-Nitrosodimethylamine |
| ClO ₂ ⁻ | Chlorite | NOM | Natural organic matter |
| ClO ₂ | Chlorine dioxide | O ₂ ⁻ | Superoxide |
| ClO ₃ ⁻ | Chlorate | O ₃ | Ozone |
| DBPs | Disinfection by-products | OD ₆₀₀ | Optical density at 600 nm |
| DNA | Deoxyribonucleic acid | ·OH | Hydroxylradical |
| DOC | Dissolved organic carbon | $\int [Ox]dt$ | Oxidant exposure |
| O ₃ | Ozone | PBS | Phosphate-buffered saline |
| FAB | Free available bromine | pK _a | Dissociation constant |
| FAC | Free available chlorine | PP | Polypropylene |
| FAI | Free available iodine | ROS | Reactive oxygen species |
| GSH | Glutathione | SMX | Sulfamethoxazole |
| HAA | Haloacetic acid | SRFA | Suwannee River fulvic acid |
| HAN | Halogenated acetonitrile | SRNOM | Suwannee River natural organic matter |
| HGT | Horizontal gene transfer | SQ | Semiquinone |
| HOBr | Hypobromous acid | t-BuOH | tert-Butanol |
| HOCl | Hypochlorous acid | TEM | Transmission electron microscopy |
| HOI | Hypoiodous acid | THM | Trihalomethane |
| HPLC | High performance liquid chromatography | UV | Ultraviolet |
| $I_{min/max/ave}$ | Inactivation | WHO | World health organization |
| IC | Ion chromatography | ϵ | Adsorption coefficient |
| k | Reaction rate constant | λ | Wavelength |

Table of content

| | |
|---|-------------|
| Acknowledgment | v |
| Abstract | vii |
| Kurzfassung | x |
| Abbreviation | xiii |
| Table of content | xiv |
| 1. Introduction | 3 |
| 1.1 Background | 3 |
| 1.2 Bacterial inactivation processes in water disinfection – mechanistic aspects of primary and secondary oxidants – a critical review | 7 |
| 1.2.1 Introduction | 9 |
| 1.2.1.1 Kinetic considerations and competing reactions | 11 |
| 1.2.1.2 Secondary oxidants | 17 |
| 1.2.2 Target structures reactivity and effect on viability | 18 |
| 1.2.2.1 Lipid layer and effect on viability | 19 |
| 1.2.2.2 Proteins & Amino acids reactivity and effect on viability | 20 |
| 1.2.2.3 genetic material reactivity and effect viability | 22 |
| 1.2.3 Free available chlorine | 22 |
| 1.2.3.1 Reaction with the water matrix | 23 |
| 1.2.3.2 Reaction with cell constituents | 24 |
| 1.2.3.3 Reaction with genetic material | 26 |
| 1.2.4 Chlorine dioxide | 28 |
| 1.2.4.1 Reaction with the matrix constituents | 28 |
| 1.2.4.2 Reaction with cell constituents | 29 |
| 1.2.4.3 Reaction with genetic material | 30 |
| 1.2.5 Ozone | 31 |
| 1.2.5.1 Reaction with the water matrix constituents | 32 |
| 1.2.5.2 Reaction with cell constituents | 33 |
| 1.2.5.3 Reaction with genetic material | 34 |
| 1.2.6 Defense response | 35 |
| 1.2.7 Additional <i>in vivo</i> effects | 37 |

Table of content

| | |
|---|-----------|
| 1.2.8 Conclusion and further research suggestions | 38 |
| 2. Research gaps and objective..... | 43 |
| 3. Results | 51 |
| 3.1 Novel insights in chlorine dioxide-based disinfection mechanism –Investigation of the reaction with amino acids | 51 |
| 3.1.1 Introduction | 52 |
| 3.1.2 Material and Method | 54 |
| 3.1.2.1 Chemicals and Instruments | 54 |
| 3.1.2.2 Production of ClO ₂ | 54 |
| 3.1.2.3 Preparation of FAC | 55 |
| 3.1.2.4 Determination of reaction kinetics | 55 |
| 3.1.2.5 Stoichiometry | 58 |
| 3.1.2.6 Chlorine balance..... | 58 |
| 3.1.4 Results and Discussion..... | 59 |
| 3.1.4.1 Reaction kinetics | 59 |
| 3.1.4.2 Chlorine balance..... | 65 |
| 3.1.4.3 Reaction mechanism of NAL-tyrosine..... | 67 |
| 3.1.4.4 Reaction mechanism of NAL-tryptophan | 68 |
| 3.1.5 Conclusion..... | 70 |
| 3.2 Reaction mechanisms of chlorine dioxide with phenolic compounds – Influence of different substituents on stoichiometric ratios and intrinsic formation of free available chlorine..... | 73 |
| 3.2.1 Introduction | 75 |
| 3.2.2 Material and Methods..... | 78 |
| 3.2.2.1 Chemicals, Instruments, and Analytical methods | 78 |
| 3.2.2.2 Production of ClO ₂ and FAC | 78 |
| 3.2.2.3 Intrinsic FAC formation | 78 |
| 3.2.2.4 Stoichiometric ratios | 79 |
| 3.2.3 Results and discussion..... | 80 |
| 3.2.3.1 Effect of substituents in different locations..... | 80 |
| 3.2.3.2 Effect of different functional substituents | 85 |

Table of content

| | |
|---|------------|
| 3.2.3.2.1 Halogenated phenols | 87 |
| 3.2.3.2.2 Hydroxyphenols | 89 |
| 3.2.3.3.3 Aminophenols | 94 |
| 3.2.4. Practical implications | 96 |
| 3.3 Investigation of methionine as a selective scavenger for free available chlorine in chlorine dioxide-based reactions..... | 99 |
| 3.3.1 Introduction | 101 |
| 3.3.2 Material and Methods..... | 103 |
| 3.3.2.1 Chemicals, Instruments, & Methods | 103 |
| 3.3.2.2 Determination of reaction kinetics | 103 |
| 3.3.2.3 Formation of Chloride and MSO in methionine oxidation by FAC | 103 |
| 3.3.2.4 Model compounds | 104 |
| 3.3.2.5 Chlorite reactions | 105 |
| 3.3.3 Results and Discussion..... | 106 |
| 3.3.3.1 Reaction kinetics | 106 |
| 3.3.3.2 Formation of Chloride and MSO | 107 |
| 3.3.3.3 Chlorine balance of model compounds | 108 |
| 3.3.3.4 MSO formation by chlorite | 114 |
| 3.3.4 Conclusion and Outlook..... | 116 |
| 3.4 Participation of free available chlorine as secondary oxidant during chlorine dioxide-based disinfection of <i>Escherichia coli</i> – Effect of extracellularly formed FAC | 119 |
| 3.4.1 Introduction | 120 |
| 3.4.2 Materials and Methods | 122 |
| 3.4.2.1 Chemicals, Instruments, and Analytical Methods..... | 122 |
| 3.4.2.2 Bacterial Strains | 122 |
| 3.4.2.3 Production of ClO ₂ and FAC | 122 |
| 3.4.2.4 Inactivation kinetics | 123 |
| 3.4.2.5 Novel approach to determine inactivation | 123 |
| 3.4.2.6 Participation of FAC in ClO ₂ based disinfection | 124 |
| 3.4.3 Results and Discussion..... | 125 |
| 3.4.3.1 Inactivation kinetics | 125 |

Table of content

| | |
|---|------------|
| 3.4.3.2 Participation of FAC in ClO ₂ based inactivation | 128 |
| 3.4.3.3 pH dependent inactivation..... | 130 |
| 3.4.4 Conclusion and Outlook..... | 132 |
| 4. General conclusion and further perspective | 135 |
| 5. Literature | 141 |
| List of Figures | 161 |
| List of Tables..... | 165 |
| Appendix I..... | 169 |
| Appendix II | 177 |
| Appendix III..... | 189 |
| Appendix IV | 215 |
| Appendix V | 223 |

Chapter 1

Introduction

1. Introduction

Planet earth contains more than 1.3 billion km³ of water in the whole hydrosphere, whereby only 2.5% can be considered as freshwater (Shiklomanov and Rodda, 2003). A significant part of the freshwater fraction ($\approx 70\%$) is frozen and present as permanent frost, which leaves an even smaller fraction of freshwater for human usage. Therefore, freshwater should be considered one of the most important resources of human kind. In 2006 the water withdrawn by humans was estimated to be 3800 km³ per year (Oki and Kanae, 2006), which is very likely to increase proportionally to the ongoing rise in the world population. Withdrawn water is mainly used for domestic, industrial, and agricultural purposes. Each purpose is causing a different kind of pollution to the used water (i.e., bacterial and/or chemical pollution). The consumption of polluted wastewater is very dangerous and can cause intoxication and/or infection with severe waterborne diseases. As it happened during the cholera outbreak of 1892 in the city of Hamburg (Awofeso and Aldabk, 2018). Cases like this demonstrate that the treatment of used water is one of the most important inventions for human health. Two of the major sections in water treatment are disinfection and pollutant control. The combination of inactivating pathogenic bacteria and removing harmful chemical compounds leads to the production of safe drinking water.

1.1 Background

Many different chemical oxidants can be used for achieving disinfection and/or pollutant control. Chlorine has been used since the beginning of the 20th century, mainly for disinfection purposes. However, in the 1970s the formation of harmful disinfection by-products (DBPs) during chlorination was observed (Rook, 1974). This observation started a whole new research brand to investigate alternatives for chlorine. The most promising alternatives are ozone (O₃) and chlorine dioxide (ClO₂).

O₃ has been very intensively studied over the last decades (von Sonntag and von Gunten, 2012). O₃ is a broadband oxidant, which reacts with a large spectrum of different compounds and shows very powerful disinfection strength. Due to the fast reaction rates with many compounds, the formation of undesired DBPs is not unexpected. In bromide-containing water matrices, O₃ reacts with bromide (Br⁻) and forms harmful bromate (BrO₃⁻) (von Gunten, 2003a). Additionally, O₃ can form carcinogenic nitrosamines if dimethylamines are present as a precursor (Andrzejewski et al., 2008). Thus, the applicability of O₃ strongly depends on the water matrix composition.

A more selective option is ClO_2 , which reacts with a smaller range of different compounds (Abdighahroudi et al., 2021) and is also a strong disinfectant (Cho et al., 2010). However, the reaction of ClO_2 leads to the formation of chlorite (ClO_2^-) and chlorate (ClO_3^-) as harmful DBPs with a drinking water standard of $200 \mu\text{g L}^{-1}$ (Germany) or 1.0mg L^{-1} (USA). Thus, the formation of ClO_2^- and ClO_3^- is limiting the application of ClO_2 . However, removal techniques for these DBPs are also investigated (e.g.; reduction by ferrous salts (Fe^{2+}) (Katz and Narkis, 2001)). Additionally, ClO_2 does form significantly lower amounts of halogenated DBPs compared to chlorine (Zhang et al., 2000) and is more effective over a broader pH range (Junli et al., 1997).

An interesting observation is the formation of secondary oxidants. The formation of hydroxyl radicals ($\cdot\text{OH}$) in O_3 reactions has been intensively studied (von Sonntag and von Gunten, 2012). Recently, the intrinsic formation of free available chlorine (FAC) during ClO_2 reactions has been demonstrated (Rougé et al., 2018; Terhalle et al., 2018). The reaction of ClO_2 with phenolic compounds is proposed to be a two-step reaction. The first reaction step is an electron transfer from phenol to ClO_2 forming ClO_2^- and a phenoxy radical, which reacts with another ClO_2 molecule by oxygen transfer forming benzoquinone and FAC in form of HOCl (Wajon et al., 1982). FAC and ClO_2 show different reaction behavior towards different reactive moieties. Therefore, FAC as secondary oxidant might play a major role in the application of the primary oxidant ClO_2 , in form of synergistic effects for pollutant control or disinfection purposes (Abdighahroudi et al., 2021). However, studies about the intrinsic FAC formation (i.e., what is influencing FAC formation and how) and disinfection mechanisms (i.e., participation of FAC during ClO_2 disinfection) are still lacking.

Chapter 1.2

Bacterial inactivation processes in water disinfection – mechanistic aspects of primary and secondary oxidants – a critical review

Mischa Jütte, Mohammad S. Abdighahroudi, Torsten Waldminghaus, Susanne Lackner, and Holger V. Lutze

This chapter has been adapted from: M. Jütte, M. S. Abdighahroudi, T. Waldminghaus, S. Lackner, and H. V. Lutze, “Bacterial inactivation processes in water disinfection – mechanistic aspects of primary and secondary oxidants – A critical review,” in *Water Research*, Elsevier, DOI: 10.1016/j.watres.2023.119626

1.2 Bacterial inactivation processes in water disinfection – mechanistic aspects of primary and secondary oxidants – a critical review

Water disinfection during drinking water production is one of the most important processes to ensure safe drinking water, which is gaining even more importance due to the increasing impact of climate change. With specific reaction partners, chemical oxidants can form secondary oxidants, which can cause additional damage to bacteria. Cases in point are chlorine dioxide which forms free available chlorine (e.g., in the reaction with phenol) and ozone which can form hydroxyl radicals (e.g., during the reaction with natural organic matter). The present work reviews the complex interplay of all these reactive species which can occur in disinfection processes and their potential to affect disinfection processes. A quantitative overview of their disinfection strength based on inactivation kinetics and typical exposures is given. By unifying the current data for different oxidants it was observable that cultivated wild strains (e.g., from wastewater treatment plants) are in general more resistant to chemical oxidants compared to lab-cultivated strains from the same bacterium. Furthermore, it could be shown that for selective strains chlorine dioxide is the strongest disinfectant (highest maximum inactivation), however as a broadband disinfectant ozone showed the highest strength (highest average inactivation). Details in inactivation mechanisms regarding possible target structures and reaction mechanisms are provided. Thereby the formation of secondary oxidants and their role in the inactivation of pathogens is decently discussed. Eventually, possible defense responses of bacteria and additional effects which can occur *in vivo* are discussed.

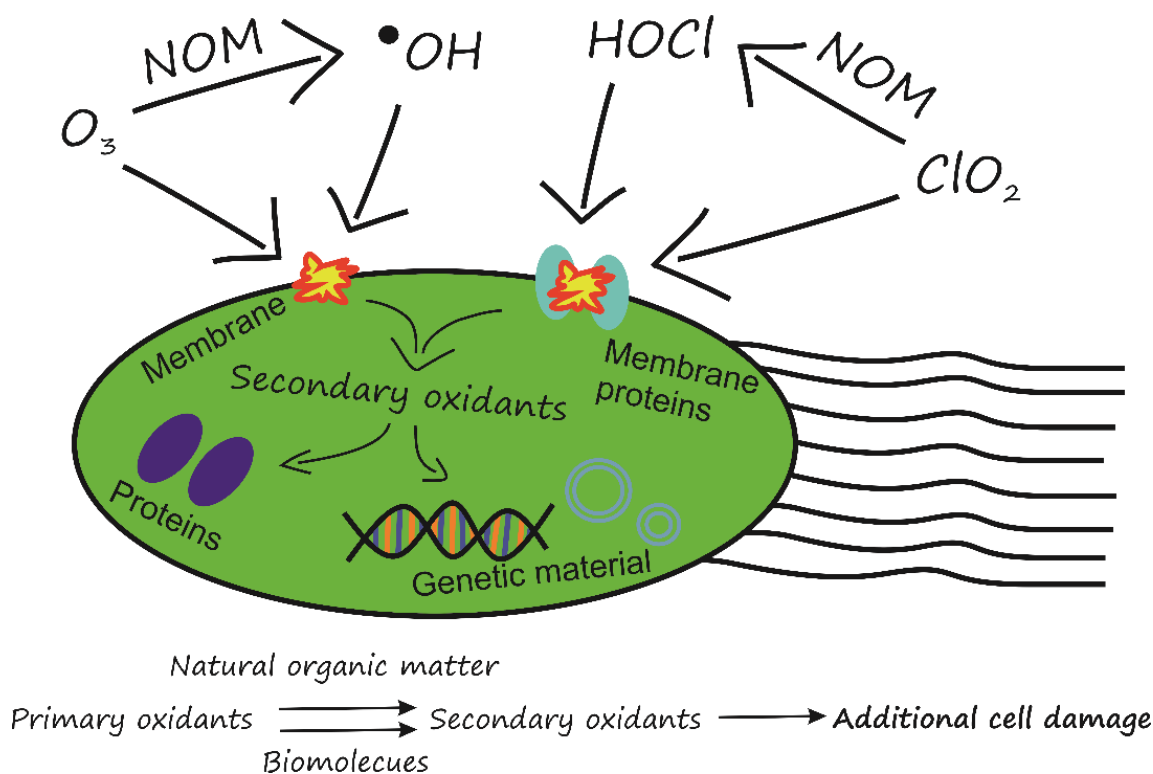


Figure 1: Graphical abstract of chapter 1.2 – Bacterial inactivation processes in water disinfection – mechanistic aspects of primary and secondary oxidants – a critical review

1.2.1 Introduction

Drinking water is safe if it is free of pathogens and other pollutants. However, approximately 30 % of the world's population has no access to safe drinking water, and more than one-third is living under hygienically poor conditions (Sanitation, 2019). The consumption of unsafe drinking water can cause severe diseases such as cholera, hepatitis, or acute gastroenteritis (Pal et al., 2018; Sanitation, 2019) and thus, adversely affect public health. The availability of safe drinking water is aggravated by the ongoing climate change. According to a report by the European environment agency, it is estimated that the average global temperature will increase by 2 °C in the next 20 years if no countermeasures are carried out (European environment agency, 2020; Masson-Delmotte et al., 2021). The increased temperature strongly favors the development of emergent waterborne diseases because the growth of many relevant bacteria, as well as other waterborne diseases like viruses and parasites, increases with increasing temperature (Ratkowsky et al., 1982; Walker, 2018). Additionally, the change in the water cycle behavior (such as heavy rainfall and flooding) is accelerating the spread and the transport of waterborne diseases (Semenza, 2020). Furthermore, the increased frequency and intensity of heatwaves combined with droughts may favor the growth of pathogens in source waters and water distribution systems. Hence, water disinfection is of utmost importance as a powerful tool to provide hygienically safe drinking water from polluted sources. An effective option for water disinfection is the application of chemical oxidants such as free available chlorine (FAC), chlorine dioxide (ClO₂), or ozone (O₃).

Besides the inactivation of pathogens, chemical oxidants can also be used to reduce antibiotic-resistant genes (ARGs), which are present in, e.g., municipal wastewater and hospital wastewater and can be taken up by other pathogens (Jäger et al., 2018; Pazda et al., 2019). Antibiotic-resistant bacteria (ARB) developed different ways to survive antibiotic treatment (Text A1.1). Indeed, ARBs can have severe consequences for human health, and WHO defined antibiotic resistance as one of the largest global health threats. The spread of ARGs can result in pathogens taking up/acquiring multiple (new) ARGs. If severe diseases such as pneumonia, tuberculosis, blood poisoning, and gonorrhoea are caused by such (multi-resistant) pathogens, there are not many effective antibiotics against them and therefore possible treatment methods are reduced (Antibiotic resistance, 2018). The extensive spread of ARGs and the importance of their removal have been reviewed recently by Pazda et al. (2019), showing that different ARGs can be found in severe amounts of effluents from WWTPs.

Antibiotics are widely used in human and veterinary medicine, but also, for example, as growth promoters or for prophylactic reasons in animal husbandry (Hao et al., 2014). The increase in the world's population, the higher demand for food, and the further emerging/reemerging of diseases due to climate change (Smol, 2012) lead to a significantly higher consumption of antibiotics (Roberts and Zembower, 2020). Furthermore, the fact that antibiotics are easily accessible (e.g., in grocery stores) in some countries and the prophylactic usage in animal husbandry further accelerates the development and spreading of ARGs (Davies and Davies, 2010). In fact, ARGs could be detected in wastewater (Alcaide and Garay, 1984; Filali et al., 2000; Pazda et al., 2019; Schwartz et al., 2003; Zhang et al., 2009), in the aquatic environment (Czekalski et al., 2015; Pruden et al., 2006; Su et al., 2020; Zhao et al., 2020), in soil samples (Bougnom et al., 2020; Chen et al., 2016; Knapp et al., 2010; Marti et al., 2013; Martínez-Carballo et al., 2007; Wang et al., 2014; Zhu et al., 2013), in water sediments (Chen et al., 2013; Czekalski et al., 2014; Mao et al., 2014; Thevenon et al., 2012), and even in drinking water (Bergeron et al., 2015; Destiani and Templeton, 2019; Sanganyado and Gwenzi, 2019; Yu et al., 2022) worldwide. Nowadays, the development of multidrug resistance genes (MRGs) is observed, whereby bacteria developed or acquired resistance mechanisms against several antibiotics (Pazda et al., 2019).

ARGs are particularly relevant in water disinfection because they can be transferred horizontally amongst bacteria which facilitates their alarming spreading (Karkman et al., 2018). While the vertical transfer of genetic information describes the transfer from parents to siblings or cells to daughter cells, horizontal gene transfer (HGT) is the transfer from “adult” cells to other “adult” cells. This HGT is mostly limited to short pieces of DNA as ARGs and does not result in the transfer of entire genomes as it happens in the vertical gene transfer. HGT might appear through cell-cell contact by a process called conjugation, through a viral vector by a process called transduction, or by bacteria acquiring free DNA from the environment, a process called transformation. The latter mechanism is relevant for the water disinfection process since the inactivation of some bacteria might release genetic material as ARGs that could be taken up by surviving and environmental bacteria and render them resistant to antibiotics. The deactivation of ARGs is, therefore, a central topic in water disinfection. One should distinguish between free extracellular ARGs in the water matrix and the intracellular ARGs that do require different considerations due to different accessibilities.

1.2.1.1 Kinetic considerations and competing reactions

An important parameter for describing the inactivation of pathogens or degradation of pollutants by chemical oxidants is oxidant exposure. It can be interpreted as oxidant concentration available for pollutant degradation or disinfection and is the integral of oxidant concentration over time (von Gunten and Hoigne, 1994). The presence of water matrix constituents can largely decrease the oxidant exposure available for pathogen inactivation. Especially in the case of wastewater, nitrite can cause a significant oxidant depletion ($k_{app}(\text{FAC} + \text{NO}_2^-) = 7.4 \times 10^3 \text{ M}^{-1} \text{ s}^{-1}$ at pH 7 (Panasencko et al., 1997), $k_{app}(\text{ClO}_2 + \text{NO}_2^-) = 1.1 \times 10^2 \text{ M}^{-1} \text{ s}^{-1}$ at pH 7 (Hoigné and Bader, 1994), $k_{app}(\text{O}_3 + \text{NO}_2^-) = 5.8 \times 10^3 \text{ M}^{-1} \text{ s}^{-1}$ at pH 7 (von Sonntag and von Gunten, 2012)). Ammonia may scavenge FAC as well ($k_{app}(\text{FAC} + \text{NH}_3) = 1.3 \times 10^4 \text{ M}^{-1} \text{ s}^{-1}$ at pH 7) (Deborde and von Gunten, 2008), however, oxidation in wastewater treatment is typically applied to treated wastewater which should contain a low level of ammonia. Natural organic matter (NOM) is the most important matrix constituent that results in oxidant depletion. Indeed, NOM has various functional groups (Figure AI.1), which are reactive toward most oxidants (Świetlik et al., 2004; Westerhoff et al., 2004).

Hence, the reactivity of an oxidant with critical cell structures in pathogens has to be compared with undesired side reactions (e.g., with NOM). Table 1 – Table 3 compile reaction rates of common oxidants with bacteria.

It has to be mentioned that the rate of inactivation per time (inactivation kinetics (k)) of bacteria depends on many factors (e.g., strain, temperature, pH) (Hunt and Mariñas, 1997; Jamil et al., 2017). However, most of the available inactivation data are not unified or reported these factors, aggravating a comparison between studies. Furthermore, most of the reaction rates are not given on a molar scale, which complicates comparing with other oxidants. Therefore, reaction rate constants presented in Table 1 – Table 3 have been unified on a molar scale based on the chemical disinfectant (i.e., $k / \text{M}^{-1} \text{ s}^{-1}$) (Equation 1). We also recommend using the molar scale in future studies. The collected data is visualized in Figure 2. It is worth mentioning that the kinetics of bacterial inactivation in real applications is complex and might follow non-linear curves (shouldering or tailing) (Jensen, 2010). However, using the simple Chick-Watson model with linear second-order kinetics and calculation of ct values is common in practice to compare to more sophisticated empirical models. Yet the Chick-Watson model does not include for instance the so-

called lag phase, which describes the range between the first data point of monitored disinfection and the first data point of an observed effect (Gyürek and Finch, 1998). This delay can be caused by the resistance of bacteria toward specific oxidants for instance.

$$\ln\left(\frac{N_t}{N_0}\right) = -k \times \int[Ox]dt \quad \text{Equation 1}$$

$\left(\frac{N_t}{N_0}\right)$ = Number of bacteria at time t / Initial number of bacteria

k = Reaction rate constants for inactivation / $M^{-1} s^{-1}$

$\int[Ox]dt$ = Oxidant exposure / $M \times s$

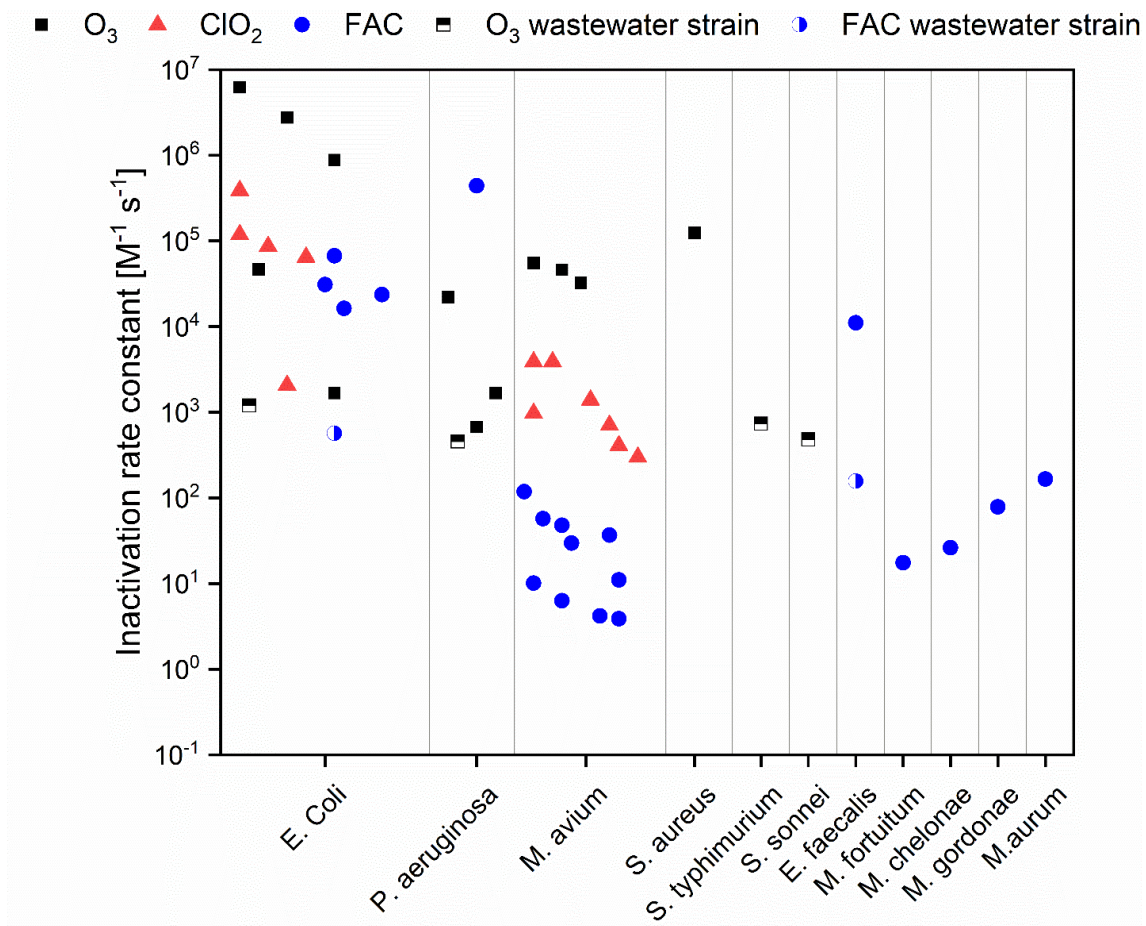


Figure 2: Available inactivation rates of different bacteria with different chemical oxidants from literature. Datasets are separated by laboratory-cultivated strains (full symbol) and wastewater isolates (half full symbols).

Table 1: Comparison of inactivation kinetics of different bacteria with ozone.

| Bacterium | Strain | pH | Temp / °C | $k / \text{M}^{-1} \text{s}^{-1}$ | Ref. |
|-------------------------------|-------------------|------|-----------|-----------------------------------|--------------------------|
| <i>Escherichia coli</i> | ATCC 11775 | 6 | 20 | 6.24×10^6 | (Hunt and Mariñas, 1997) |
| | Strain C | 7.2 | 23 | 2.76×10^6 | (Taylor et al., 2000) |
| | ATCC 8739 | 7.1 | 20 | 8.77×10^5 | (Cho et al., 2010) |
| | J53 (R388, sul1) | 7.4 | 22 | 4.64×10^4 | (Czekalski et al., 2016) |
| | ATCC 25922 | 7.2 | 25 | 1.68×10^3 | (Lezcano et al., 1999) |
| | Isolated from WW | 7.2 | 25 | 1.2×10^3 | (Lezcano et al., 1999) |
| <i>Pseudomonas aeruginosa</i> | Clinical isolates | N.A. | N.A. | 2.21×10^4 | (Choudhury et al., 2018) |
| | ATCC 27853 | 7.2 | 25 | 1.68×10^3 | (Lezcano et al., 1999) |
| | No information | N.A. | 25 | 6.70×10^2 | (Zuma et al., 2009) |
| | Isolated from WW | 7.2 | 25 | 4.56×10^2 | (Lezcano et al., 1999) |
| <i>Staphylococcus aureus</i> | Clinical isolates | N.A. | N.A. | 1.24×10^5 | (Choudhury et al., 2018) |
| <i>Salmonella typhimurium</i> | Isolated from WW | 7.2 | 25 | 7.36×10^2 | (Lezcano et al., 1999) |
| <i>Shigella sonnei</i> | Isolated from WW | 7.2 | 25 | 4.80×10^2 | (Lezcano et al., 1999) |
| <i>Mycobacterium avium</i> | 5502 | 7 | 23 | 5.53×10^4 | (Taylor et al., 2000) |
| | 5002 | 7 | 23 | 4.61×10^4 | (Taylor et al., 2000) |
| | 1060 | 7 | 23 | 3.25×10^4 | (Taylor et al., 2000) |

Table 2: Comparison of inactivation kinetics of different bacteria with chlorine dioxide.

| Bacterium | Strain | pH | Temp./ °C | $k / \text{M}^{-1} \text{s}^{-1}$ | Ref. |
|----------------------------|------------|------|-----------|-----------------------------------|-----------------------------|
| <i>Escherichia coli</i> | Strain C | 7 | 23 | 3.88×10^5 | (Taylor et al., 2000) |
| | ATCC 35218 | 8 | 4 | 1.19×10^5 | (Ofori et al., 2017) |
| | ATCC 8739 | 7.1 | 20 | 8.63×10^4 | (Cho et al., 2010) |
| | ATCC 8739 | N.A. | N.A. | 6.47×10^4 | (Cho et al., 2004) |
| | ATCC 35218 | 8 | 22 | 2.07×10^3 | (Ofori et al., 2017) |
| <i>Mycobacterium avium</i> | 5502 | 7 | 23 | 3.88×10^3 | (Taylor et al., 2000) |
| | 15769 | 6 | 30 | 3.88×10^3 | (Vicuña-Reyes et al., 2008) |
| | 15769 | 10 | 20 | 1.39×10^3 | (Vicuña-Reyes et al., 2008) |
| | 1060 | 7 | 23 | 9.71×10^2 | (Taylor et al., 2000) |
| | 5002 | 7 | 23 | 7.06×10^2 | (Taylor et al., 2000) |
| | 15769 | 6 | 10 | 4.08×10^2 | (Vicuña-Reyes et al., 2008) |
| | 15769 | 6 | 5 | 3.00×10^2 | (Vicuña-Reyes et al., 2008) |

Table 3: Comparison of inactivation kinetics of different bacteria with free available chlorine.

| Bacterium | Strain | pH | Temp. / °C | $k / \text{M}^{-1} \text{s}^{-1}$ | Ref. |
|--------------------------------|------------------------------|-----------|--------------------|---|--------------------------------|
| <i>Escherichia coli</i> | Strain C | 7 | 23 | 6.71×10^4 | (Taylor et al., 2000) |
| | ATC 8739 | N.A. | N.A. | 3.10×10^4 | (Cho et al., 2004) |
| | ATC 8739 | 7.1 | 20 | 2.37×10^4 | (Cho et al., 2010) |
| | ATCC 10798 | 7.6 | 19 | 1.63×10^4 | (Mwatondo and Silverman, 2021) |
| | Waste water isolate | 7.6 | 19 | 5.68×10^2 | (Mwatondo and Silverman, 2021) |
| <i>Pseudomonas aeruginosa</i> | PAO1 | 7 | 22 | 4.42×10^5 | (Xue et al., 2013) |
| <i>Enterococcus faecalis</i> | ATCC 19433 | 7.6 | 19 | 1.11×10^4 | (Mwatondo and Silverman, 2021) |
| | Waste water isolate | 7.6 | 19 | 1.57×10^2 | (Mwatondo and Silverman, 2021) |
| <i>Mycobacterium avium</i> | 5502 (media grown) | 7 | 23 | 1.18×10^2 | (Taylor et al., 2000) |
| | A 5 (media grown) | 7 | 23 | 5.70×10^1 | (Taylor et al., 2000) |
| | 5002 (media grown) | 7 | 23 | 4.79×10^1 | (Taylor et al., 2000) |
| | 1508 (media grown) | 7 | 23 | 3.68×10^1 | (Taylor et al., 2000) |
| | 1060 (media grown) | 7 | 23 | 2.96×10^1 | (Taylor et al., 2000) |
| | 5502 (water grown) | 7 | 23 | 1.10×10^1 | (Taylor et al., 2000) |
| | 1508 (water grown) | 7 | 23 | 1.01×10^1 | (Taylor et al., 2000) |
| | 5002 (water grown) | 7 | 23 | 6.28×10^0 | (Taylor et al., 2000) |
| | 1060 (water grown) | 7 | 23 | 4.18×10^0 | (Taylor et al., 2000) |
| A 5 (water grown) | 7 | 23 | 3.89×10^0 | (Taylor et al., 2000) | |
| <i>Mycobacterium fortuitum</i> | public water supply isolates | 7 | RT | 1.75×10^1 | (Le Dantec et al., 2002) |
| <i>Mycobacterium chelonae</i> | public water supply isolates | 7 | RT | 2.62×10^1 | (Le Dantec et al., 2002) |
| <i>Mycobacterium gordonae</i> | Drinking water isolate | 7 | RT | 7.87×10^1 | (Le Dantec et al., 2002) |
| <i>Mycobacterium aurum</i> | public water supply isolates | 7 | RT | 1.66×10^2 | (Le Dantec et al., 2002) |

Remarkably, the reaction rate of the same bacteria can largely vary for different strains, i.e., the reaction rate of *Escherichia coli* with O_3 can differ by three orders of magnitude dependent on the investigated strain. In general, it can be stated that environmental strains isolated from wastewater are more resistant to chemical oxidants compared to commercially available references (Mwatondo and Silverman, 2021). Reliable kinetic data on inactivation rates is decisive for precise predictions

of pathogen abatement, which can be done based on a given exposure and standardization (von Sonntag and von Gunten, 2012). Both a standardized and representative procedure for determining reaction rate and more reliable data on inactivation kinetics are needed to improve the understanding and prediction of inactivation processes in oxidative treatment.

To compare the efficiency of pathogen inactivation by different oxidants, it is necessary to multiply the inactivation rate with typical exposures of the corresponding oxidant. Therefore, literature values for oxidant exposure were taken, which resembles typical oxidant exposures for the corresponding oxidants in secondary wastewater effluent at pH 8. The exposures were determined by adding 45 μM of each oxidant and monitoring the oxidant depletion for 1 hour by using colorimetric methods (Lee and von Gunten, 2010). The final exposure can be calculated by the integral of the residual oxidant concentration over time. The product of the exposure and the inactivation rate (k) allows calculating the logarithmic inactivation effect according to the Chick-Watson model (equation 1). The range of pathogen inactivation (I_{\min} and I_{\max}) and the average inactivation (I_{ave}) are shown in Table 4.

Table 4: Range of inactivation efficiency in wastewater of the oxidants ozone, chlorine dioxide, and chlorine. The exposures of the different oxidants have been determined for the same wastewater and were obtained from Lee and von Gunten (2010).

| Oxidant | Exposure / M s | $k_{\min} /$ M⁻¹ s⁻¹ | $k_{\text{ave}} /$ M⁻¹ s⁻¹ | $k_{\max} /$ M⁻¹ s⁻¹ | I_{min} (N/N₀) | I_{ave} (N/N₀) | I_{max} (N/N₀) |
|-------------------------|---------------------------------|--|--|--|--|--|--|
| Ozone | 6.0×10^{-4} | 1×10^2 | 6.4×10^5 | 1×10^6 | 6×10^{-2} | 3.8×10^2 | 6×10^2 |
| Chlorine dioxide | 4.5×10^{-2} | 1×10^2 | 5.6×10^4 | 1×10^5 | 4.5×10^0 | 3.4×10^1 | 4.5×10^3 |
| Chlorine | 3.6×10^{-2} | 1×10^0 | 3.1×10^4 | 1×10^4 | 3.6×10^{-2} | 1.9×10^1 | 3.6×10^2 |

Table 4 shows that the low inactivation kinetics of ClO_2 is compensated by the high oxidant exposure in wastewater, indicating that ClO_2 is most effective, followed by O_3 and FAC, which have a similar effect on disinfection. It must be mentioned that the effectiveness order may also vary depending on the composition of the water matrix. E.g., the effectivity of FAC largely depends on the N -content in the organic matter since it has high reaction rates with amines (Deborde and von Gunten, 2008). Although ClO_2 shows the highest possible inactivation, the average value for O_3 is one order of magnitude higher than ClO_2 . This shows that although ClO_2 has higher exposure

and fast inactivation with specific bacterial strains, O₃ is a more broadband disinfectant. Furthermore, one has to consider the formation of secondary oxidants, which can contribute to disinfection.

The assessment of the oxidant exposure becomes even more complicated when it comes to the deactivation of intracellular ARGs. Here cell wall, cell membrane, and endoplasmic matter contribute to oxidant depletion. By critically reviewing the available literature for reaction rate constants of the different oxidants with different bacterial constituents, Dodd concluded that the effectiveness of a disinfectant to deactivate ARGs depends strongly on the reactivity towards the endoplasmic constituents, including amino acids, lipids, saccharides, and nucleic acids (Dodd, 2012).

To this end, coherent data is still lacking on inactivation kinetics, oxidant exposures in real water matrices, and intracellular biochemical reactions and their effect on the viability of bacteria. Further research with standardized experimental conditions is needed, combining reaction rate with oxidant exposure in different matrices for different oxidants to improve the understanding of disinfection processes. For instance, investigating the inactivation kinetics of the same bacterial strain under a broader range of different conditions (e.g., pH, Temperature) would increase the understanding of inactivation processes during (waste)water treatment and promote disinfection optimization.

1.2.1.2 Secondary oxidants

In oxidative water treatment, the primary oxidants (e.g., FAC, ClO₂, and O₃) can form numerous secondary oxidants, which can contribute to pollutant degradation, disinfection, and by-product formation (Table 5).

Table 5: Known and conceivable secondary oxidants for different primary oxidants.

| Primary oxidant | Secondary oxidant | Ref |
|---|--|---|
| Free available chlorine (Chapter 1.2.3) | Chloramines | (Fayyad and Al-Sheikh, 2001) |
| | Free available bromine | (Heeb et al., 2014) |
| | Bromamines | (Heeb et al., 2014) |
| | Hydroxyl radicals | (Rodríguez and von Gunten, 2020) |
| Chlorine dioxide (Chapter 1.2.4) | Chlorite | (Abdighahroudi et al., 2022, 2021; Hupperich et al., 2020; Jütte et al., 2022; Rougé et al., 2018; Terhalle et al., 2018) |
| | Free available chlorine | (Abdighahroudi et al., 2021; Hupperich et al., 2020; Jütte et al., 2022; Rougé et al., 2018; Terhalle et al., 2018) |
| | Chlorate | (Abdighahroudi et al., 2021; Hupperich et al., 2020) |
| Ozone (Chapter 1.2.5) | Hydroxyl radicals | (von Sonntag and von Gunten, 2012) |
| | Free available bromine | (Haag and Holgné, 1983) |
| | Peroxyl radicals | (von Sonntag and von Gunten, 2012) |
| | Singlet oxygen | (von Sonntag and von Gunten, 2012) |
| | Superoxide | (von Sonntag and von Gunten, 2012) |
| | Oxyl radicals | (von Sonntag and von Gunten, 2012) |
| | Reactive organic species (e.g., quinones) | (Fischbacher et al., 2015; von Sonntag and von Gunten, 2012) |

It is important to consider that the formation and the yield of secondary oxidants strongly depend on the reaction partner of the primary oxidant (Abdighahroudi et al., 2021; Hupperich et al., 2020; von Sonntag and von Gunten, 2012). However, which secondary oxidants and how they are formed during disinfection in intracellular reactions and cell-matrix conditions remain unrevealed. The participation of the formed secondary oxidants in the disinfection mechanism of the corresponding primary oxidant is not revealed yet. Although the inactivation efficiency of the secondary oxidants might be lower (e.g., in the case of chloramines by using FAC as the primary oxidant), the low reactivity can lead to longer lifetimes of the secondary oxidant and, therefore higher exposures.

The high exposure to secondary oxidants can indeed effect the inactivation efficiency of the corresponding primary oxidants.

The present review deals with mechanistic aspects of disinfection of several oxidants, considering the formation and fate of secondary oxidants during the inactivation mechanism, and shows that further research is needed to understand these mechanisms fully.

1.2.2 Target structures reactivity and effect on viability

The primary site of attack on bacteria and the corresponding inactivation mechanism differs strongly for each oxidant. A scheme of possible reaction partners is shown in Figure 3. The oxidants can react with different chemical structures of the cell membrane (e.g., double bonds of the lipid double layer or the amino acids of the membrane proteins) or the cytoplasm (e.g., the amino acids of proteins or the nucleotides within DNA). Most of these reactions are pH-dependent since reactive functional groups occur in different species. For instance, phenol which resembles a reactive moiety of the amino acid tyrosine has a pK_a of 10 (Hoigné and Bader, 1994); thus, the predominant species at $pH < 10$ is the neutral phenol species, and only at $pH > 10$ the deprotonated phenolate species becomes predominant. However, phenolate reacts several orders of magnitude faster than the neutral phenol species with most chemical oxidants (Neta et al., 1988). Therefore, the phenolate species controls the reaction rate even at neutral pH. It has to be mentioned that also the speciation of the oxidant affects the reaction rate, in that the different species show significant differences in reactivity (e.g., $HOCl/OCl^-$, in the case of FAC (Deborde and von Gunten, 2008)). Speciation of both reactants (oxidant and target structure) results in quite a complex pH-dependent reaction rate, whereby reaction rate constants can vary by several orders of magnitude. Since reaction rates are the key to identifying the most important oxidant target among the cells' constituents, reliable pH-dependent reaction rates are decisive in understanding inactivation mechanisms by calculating reaction rates at specific pH values. Although the reaction on the surface of the cell can happen at different pH values, the cytoplasm of bacteria has a typical pH of around 7 (Padan et al., 1981; Porcelli et al., 2005; Zilberstein et al., 1984).

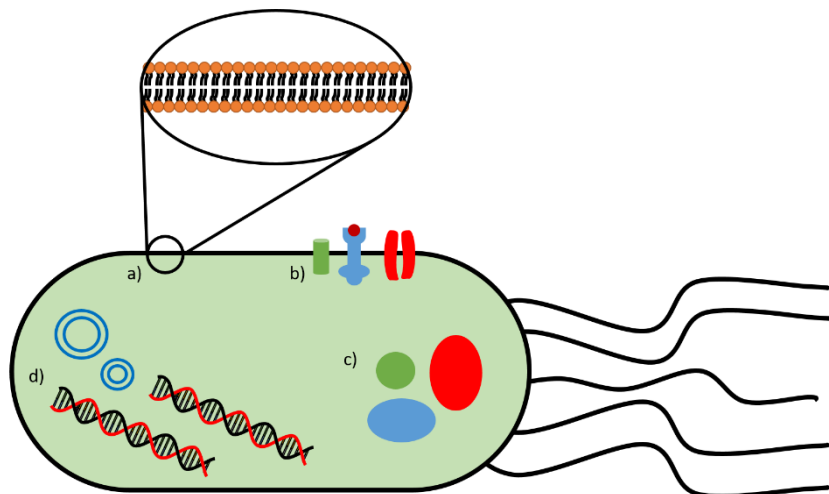


Figure 3: Schematic representation of a cell with different points of attack for inactivation. The possible target structures are a) the double bonds of the lipid bilayer, b) the amino acids of the membrane proteins, c) intracellular proteins, and d) the DNA nucleotides (chromosomal DNA and plasmids).

1.2.2.1 Lipid layer and effect on viability

The phospholipid bilayer surrounding bacterial cells consists of unsaturated fatty acids, as shown in Figure AI.2. The double bonds in these fatty acids display a high electron density, where electrophilic oxidants might attack (e.g., O_3 (von Sonntag and von Gunten, 2012)). A reaction with the membrane may lead to membrane lysis and leakage of inner cell components and eventually to a lethal event (Cho et al., 2010). However, in this scenario, the inner cell compounds (e.g., genetic material) may stay intact (Yoon et al., 2017) and can arrive at the bulk solution. This means ARGs might be transferred to other bacteria via HGT.

The reactivity of common oxidants with double bonds follows the order O_3 ($\approx 10^4 \text{ M}^{-1} \text{ s}^{-1}$) $\gg \gg$ $FAC \approx ClO_2 \approx NH_2-Cl$ ($< 1 \text{ M}^{-1} \text{ s}^{-1}$), (Abdighahroudi et al., 2021; Deborde and von Gunten, 2008; von Sonntag and von Gunten, 2012); hence O_3 is the most effective in attacking double bonds. Thereby, a fast Criegee reaction may break down the carbon chain structure, which can explain the loss in membrane integrity of bacteria observed in ozonation (Cho et al., 2010). Thereby, O_3 binds to the double bond and causes cleavage of the Pi-bond (partial oxidation), or cleavage of the whole double bond and formation of carbonyl moieties (von Sonntag and von Gunten, 2012). Other oxidants cannot interact with the membrane significantly but cause damage to membrane proteins or diffuse into the cytoplasm and cause inner cell damage (Cho et al., 2010).

1.2.2.2 Proteins & Amino acids reactivity and effect on viability

Other points of attack in bacterial cells are proteins, peptides, and amino acids. Since proteins have different functions in bacterial cells, their inactivation may affect the viability of bacterial cells more critically than the degradation of free amino acids in bacterial cells. Proteins are chains of amino acids, whereby the primary amine of the free amino acids is present as secondary amines with a ketone group at the alpha carbon, known as amides (Figure AI.3). Amides are strongly deactivated, making peptide bonds hard to break (Deborde and von Gunten, 2008; von Sonntag and von Gunten, 2012). Hence, a reaction of oxidants will mainly happen at the functional side groups of the amino acids of peptides and proteins. Figure AI.4 shows the structure of the functional side groups of the 20 canonical (proteinogenic) amino acids and categorizes these groups according to their structure. Figure 4 summarizes the range of the reactivity at pH 7 of different oxidants towards the functional groups in amino acid side groups.

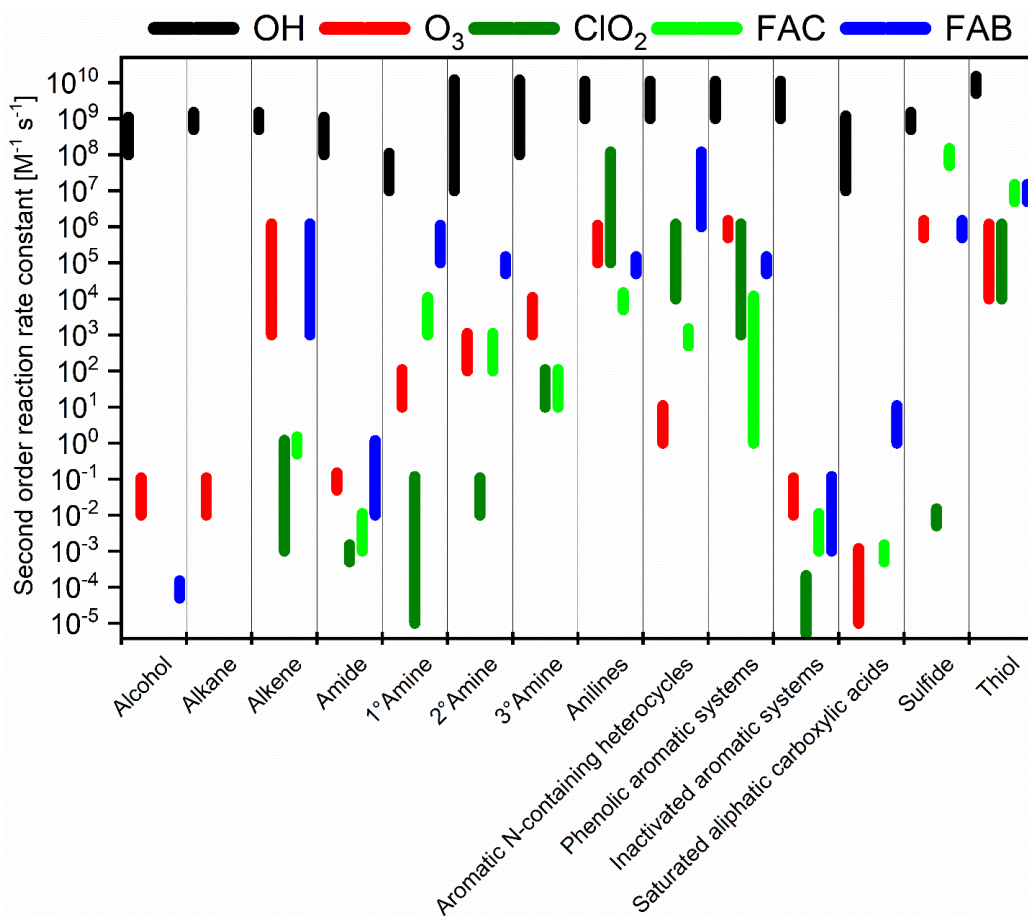


Figure 4: Range of reaction rates of different oxidants towards functional groups present in the side groups of amino acids at pH 7.

•OH reacts with all structures at near diffusion-controlled rates (Buxton et al., 1988) and, thus, is not selective toward specific moieties. This results in a very short lifetime and low **•OH** exposures and, thus, a limited effect on the pathogens' viability. However, if **•OH** are formed as secondary oxidants, e.g., from the reaction of O_3 (von Sonntag and von Gunten, 2012) at sites in pathogens that are crucial for their vitality, their immediate reaction at surrounding sites may enhance the cell damage significantly. O_3 reacts more selectively than **•OH** with secondary and tertiary amines, olefins, phenols, and reduced sulfur-containing groups (Hoigné et al., 1983; Hoigné and Bader, 1983; Lee and von Gunten, 2012; von Sonntag and von Gunten, 2012). Overall, 7 out of 20 canonical amino acids can be considered reactive with O_3 (i.e., *N*-containing, *S*-containing, and aromatic sidechains). Free available bromine (**FAB**) is a quite reactive oxidant showing reactivity towards alkenes, phenols, anilines, *N*-containing compounds, and *S*-containing compounds (Heeb et al., 2014). The selectivity of FAB is therefore comparable with O_3 . However, the currently available data for FAB reaction rates is quite limited, and more research is needed. **FAC** reacts with most *N*-containing side groups and all *S*-containing amino acids (Deborde and von Gunten, 2008) (i.e., 7 out of 20 canonical amino acids) and is similarly selective as O_3 and FAB in its reaction with amino acids. The reaction of FAC with *N*-containing moieties may also form chloramines (see Chapter 1.2.3). These chloramines can principally cause further cell damage or reform the original amino acid in a reaction with a reductant. **ClO₂** is way more selective than **•OH**, O_3 , and FAC since it mainly reacts with phenolic moieties, aromatic amines, and thiols (Sharma and Sohn, 2012). Hence, it may build up high exposures in the endoplasm. Additionally, **ClO₂** probably forms significant yields of FAC and chlorite (ClO_2^-) at the reactive sites in the endoplasm, which may increase its disinfection strength (see chapter 1.2.4). Indeed, FAC and **ClO₂** act together very synergistically since their target structures are nearly complementary (only cysteine and tryptophan are degraded by both oxidants).

The reaction of chemical oxidants with (membrane)proteins may reduce the biological function by changing, e.g., their quaternary structure. In that regard, the kind of degradation is very much dependent on the kind of oxidant present, due to the different target structures inside the protein.

1.2.2.3 genetic material reactivity and effect viability

The oxidation of the genetic material (cf. further information in Appendix I, Figure AI.5 and Text AI.2) can lead to a single base lesion (He et al., 2019; von Sonntag and von Gunten, 2012), DNA double-strand breaks (fragmentation) (Suquet et al., 2010; von Sonntag, 2006; von Sonntag and von Gunten, 2012), and consequently alteration in the supercoiled structure (Ishizaki et al., 1987; Sawadaishi et al., 1985). If these reactions occur at ARGs, these genes would lose their transformation activity due to modification of the chemical structure, which means that the ARGs are deactivated. It is noteworthy that the deactivation of genes is dependent on the oxidant exposure but independent of the oxidant concentration (Choi et al., 2021; Yoon et al., 2021). It has been reported that the reactivity of the oxidants toward the amplicon is increasing with the increasing length of the genome, which can be explained by the increased number of possible reaction partners (Choi et al., 2021; He et al., 2019; Nihemaiti et al., 2020). Thereby, $\cdot\text{OH}$ is causing very effective double-strand breakage (Nihemaiti et al., 2020), resulting in an instant loss of transforming activity (He et al., 2019). This high efficiency in double-strand breakages is caused by the high reaction rate constants of $\cdot\text{OH}$ with amplicons (He et al., 2019; Nihemaiti et al., 2020). Compared to $\cdot\text{OH}$, the loss of transforming activity was less pronounced in the case of O_3 , followed by FAC, ClO_2 , and chloramines (He et al., 2019). Bacteria can initiate countermeasures such as repair mechanisms (Friedberg et al., 2005), which explains why the loss of transformation activity was slower than the corresponding gene degradation (Nihemaiti et al., 2020). However, different bacteria have different repair mechanisms. This is one reason lag phases and inactivation rates can largely vary for different bacteria or strains (Table 1 – 3). Considering that nearly all oxidants also form secondary oxidants (Table 5), the inactivation mechanisms are very complex and will be discussed for each oxidant in the following chapters.

1.2.3 Free available chlorine

FAC is the most common disinfectant used for water treatment. The inactivation of bacteria and viruses by FAC has been proven by various studies (De Beer et al., 1994; Engelbrecht et al., 1980; Floyd et al., 1979; Le Dantec et al., 2002; Nakagawara et al., 1998; Nuanualsuwan and Cliver, 2003; Page et al., 2010; Venkobachar et al., 1977; Wigginton et al., 2012). FAC is a selective oxidant that predominantly reacts with amines, sulfides, activated double bonds, aromatic compounds, and some inorganic compounds such as reduced iron, manganese, and dihydrogen sulfide (Deborde and von Gunten, 2008). The active agent in chlorination is hypochlorous acid

(HOCl) which can dissociate to hypochlorite (OCl^-) ($\text{p}K_a = 7.54$ (Deborde and von Gunten, 2008)).

The reactivity of the conjugated base OCl^- is several orders of magnitude lower than HOCl (Deborde and von Gunten, 2008); hence disinfection and reaction with organic and inorganic compounds become significantly weaker at $\text{pH} > 7$ (Deborde and von Gunten, 2008). Chloramines can be produced by the addition of ammonia prior to chlorination (Berliner, 1931). Chloramines have higher selectivity than FAC and can be applied in waters that have a strong FAC demand and high pH (Vikesland et al., 1998).

1.2.3.1 Reaction with the water matrix

The reaction of FAC with NOM leads to the formation of harmful halogenated organic compounds such as trihalomethanes (THM), halogenated acetonitriles (HAN), and haloacetic acids (HAA) (Gallard and von Gunten, 2002; Lu et al., 2009; Richardson et al., 2007; Zhang et al., 2012). Besides the formation of harmful halogenated disinfection by-products (DBPs) (Gallard and von Gunten, 2002), the reaction of FAC with specific matrix constituents can lead to the formation of secondary reactive species such as chloramines and FAB (Berliner, 1931; Farkas et al., 1949). Chloramine formation is observed in wastewater matrices treated with FAC (Fayyad and Al-Sheikh, 2001). Although chloramines can be considered a reactive species, their inactivation rate is much lower than FAC. Indeed, the addition of different amino acids to wastewater, increases the chloramine formation, resulting in a decrease in *E. coli* inactivation efficiency (Fayyad and Al-Sheikh, 2001).

Typical matrices of natural waters and municipal wastewaters contain bromide (Br^-) and sometimes iodide (I^-) (Gruchlik et al., 2014; Li et al., 2020; Magazinovic et al., 2004), and the treatment of Br^- and I^- containing water by FAC or chloramine has been reported to increase the cytotoxicity, due to formation of brominated and iodinated products (Criquet and Allard, 2021; Dong et al., 2017). Indeed, FAC reacts fast with Br^- and I^- ($k_{app}(\text{HOCl} + \text{Br}^-) = 5.3 \times 10^3 \text{ M}^{-1} \text{ s}^{-1}$ and $k_{app}(\text{HOCl} + \text{I}^-) = 1.1 \times 10^8 \text{ M}^{-1} \text{ s}^{-1}$ at $\text{pH} 7$ (Deborde and von Gunten, 2008)). In the case of Br^- , the reaction results in FAB, while I^- is oxidized by FAC to free available iodine (FAI), which is further oxidized to iodate rapidly. Thus, significant FAI exposures are unlikely to happen in the presence of FAC. However, chloramines can also form FAI but not further oxidize it to form iodate (Bichsel and von Gunten, 1999). Hence, FAI is a potential secondary oxidant of chloramines. FAB reacts fast with amines to form bromamines (e.g., $k_{app}(\text{HOBr} + \text{Ammonia}) \approx 10^5 \text{ M}^{-1} \text{ s}^{-1}$ at $\text{pH} 7$)

(Heeb et al., 2014). However, the knowledge about the disinfection strength of FAB, bromamines, and FAI is limited. Potentially formed free available halogen species can indeed play a role in water disinfection mechanisms. The disinfection strength of FAB is only marginally lower compared to FAC (e.g., 57 μM FAC leads to 4 log inactivation of *Enterococcus faecalis* and *Pseudomonas aeruginosa* after 2 min at 25 °C at pH 7 while 52 μM FAB yield 92.8 and 85.5 % inactivation under the same conditions, respectively and 3 log inactivation was reached after 4 minutes (Wojtowicz, 2004)) and it is used for disinfection of, for instance, spa and pool water (Daiber et al., 2016). Br^- and NOM concentration in natural waters and wastewater largely varies from a few $\mu\text{g L}^{-1}$ up to mg L^{-1} (Magazinovic et al., 2004). Formed FAB may contribute to the disinfection but also form undesired by-products (bromate (BrO_3^-) and halo-organic) (Haag and Holgné, 1983). FAB can undergo reactions with matrix compounds, for instance, phenolic compounds ($k(\text{HOBr} + \text{Phenol}) = 1.8 \times 10^5 \text{ M}^{-1} \text{ s}^{-1}$ at pH 7) (Heeb et al., 2014) and forms halogenated DBPs (Judd and Jeffrey, 1995). The formation of toxic DBPs is known to be strongly matrix-dependent (Wirzberger et al., 2021). The efficiency of bacterial inactivation during the water and wastewater treatment due to secondary formed FAB stills lacks decent investigations.

Recent research indicated that FAC could also form hydroxyl radicals ($\cdot\text{OH}$) as another secondary oxidant (Rodríguez and von Gunten, 2020). In the postulated pathway, FAC reacts with hydroquinone and forms benzoquinone (BQ). BQ reacts with another hydroquinone molecule to two semiquinone radicals (SQ), which further reacts with O_2 and forms a superoxide radical ($\text{O}_2^{\cdot-}$). Eventually, $\text{O}_2^{\cdot-}$ reacts with FAC and forms $\cdot\text{OH}$ (Rodríguez and von Gunten, 2020). Intrinsic formed $\cdot\text{OH}$ might contribute to the inactivation of pathogens (chapter 1.2.5).

1.2.3.2 Reaction with cell constituents

The chlorination of an *E. coli* suspension leads to the leakage of inner cell compounds (e.g., proteins). Therefore, it was concluded that FAC mainly inactivates bacterial cells by changing the membrane's permeability (Venkobachar et al., 1977). Since FAC shows only a low reactivity towards unsaturated fatty acids in the double lipid layer (Deborde and von Gunten, 2008; Pattison et al., 2003), the main target structures probably are in the membrane proteins. Therefore, the reaction of FAC with proteins and with amino acids, as their building blocks, have been widely studied (Hawkins and Davies, 1998a; Hazell and Stocker, 1993; How et al., 2017; Hureiki et al., 1994; Na and Olson, 2007; Pattison et al., 2007; Tan et al., 1987b; Winterbourn, 1985). The

reactions of FAC with proteins showed irreversible denaturation, fragmentation, and amino acid cross-linking (Vissers and Winterbourn, 1991). The latter can be developed either by forming covalent bonds between sulfur and nitrogen of thiol and lysine, respectively (Fu et al., 2002), or by the oxidation of tyrosine, which leads to the formation of tyrosine phenoxyl radicals, which eventually form bityrosines (Vissers and Winterbourn, 1991).

In general, the primary amines of the free amino acids react very fast with FAC (Deborde and von Gunten, 2008) and lead to chlorination of the primary amine (How et al., 2017; Tan et al., 1987a); however, in the peptide bond, the nitrogen atoms are present as amides, largely hampering an oxidative attack at the nitrogen (Jensen et al., 1999). Thus, it is more likely that the reaction of FAC occurs at other functional groups of the amino acid side groups, such as phenolic groups, sulfides, primary amines, and olefins. A case in point is cysteine which contains a highly reactive thiol group that even reacts faster than the free amino group with FAC. Indeed, the degradation of the amino group could only be observed after the sulfhydryl group was fully degraded (Arnhold et al., 1991). Moreover, primary amines also exist in peptides as side groups of incorporated amino acids that also could react with FAC (lysine). In fact, amino acids with amine-containing amino groups are in excess over sulfur-containing amino acids (Ulmschneider and Sansom, 2001; Winterbourn, 1985). Therefore, it can be assumed that these functional groups are the main reaction partners of FAC in protein reactions.

It was experimentally proven that chloramines are formed during the reaction of FAC with proteins (Hawkins and Davies, 1998b; Hazell and Stocker, 1993; Vissers and Winterbourn, 1991). During the reaction of FAC with protein amino groups, approximately 20 – 30 % of the added FAC is converted to chloramines (Hawkins and Davies, 1999). These protein-derived chloramines can decompose to form nitrogen-centered radicals with diverse follow-up reactions such as inter- and intra-molecular hydrogen atom abstraction and protein fragmentation (Hawkins and Davies, 1998b) and are thus, substantially transformed (see Figure 5). Hence, the reaction of FAC with amines to chloramines can effectively inactivate pathogens. However, contradictory to the mechanism reported by Hawkins et al., protonated amines are less reactive compared to the corresponding neutral species (Abdighahroudi et al., 2022). Therefore, the neutral amines are the main reaction partners with FAC.

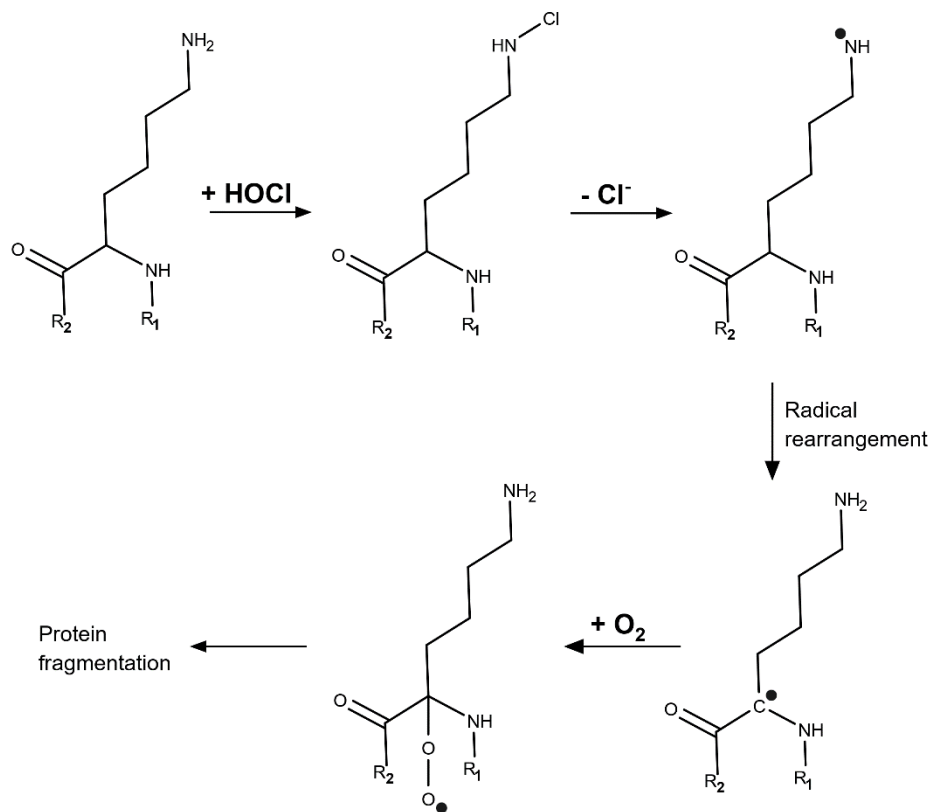


Figure 5: Reaction of FAC with the primary amine of lysine side chains leads to the formation of N -centered radicals and causes protein fragmentation. Pathway adapted from (Hawkins and Davies, 1998a).

It has been shown that low-dosed FAC concentrations significantly increased the conjugation frequency (Guo et al., 2015). As mentioned before, the application of FAC increases the permeability of bacteria by forming more potential pili or pores on the surface (Guo et al., 2015). This causes an easier donation and acceptance of ARG during conjugation. Additionally, the inactivation of ARB by FAC is causing the release of their ARGs, which can be easier incorporated by bacteria that are only partly damaged during FAC treatment. This overall causes the enrichment of ARGs in bacteria after FAC treatment (Jin et al., 2020). Thus it can be concluded that FAC disinfection can promote HGT by conjugation (Guo et al., 2015; Jin et al., 2020).

1.2.3.3 Reaction with genetic material

Recent studies provided evidence that FAC not only causes protein damage but also damages the genetic material of bacteria. A two-step reaction model has been postulated for the reaction of amplicons with FAC, whereby the reversible N -chlorination of nucleotide bases is the first step. The N -chlorination is causing a disruption of the H -bonding with the pairing base. These bases are further reacting with FAC causing irreversible C -chlorination (Choi et al., 2021; He et al., 2019).

It was shown that the kinetic of the irreversible C-chlorination is accelerated by higher FAC exposures and by a higher abundance of nucleotide bases (Choi et al., 2021). In general, the reaction of FAC with amplicons is also reported to be pH-dependent (Choi et al., 2021; Yoon et al., 2021), which can be explained by the speciation of FAC (HOCl/OCl^- $\text{p}K_a = 7.54$ (Deborde and von Gunten, 2008)).

For *E. coli*, inner protein damage (Cho et al., 2010) and a correlation between DNA fragmentation and FAC exposure (Suquet et al., 2010) were reported. The reaction rate of FAC with free DNA that is not associated with bacterial cells ranges from 3.9 to $9.2 \times 10^3 \text{ M}^{-1} \text{ s}^{-1}$ at pH 7 (He et al., 2019), which indicates that the reaction is fast enough to degrade genetic material at typical conditions of water treatment. Additionally, the inactivation of extracted DNA from bacteriophages is enhanced with increasing chloride (Cl^-) concentrations (Szczyka et al., 2022), which might be related to elevated intracellular deactivation of the genetic material. As mentioned above, the formation of $\cdot\text{OH}$ during FAC-based reaction was postulated recently (Rodríguez and von Gunten, 2020). Indeed, Yoon et al. showed that the degradation of DNA segments could be significantly hampered in the presence of *t*-BuOH, which is a selective scavenger for $\cdot\text{OH}$ (Yoon et al., 2021). Additionally, the absence of *t*-BuOH caused a conformational change from the supercoiled to the linear form and later also caused fragmentation. In the presence of *t*-BuOH, none of these conformational changes were observed (Yoon et al., 2021). The formation of $\cdot\text{OH}$ as a secondary oxidant of FAC seems, therefore, very likely.

The deactivation of intracellular genetic material such as intracellular ARGs is much slower compared to the inactivation of the bacteria itself; thus, ARGs can still be intact while the bacteria itself is inactivated (He et al., 2019). This observation is explainable by the fact that FAC and its secondary oxidants are much stronger scavenged by constituents of the cytoplasmic matter than the wastewater or drinking water matrix (e.g., by envelope lipids and proteins), which largely hampers ARG deactivation by FAC.

By reviewing the literature about the application of FAC for disinfection, Dodd (2012) concluded that the deactivation of ARGs might be possible; however, the required concentration and contact time (exposure) would be above the upper limit of the drinking water regulations (Dodd, 2012; Suquet et al., 2010). This is in accordance with more recent results, which showed that the required FAC concentration for ARG deactivation and suppression of ARG transfer is significantly higher

than that of ARB inactivation (Guo et al., 2015; Jin et al., 2020). This fact can become problematic since FAC is known to form harmful DBPs (Rook, 1976). The toxicity of these DBPs is known (Pan et al., 2014; Wang et al., 2007); therefore, these compounds are regulated in drinking water. Thus, the formation of harmful DBPs may indeed limit the application of FAC for ARGs deactivation.

1.2.4 Chlorine dioxide

ClO_2 is used as an alternative for FAC during waste(water) treatment processes to avoid the formation of the harmful halogenated DBPs formed during the application of FAC in water treatment (Zhang et al., 2000). Compared with FAC, ClO_2 is a stronger disinfectant that does not dissociate and, therefore, shows higher efficiency in a broader pH range (Junli et al., 1997). ClO_2 reacts very fast with electron-rich functional groups, such as activated aromatic systems (Huber et al., 2005) with activated double bonds (Hoigné and Bader, 1994) and activated neutral amines in the order tertiary > secondary > primary amines (Figure 4) (Rosenblatt et al., 1967). However, as mentioned earlier, the reactivity with dissociating functional groups is pH-dependending. For example, ClO_2 reacts only very slowly with protonated amines (Abdighahroudi et al., 2022; Wang et al., 2010).

1.2.4.1 Reaction with the matrix constituents

In the water matrix, ClO_2 undergoes reactions with all the mentioned functional groups of the NOM of the water matrix. This is the main driver of ClO_2 depletion in the water matrix, which is rather slow due to the high selectivity of ClO_2 . Hence, ClO_2 can also be applied in waters with high organic matter contents (Lee and von Gunten, 2010).

Apart from direct reactions of ClO_2 , the disinfection may also be controlled by several secondary oxidants (Table 5). ClO_2 forms FAC in the reaction with phenol and phenolic compounds (Hupperich et al., 2020; Rougé et al., 2018; Terhalle et al., 2018). Therefore, the reaction of ClO_2 with functional phenolic and olefinic moieties of NOM is responsible for FAC formation during water treatment (Hupperich et al., 2020). The yields of FAC by using, e.g., Suwannee River natural organic matter (SRNOM) vary between 22 and 25 % per consumed ClO_2 (Hupperich et al., 2020; Rougé et al., 2018). This shows that ClO_2 -based disinfection can include a considerable amount of FAC as a secondary oxidant and the secondary oxidants formed by FAC, as described above. FAC formation also leads to the formation of chlorine-derived DBPs. However, it seems that the formed

yield of FAC is not high enough to form the known undesired DBPs from FAC disinfection since no or only low concentrations of DBPs are observed during ClO₂ treatment (Al-Otoum et al., 2016) compared to chlorination (Zhang et al., 2000). For example, the addition of 4.5 mg L⁻¹ FAC to 3 mg L⁻¹ DOC (Suwannee River fulvic acid (SRFA)), buffered at pH 7.4, leads to the formation of 211 µg L⁻¹ chloroform after five days of reaction time, while 6 mg L⁻¹ ClO₂ lead to only 0.36 µg L⁻¹ chloroform under the same experimental conditions (Zhang et al., 2000). One has to take into account that due to the low concentrations of intrinsically formed FAC, FAC may be consumed immediately by the water matrix; however, the behavior of intrinsically formed FAC in different water matrices is yet not investigated. It is conceivable that the reaction of ClO₂ with the organic matter can be considered pre-oxidation, which hampers the formation of DBPs during the reaction of intrinsic formed FAC with DOC. This is in analogy to ozonation since ozonation also results in a lower DBPs formation potential of FAC in a subsequent chlorination step (Hua and Reckhow, 2013).

1.2.4.2 Reaction with cell constituents

Although the bactericidal effect of ClO₂ has been known since the first half of the 20th century (Ridenour and Ingols, 1947), the inactivation mechanism of ClO₂ is not fully revealed. The efficiency of the inactivation of *E. coli* by ClO₂ depends on the disinfection dose, pH (faster in alkaline media), and temperature. Whereby the latter had the smallest impact (Ofori et al., 2017). The application of ClO₂ to *E. coli* leads to an inhibition of different enzymes (e.g., dehydrogenase (Roller et al., 1980), β-D-galactosidase (Ofori et al., 2017)) already after a very short reaction time, while the cells remain viable. Furthermore, ClO₂ partially inhibits the protein synthesis of *E. coli*, which is proportional to the dose of ClO₂ (Roller et al., 1980). The inactivation of *E. coli* correlates with the protein release into the bulk solution, which indicates that ClO₂ is also damaging the cell membrane. Furthermore, using transmission electron microscopy (TEM) and a polyacrylamide gel electrophoresis protein assay after 1-log inactivation, evidence was provided that ClO₂ causes damage to cell surface proteins and the cytoplasm (Cho et al., 2010). Based on the current state of knowledge, it can be stated that the inactivation step which is causing the lethal event is the damage of the cell membrane followed by leakage of cytoplasmic material. Since ClO₂ is unreactive towards double bonds similar to FAC (Abdighahroudi et al., 2021; Deborde and von Gunten, 2008), which are present in the membrane lipid double layer, the observed membrane damage may also be caused by the reaction with membrane proteins. Some amino acids show a significant reactivity

toward ClO₂ (Jütte et al., 2022), and their transformation might be responsible for the primary inactivation step during ClO₂ disinfection. Although cysteine shows the highest reaction rate among the amino acids towards ClO₂ (Ison et al., 2006), a significant decrease in tyrosine and tryptophan residues was observed in proteins after ClO₂ treatment, whereby most other amino acids did not degrade significantly (Ogata, 2007). Therefore, it can be concluded that these residues are the main target for ClO₂-based oxidation. For the proteins albumin and glucose-6-phosphate dehydrogenase of *Saccharomyces cerevisiae*, loss of enzymatic activity, decrease in α -helix content, and protein denaturation has been reported (Ogata, 2007). Similar results are reported for lysozyme (Ooi and Branning, 2017). However, until today only a few studies investigated the behavior of bacterial cell proteins during ClO₂ treatment.

If the reaction of amino acids with ClO₂ is considered the primary inactivation step, this reaction may lead to the formation of FAC, which might contribute to the inactivation mechanism. Indeed, possible pathways are postulated, stating the formation of FAC in the reaction of ClO₂ with cysteine, tyrosine, and tryptophan (Ison et al., 2006; Napolitano et al., 2005; Stewart et al., 2008) which has been confirmed recently for tyrosine and tryptophan (50 % of [ClO₂]) (Jütte et al., 2022). (Note that these amino acids belong to the most reactive towards ClO₂ (Noss et al., 1986; Sharma and Sohn, 2012)). Hence, it can be assumed that FAC is formed inside bacterial cells and may thus, enhance the disinfection effect of ClO₂.

1.2.4.3 Reaction with genetic material

The reactivity of ClO₂ towards genetic material has been barely studied yet. Even less is known about the DNA alterations caused by ClO₂. Recently it has been reported that ClO₂ causes changes in the conformation and structure of DNA (Zhao et al., 2022). When ClO₂ was applied to *Haemophilus influenza* cells, the DNA transforming activity was not affected, even after 6-log inactivation, which indicates that intracellular bacterial DNA seems inert toward ClO₂ (Roller et al., 1980). In general, the reaction rate of bacterial ARGs towards ClO₂ is very slow (k_{app} ranging from $0.35 - 1.2 \times 10^1 \text{ M}^{-1} \text{ s}^{-1}$ at pH 7 (He et al., 2019)). However, even though the reaction of other constituents would outcompete the reaction of ClO₂ towards ARGs, a very slight deactivation of intracellular ARGs was observed after ClO₂ addition to a multidrug-resistant strain of *Bacillus subtilis* (He et al., 2019). ClO₂ itself cannot explain the observed deactivation of ARGs; indeed, ClO₂ is not the only present disinfectant, as mentioned before. Taking this into account, it becomes

clear that the disinfection by ClO_2 in real water matrices can include $\approx 25\%$ FAC disinfection (Hupperich et al., 2020), which can improve disinfection. Additionally, FAC might be formed in intracellular ClO_2 reactions and could be the reason for the observed slight ARG deactivation. Although the formation of FAC with specific reaction partners has been demonstrated (Jütte et al., 2022), the intrinsic formation and the corresponding participation of FAC in ClO_2 -based disinfection processes (e.g., ARG deactivation) has not been reported yet.

The formation of all possible secondary oxidants formed in the application of ClO_2 is summarized in Figure 6. To this end, it can be assumed that ClO_2 inactivates bacteria by reacting with membrane proteins and cytoplasmic proteins. In these reactions, secondary oxidants such as FAC can also be formed, which cause further cell damage (eventually including gene damage). Besides FAC, the other main transformation product is ClO_2^- (Abdighahroudi et al., 2021), a cytotoxic compound (Van Wijk et al., 1998), which could also be formed in the cytoplasm and participate in cell inactivation. However, reactions of ClO_2^- with organic compounds are barely investigated yet. Furthermore, ClO_2^- is regulated by drinking water guidelines (recommended threshold concentration by WHO of 0.7 mg L^{-1} (*Guidelines for Drinking-water Quality*, 2011)), which means that the formation of ClO_2^- limits the application of ClO_2 . Possible countermeasures are the reduction of ClO_2^- by ferrous salts (Fe^{2+}) or by sulfur-dioxide-sulfite ion (Gordon et al., 1990; Katz and Narkis, 2001).

1.2.5 Ozone

The application of O_3 in (waste)water treatment can be used for the removal of micropollutants (Lee and von Gunten, 2012), abatement of taste and odor compounds (Glaze et al., 1990), and disinfection purposes (Morrison et al., 2022; von Gunten, 2003a). O_3 has been used for water disinfection since the beginning of the last century and has gained increasing interest after discovering that the application of chlorination may result in the formation of undesired taste and odor compounds and harmful DBPs (Rook, 1974). The reaction mechanisms and the application of O_3 for water and wastewater treatment have been reviewed frequently over the last decades (Glaze et al., 1987; Lawrence and Cappelli, 1977; von Gunten, 2018, 2003b, 2003a; von Sonntag and von Gunten, 2012).

1.2.5.1 Reaction with the water matrix constituents

O₃ is more reactive than the oxidants discussed above, which means it undergoes a fast reaction with the water matrix compounds (e.g., NOM) and is, therefore, less stable and less selective (Lee and von Gunten, 2010). The O₃ demand necessary for disinfection is much higher than the demand for micropollutant degradation. In fact, 10⁸ molecules of O₃ are necessary for the inactivation of one bacterial cell (von Sonntag and von Gunten, 2012).

O₃ reacts with matrix constituents in various ways, forming several secondary oxidants, which can contribute to the inactivation of pathogens. Thereby, the most important secondary oxidants are FAB (Haag and Holgné, 1983) and [•]OH (von Sonntag and von Gunten, 2012), which are formed in the presence of Br⁻ (Haag and Holgné, 1983) ($k(\text{O}_3 + \text{Br}^- \rightarrow \text{OBr}^- + \text{O}_2) = 1.6 \times 10^2 \text{ M}^{-1} \text{ s}^{-1}$) (Neta et al., 1988) and organic matter, respectively. Experiments in artificial seawater with high Cl⁻ and Br⁻ concentrations showed that O₃ is depleted within a few seconds, and FAB is formed, which is fairly stable (Jung et al., 2017). Thereby the reaction of O₃ with Br⁻ outcompetes the slow reaction of O₃ with Cl⁻. For the removal of *Artemia salina* during seawater ozonation, the degree of inactivation by O₃ and FAB has been determined to be 51.9 and 6.8 %, respectively (Jung et al., 2017). Thus, it can be assumed that FAB is indeed playing a role during O₃-based disinfection. The formation of FAC in the presence of Cl⁻ is less relevant under typical conditions of water treatment since the reaction of O₃ and hydroxyl radicals with Cl⁻ is very slow ($k(\text{O}_3 + \text{Cl}^-) \approx 10^{-3} \text{ M}^{-1} \text{ s}^{-1}$ at pH 7, $k(\text{OH}^\bullet + \text{Cl}^-) = 10^3 \text{ M}^{-1} \text{ s}^{-1}$ at pH 7 (Levanov et al., 2018; von Gunten, 2003a)) and will therefore be outcompeted by other reactions.

Another important secondary oxidant is the [•]OH, formed in O₃ reactions with organic matter. The yields of [•]OH depend on the molecular structure of NOM and vary between 15 and 70 % per consumed equivalent O₃ (von Sonntag and von Gunten, 2012). The reaction rate of [•]OH is very fast with many matrix components, and the exposure is therefore very small; thus, it seems reasonable that [•]OH is scavenged by matrix components. However, the reported literature is contradictory in this regard. For instance, the inactivation of *B. subtilis* was hampered in the presence of *t*-BuOH, a selective scavenger for [•]OH (Cho et al., 2003). On the other hand, the inactivation of *E. coli* in the presence or absence of a different scavenger, humic acid, is similar (Hunt and Mariñas, 1999). The reason for this observation might be that humic acid also initiates [•]OH formation during the reaction with O₃ and thus, enhances the inactivation of *E. coli* by [•]OH. Secondary oxidants are generally

formed in drinking and wastewater treatment in the bulk solution. Their effect on disinfection is often hard to assess since different matrix constituents scavenge these secondary oxidants. $\cdot\text{OH}$ is a very unselective oxidant, which mostly reacts with diffusion-controlled kinetics resulting in average lifetimes of a few μs (Buxton et al., 1988). This results in a very low steady-state concentration of $\cdot\text{OH}$ (pM range) and thus, in rather low disinfection strength compared to the primary disinfectant and hardly contributes to the inactivation of the bacterial cells (Hao et al., 2012). It is reported that intracellular ARG deactivation does not change significantly if extracellular produced $\cdot\text{OH}$ are scavenged or not (Choi et al., 2021).

1.2.5.2 Reaction with cell constituents

Compared to ClO_2 and FAC, O_3 is way less selective (Lee and von Gunten, 2010) and therefore has more possible target structures for cell inactivation. The O_3 attack on bacterial cells has been observed in the cytoplasmic material (Hunt and Mariñas, 1999; Ishizaki et al., 1987; von Sonntag and von Gunten, 2012) and the cell wall or membrane (Cho et al., 2010; Christensen and Giese, 1954; Girgin Ersoy et al., 2019; McNair Scott and Lesher, 1963). Thereby, O_3 undergoes reactions with the double bonds present in the cell membrane (Pryor et al., 1991), which increases the cell membrane's permeability and leakage of inner cell compounds (McNair Scott and Lesher, 1963). Additionally, O_3 reacts with different amino acids present in (membrane)proteins (Sharma and Graham, 2010). In the case of amino acids, it is again important to mention that O_3 does not react with the peptide bond itself (Cataldo, 2006; Pryor et al., 1984), so only the side chains are available for an O_3 attack. The oxidation of amino acid side groups by O_3 results in a change in the folding and binding ability of the peptide chain (Cataldo, 2006), which may result in a loss of protein functionality. The denaturation and thus the loss of the biological activity of proteins after ozonation has been reported before (Cataldo, 2006; Zhang et al., 2015).

The formation of secondary oxidants may also be important in intracellular reactions with O_3 (von Sonntag and von Gunten, 2012). This could lead to the intracellular generation of FAB in the presence of Br^- , peroxy radicals, and $\cdot\text{OH}$. If FAB is formed, it will react with other inner cell compounds (e.g., amino acids) (Heeb et al., 2014; Pattison and Davies, 2004) and might thus, increase the inactivation rate of bacteria. Even though the reaction of O_3 with Cl^- to form FAC is very slow, it might be important in the endoplasmaticum since Cl^- can be present in very high concentrations compared to other cell constituents ($c(\text{Cl}^- \text{ in } E. coli) = 207 \pm 41 \text{ mM}$ (Szatmári et

al., 2020)). It is experimentally proven that BrO_3^- formation during ozonation is accelerated if high concentrations of Cl^- are present (Grguric et al., 1994). If FAC is formed, it can either directly react with vital cell compartments or with Br^- to form FAB ($k(\text{HOCl} + \text{Br}^- \rightarrow \text{HOBr} + \text{Cl}^-) = 6.84 \times 10^3 \text{ M}^{-1} \text{ s}^{-1}$ at pH 7 (Deborde and von Gunten, 2008; Heeb et al., 2014)), which eventually forms toxic BrO_3^- (Fischbacher et al., 2015). Therefore, it can be concluded that the high Cl^- concentrations indeed accelerate the inactivation of bacterial cells during O_3 -based disinfection.

Furthermore, the reaction of O_3 with cytoplasmic constituents may also yield $\cdot\text{OH}$ as a secondary oxidant (Nöthe et al., 2009; von Sonntag and von Gunten, 2012). The mechanistic pathways and kinetics are already well described (von Sonntag and von Gunten, 2012). The formation of intracellular $\cdot\text{OH}$ seems very likely to accelerate the inactivation of bacterial cells by fast reaction with a broad range of functional groups (Figure 4), thus, damaging inner cell compounds.

1.2.5.3 Reaction with genetic material

The main site of the O_3 attack was already concluded in the 1950s to be the cell surface, even though the reaction between O_3 and DNA-containing compounds was also observable (Christensen and Giese, 1954). By now, many studies have proven that O_3 -based treatment of bacteria leads to a decomposition of the cell membrane (Cho et al., 2010; Girgin Ersoy et al., 2019; Mcnair Scott and Leshner, 1963). O_3 also may diffuse into bacterial cells, and the average travel distance can be estimated by the mean kinetics and the average travel distance of $\cdot\text{OH}$, which is 6 – 9 nm (von Gunten, 2003a). The reactivity of O_3 is four orders of magnitude slower compared to $\cdot\text{OH}$ on average; therefore, it can be estimated that the average travel distance of O_3 is around four orders of magnitude longer inside the cell. This means O_3 has an estimated average travel distance of 60 – 90 μm . Considering about 2 μm length of an *E. coli* cell, O_3 could indeed reach genetic material and react with the nucleotides, which eventually results in the inactivation of vital genes and, thus, cell death. The reactivity of $\cdot\text{OH}$ with ARGs was reported to be very fast ($k = 0.59 - 2.3 \times 10^{11} \text{ M}^{-1} \text{ s}^{-1}$ (He et al., 2019)). Additionally, the reaction of O_3 with other cell constituents may also form the abovementioned secondary oxidants, contributing to the inactivation of genetic material. Finally, the reaction of O_3 with the genetic material itself results in the formation of $\cdot\text{OH}$ (von Sonntag, 2006). In this case, $\cdot\text{OH}$ are formed close to the genetic material, which largely facilitates their reaction with the genetic material since the traveling distance of hydroxyl radicals in bacterial cells is estimated to be 6 – 9 nm (von Gunten, 2003a). It is worth mentioning that $\cdot\text{OH}$ attack at

DNA/RNA is extremely effective in gene inactivation due to string breaking, which inhibits transforming activity (von Sonntag, 2006). Evidence for the participation of $\cdot\text{OH}$ during O_3 -based reaction with DNA has been reported recently (Yoon et al., 2021). O_3 treatment of supercoiled DNA has been reported to cause single-strand cleavage of circular DNA, resulting in a supercoiled structure alteration (Sawadaishi et al., 1985). However, this observation did not occur in the presence of *t*-BuOH (Yoon et al., 2021), indicating that $\cdot\text{OH}$ are responsible for the change in the supercoiled structure. Additionally, the reaction rate constant of O_3 with ARGs was lower in the presence of a selective $\cdot\text{OH}$ scavenger (Choi et al., 2021). These findings show that $\cdot\text{OH}$ might play a role in intracellular ARGs deactivation if it is intrinsically formed. It has to be considered that the genetic material is also protected by intracellular structures, e.g., the cell membrane or other cell components, which can hamper a direct reaction with oxidants. For instance, even after 5 log inactivation of *E. coli* by O_3 , the intracellular ARGs stay intact (Czekalski et al., 2016). An increase in the dosage of O_3 would cause several adverse effects, such as the formation of carcinogenic BrO_3^- (Fischbacher et al., 2015; von Gunten, 2003a) or *N*-Nitrosodimethylamine (NDMA) (Andrzejewski et al., 2008). Additionally, $\cdot\text{OH}$ revealed another drawback in ARGs deactivation monitoring. The reaction of $\cdot\text{OH}$ with DNA mainly leads to strand fragmentation by cleavage of the phosphate backbone (He et al., 2019). By shortening the strand, the ARG transformation activity is lowered; however, it might be possible that the region of the monitored ARG amplicons stays intact, which gives a biased result of faster ARG deactivation than amplicon degradation (He et al., 2019).

All secondary oxidants which are known to be formed in O_3 reactions are shown in Figure 6 as well. It becomes clear that the synergy of all secondary oxidants together with O_3 as the primary oxidant is eventually responsible for bacterial inactivation.

1.2.6 Defense response

Especially aerobic bacteria are continuously exposed to oxidative stress by reactive oxygen species (ROS) such as H_2O_2 or $\text{O}_2^{\cdot-}$ (Forman et al., 2009). To encounter ROS exposure, bacterial cells have developed a defense mechanism in the form of antioxidants such as glutathione (GSH). It was shown that the production of this tripeptide (cysteine, glutamic acid, and glycine) is induced by oxidative stress in *E. coli* and *S. cerevisiae* (Carmel-Harel and Storz, 2000). The intracellular concentration of GSH in glucose-fed, exponentially growing *E. coli* was detected to be 17 mM,

which makes it the second most abundant metabolite after glutamate (96 mM) (Bennett et al., 2009). Thus, GSH is in excess over the reactive amino acids (e.g., methionine 0.15 mM, tyrosine 0.029 mM (Bennett et al., 2009)) and, therefore, scavenges most of the oxidants and hamper the bacterial inactivation.

Table 6 summarizes the known reaction constants of GSH for the different primary and secondary oxidants that might be relevant during chemical water disinfection.

Table 6: Summary of the known reaction rates of GSH towards different oxidative species

| Oxidant | pH | $k / M^{-1} s^{-1}$ | Reference |
|-------------------------|-----------|----------------------|------------------------------------|
| O₃ | 7 | 3.9×10^6 | (von Sonntag and von Gunten, 2012) |
| FAB* | 7 | $\sim 10^7$ | (Heeb et al., 2014) |
| NH₂Br | 7.2 | $> 10^5$ | (Heeb et al., 2014) |
| FAC | 5, 7.4, 9 | $\geq 10^7$ | (Deborde and von Gunten, 2008) |
| | 7.4 | 1.2×10^8 | (Storkey et al., 2014) |
| NH₂Cl | 7.4 | 1.2×10^2 | (Peskin and Winterbourn, 2001) |
| ClO₂ | 7 | 2.5×10^6 | (Ison et al., 2006) |
| ·OH | 5.5 | 1.3×10^{10} | (Buxton et al., 1988) |

***The reaction rate of FAB + cysteine is shown.**

The reaction rate of FAB has not been determined yet. However, it can be estimated from the reaction rate with cysteine (k (HOBr + cysteine) = $1.7 \times 10^7 M^{-1} s^{-1}$ at pH 7.2 – 7.5) (Heeb et al., 2014) since cysteine is the most reactive moiety in this tripeptide. In the case of O₃ and FAC, the reaction rate with cysteine (k (O₃ + cysteine) = $4.2 \times 10^4 M^{-1} s^{-1}$ at pH 7) (Pryor et al., 1984) and k (HOCl + cysteine) = $6.7 \times 10^7 M^{-1} s^{-1}$ at pH 7 (Deborde and von Gunten, 2008)) is slower or in the same order of magnitude as the reported reaction rate for GSH (see Table 6). Therefore, it can be assumed that the reaction rate of FAB with GSH is in the same order of magnitude or faster than the reaction rate of FAB and cysteine. This shows that all primary and secondary oxidants are highly reactive toward GSH and at concentrations in the mM range GSH is probably capable of

effectively scavenging most of the disinfectants and their secondary reactive species. This may be one of the reasons why disinfectants are typically added in large surplus over potential pathogens (von Sonntag and von Gunten, 2012).

Besides the production of scavengers, repair mechanisms have been observed, especially for DNA damage. Thereby, transforming activity elimination depends on the type of DNA repair genes (Nihemaiti et al., 2020). The influence of repair mechanisms becomes clear by comparing the gene degradation and the loss of transforming activity. Loss of transforming activity is reported to be significantly slower than the overall degradation rate of the plasmid with the same oxidant (Nihemaiti et al., 2020; Yoon et al., 2021).

The combination of the repair mechanism and production of chemical scavengers may be responsible for the extremely high number of collisions between bacteria and oxidants (10^8 in the case of O_3 (von Sonntag and von Gunten, 2012)) until a lethal event happens and the lag phase is observed. This number of collisions may be similar or even higher in the case of FAC, ClO_2 , and chloramines since their inactivation kinetics is similar or slower. The stress response is surely way more complex in bacterial consortia (biofilms), which are hardly investigated.

1.2.7 Additional *in vivo* effects

One must consider that the above-mentioned reaction rates do not necessarily apply to amino acids associated with peptides or proteins. By investigating the influence of other amino acids in oligopeptides and proteins on the reactivity of tryptophan towards ClO_2 , it was observed that several further factors influence the reactivity under real conditions (Ge et al., 2020). For instance, the position of the amino acid in the peptide, the accessibility, the protein folding, and the surrounding amino acid moieties influence the reaction rate. The attached amino acids may lead to a shift of the pK_a of the reactive moieties, which has a strong influence on the apparent second-order reaction rate, especially at pH 7. Additionally, the electron density is changed, and therefore an electrophilic attack is either accelerated or hampered. Furthermore, the accessibility of the reactive moiety in the polypeptide has a strong influence on the reaction rate (Ge et al., 2020).

Other important factors for ARG deactivation might be the accessibility of the ARG on the genome, the supercoiling of the DNA helix strand, and the type of DNA. For instance, it has been shown for extracellular DNA that the deactivation efficiency of genomic DNA is higher than plasmid DNA (Zhang et al., 2019). In Contradictory, two other studies determined similar reactivity of

plasmid-borne and chromosomal DNA toward O₃ (He et al., 2019; Yoon et al., 2021). Thus, it seems very reasonable that all observed *in vivo* effects are also oxidant-dependent. Additionally, it has been shown that double-stranded DNA is less reactive than single-stranded DNA toward FAC (Szczuka et al., 2022). The deactivation efficiency also depends on the length of the gene since longer amplicons have higher reactivity due to more possible points of attack (Choi et al., 2021; He et al., 2019; Yoon et al., 2021).

1.2.8 Conclusion and further research suggestions

Based on the current knowledge, it can be concluded that all oxidants applied in water treatment also form a different set of secondary oxidants in their reaction with the water matrix and their reaction with bacterial cells (see Figure 6).

All the primary and secondary oxidants might more or less contribute to the inactivation mechanism of cells of different bacterial species. Although the formation of secondary oxidants is known, little is known about their influence on the overall disinfection mechanism. Therefore, it is impossible to estimate the full inactivation mechanism of the primary oxidant at this point. Further research is necessary about the inactivation in the absence or presence of different scavengers to scavenge secondary oxidants. As discussed above, the participation of [•]OH during O₃ disinfection processes has been shown recently. The same procedure can be carried out for ClO₂ by using, e.g., methionine to scavenge intrinsically formed FAC. The participation of FAC in ClO₂-based disinfection processes is a very interesting research field. However, besides the possible formation of FAC during the reaction with NOM or specific amino acids (see above) no data is available so far.

It is crucial to further normalize the available data in the literature regarding the inactivation kinetics of different oxidants on a molar scale. This review summarized the available data for the inactivation of bacteria with the oxidants O₃, ClO₂, and FAC in water. In the literature also, the molar inactivation rate constants for the inactivation of viruses with O₃ are available (Morrison et al., 2022). As shown above, the inactivation rate constants can vary strongly regarding species, strain, or oxidant. It would be of great advantage to increase the available data on the inactivation rates in the molar scale, which allows the comparison between different oxidants and also will help to improve the understanding of disinfection mechanisms. Furthermore, it allows to predict

disinfection of pathogens based on oxidant exposures and thus may help to improve water disinfection processes (e.g., by more precise oxidant dosage).

Furthermore, it would be very useful to investigate the exact reaction mechanism of the different oxidants toward DNA. The reaction mechanism for FAC with different amplicons has been described in detail. However, the available data for other oxidants is still lacking. Therefore, additional data would be of great use for understanding which oxidant (primary or secondary) is responsible for which part of the degradation or deactivation of the genome.

It is necessary to investigate further which secondary oxidants are formed in which reactions and determine the yields, for instance, the formation of FAC during the reaction of ClO₂ with different functional groups of amino acids. This might be done by comparing the inactivation of mutated strains of the same bacteria. The mutations should be in a way that the results reveal insights into the intrinsic formation and participation of secondary oxidants (e.g., lack of specific defense proteins). Furthermore, as discussed in this review, secondary oxidants can form further oxidants, which can be named tertiary oxidants. This chain of different reactive species gives a very complicated system but also opens a great field of research. Further *in vivo* effects should be investigated as well. For instance, the supercoiling/ folding extends influence on ARGs deactivation by different oxidants or the ARGs accessibility towards chemical inactivation regarding the location on the genome.

Only if the inactivation mechanisms are fully revealed and understood can the oxidant applications be optimized to achieve an efficient deactivation of ARGs.

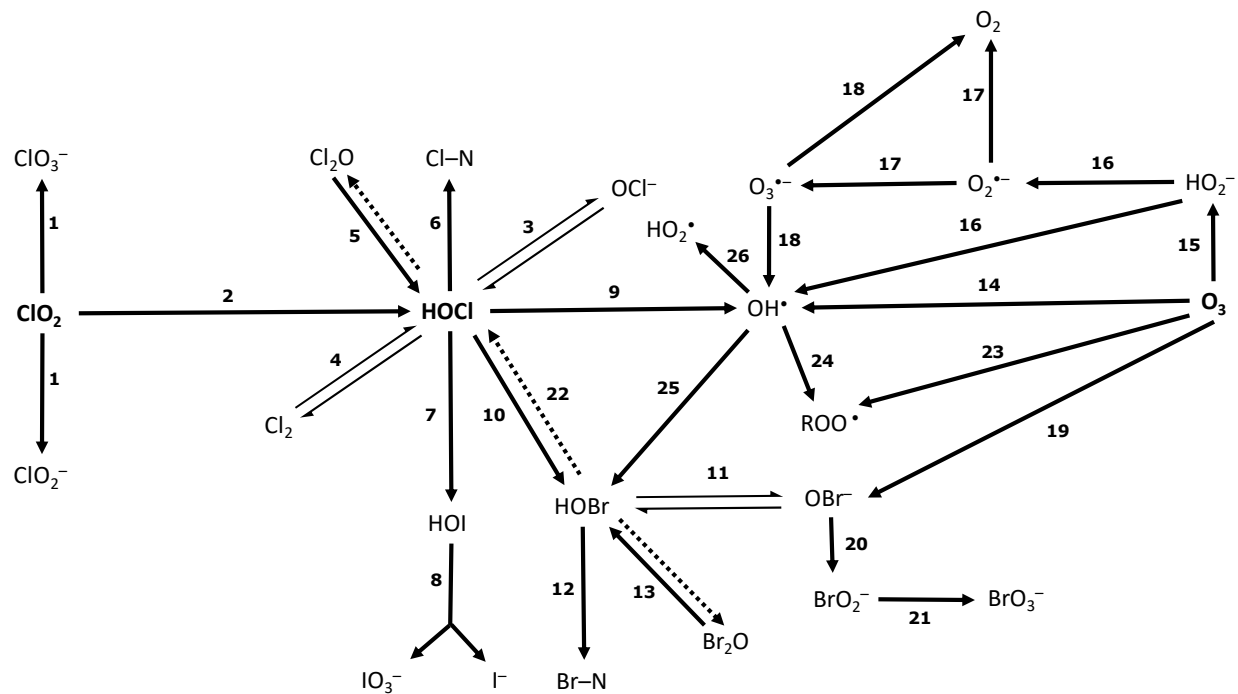


Figure 6: Overview of all possible secondary oxidants formed during FAC, ClO_2 , and O_3 disinfection. Explanation of reactions: **1.** The reaction of ClO_2 leads to the formation of inorganic DBPs (Abdighahroudi et al., 2021; Hupperich et al., 2020), whereby ClO_2^- and ClO_3^- can be considered as weak secondary oxidants. **2.** The reaction of ClO_2 with (e.g., phenolic compounds) leads to the formation of FAC in form of HOCl (Hupperich et al., 2020; Jütte et al., 2022; Rougé et al., 2018; Terhalle et al., 2018). **3.** HOCl dissociates to OCl^- ($\text{pK}_a = 7.54$), which is nearly unreactive (Deborde and von Gunten, 2008). **4.** $\text{Cl}_2 + \text{H}_2\text{O} \rightleftharpoons \text{HOCl} + \text{H}^+ + \text{Cl}^-$. Cl_2 is only present at $\text{pH} < 4$, therefore not relevant for typical water treatment conditions (Deborde and von Gunten, 2008). **5.** $2 \text{HOCl} \rightleftharpoons \text{Cl}_2\text{O}$ Equilibrium is strongly on the reactant side ($K_{\text{Cl}_2\text{O}} = 8.7 \times 10^{-3}$) (Deborde and von Gunten, 2008). **6.** FAC reacts with (mostly primary) amines under the formation of chloramine (Deborde and von Gunten, 2008; Hawkins and Davies, 1998a; Hazell and Stocker, 1993; Vissers and Winterbourn, 1991). **7.** FAC reacts iodide ($k(\text{HOCl} + \text{I}^-) = 10^8 \text{ M}^{-1} \text{ s}^{-1}$ at $\text{pH} 7$) and forms HOI (Deborde and von Gunten, 2008). **8.** HOI further oxidizes or decomposes under the formation of IO_3^- and/or I^- (Li et al., 2020). **9.** Reaction of FAC with $\text{O}_2^{\cdot-}$ induced by the hydroquinone- HOCl reaction (Rodríguez and von Gunten, 2020). **10.** FAC reacts with Br^- ($k(\text{HOCl} + \text{Br}^-) = 10^3 \text{ M}^{-1} \text{ s}^{-1}$ at $\text{pH} 7$) and forms HOBr (Deborde and von Gunten, 2008). **11.** HOBr dissociates to OBr^- ($\text{pK}_a \approx 8.7$) (Heeb et al., 2014). **12.** HOBr reacts with amines and forms brominated amines (e.g. $k(\text{HOBr} + \text{NH}_3) \approx 10^5 \text{ M}^{-1} \text{ s}^{-1}$ at $\text{pH} 7$) (Heeb et al., 2014). **13.** $2 \text{HOBr} \leftrightarrow \text{Br}_2\text{O} + \text{H}_2\text{O}$ $K_{\text{Br}_2\text{O}} = 6.31 \text{ M}^{-1}$ (Heeb et al., 2014). **14.** Reaction of O_3 with a various number of functional groups forms $\cdot\text{OH}$ (e.g. phenolic moieties & amines) (Nöthe et al., 2009; von Gunten, 2003b; von Sonntag and von Gunten, 2012). **15.** $\text{O}_3 + \text{OH}^- \rightleftharpoons \text{HO}_2^- + \text{O}_2$ $k = 70 \text{ M}^{-1} \text{ s}^{-1}$ (Fischbacher et al., 2015) **16.** $\text{O}_3 + \text{HO}_2^- \rightleftharpoons \text{O}_2^{\cdot-} + \cdot\text{OH}$ $k = 5.5 \times 10^6 \text{ M}^{-1} \text{ s}^{-1}$ (Fischbacher et al., 2015; Neta et al., 1988) **17.** $\text{O}_3 + \text{O}_2^{\cdot-} \rightleftharpoons \text{O}_3^{\cdot-} + \text{O}_2$ $k = 10^9 \text{ M}^{-1} \text{ s}^{-1}$ (Fischbacher et al., 2015; Neta et al., 1988) **18.** $\text{O}_3^{\cdot-} + \text{H}_2\text{O} \rightleftharpoons \cdot\text{OH} + \text{O}_2 + \text{OH}^-$ (Fischbacher et al., 2015) **19.** $\text{O}_3 + \text{Br}^- \rightleftharpoons \text{OBr}^-$ $k = 10^2 \text{ M}^{-1} \text{ s}^{-1}$ (Neta et al., 1988) **20.** $\text{O}_3 + \text{OBr}^- \rightleftharpoons \text{BrO}_2^-$ $k = 10^2 \text{ M}^{-1} \text{ s}^{-1}$ (Neta et al., 1988) **21.** $\text{O}_3 + \text{BrO}_2^- \rightleftharpoons \text{BrO}_3^-$ $k > 10^5$ (Neta et al., 1988) **22.** $\text{HOBr} + \text{Cl}^- \rightleftharpoons \text{HOCl} + \text{Br}^-$ $k = 1.03 \times 10^{-2} \text{ M}^{-1} \text{ s}^{-1}$ (Based on $K = 1.5 \times 10^5$ & $k_{-1} = 1.55 \times 10^3 \text{ M}^{-1} \text{ s}^{-1}$) (Heeb et al., 2014) **23.** The reaction of O_3 with organic molecules leads to the formation of carbon-centered radicals. These radicals can react with O_2 to form peroxy radicals: $\text{R}^{\cdot} + \text{O}_2 \rightarrow \text{ROO}^{\cdot}$ $k = 2 \times 10^9 \text{ M}^{-1} \text{ s}^{-1}$ (von Sonntag and von Gunten, 2012). **24.** $\cdot\text{OH}$ can also form peroxy radicals in the presence of oxygen (von Sonntag and von Gunten, 2012). **25.** $\cdot\text{OH}$ reacts with Br^- at diffusion-controlled reaction rates ($10^{10} \text{ M}^{-1} \text{ s}^{-1}$) which forms reactive bromine species and eventually HOBr (Buxton et al., 1988). **26.** $\text{O}_3 + \cdot\text{OH} \rightarrow \text{HO}_2^{\cdot} + \text{O}_2$ $k = 10^8 \text{ M}^{-1} \text{ s}^{-1}$ (Neta et al., 1988)

Chapter 2

Research gaps and objective

2. Research gaps and objective

Former research has shown that FAC can be formed in ClO₂ reactions with phenols, amines, and NOM. However, no study has investigated the participation of intrinsically formed FAC in ClO₂-based disinfection mechanisms. To study this hypothesis and to get deeper insights into ClO₂ disinfection the following chapters were carried out.

Chapter 3.1: The first research chapter investigates the reaction of ClO₂ with specific amino acids regarding their reactivity and their potential to form FAC. Due to the different reactive moieties, amino acids most likely an important reaction partner of chemical oxidants. Examples are tyrosine (phenol-containing moiety) and tryptophan (indole-containing moiety). Thus, the primary reaction partner of ClO₂ might be these reactive amino acids. If FAC is formed in a reaction between an amino acid and ClO₂ the intrinsically formed FAC may cause further oxidative damage to the bacterial cell and thus, improve the inactivation process. Therefore, a detailed study of the reaction of ClO₂ with tyrosine and tryptophan is carried out in Chapter 3.1. This includes the determination of pH-dependent reaction kinetics of amino acids with ClO₂ and FAC, quantification of intrinsically formed FAC and other chlorine species, determination of stoichiometric ratios, and postulation of the corresponding reaction mechanisms.

Chapter 3.2: NOM is the major ingredient of natural water bodies, and the chemical structure of NOM consists of complex molecules, containing mainly phenolic moieties. During ClO₂ treatment of natural water sources, ClO₂ is mainly consumed by NOM, due to the reactivity of ClO₂ with phenols. This chapter deals with the reaction of ClO₂ with different phenolic compounds. The reaction of NOM with ClO₂ has been reported to form 25 % FAC. Therefore, this chapter tackles the question, ‘which phenols form intrinsically FAC, and which characteristics are hampering the FAC formation?’ Thus, major reaction mechanisms of *ortho*-, *meta*-, and *para*-substituted phenols containing different functional groups are investigated regarding the quantification of intrinsically formed FAC and other chlorine species and determination of stoichiometric ratios. Since the investigated phenols are potential moieties of NOM, proposed reaction mechanisms are intensively discussed in Chapter 3.2.

Chapter 3.3: For the quantification of intrinsic FAC in the reaction of ClO₂ with phenols or aromatic amines the so-called glycine method can be used. Thereby glycine is added as a selective scavenger for FAC. The key element is the low reactivity of FAC with the compound under study (e.g.,

phenol) compared to the reaction of FAC with glycine. Thus, glycine is a very suitable scavenger for investigating phenolic compounds due to the low reactivity with ClO_2 and the relatively high reactivity with FAC. Therefore, FAC will be scavenged by glycine, and the yield of formed chloroglycine (Cl-Gly) can be used for quantification of formed FAC. However, for investigating the reaction of compounds that react fast with FAC (e.g. thiol-containing molecules), the glycine method may not be applicable. A case in point is the reaction with the fast-reacting antioxidant GSH, which could not be investigated because FAC reacts many orders of magnitude faster with GSH than with glycine. The application of the glycine method would bias the results regarding reactivity and yields of FAC (i.e., the reaction of FAC with GSH would outcompete the reaction of FAC with glycine and form other chlorine species instead of Cl-Gly). Thus, another method needs to be developed to characterize the reaction of ClO_2 with compounds that react fast with FAC. In Chapter 3.3, it is attempted to develop a new scavenging method based on methionine as a selective scavenger. It has been shown that methionine reacts very slowly with ClO_2 and very fast with FAC. The method is tested with compounds of which the yield of inorganic chlorine species is known for method validation. Then the formation of FAC in the reaction of ClO_2 with GSH is studied using the methionine method. The formation of FAC in the reaction of ClO_2 with GSH might be of great interest. GSH is an antioxidant produced during bacterial defense mechanisms. If this reaction forms FAC, another disinfecting species is formed, which can cause further damage.

Chapter 3.4: The final chapter of this work applies the achieved knowledge from Chapter 3.1 – 3.3 to investigate the inactivation mechanisms and roles of primary and secondary oxidants of ClO_2 disinfection. Although it is known that ClO_2 is suitable to inactivate *E. coli*, the participation of intrinsically formed FAC has not been revealed yet. Therefore, a novel technique of cell inactivation will be developed, which provides higher and faster data and consumes less laboratory consumables compared to the commonly used methods (e.g., spread plate method). To induce intrinsic FAC formation, bacteria solutions containing NOM and different concentrations of methionine are treated with ClO_2 . NOM is the main reaction partner of ClO_2 and forms FAC under real conditions of water treatment. By adding different concentrations of methionine, FAC will be scavenged and not interact with the bacteria. Thereby, the participation of extracellular formed FAC can be estimated.

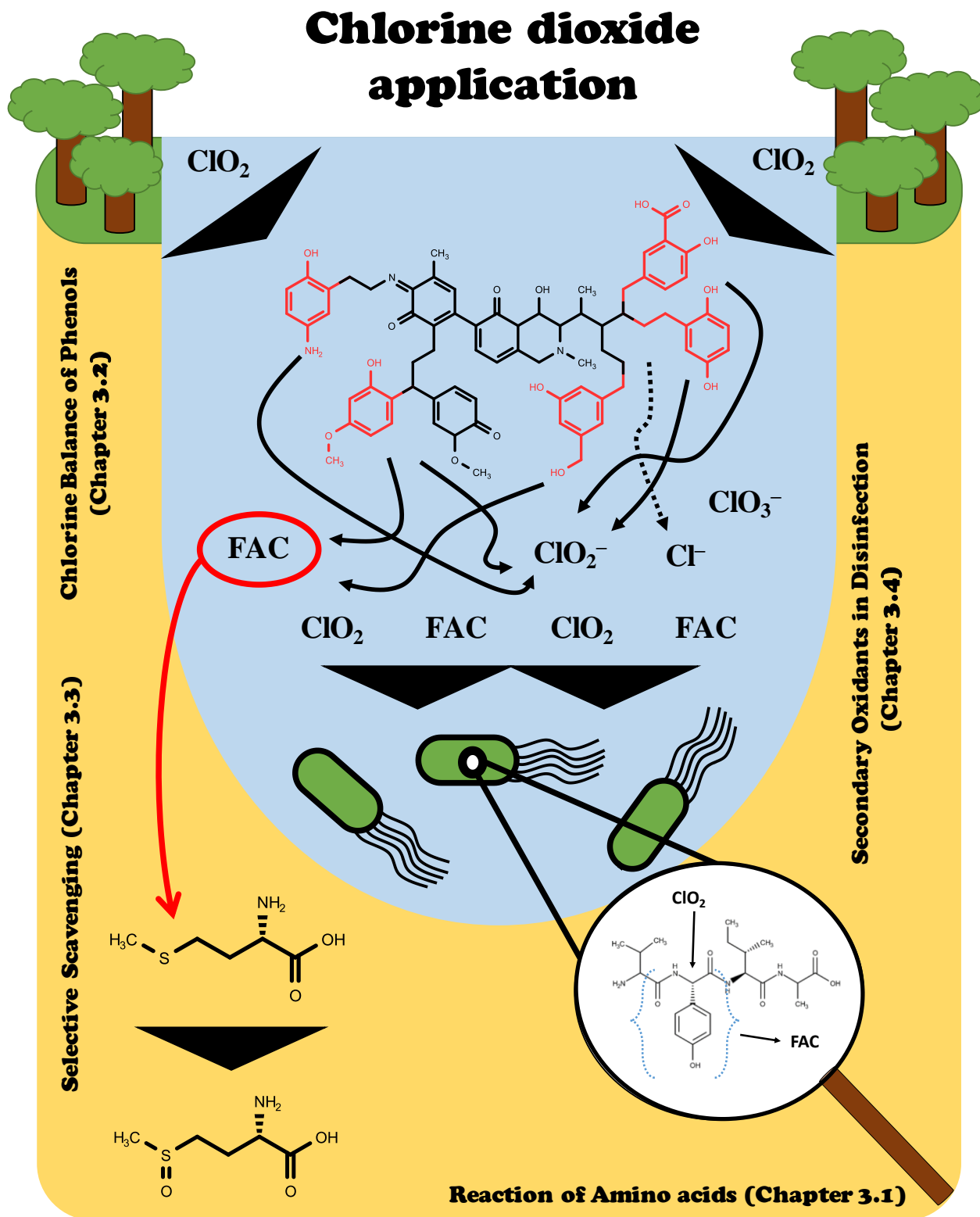


Figure 7: Graphical overview of the thesis content and different chapters.

Results and Discussion

Novel insights in chlorine dioxide-based disinfection mechanism – Investigation of the reaction with amino acids

Mischa Jütte, Mohammad S. Abdighahroudi, Janine V. Große, Christoph Schüth, and Holger V. Lutze

This chapter has been adapted from: M. Jütte, J. V. Große, M. S. Abdighahroudi, C. Schüth, and H. V. Lutze, “Novel insights into chlorine dioxide based disinfection mechanisms – investigation of the reaction with amino acids,” in *Environmental Science Water Research & Technology*, Royal Society of Chemistry, DOI: 10.1039/d1ew00812a

3. Results

3.1 Novel insights in chlorine dioxide-based disinfection mechanism – Investigation of the reaction with amino acids

This study systematically investigated the reactions of *N*-Acetyl-L-tyrosine (NAL-tyrosine) and *N*-Acetyl-L-tryptophan (NAL-tryptophan) with ClO_2 and FAC. NAL-tyrosine and NAL-tryptophan are examples of reactive amino acids included in peptides and incorporated in microbial membrane proteins, which can react with these oxidants during chemical water disinfection. The pH-dependent reaction kinetics revealed the following order at pH 7: NAL-tyrosine + ClO_2 ($k = 3.16 \times 10^4 \text{ M}^{-1} \text{ s}^{-1}$) > NAL-tryptophan + ClO_2 ($k = 1.81 \times 10^4 \text{ M}^{-1} \text{ s}^{-1}$) > NAL-tryptophan + FAC ($k = 7.31 \times 10^3 \text{ M}^{-1} \text{ s}^{-1}$) >>> NAL-tyrosine + FAC ($k = 22.6 \text{ M}^{-1} \text{ s}^{-1}$). Furthermore, this study showed that in the reactions of NAL-tyrosine and NAL-tryptophan with ClO_2 , free available chlorine (FAC) can form: NAL-tyrosine (50 % per ClO_2 consumed) and NAL-tryptophan (36 % per ClO_2 consumed). These results are in accordance with phenol and indol, which are the reactive moieties in NAL-tyrosine (phenolic moiety) and NAL-tryptophan (indol-moiety). Based on the achieved results, it can be assumed that in ClO_2 -based disinfection FAC may be an important secondary oxidant significantly contributing to the inactivation of pathogens by reacting with other cell compartments.

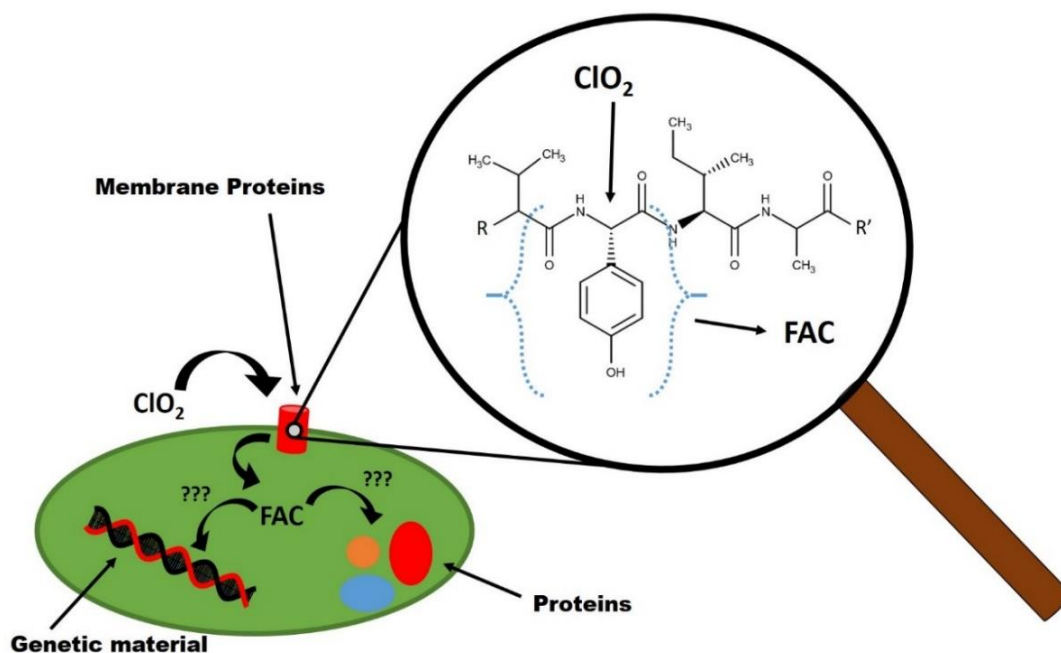


Figure 8: Graphical abstract of Chapter 3.1 – Novel insights in chlorine dioxide-based disinfection mechanisms - investigation of the reaction with amino acids.

3.1.1 Introduction

The disinfection of drinking water is a crucial step to preserve human health and prevent the spread of waterborne diseases. Worldwide, chlorine (free available chlorine (FAC)) has been successfully used to produce microbial-safe drinking water in the form of hypochlorous acid (HOCl). However, especially at high pH (> 7), the disinfection efficiency decreases due to the formation of OCl^- ($\text{p}K_a$: 7.54 (Deborde and von Gunten, 2008)), which is 80 – 100 times weaker disinfectant than HOCl (Rossi-Fedele et al., 2011). Furthermore, in dissolved organic carbon (DOC) rich water, the excessive formation of harmful halogenated disinfection by-products (DBPs) can occur (Pan et al., 2014; Rook, 1974; Wang et al., 2007). One alternative for HOCl is chlorine dioxide (ClO_2), which is less affected by pH (Junli et al., 1997) and does not form halogenated DBPs (Zhang et al., 2000). The main DBPs formed during ClO_2 treatment, however, are chlorite (ClO_2^-) and chlorate (ClO_3^-) (Korn et al., 2002; Lee et al., 2004; Werdehoff and Singer, 1987), which are also potentially harmful (Couri et al., 1982). In contrast to halogenated DBPs, ClO_2^- and ClO_3^- can be easier removed from the water, for instance, by adding ferrous salts (Fe^{2+}) or sulfite (SO_3^{2-}) and causing the reduction, which eventually forms harmless chloride (Cl^-) (Gordon et al., 1990; Katz and Narkis, 2001).

Besides ClO_2^- and ClO_3^- , ClO_2 might also form FAC as a secondary oxidant as well as Cl^- . The formation of FAC in the reaction of ClO_2 with phenol was first postulated by Wajon et al. (1982) and evidenced recently (Rougé et al., 2018; Terhalle et al., 2018). The proposed mechanism of intrinsic FAC formation during the reaction of phenol with ClO_2 by Wajon et al. (1982) is shown in Figure AII.1. The measured chlorine species formed in the reaction of ClO_2 with phenol consists of around 60 % ClO_2^- and 40 % FAC (Terhalle et al., 2018). Additionally, it is shown that the reaction of ClO_2 with the natural organic matter (NOM) of the water matrix also leads to the formation of ≈ 25 % FAC per consumed ClO_2 (Hupperich et al., 2020; Rougé et al., 2018). Previous works indicated that the yield of FAC displays a very strong structure dependency (Abdighahroudi et al., 2021). While phenol yields FAC, Hupperich et al. 2020 observed that the reaction of the phenol derivative vanillin with ClO_2 resulted in the formation of $\approx 50\%$ ClO_2^- and $\approx 50\%$ Cl^- as major products, whereby no FAC was observed (Hupperich et al., 2020). Yet, a mechanistic understanding of this observation is lacking.

The bactericidal effect of ClO₂ has been known for more than a century and has been demonstrated many times over the years (Benarde et al., 1965; Cho et al., 2010; Ofori et al., 2017; Ridenour and Ingols, 1947; Roller et al., 1980), however, it is not fully understood how ClO₂ inactivates pathogens. Former research has shown that the reaction of ClO₂ leads to leakage of endo-plasmatic matter, which indicates membrane damage in *E. coli* (Cho et al., 2010). Furthermore, the inactivation of inner cell functions (e.g., enzymes) was observed, indicating intracellular damage (Cho et al., 2010). The membrane damage could be explained by the reaction of ClO₂ with membrane proteins (note that the double bonds of lipids hardly react with ClO₂ (Abdighahroudi et al., 2021)). Former research has shown that ClO₂ reacts with specific amino acids (e.g., tyrosine, tryptophan, and cysteine (Ison et al., 2006; Napolitano et al., 2005; Stewart et al., 2008)). However, in most of these cases, the investigation was only carried out for the free amino acid, which is not present in this form under real conditions. In proteins, the amino acids are connected via peptide bonds; therefore, the primary amines are present as amides. This has a big impact on the reactivity of the nitrogen towards different oxidants, especially FAC, which reacts very fast with primary amines (Deborde and von Gunten, 2008). In analogy to phenols, FAC may also be formed in the reaction of ClO₂ with the functional groups of amino acid sidechains such as tyrosine which indeed has a phenolic moiety.

This study aims to investigate the reaction of tryptophan and tyrosine with ClO₂. For this purpose, *N*-acetylated amino acids, which resemble peptide bonds, were investigated. Thereby pH-dependent kinetics and formation of the inorganic products FAC, ClO₂⁻, Cl⁻, and ClO₃⁻ were investigated to estimate the potential of intracellular FAC formation, which could be a part of the ClO₂-based inactivation mechanism.

3.1.2 Material and Method

3.1.2.1 Chemicals and Instruments

All chemicals and instruments used in this study are listed in Table AII.1 and Table AII.2, respectively. The developed methods for liquid and ion chromatography, including the retention times of the compounds, are listed in Table AII.3 and Table AII.4, respectively.

3.1.2.2 Production of ClO₂

To produce aqueous ClO₂, the persulfate-chlorite method was used (Hupperich et al., 2020; Terhalle et al., 2018). In brief: 100 mL 0.885 M sodium chlorite (NaClO₂) and 100 mL 0.168 M sodium-persulfate (Na₂S₂O₈) were mixed in a gas washing bottle and continuously stirred. The formed ClO₂ was stripped by N₂ and the off-gas was purified by passing through a 0.111 M NaClO₂ solution, which scavenges residual FAC, a possible by-product of ClO₂ production. After the purification process, the gas was absorbed in ice-cooled pure water. The concentration of ClO₂ was determined directly after the production and before every experiment by measuring the extinction at $\lambda = 359 \text{ nm}$ ($\epsilon_{359} = 1250 \text{ M}^{-1} \text{ s}^{-1}$ (Gates et al., 2009)). If the concentration of the stock solution dropped below 80 % of the initial concentration, a new stock solution was produced.

Additionally, the possible residual concentration of ClO₂⁻, FAC, Cl⁻, and ClO₃⁻ in the ClO₂ solution were also determined. Therefore, aliquots of 5 mL ClO₂ stock solution were transferred into 15 mL of pure H₂O and 15 mL of a 10 mM glycine solution, respectively. The additional glycine solution was used to determine the residual concentration of FAC. Thereby, FAC reacts with glycine to form chloro-glycine (Cl-Gly). The solutions were stripped by N₂ until ClO₂ was fully removed (time = 20 – 30 min) (note that minimal low concentrations of residual ClO₂ may result in an overestimation of inorganic chlorine species in the ClO₂ solution. However, this is not important in this case since the impurities were determined to be very low < 2.5 % per ClO₂). Afterward, the samples were measured by using ion chromatography (conductivity detector) with a post-column reaction (UV detector) (IC-CD-PCR-UV). This procedure was only carried out for measuring the impurities of the ClO₂ stock solution. For detailed information about determining the concentration of ClO₂⁻, FAC, Cl⁻, and ClO₃⁻ formed during ClO₂-based reactions, see Chapter 3.1.2.6 Chlorine balance.

3.1.2.3 Preparation of FAC

FAC solution was freshly prepared daily before every experiment. From the 15% FAC solution mentioned in the chemical section, an aliquot of 125 μM was diluted in 50 mL pure water. FAC concentration was measured photometrical at $\lambda = 292 \text{ nm}$ ($\epsilon_{292} = 350 \text{ M}^{-1} \text{ s}^{-1}$ (Abdighahroudi et al., 2020)) by using a UV/Vis photometer. One has to take into account that the concentration was determined by measuring the OCl^- concentration. Therefore, it has to be ensured that OCl^- is the dominant species ($\text{p}K_a$: 7.54 (Deborde and von Gunten, 2008)); thus, all determined solutions had a pH of > 10 .

3.1.2.4 Determination of reaction kinetics

It is important to resemble the situation of amino acids in peptides, which have the primary amine inactivated by acetylation; therefore, derivatives of the amino acids tryptophan and tyrosine were used. The pH-dependent reaction rates of *N*-Acetyl-L(NAL)-tyrosine and NAL-tryptophan with ClO_2 and HOCl were determined using competition kinetics (von Sonntag and von Gunten, 2012). Therefore, suitable competitors are necessary, which are reacting in the same order of magnitude as the compound under study. For this purpose, phenol, indol, and sulfamethoxazole (SMX) were chosen as competitors (cf. Table 7). The reaction rates of the competitors were obtained from the literature (cf. Table 8). One needs to take into account that the pH-dependent reactivity of the competitors might behave differently compared with the compound under study; thus, at different pH values, different competitors have to be used. An overview of the used competitors and the investigated pH range is shown in Table 7.

Table 7: pH range of competitors used to determine the second-order reaction rate constants for NAL-tyrosine & NAL-tryptophan.

| Compound | Oxidant | Competitor | pH range |
|----------------|------------------|------------|------------|
| NAL-tyrosine | ClO ₂ | Phenol | 1.5 – 13 |
| | HOCl | Phenol | 5.5 – 12.5 |
| NAL-tryptophan | ClO ₂ | Indol | 6 – 10 |
| | | Phenol | 7 |
| | HOCl | SMX | 5 – 9.5 |
| | | Phenol | 9 – 12.5 |

For the competition kinetics experiments, a solution was prepared to contain 100 µM compound under study, 100 µM competitor, 5 mM phosphate buffer, and, in case of determining the second-order reaction rate for ClO₂, 10 mM glycine. Phosphate buffer was used to adjust and maintain the adjusted pH value, and glycine was added to scavenge possible intrinsically formed HOCl, which would bias the measured reaction rate (calculation to scavenge 99.9% HOCl is explained in Text AII.1). The solution was aliquoted into ten 15 mL reaction tubes (polypropylene (PP)), and different concentrations of ClO₂ (0 – 100 µM) were added by using glass syringes with stainless steel cannulas. The degradation of the compounds under study and respective competitors was measured by HPLC-UV. Plotting $\ln(c/c_0)$ of the compound under study vs. $\ln(c/c_0)$ of the competitor yields a linear function, with a slope equaling the ratio of the reaction rates of the compound under study and competitor. Multiplication of the slope with the apparent second-order reaction rate constant (k_{app}) of the competitor gives the k_{app} of the compound under study (von Sonntag and von Gunten, 2012). The used reaction rate constants for the competitors are listed in Table 8.

Table 8: Species-specific reaction kinetics of competitors taken from literature. Reaction rates are given for protonated (HB) and deprotonated (B⁻) species.

| | Phenol (Deborde and von Gunten, 2008; Neta et al., 1988) | Indol (Neta et al., 1988) | SMX (Dodd and Huang, 2004) |
|--|--|-------------------------------------|--------------------------------------|
| pK_a | 10 | – | 5.6 |
| k (ClO₂ + HB) [M⁻¹ s⁻¹] | 0.24 | 1.2 × 10 ⁴ | |
| k (ClO₂ + B⁻) [M⁻¹ s⁻¹] | 2.7 × 10 ⁷ | – | |
| k (HOCl + HB) [M⁻¹ s⁻¹] | 0.36 | – | 1.1 × 10 ³ |
| k (HOCl + B⁻) [M⁻¹ s⁻¹] | 3.5 × 10 ⁴ | – | 2.4 × 10 ³ |

The experiments were performed over a wide pH range. The statistical significance was derived from kinetic modeling. Eventually, it is possible to calculate the standard error and identify outliers with this procedure. Additionally, this model gives a greater overview of the pH spectra with the same time and cost investment. Since NAL-tryptophan does not dissociate in the investigated pH range, reaction kinetics was determined for 5 pH values in triplicates.

To calculate the apparent kinetic constant (k_{app}) as a function of pH, the speciation and the species-specific reaction kinetics of the compound under study has to be taken into account (Equation 2).

$$k_{app} = \sum_i^n \sum_j^n k_{ij} \alpha_i \beta_j \quad (\text{Equation 2})$$

k_{app} is described as the sum of the product of the fraction at this pH of the compound under study (α_i), the oxidant (β_j), and the species-dependent reaction rate (k_{ij}). The fractionation of the compound and the oxidants can be calculated according to the pK_a. Note that ClO₂ does not dissociate; thus, ClO₂ β equals 1. Additionally, the reactive moiety NAL-tryptophan does not dissociate, and therefore, α_i equals 1 as well in the case of NAL-tryptophan. The statistical program MATLAB[®] was used to calculate k_{ij} , based on Equation 2. For further details, see Wang et al. (2011).

3.1.2.5 Stoichiometry

The consumption of ClO_2 and FAC per degraded NAL-tyrosine and NAL-tryptophan (stoichiometry) was determined as follows. A stock solution was prepared to contain 100 μM of the compound under study, 5 mM phosphate buffer, and 10 mM glycine in the case of determination of ClO_2 stoichiometry. Sodium phosphate salts were used to adjust the pH of the reaction solution to pH 7. Aliquots were transferred into ten 15 mL reaction tubes (PP), and the oxidant was added in different concentrations (0 – 200 μM). After a reaction time of at least 30 min, the samples were measured via HPLC-UV. The long reaction time was necessary to ensure at least 95 % degradation in the NAL-tyrosine reaction with FAC. Note that all other reactions are complete to 99 % in less than 10 seconds. All experiments were performed in triplicates.

3.1.2.6 Chlorine balance

The chlorine balance (i.e., the sum of all inorganic chlorine species formed in the reaction of ClO_2 with compounds under study (Cl^- , FAC, ClO_2^- , and ClO_3^-)) was measured in analogy to the procedure described by Abdighahroudi et al. (2020). In brief, a stock solution was prepared to contain 5 mM phosphate buffer, 10 mM glycine, and 100 μM compound under study. The pH of the stock solution was set to 7.0 to mimic the conditions representative of typical microorganisms (the pH of cytoplasm is between 7.0 – 7.4 (Padan et al., 1981)). Aliquots of the stock solution were transferred into 15 mL reaction tubes (PP), and ClO_2 was dosed in different concentrations (0– 200 μM). The chlorine balance was determined for NAL-tyrosine, NAL-tryptophan, and indol to compare the chlorine balance of NAL-tryptophan and indol (representative for the reactive moiety of tryptophan). For NAL-tyrosine, the reaction time was at least 30 minutes before the samples were transferred into HPLC-Vials (PP) and measured with IC-CD-PCR-UV (setup is shown in Figure AII.2). Since Cl-Gly is not stable in the presence of indol and NAL-tryptophan, the reaction time was reduced to 10 seconds before the samples were transferred into the cooled autosampler (5°C). The waiting time until the sample was injected was less than 5 minutes. Note that the reaction of NAL-tryptophan is > 99.9 % completed within the first ten seconds. For all compounds, the recovery of Cl-Gly was measured by adding 0.1 mM FAC into an identical aliquot of the reaction solution. By doing so, the reaction of Cl-Gly with compounds under study would be detected by an incomplete recovery. The use of glycine as a scavenger also suppresses the reaction of FAC with ClO_2^- .

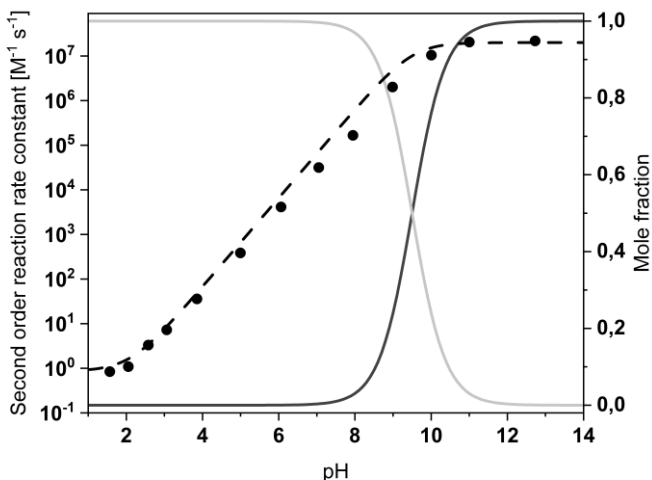
Note that, a fairly complete chlorine balance could be established (the sum of all inorganic by-products resembled > 90 % chlorine from the chlorine dioxide dose). Since there was nearly no gap in the chlorine mass balance, no other procedures were employed to determine other (e.g., organic) chlorine.

3.1.4 Results and Discussion

3.1.4.1 Reaction kinetics

Figure 9 visualizes the pH-dependent reaction kinetics of NAL-tyrosine and NAL-tryptophan with ClO₂. NAL-tyrosine shows a similar correlation in reactivity towards ClO₂ as phenol (Neta et al., 1988). The deprotonated species are reacting several orders of magnitudes faster than the protonated species (cf. Table 9). This observation is in line with the reaction rates of other phenolic compounds and can be explained by the strong activating effect of the deprotonated hydroxyl group, which favors the electrophilic attack of ClO₂. NAL-tryptophan has no dissociation center and therefore shows no pH-dependent reaction kinetics towards ClO₂. The reactivity is in the same order of magnitude compared to indol (Neta et al., 1988), which corroborates that the reactive moiety of tryptophan is the indol moiety.

A



B

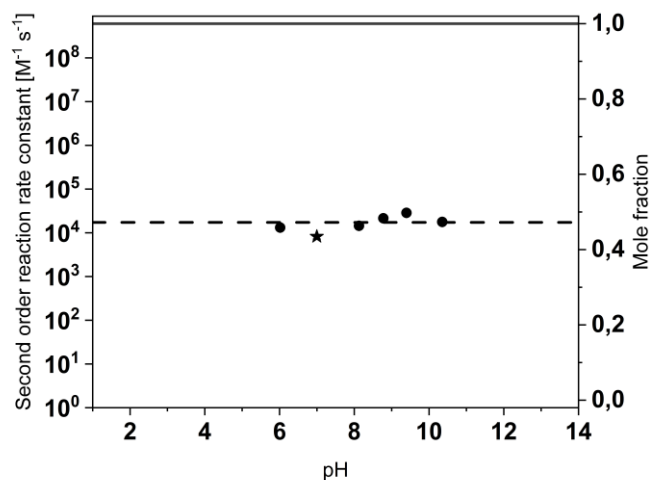
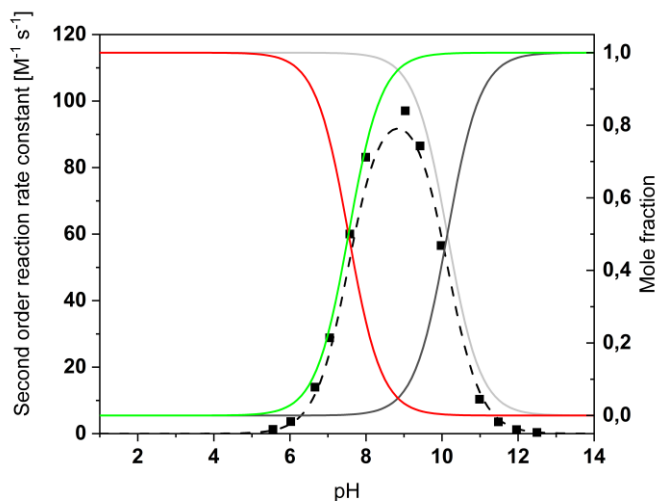


Figure 9: pH-dependent reaction kinetics of NAL-tyrosine (A) and NAL-tryptophan (B) with ClO_2 . Experimental conditions: 100 μM of NAL-amino acid, 100 μM competitor, 5 mM phosphate buffer, and 10 mM glycine. A: The grey and the black line represent the speciation of NAL-tyrosine ($\text{p}K_a = 10.22$) (Mayberry et al., 1965), grey and black represent the protonated and the deprotonated phenolic moiety, respectively. The black dots show the determined second-order reaction rate constants, and the dashed line is the kinetic model (cf. material and methods). B: NAL-tryptophan has no dissociation center, therefore the black line is representing the neutral species, which is constant over the full pH range. Black dots are representing the measured second-order reaction rates measured by using indole as a competitor, the star represents the second-order reaction rate measured with phenol as a competitor. Measurements have been done in triplicates, the relative standard deviation was $< 7\%$).

Figure 10 shows the reactivity of both amino acids with HOCl. In this case, the dissociation of HOCl ($pK_a = 7.54$ (Deborde and von Gunten, 2008)) to OCl^- at $pH > 7$ is causing a decrease in reactivity. This can be explained by the low reaction kinetics of OCl^- which is several orders of magnitude slower than the protonated species. Note that in previous studies, the reaction kinetics of OCl^- is even neglected (Deborde and von Gunten, 2008). Since the indole moiety of NAL-tryptophan does not dissociate at low pH, the reactivity is constant at low pH. At high pH values, the unreactive OCl^- dominates; therefore, the overall reactivity becomes slower. The fraction of the reactive phenolate species of NAL-tyrosine, however, increases with pH. Thus, the reactivity has a maximum at the average of the pK_a values of NAL-tyrosine and HOCl. At pH values < 6 , the neutral phenolic species are predominant, which hardly react with HOCl.

Table 9 compiles the species-specific reaction kinetics of the compounds under study, as well as k_{app} at pH 7. Although the species-specific reaction rate for ClO_2 of NAL-tyrosine and NAL-tryptophan differs by several orders of magnitude, their reaction rate at pH 7 is in the same order of magnitude. This can also be explained by the speciation of the compounds. Since NAL-tryptophan reactivity remains constant at the studied pH range, NAL-tyrosine reactivity shows a peak-shaped pattern. At pH 7 both of the calculated functions intersect. Therefore, it can be assumed that ClO_2 will react with both amino acids in the endoplasm to a similar extent.

A



B

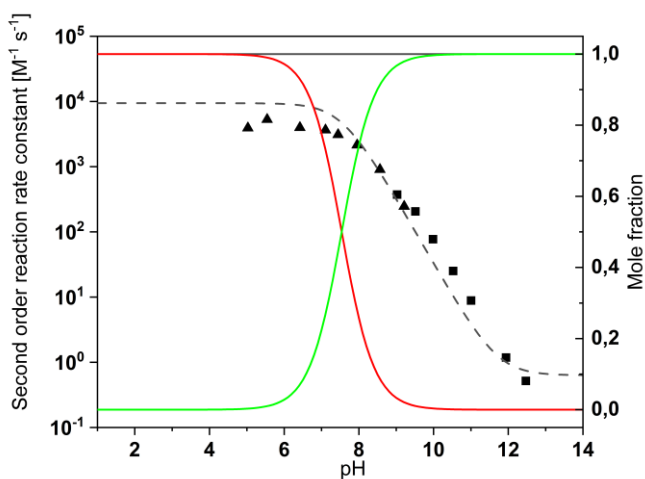


Figure 10: pH-dependent reaction rate of (A) NAL-tyrosine and (B) NAL-tryptophan with HOCl. Experimental conditions: 100 μM of NAL-amino acid, 100 μM competitors, and 5 mM phosphate buffer. (A): The black and grey line represents the speciation of NAL-tyrosine ($\text{p}K_{\text{a}} = 10.22$) (Mayberry et al., 1965), whereby grey and black are representing the protonated and the deprotonated phenolic moiety, respectively. The red and green line represents the speciation of HOCl (red = HOCl; green = OCl^-). The black squares are the measured second-order reaction rate constants, and the dashed line shows the kinetic model. (B): NAL-tryptophan does not dissociate, therefore the black line is representing the neutral species, which is constant over the entire pH range. The red and green line represents the speciation of HOCl (red = HOCl; green = OCl^-). Black triangles are representing the second-order reaction rate constants measured by competition kinetics using SMX as a competitor, and the black squares represent the second-order reaction rate constants measured with phenol as a competitor.

Chapter 3.1: Novel insights in chlorine dioxide-based disinfection mechanism – Investigation of the reaction with amino acids

Table 9: Kinetic results for amino acids reaction with ClO₂ and HOCl and comparison of second-order reaction rate constants with literature data. Reaction rate constants are given for protonated (HB) and deprotonated (B⁻) amino acids (AA). As mentioned above, the reaction kinetics of OCl⁻ is neglected.

| | <i>Ox</i> | <i>Ox + HB</i> [M ⁻¹ s ⁻¹] | <i>Ox + B⁻</i> [M ⁻¹ s ⁻¹] | <i>k_{app} at</i> <i>pH 7</i> [M ⁻¹ s ⁻¹] | <i>Degraded</i> <i>equivalent AA</i> <i>per consumed</i> <i>equivalent Ox</i> | <i>Ref</i> |
|------------------------------|------------------|--|---|--|--|------------|
| N-Acetyl-L-Tyrosine* | ClO ₂ | 1.07 ± 0.82 | 5.01 × 10 ⁷ ± 1.63 | 3.02 × 10 ⁴ | 0.52 ± 0.01 | A |
| | HOCl | 4.23 × 10 ⁻⁷ | 4.84 × 10 ⁴ ± 0.17 | 27.2 47 [▲] | 0.71 ± 0.10 | B |
| N-Acetyl-L-Tryptophan | ClO ₂ | 1.81 × 10 ⁴ ± 0.12 | – | 1.81 × 10 ⁴ | 0.46 ± 0.03 | |
| | HOCl | 9.42 × 10 ³ ± 3.71 | – | 7.31 × 10 ³ 7.8 × 10 ³ [▲] | 0.93 ± 0.01 | B |
| Tyrosine | ClO ₂ | | 1.8 × 10 ⁸ | | | A |
| | HOCl | | Not known | | | |
| Phenol | ClO ₂ | | 2.7 × 10 ⁷ | | | C |
| | HOCl | | 2.2 × 10 ⁴ | | | D |
| 4-Methylphenol | ClO ₂ | | 5.2 × 10 ⁸ | | | E |
| | HOCl | | 2.7 × 10 ⁴ | | | D |

*p*K_a* used for calculating *k_{app}* at pH 7 was 10.22 (Mayberry et al., 1965).

▲ Reported results by Pattison et al. 2001, who measured the absolute reaction rate constant for pH 7.2 – 7.4 (Pattison and Davies, 2001).

Reference list: A (Napolitano et al., 2005), B (Pattison and Davies, 2001), C (Neta et al., 1988), D (Deborde and von Gunten, 2008), E (Hoigné and Bader, 1994)

The stoichiometry of both amino acids towards ClO_2 shows that 2 equivalents of ClO_2 are consumed per equivalent of amino acid degraded. NAL-tryptophan reacts with HOCl in an almost 1:1 stoichiometry. The observed stoichiometry of NAL-tyrosine with HOCl does not follow a linear trend. The degradation can be better described by an exponential plot (Figure AII.3). The reason for this observation could be that the formed transformation products (presumably chlorinated NAL-tyrosine) may react with HOCl even faster than NAL-tyrosine itself and thus compete for HOCl reaction. This phenomenon will be explained with phenol as an example. 2-chlorophenol is a possible reaction product from the reaction of phenol and HOCl . The reaction rate of the deprotonated phenolate species differs by 1 order of magnitude (k (phenolate + HOCl) = $2.19 \times 10^4 \text{ M}^{-1} \text{ s}^{-1}$ and k (2-chlorophenolate + HOCl) = $2.42 \times 10^3 \text{ M}^{-1} \text{ s}^{-1}$ (Deborde and von Gunten, 2008)). Therefore, one may assume that the reaction kinetics of 2-chlorophenolate at pH 7 should be slower and, therefore, not affect the observed stoichiometry. However, chlorination also lowers the pK_a of the phenol from 9.99 to 8.56 (Deborde and von Gunten, 2008). This results in a higher fraction of the highly reactive phenolate species at pH 7 compared with phenol and eventually results in a faster apparent reaction rate at pH 7 (k_{app} (phenol + HOCl) = $18 \text{ M}^{-1} \text{ s}^{-1}$ at pH 7 and k_{app} (2-chlorophenol + HOCl) = $50 \text{ M}^{-1} \text{ s}^{-1}$ at pH 7) (Deborde and von Gunten, 2008). This concept can now be transferred to the reaction of HOCl with NAL-tyrosine, which has a phenolic moiety as well. The formed chlorinated transformation products may have a smaller pK_a value than NAL-tyrosine and thus, reveal a similar k_{app} at pH 7 as NAL-tyrosine itself. With increasing HOCl doses, chlorinated NAL-tyrosine is increasingly formed, which competes for HOCl with NAL-tyrosine. This can explain the nonlinear increase in HOCl demand with increasing HOCl dose. However, at low HOCl doses, a linear correlation was observed, which was used to determine the stoichiometry of HOCl in the reaction with NAL-Tyrosine. Table 9 compiles all determined stoichiometry.

Table 9 additionally compares the reactivity of the deprotonated species of NAL-tyrosine with phenol and methyl-phenol. In general, it can be stated that the measured kinetic data matches the previously reported data very well and thus, phenol can be confirmed as a reactive moiety. Furthermore, by comparing the reactivity of tyrosine and NAL-tyrosine with ClO_2 , it can be deduced that the reactivity of the amino acid under conditions similar to peptide bonds is slower than the free amino acid, which may play a role in the inactivation mechanism of microbial cells. It could be shown that the choice of a representative model compound such as N-acetylated amino acids is decisive to understanding their reactions in complex systems such as peptides or proteins.

Additionally, as shown in Table 9, the calculated reaction rate for HOCl at pH 7 can be compared with previously reported results by Pattison et al. 2001, who measured the absolute reaction rate constant for pH 7.2 – 7.4 (Pattison and Davies, 2001). It can be observed that the determined data is matching the previously reported data very well.

3.1.4.2 Chlorine balance

Table AII.5 summarizes the formation of conceivable inorganic by-products from ClO₂ production, which may be present in the ClO₂ stock solution. Cl⁻, ClO₂⁻, and FAC impurities are very low (<0.2 % of the molar equivalent of ClO₂) and be neglected in further data evaluation. However, the ClO₃⁻ impurity was 2.1 % per ClO₂ concentration, which was subtracted from determined ClO₃⁻ concentrations in the chlorine balances.

Figure 11 shows the determined chlorine balance for NAL-tyrosine and NAL-tryptophan. ClO₂ was added in different concentrations to investigate if the ratio between ClO₂ and the amino acid under study affects by-product formation. In the case of NAL-tyrosine, ≈ 50 % ClO₂⁻ and ≈ 50 % FAC per consumed ClO₂ were detected for the whole range of ClO₂ / amino acid ratios. It was reported that the reaction of phenol with ClO₂ leads to the formation of 60 % ClO₂⁻ and 40 % FAC, which agrees well with NAL-tyrosine, which has a phenolic reactive moiety (Terhalle et al., 2018). In the case of NAL-tryptophan, however, ≈ 50 % ClO₂⁻, ≈ 35 % FAC, and ≈ 10 % Cl⁻ were detected. Preliminary experiments have shown that Cl-Gly is not stable in the presence of NAL-tryptophan and indol, even if the samples are cooled at 5 °C. Thus, the samples (in the case of NAL-tryptophan and indol) were injected 5 min after ClO₂ was added to the sample to achieve minimal loss in recovery. However, even at very low reaction times (immediate measurement after oxidant injection FAC recovery was incomplete (≈ 85 %) (see Table 10). Hence, the real FAC yields may be somewhat higher (max. 15%) than the determined ones. The reaction of NAL-tryptophan with Cl-Gly might lead to the formation of Cl⁻, which would explain the formation of ≈ 10 % Cl⁻. Taking the FAC recovery into account, one would arrive at approximately 50% FAC yield per ClO₂ consumed. Additionally, Figure 11 shows that the ClO₂ dose up to a ratio of 2:1 ClO₂:amino acid had hardly any effect on the chlorine balance, corroborating that ClO₂ reacts in two steps with the amino acids. This indicates that even if low concentrations of ClO₂ are reaching the microbial cells and react with the amino acid side moiety, FAC can be formed.

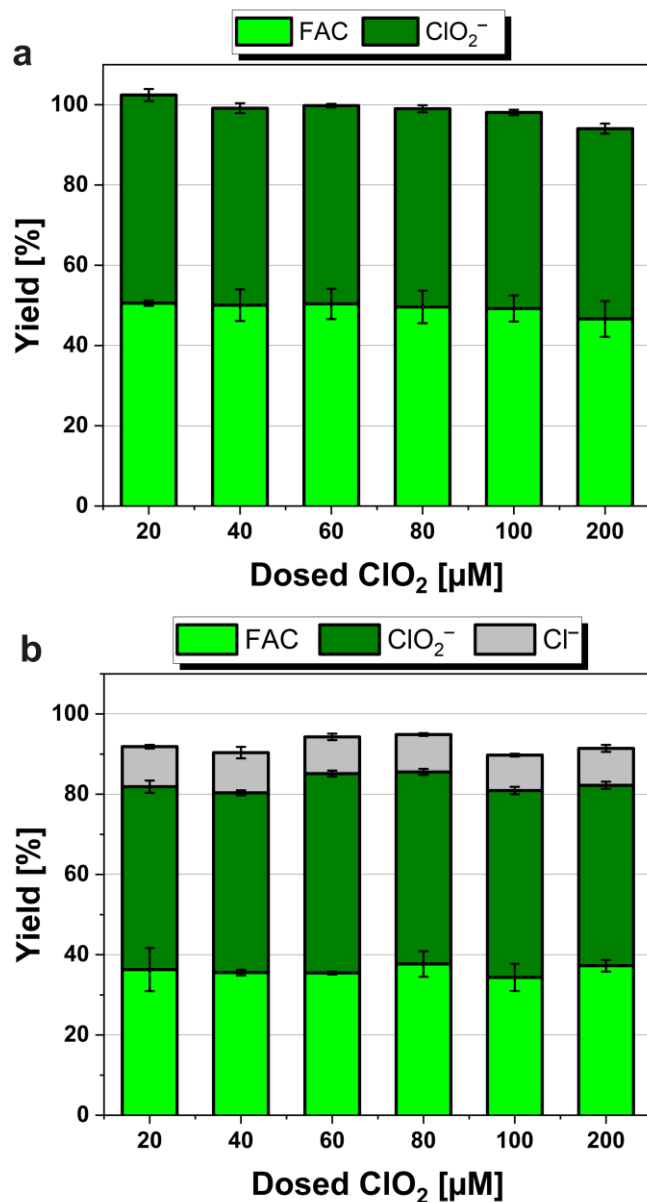


Figure 11: Chlorine balance of N-Acetyl-L-tyrosine (a) and N-Acetyl-L-tryptophan (b). Both balances were determined at pH 7. The reaction solution contained 10 mM glycine, 5 mM phosphate buffer, and 0.1 mM of the corresponding N-acetylated amino acid. All experiments were measured in triplicates. The error bars represent the standard deviation of the results. If the yield of a species was below 2.5 %, it is not shown in the chart. A complete overview of the detected yields of inorganic chlorine species is given in Table 10.

Table 10: Quantification of chlorine species during the reaction of both amino acids and ClO₂.

| Compound | ClO ₂ ⁻ | FAC | Cl ⁻ | ClO ₃ ⁻ | Σ | Recovery FAC |
|----------------|-------------------------------|------------|-----------------|-------------------------------|-------|-----------------|
| | [%] | | | | | |
| NAL-tyrosine | 49.2 ± 1.3 | 48.9 ± 2.0 | 1.0 ± 0.3 | 2.1 ± 1.3 | 101.2 | 114.4 ± 4.9 |
| NAL-tryptophan | 46.6 ± 1.9 | 36.1 ± 1.2 | 9.4 ± 0.5 | < 1.0 | 92.1 | 84.9 ± 2.0 |

To confirm the reactive moiety of NAL-tryptophan, the model compound indol was investigated as well. Thereby the chlorine balance of NAL-tryptophan and indol were compared (Figure AII.4). The results show that the measured chlorine balance and the overall FAC recovery were very similar. Thus, it can be assumed that the reactions of both compounds are accomplished by the same reaction pathway.

3.1.4.3 Reaction mechanism of NAL-tyrosine

The results confirm the previous observations by Napolitano et al., who proposed a two-step reaction pathway for the free amino acid tyrosine with ClO₂ (2005). However, previous research did not quantify the formed FAC. By using the glycine method (Abdighahroudi et al., 2020), it was possible to quantify intrinsic FAC, and thus, the yield of FAC could be determined. With the knowledge that ClO₂⁻ and FAC are formed in a 1:1 ratio, it seems reasonable that NAL-tyrosine is reacting similarly to phenol, whereby ClO₂⁻ is formed in the first step of the reaction (electron transfer) and the second step leads to the formation of FAC ((oxygen transfer) for further details cf. Figure AII.5) (Napolitano et al., 2005; Wajon et al., 1982).

It was stated earlier by Hupperich et al. 2020 that the formation of FAC is hampered if the phenolic moiety is *para*-substituted. Indeed, in the case of vanillin, ClO₂⁻ and Cl⁻ were formed, and no FAC was measured (Hupperich et al., 2020). However, this observation is not in line with the present study since the *para*-substituted phenolic moiety of NAL-tyrosine formed FAC (Figure 11) (For comparison of chemical structures cf. Figure AII.6). Hence, it can be concluded that not only the presence of any substituent in *para*-substitution affects the reaction (e.g., by affecting the intramolecular bond rearrangements) but also the kind of substituent, which can affect the electron

density distribution. Thereby, substituents may have electron-donating effects (activating) or electron-withdrawing effects (inactivating), and these effects can control the point of attack and the reaction mechanisms (e.g., electron transfer or oxygen transfer) of the electrophile ClO_2 . Vanillin has an acetyl group in *para*-position which, strongly inactivates the aromatic system. In NAL-tyrosine, however, the *para*-substituent has a slightly activating effect on the aromatic system, since the reaction kinetics of NAL-tyrosine is slightly higher compared to phenol (note that tyrosine reacts even 10-fold faster than phenol). Additionally, vanillin has an activating methoxy group in *ortho*-position, which is lacking in NAL-tyrosine. Hence FAC forming oxygen transfer reaction of ClO_2 may occur in the *ortho*-position of NAL-tyrosine, which is not substituted in this molecule. It might be possible that the presence of a substituent (activating or deactivating) at one *ortho*-position of NAL-tyrosine might also influence FAC formation and the reaction would work as described by Hupperich et al. (2020). However, to investigate the exact reason why vanillin does not form FAC and to further prove the proposed hypotheses is out of scope and further experiments with different model compounds are necessary.

3.1.4.4 Reaction mechanism of NAL-tryptophan

For the reaction of the free amino acid tryptophan, a reaction pathway has been proposed by Stewart et al. (2008). However, according to that mechanism, the formed OCIO-intermediate (formed during the second step of the reaction pathway) cannot lead to the formation of FAC. Thus, based on the results of this study, it seems more reasonable that the point of the first attack of ClO_2 in the indol moiety is the nitrogen atom (see Figure 12). In the first step, ClO_2 may react *via* electron transfer yielding ClO_2^- and a nitrogen-centered radical (step a, Figure 12)). Afterward, intramolecular reactions result in the formation of a carbon-centered radical in the aromatic ring, where it can be stabilized in the π -system (step b, Figure 12). The carbon-centered radical reacts with a second molecule of ClO_2 and forms an OCIO-adduct similar to the reaction pathway of phenolic moieties. Eventually, the formed intermediate undergoes a cleavage reaction and forms HOCl and a ketone group (step c Figure 12). The described reaction pathway is in accordance with the experimental results since 2 equivalents of ClO_2 are necessary to react with 1 equivalent of NAL-Tryptophan and the chlorine balance shows a yield of 50 % ClO_2^- and, as the authors assume, 50 % FAC per consumed ClO_2 .

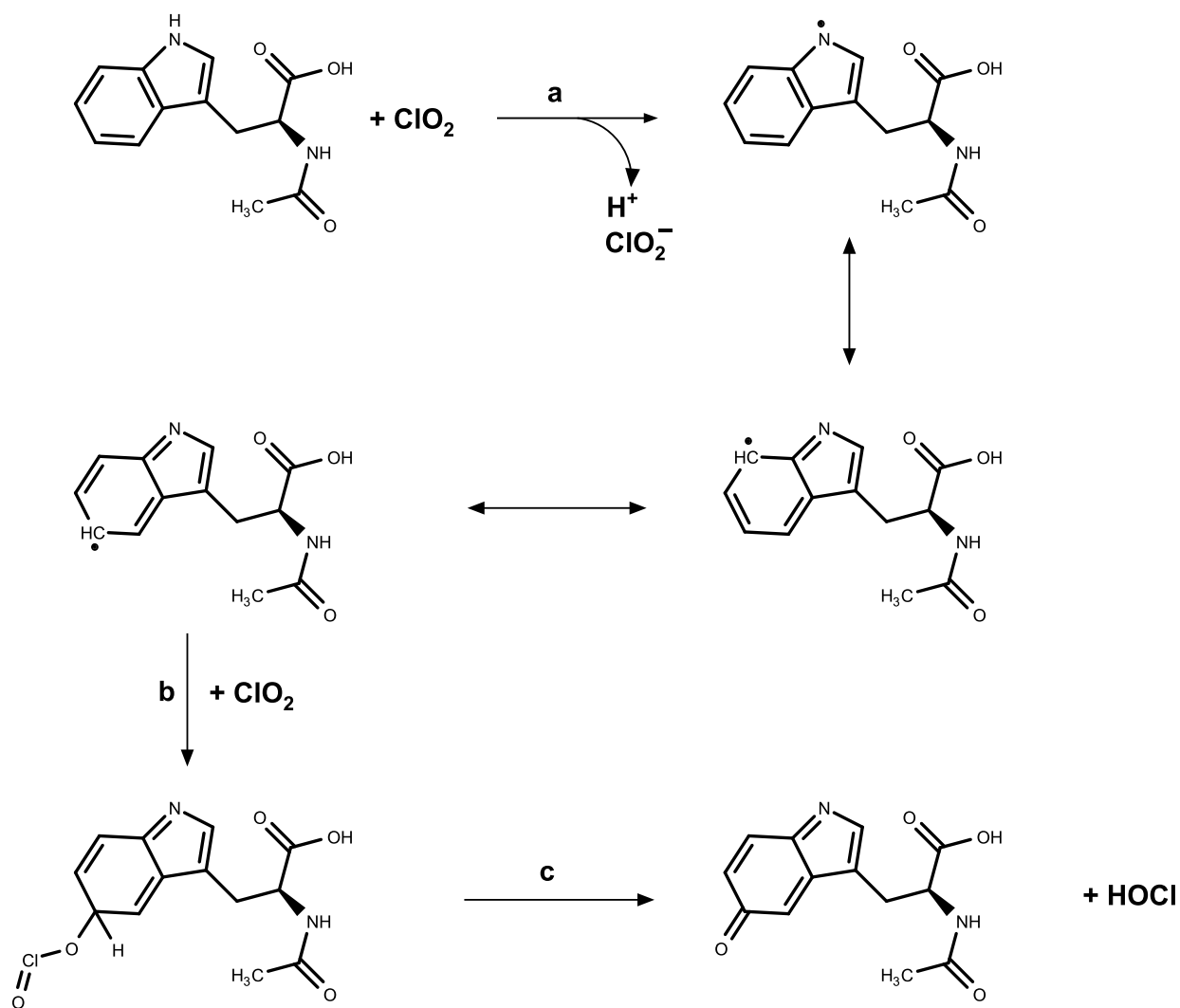


Figure 12: Proposed reaction pathway of the reaction of NAL-tryptophan with ClO_2 .

3.1.5 Conclusion

Since this study could prove that up to 50 % of applied ClO_2 is transformed to FAC during the reaction with specific amino acids, FAC might play a major role in the inactivation processes of pathogens during ClO_2 -based disinfection. The relative abundance of the amino acids tyrosine and tryptophan is relatively high in membrane proteins of microbial cells (Ulmschneider and Sansom, 2001), and the reactivity of these amino acids, even if connected via peptide bonds, is very fast at pH 7 (Table 7). It can be assumed that ClO_2 is inactivating pathogens or at least damaging the membrane by reacting with the amino acids NAL-tyrosine and NAL-tryptophan. During this reaction, FAC is formed and might react further, either with the same amino acids (e.g., tryptophan) or different amino acids (e.g., cysteine, methionine) (Deborde and von Gunten, 2008) or diffuse inside the microbial cell and cause further inner cell damage. It was reported that strong chemical oxidants such as ozone are more likely to cause microbial membrane destruction, and weak oxidants such as FAC cause inner cell damage. ClO_2 was reported to show both effects (Cho et al., 2010). This observation underlines the above-mentioned hypothesis that ClO_2 is mainly responsible for surface damage, whereby FAC is formed as a secondary oxidant that causes the observed inner cell damage.

Reaction mechanisms of chlorine dioxide with phenolic compounds – Influence of different substituents on stoichiometric ratios and intrinsic formation of free available chlorine

Mischa Jütte, Janis A. Wilbert, Marcel Reusing, Mohammad S. Abdighahroudi, Christoph Schüth, and Holger V. Lutze

This chapter has been adapted with permission from: M. Jütte, J. A. Wilbert, M. Reusing, M. S. Abdighahroudi, C. Schüth, and H. V. Lutze, “Reaction mechanisms of chlorine dioxide with phenolic compounds – Influence of different substituents on stoichiometric ratios and intrinsic formation of free available chlorine,” *Environmental Science & Technology*. Copyright 2023 American Chemical Society.

3.2 Reaction mechanisms of chlorine dioxide with phenolic compounds – Influence of different substituents on stoichiometric ratios and intrinsic formation of free available chlorine

Chlorine dioxide (ClO_2) is an oxidant applied in water treatment processes that is very effective for disinfection and abatement of inorganic and organic pollutants. Thereby phenol is the most important reaction partner of ClO_2 in reactions of natural organic matter (NOM) and in pollutant degradation. It was previously reported that with specific reaction partners (such as phenol), free available chlorine (FAC) could form as another by-product next to chlorite (ClO_2^-). This study investigates the impact of different functional groups attached to the aromatic ring of phenol on the formation of inorganic by-products (i.e., FAC, ClO_2^- , chloride, and chlorate) and the overall reaction mechanism. The majority of the investigated compounds reacted with a 2:1 stoichiometry and formed 50 % ClO_2^- and 50 % FAC, regardless of the position and kind of the groups attached to the aromatic ring. The only functional groups strongly influencing the FAC formation in the ClO_2 reaction with phenols were hydroxyl- and amino-substituents in *ortho*- and *para*-position, causing 100 % ClO_2^- and 0 % FAC formation. Additionally, this class of compounds showed a pH-dependent stoichiometric ratio due to pH-dependent autoxidation. Overall, FAC is an important secondary oxidant in ClO_2 based treatment processes. Synergetic effects in pollutant control and disinfection might be observable, however, the formation of halogenated by-products needs to be considered as well.

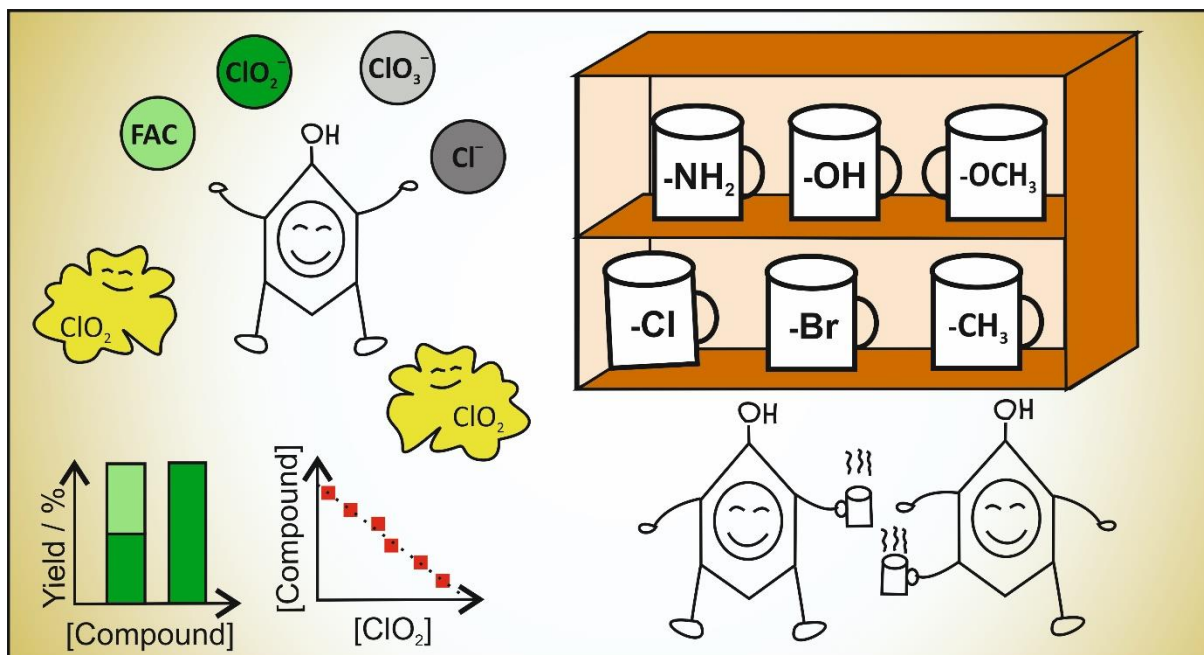


Figure 13: Graphical abstract of chapter 3.2 – Reaction mechanisms of chlorine dioxide with phenolic compounds – Influence of different substituents on stoichiometric ratios and intrinsic formation of free available chlorine

3.2.1 Introduction

Oxidation is an important tool in water treatment to provide safe drinking water by disinfection and pollutant degradation (von Gunten, 2018). Therefore, different chemical oxidants such as chlorine (free available chlorine (FAC)), chlorine dioxide (ClO_2), and ozone (O_3) are used, whereby FAC is the most common oxidant. However, by discovering the formation of undesired halogenated disinfection by-products (DBPs) in FAC application (Rook, 1974; Watson et al., 2012), the usage of other oxidants such as O_3 or ClO_2 has increased. Although ClO_2 forms only small yields of halogenated DBPs compared to FAC (Sorlini and Collivignarelli, 2005), it forms chlorite (ClO_2^-) and chlorate (ClO_3^-) as major by-products (Korn et al., 2002; Werdehoff and Singer, 1987). Recently, it was discovered that ClO_2 forms FAC as a secondary oxidant with specific reaction partners (Abdighahroudi et al., 2022; Guo et al., 2022; Rougé et al., 2018; Terhalle et al., 2018).

Due to the high reactivity, phenols are a crucial reactive moiety in ClO_2 based reaction mechanisms (Hoigné and Bader, 1994). The natural organic matters (NOM) of different water bodies contain a high amount of phenolic moieties, while, many micropollutants also contain phenolic moiety (e.g., ethylene-estradiol or bisphenol-A). This results in the fact that ClO_2 mainly reacts with phenolic moieties of natural organic matter (NOM) in a real water matrix (Wenk et al., 2013), and phenol containing micropollutants are very well degradable by ClO_2 (Lee and von Gunten, 2012, 2010; Wang et al., 2011). The reaction of ClO_2 with phenolic moieties has been proposed to be a two-step mechanism resulting in ClO_2^- (1st step, electron transfer) and FAC (2nd step, oxygen transfer upon addition of ClO_2 to the carbon-centered radical from step 1) (Wajon et al., 1982). Thereby, Wajon et al. suggested FAC formation in the presence of a hydrogen bond at the carbon of ClO_2 -addition (1982). Recent studies have proven the intrinsic formation of FAC in this reaction (Hupperich et al., 2020; Jütte et al., 2022; Rougé et al., 2018; Terhalle et al., 2018). However, the published FAC yields have been reported to depend on the substituents of the phenolic compounds. For instance, phenol itself has been reported to form 40 – 50 % FAC of the dosed ClO_2 (Rougé et al., 2018; Terhalle et al., 2018), whereby vanillin, which has a methoxy group in *ortho*-position and a formyl group in *para*-position, does not form any FAC but significant yields of chloride (Cl^-) (Hupperich et al., 2020). The observed lack of FAC formation in vanillin reaction with ClO_2 was explained by the absence of a *C-H* bond in *para*-position, which might have caused formyl radical ($\cdot\text{CHO}$) formation instead of HOCl (Hupperich et al., 2020). However, later research showed that

Chapter 3.2: Reaction mechanism of chlorine dioxide with phenolic compounds – Influence of different substituents on stoichiometric ratios and intrinsic formation of free available chlorine

N-acetyl-L-tyrosine, a *para*-substituted phenol, does form FAC ($\approx 49\%$) (Jütte et al., 2022), which contradicts the previous works on vanillin (Hupperich et al., 2020). Thereby, the question of how different substituents affect the formation of FAC during the reaction of ClO_2 with phenolic moieties arises.

Besides the investigations regarding different phenols with ClO_2 , the reaction of ClO_2 with NOM has been investigated as well. It has been shown that the reaction of ClO_2 with NOM causes degradation of high molecular weight fractions (Świetlik et al., 2004). Additionally, the reaction of ClO_2 with the phenolic moieties in NOM results in reduced aromaticity (Yang et al., 2013). It has been reported that from this reaction, 25 % of dosed ClO_2 forms FAC (Hupperich et al., 2020; Rougé et al., 2018). So far, it has not been investigated which phenolic moieties are responsible for the reported FAC yields.

This study systematically investigated the reaction of ClO_2 with different phenolic model compounds (Figure 14) regarding the formation of FAC, other chlorine species, and the reaction stoichiometry. These compounds have been chosen for investigating the effects of different groups attached to the phenol ring on the primary and secondary attack of ClO_2 . Thereby in the primary attack, the phenoxy radical is formed upon electron transfer of ClO_2 . The phenoxy radical has different resonance structures, whereby the radical can be located in *ortho*- or *para*-position of the hydroxyl group (Figure AIII.1). Since FAC is postulated to be formed in the second reaction step (Wajon et al., 1982), these positions might be crucial for hampering or forming FAC. Thereby, the FAC formation was investigated for phenolic compounds, which have one or more of these positions occupied by methyl groups. Besides the methylated phenolic compounds, it was also investigated if different substituents affect the FAC formation. Thus, hydroxyphenols, chlorophenols, bromophenols, aminophenols, and methoxyphenols in *ortho*-, *meta*-, and *para*-position were also investigated (Figure 14). Vanillin was also investigated to corroborate or refute reported data on the effect of *para*-substitution.

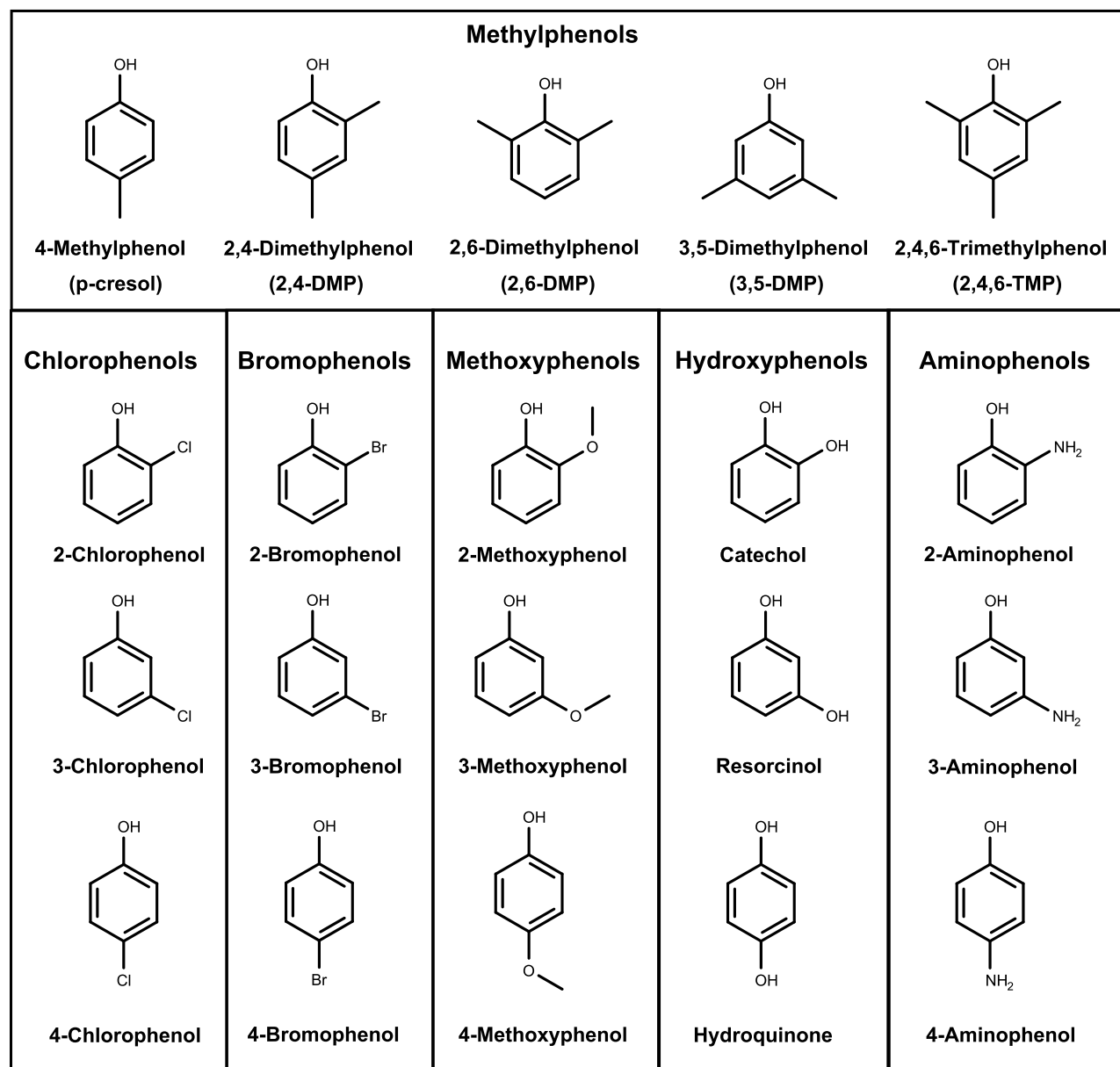


Figure 14: Phenolic model compounds investigated in this study. Besides different different methylphenols, chlorophenol, bromophenol, methoxyphenol, hydroxyphenol, and aminophenol were investigated as well.

3.2.2 Material and Methods

3.2.2.1 Chemicals, Instruments, and Analytical methods

The list of used chemicals can be found in Table AIII.1. Table AIII.2 shows a list of all instruments used in this study. Finally, the liquid and ion chromatography (LC & IC) methods used in this study, including the retention time of analytes, are shown in Table AIII.3 and Table AIII.4, respectively.

3.2.2.2 Production of ClO₂ and FAC

ClO₂ was produced on-site using the persulfate-chlorite method. The procedure has been described in the literature (Hupperich et al., 2020; Jütte et al., 2022; Terhalle et al., 2018). The concentration of ClO₂ solution was determined directly after production and before each experiment by direct measurement of the extinction at $\lambda = 359 \text{ nm}$ ($\epsilon_{359} = 1250 \text{ M}^{-1} \text{ s}^{-1}$ (Gates et al., 2009)). ClO₂ was stored in the dark at 4 °C with no headspace. Produced ClO₂ solutions were used until the concentration dropped below 80 % of the initial concentration. Additionally, possible residuals in the ClO₂ stock solution (ClO₂⁻, FAC, Cl⁻, and ClO₃⁻) were determined for every ClO₂ solution and later subtracted from the final results, as described in Hupperich et al. (2020) and Jütte et al. (2022). To determine FAC impurities in the ClO₂ stock solution, an aliquot of 5 mL ClO₂ stock solution was mixed with 15 mL of 100 mM glycine solution. This solution was bubbled by Nitrogen gas to remove ClO₂ for one hours until no absorption at $\lambda = 359 \text{ nm}$ could be observed. After ClO₂ was successfully removed, the FAC concentration was determined by measuring the Cl-Gly concentration, which were below the limit of detection (note that the sum of concentrations of all impurity anions were < 5% of the corresponding ClO₂ concentration, which also applies to persulfate). For further information about impurities in the ClO₂ solution, see Text AIII.1.

The FAC stock solution was prepared daily before every experiment. Therefore, a 15 % FAC solution was diluted (125 μL in 50 mL of pure water). The FAC concentration was determined by measuring the absorption at $\lambda = 292 \text{ nm}$ ($\epsilon_{359} = 350 \text{ M}^{-1} \text{ s}^{-1}$ (Abdighahroudi et al., 2020)). Note that the concentration was determined by measuring the concentration of OCl⁻, which is the dominant species in the pH > 10 ($pK_a = 7.54$ (Deborde and von Gunten, 2008)).

3.2.2.3 Intrinsic FAC formation

The formation of inorganic products from the reaction of ClO₂ with the different model compounds was determined by using the glycine method described in Abdighahroudi et al. (2020) with minor changes. In brief: A solution was prepared containing 5 mM phosphate buffer, 10 mM glycine, and

100 μM of the compound of interest, whereby the pH was adjusted to pH 7 (± 0.05). In this experiment, glycine was used as a selective scavenger for FAC, which results in chloro-glycine (Cl-Gly) formation. Aliquots of the stock solution were transferred into polypropylene (PP) reaction tubes, and ClO_2 was dosed in different concentrations (20 – 200 μM). After ClO_2 dosage and a reaction time of precisely 30 seconds, the sample was transferred into the temperature-controlled autosampler to slow down follow-up reactions (cooled at 5°C), followed up by injection of the sample into the ion chromatography (IC) system within five minutes to determine formed chlorine species (Cl^- , ClO_2^- , ClO_3^- , and Cl-Gly). Due to the high reaction rate of phenolic compounds toward ClO_2 , more than 99.9 % of the dosed ClO_2 concentration was consumed in less than two seconds (see Table AIII.5), and thus full ClO_2 consumption was always achieved. However, to avoid follow-up reactions of the scavenging product Cl-Gly and ClO_2^- a reaction time of 30 seconds was chosen. The time between dosing of ClO_2 and injection to IC was always precisely 5 min. This method uses the advantage of the fast reaction between FAC and glycine ($k_{\text{app}} = 10^5 \text{ M}^{-1} \text{ s}^{-1}$ at pH 7 (Deborde and von Gunten, 2008)) compared to the slower reactivity of FAC with phenolic compounds ($k_{\text{app}} = 10^1 - 10^3 \text{ M}^{-1} \text{ s}^{-1}$ at pH 7 (Deborde and von Gunten, 2008)). In addition, glycine is present in excess to model phenols so FAC mainly reacts with glycine.

To confirm that intrinsically formed FAC has been successfully scavenged by glycine within 5 min reaction time, an experiment was carried out to determine the recovery rate of FAC. Therefore, 100 μM FAC was added directly to one aliquot of the reaction solution, which was treated identically to the ClO_2 samples.

To monitor the stability of the chlorine balance 200 μM ClO_2 was added to one sample of 2,4-dimethylphenol and 2,6-dimethylphenol, respectively. The chlorine balances of both samples were measured five times in a row with a time interval of 40 minutes.

3.2.2.4 Stoichiometric ratios

In the present study, the stoichiometric ratios describe the number of ClO_2 molecules reacting with one molecule of the model compound under study. To determine the stoichiometric ratios, aliquots of the samples described above (Chapter 3.2.2.3 Intrinsic FAC formation) were transferred to the HPLC system described in Table AIII.2, and the degradation of the model compounds was measured. A plot of model compound degradation vs. the ClO_2 consumption (molar scale) yields a linear function with the slope representing the reciprocal stoichiometric ratio.

3.2.3 Results and discussion

3.2.3.1 Effect of substituents in different locations

The effect of different methyl groups attached at different positions to the phenol on the reaction mechanism was studied. For all investigated compounds, a FAC recovery between 90 – 110 % was measured (Text AIII.2 & Figure AIII.2), showing that reliable information about intrinsic FAC yields can be achieved. The detailed chlorine balances for different ClO₂ dosages and the stoichiometric ratios of these compounds are shown in Figure AIII.3 and Figure AIII.4. For all methylphenols, a stoichiometric ratio of 2 molecules of ClO₂ per consumed molecule of the compound under study was observed at pH 7. This is in accordance with the stoichiometric ratio of the ClO₂ reaction with unsubstituted phenol (Rougé et al., 2018; Terhalle et al., 2018; Wajon et al., 1982). Therefore, it seems that, independent of their position, methyl substituents do not affect the main reaction mechanism. Figure 15 shows the established chlorine balances (sum of ClO₂⁻, Cl⁻, ClO₃⁻, and FAC) for the model compounds, which contain additional methyl substituents to the phenolic moiety and vanillin. It was possible to establish a fairly complete chlorine balance for all compounds. The reaction of all methylated phenolic compounds resulted in expected yields of ClO₂⁻ (49.5 ± 3.1 %) and FAC (46.9 ± 6.3 %), which follows the reported data for phenol itself and the proposed two-step reaction mechanism (Rougé et al., 2018; Terhalle et al., 2018; Wajon et al., 1982). Only the *para*-substituted compounds (4-methylphenol, 2,4-dimethylphenol, 2,4,6-trimethylphenol, and vanillin) are showing lower FAC yield, whereby the observed effect in case of 2,4,6-trimethylphenol was only minor. For example, vanillin displayed FAC formation, albeit at lower yields compared to the other model compounds (20 – 25 %). This observation contradicts the results reported by Hupperich et al., where no FAC formation from the reaction of ClO₂ with vanillin was detected (Hupperich et al., 2020).

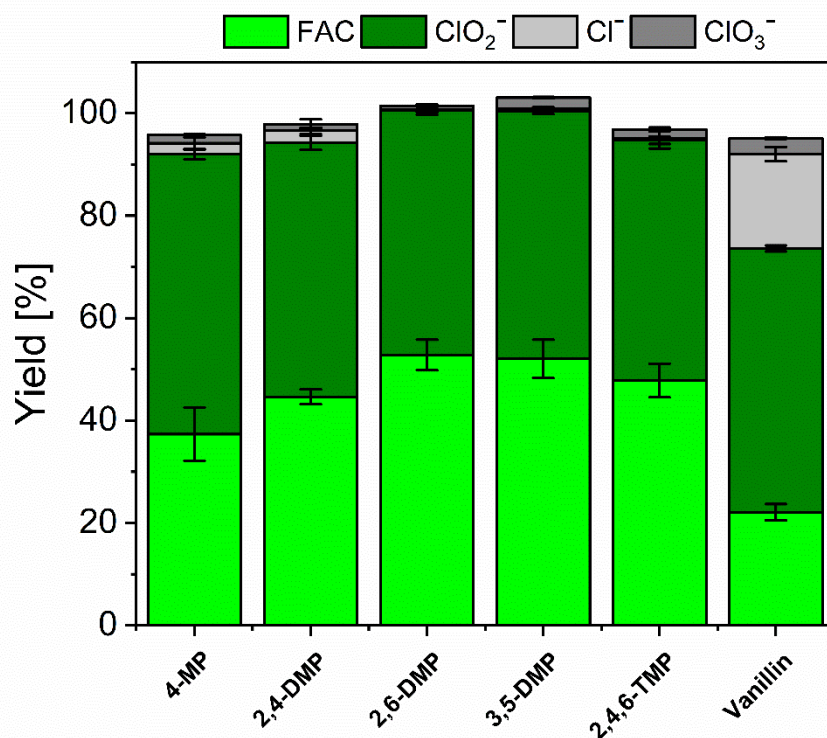


Figure 15: Chlorine balance of methyl-substituted compounds. The reaction solution contained 0.1 mM of the compound under study, 5 mM phosphate buffer to retain the pH at 7, and 10 mM glycine to scavenge intrinsically formed FAC. ClO₂ was dosed in six different ratios to the model compounds (4-MP: 4-Methylphenol, 2,4-DMP: 2,4-dimethylphenol, 2,6-DMP: 2,6-dimethylphenol, 3,5-DMP: 3,5-dimethylphenol, 2,4,6-TMP: 2,4,6-trimethylphenol, and vanillin), and each ratio was carried out in triplicates. This figure shows the mean values of all 18 measurements, and the error bars represent the standard deviation of those.

The disparity can be explained by the different reaction times between the dosing of ClO₂ and analysis. Hupperich et al. dosed ClO₂ to all samples simultaneously, followed by a reaction time of at least 30 minutes before analysis (2020). Furthermore, some samples resided in the room-temperature autosampler queue for several hours. This reaction time may have resulted in the consumption of formed Cl-Gly, which would have indicated the formation of FAC. The reason for this observation was investigated based on the differences between 2,4-dimethylphenol and 2,6-dimethylphenol reactions with ClO₂:

Chapter 3.2: Reaction mechanism of chlorine dioxide with phenolic compounds – Influence of different substituents on stoichiometric ratios and intrinsic formation of free available chlorine

In this experiment, 2,4-dimethylphenol resembles the location of the substituents in vanillin. While the chlorine balance for 2,6-dimethylphenol can be considered to be constant, for 2,4-dimethylphenol the concentration of Cl-Gly decreases over time, whereby the concentration of Cl⁻ increases. It has to be noted that the overall chlorine balance of 2,4-dimethylphenol decreases over time (Figure 16).

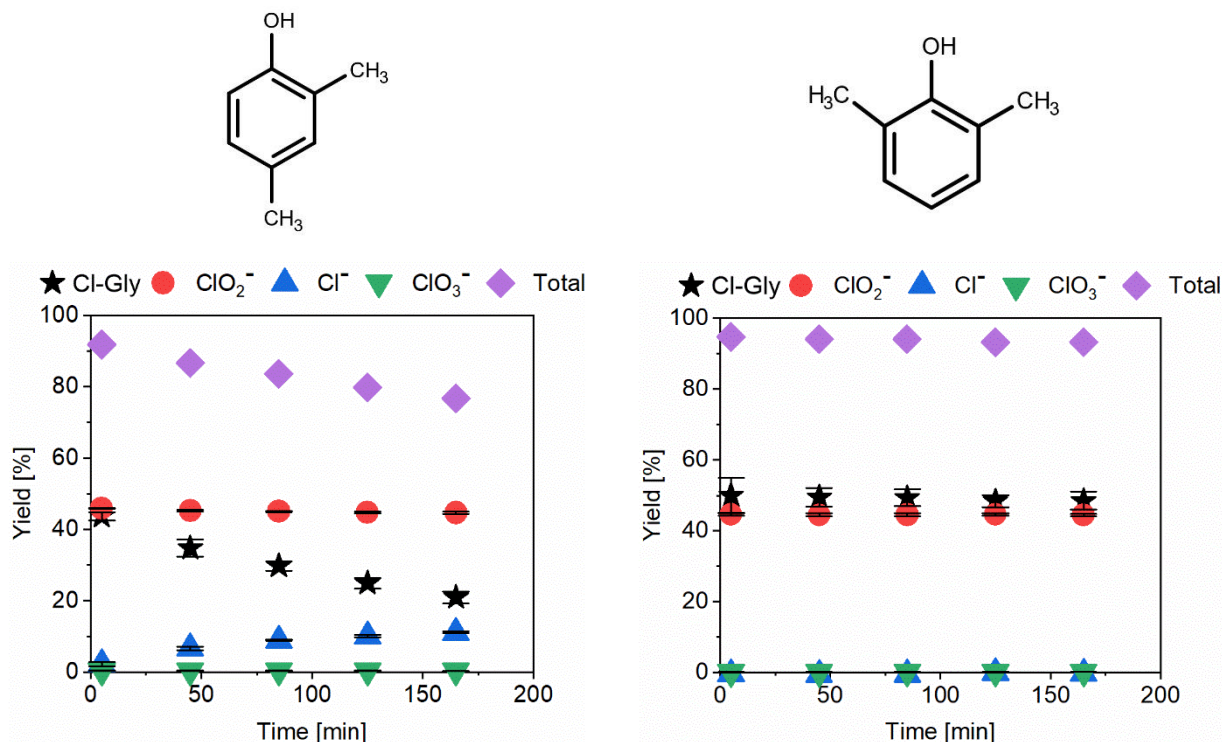


Figure 16: Repetitive measurement of the same sample of 2,4-dimethylphenol (left) and 2,6-dimethylphenol (right) after dosing 200 μM ClO₂. The samples contained 200 μM compound under study, 10 mM glycine, and 5 mM phosphate buffer at pH 7. The first sample was treated identically to the previous experiments. After each injection, the sample remained in the autosampler at 5 °C and was measured five times in a row. The time between every injection was 40 minutes.

It can be assumed that ClO₂ reacts with 2,4-dimethylphenol via electron abstraction to form ClO₂⁻ in the first step (yield of 50 %). The ensuing phenoxy radical reacts fast with another molecule of ClO₂ and forms an OClO-adduct in *ortho*-position, which then cleaves FAC and forms an *ortho*-benzoquinone (*ortho*-BQ). This hypothesis is supported by literature, where *ortho*-BQ formation is reported during oxidation of *para*-substituted phenols by potassium nitrosodisulfonate (Teuber reaction), an oxidant which also reacts via electron abstraction (Zimmer et al., 1971). The formed *ortho*-BQ has dienic and dienophilic characteristics and undergoes e.g., polymerization (Diels-Alder reaction) (Bruins et al., 2018; Mazza et al., 1974). Therefore, *ortho*-BQ can be assumed to

be very reactive and unstable. However, the reported data about *ortho*-BQ stability is very limited. Therefore, it may be intrinsically formed in the reactions of *para*-substituted phenols with ClO₂ and immediately react with Cl-Gly (Figure 17), which would result in an underestimation of the FAC yield. Chloramines are known for their instability and reactivity (Heeb et al., 2017) and, thus, may be a favored reaction partner of *ortho*-BQ. Due to the high stability of Cl-Gly after 2,6-dimethylphenol oxidation, it can be assumed that contradictory to *ortho*-BQ, *para*-BQ shows no reactivity towards Cl-Gly. This shows that *para*-substitution or *ortho*-/ and *para*-substitution do not affect the FAC formation in general, albeit it reduces the detected FAC. However, immediate analysis of Cl-Gly, as done in this study, may have partially prevented the Cl-Gly scavenging by *ortho*-BQ, and intrinsically formed FAC could indeed be measured (note that the actual FAC yield may be higher than measurements here). Additionally, the autosampler cooling slows the reaction kinetics of Cl-Gly further down, which may have enabled Cl-Gly determination in this study. Note that the direct reaction of FAC with *ortho*-BQ can be ruled out by the nearly full chlorine balance after 5 min of reaction time. This indicates that FAC was successfully scavenged by glycine and did not undergo side reactions with *ortho*-BQ.

The results indeed suggest that Cl-Gly reacts with a transformation product of 2,4-dimethylphenol (postulated to be an *ortho*-BQ) and forms Cl⁻, which would explain the high Cl⁻ yields (35.34 ± 1.03 %) reported by Hupperich et al. for vanillin (2020). The increasing gap in the chlorine mass balance over time may indicate the formation of chlorinated organic compounds through chlorine transfer from Cl-Gly to *ortho*-BQ. Similar trends have been observed for other *para*-substituted phenols (Figure AIII.5). Another observation is that the UV absorption spectra of both reaction solutions 20 seconds after dosage show formation of a peak between 400 and 450 nm. This spectrum, in the case of the 2,6-dimethylphenol reaction solution, remained almost unchanged for 5 min of reaction time. In contrast, the absorption spectra for 2,4-dimethylphenol reaction change significantly. In that, the before-mentioned peak completely disappears after 5 minutes, and a new maxima forms between 500 and 550 nm (Figure AIII. 6). Additionally, the color of the samples turned visibly pink. This may be explained by a bathochromic shift due to the before-mentioned polymerization of *ortho*-BQ, which result in an extension of the conjugated π-systems (Su, 2013), further proving the formation of *ortho*-BQ as a transformation product of this reaction. Meanwhile, for 2,6-dimethylphenol, which forms *para*-BQ, the spectrum remains almost unchanged for 5 min of reaction time, and the peak at 400 – 450 nm stays constant.

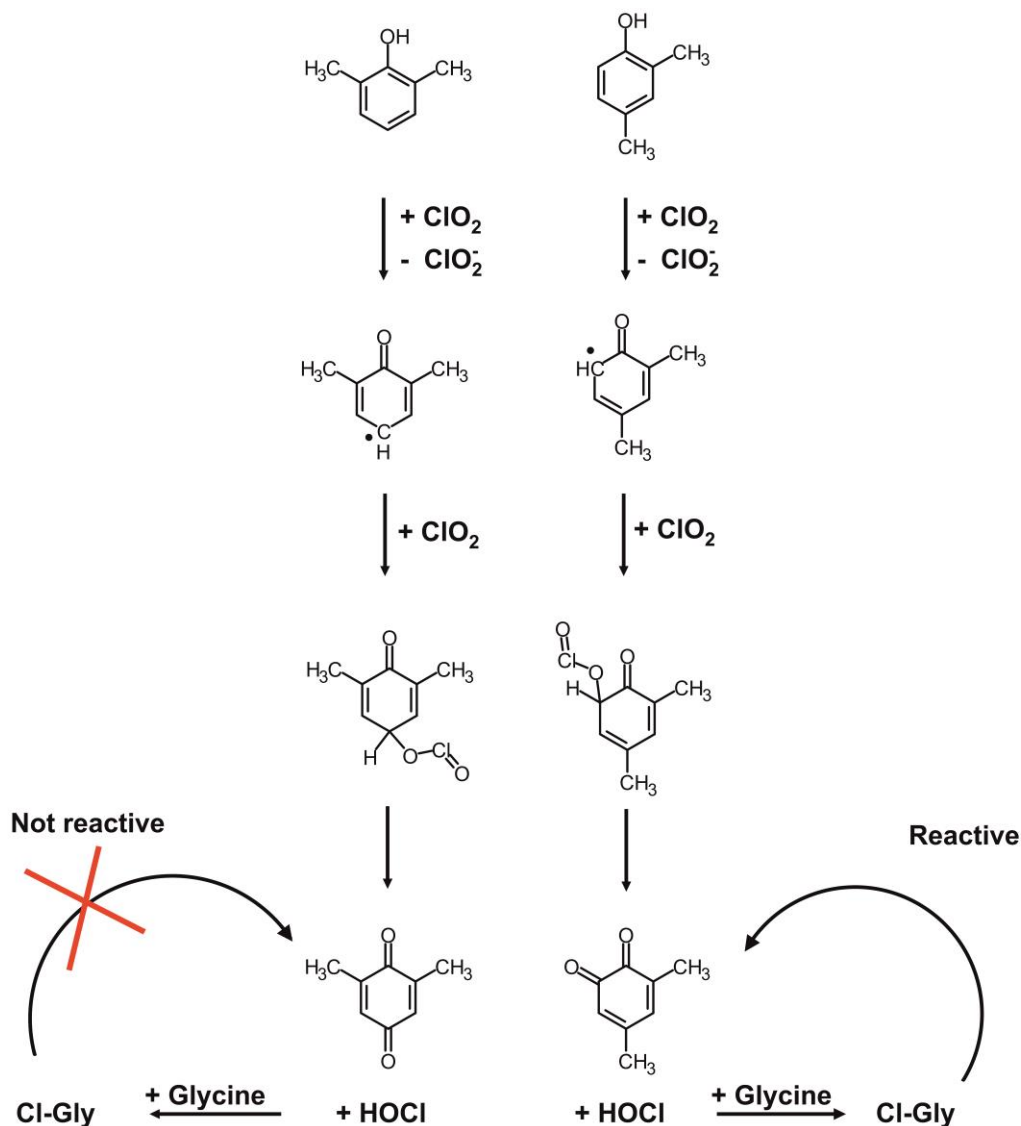


Figure 17: Postulated pathway of *para*-unsubstituted phenolic moieties (e.g., 2,6-dimethylphenol) compared to *para*-substituted phenolic compounds (e.g., 2,4-dimethylphenol) reacting with ClO₂.

It seems contradictory that the recovery rate of FAC for all compounds reported in this study is close to 100 % (Figure AIII.2). However, *ortho*-BQ as a transformation product does not exist in the performed recovery test. The model compounds themselves react slowly with FAC and chloramines (Deborde and von Gunten, 2008; Heeb et al., 2017). Therefore, glycine is a suitable scavenger, and Cl-Gly remains stable over a relatively long time in the presence of the compounds studied in our work (see Figure 16). However, some products from the reaction of ClO₂ with the

compounds under study may be quite reactive with Cl-Gly, such as (presumably) *ortho*-BQ. This might explain the low stability of Cl-Gly, e.g., in the case of ClO₂ reactions with 2,4-dimethylphenol.

It can be concluded that in the case of non *para*-substituted phenolic compounds, the formation of *para*-BQ is favored, leading to 50% FAC and 50% ClO₂⁻ formation, as shown for 2,6- and 3,5-dimethylphenol. If the *para*-position is substituted by a methyl group, *ortho*-BQ might be formed, which seems to cause the degradation of Cl-Gly. Taking the potential losses of Cl-Gly within the first five minutes into account, it can be stated that the formed FAC yields of *para*-substituted phenolic compounds are higher than the measurements. It seems reasonable that for all investigated compounds FAC is formed in a two-step mechanism that forms 50% ClO₂⁻ and 50% FAC shown in Figure 17. The reason for the fast initial degradation of Cl-Gly in the case of vanillin might be explained by the formation of a more reactive *ortho*-BQ, due to the substituents.

The results of 2,4,6-trimethylphenol seem to contradict the statement above since the degradation of Cl-Gly is relatively slow. However, this can be explained by a different reaction mechanism in case the *para*-position and both *ortho*-positions are occupied. In this case, no *H* is available, which is necessary for FAC formation. However, in this study, 50% FAC formation was observed, which indicates that FAC formation is possible even if *H* is substituted (e.g., by alkyl groups) at all possible locations where carbon-centered radicals could exist. In addition, the chlorine balance shows similar stability as the chlorine balance of 2,6-dimethylphenol (Figure AIII.5b). This shows that no reactive species is formed in this reaction, which would react with Cl-Gly.

3.2.3.2 Effect of different functional substituents

Figure 18 shows the chlorine balance of phenolic compounds with different functional groups attached to the aromatic ring. It can be stated that most of the compounds under study showed a yield of around 50% FAC and 50% ClO₂⁻. In the case of chloro-, bromo-, and methoxyphenol, no significant change in FAC formation can be observed independent of the substituent or the position. The stoichiometric ratios of all compounds were determined, and the results are shown in the ESI (methoxyphenols Figure AIII.7, chlorophenols Figure AIII.8, bromophenols Figure AIII.9, hydroxyphenols Figure AIII.10, aminophenols Figure AIII.11). All methoxyphenols, chlorophenols, bromophenols, and resorcinol show a ≈ 2:1 stoichiometric ratio (2 molecules of ClO₂ react with 1 molecule of the model compound). This is in accordance with the results of

methylphenols and with literature also reporting a 2:1 stoichiometry for phenol and vanillin (Hupperich et al., 2020; Terhalle et al., 2018). The achieved results follow the two-step reaction mechanism proposed by Wajon et al. (1982). This observation indicates that the number and position of these aromatic ring substituents do not affect the stoichiometry. It is noteworthy that all investigated compounds, that form FAC show a 2:1 stoichiometry.

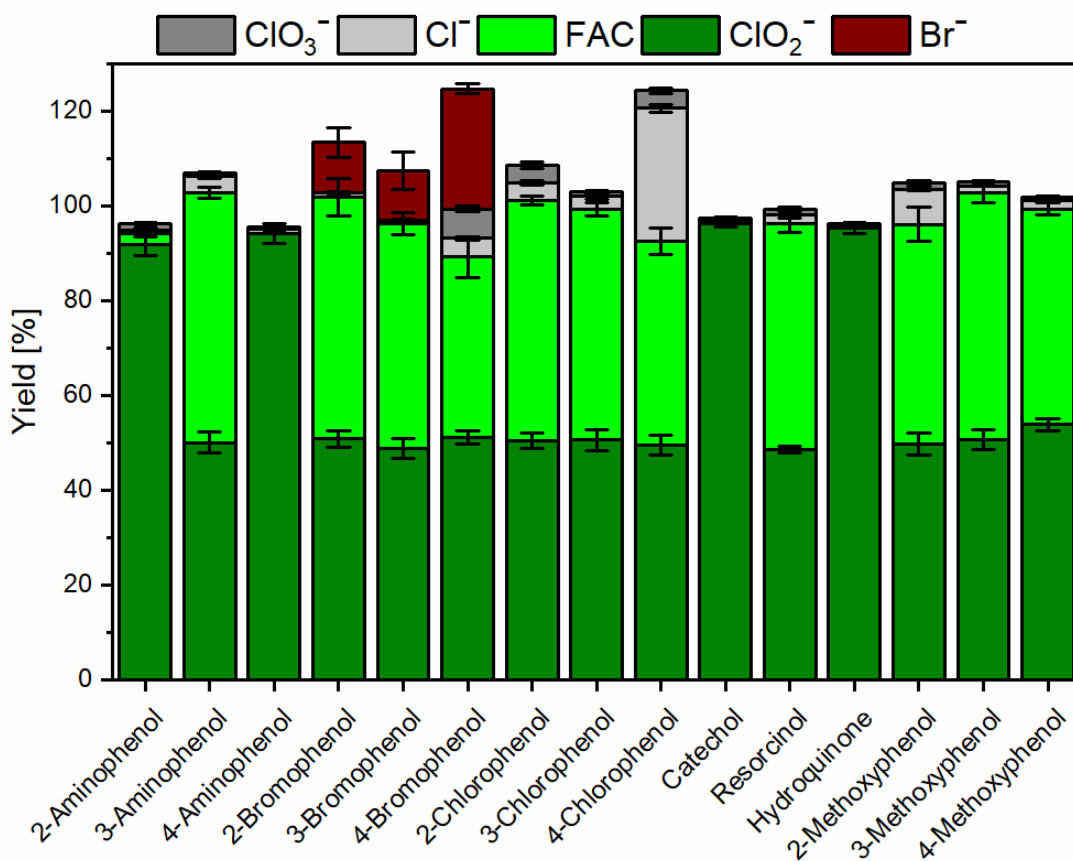


Figure 18: Chlorine balances of the phenolic compounds which contain an amino-, hydroxyl, methoxy, bromo-, or chloro-substituent. The reaction solution contained 0.1 mM of the compound under study, 5 mM phosphate buffer to keep a constant pH of 7, and 10 mM glycine to scavenge intrinsically formed FAC. ClO₂ was dosed in six different ratios to the model compounds and each ratio was carried out in triplicates (see Figure AIII.7 – Figure AIII.11). Here the mean values of all 18 measurements are shown and the error bars represent the standard deviation. Note that due to the dose-dependent results of resorcinol (see Figure AIII.10), the results in the case of resorcinol shown in this figure display the results for the lowest dose of ClO₂ (0.02 mM).

3.2.3.2.1 Halogenated phenols

In literature, it was reported that *para*-substituted phenols are oxidized by the Teuber reaction (electron transfer) to form *ortho*-BQ. However, if the *para*-substituent is chlorine the mechanism changes. In that case, *para*-BQ is formed by additional loss of chlorine (Zimmer et al., 1971). If this applies to ClO₂, one would assume a chlorine balance of 50 % ClO₂⁻, 50 % FAC, and 50 % Cl⁻ for 4-chlorophenol. However, the Cl⁻ yields are only ≈ 30 % per consumed ClO₂. This indicates that the phenoxy radical, can be established both in *ortho*-/ and *para*-position (Figure 19 Step 1). In the second step, two different pathways may follow, i.e., 50 % reaction in the *ortho*-position and 50 % in the *para*-position. The phenoxy radical in *ortho*-position further reacts to form *ortho*-BQ and FAC (Step 2a & 3a). Afterward the *ortho*-BQ may react with Cl-Gly (formed by scavenging FAC), yielding Cl⁻ (Step 4a), in accordance with 2,4-dimethylphenol. In *para*-position, the second step causes the formation of *para*-BQ and dichlorine monoxide (Cl₂O) (Steps 2b & 3b). Cl₂O reacts with water to form two molecules of FAC (Step 4b) (Renard and Bolker, 1976). Eventually, four molecules of ClO₂ react with two molecules of 4-chlorophenol forming two molecules of ClO₂⁻, two molecules of FAC, and one molecule of Cl⁻. The stability of the chlorine balance over time (Figure AIII.5c) might be explained by full consumption of *ortho*-BQ since Cl-Gly will be three times in excess over *ortho*-BQ. Another reason for the reduced recovery of chlorine might be the very strong chlorinating characteristic of Cl₂O (Sivey et al., 2010), which may have occurred in this reaction. The assumption of both pathways taking place originates from the determined chlorine balance. If the reaction only proceeded through pathway A, no yields of Cl⁻ should be detected, and the chlorine balance would not be stable over time. On the other hand, if pathway B was dominant, 50 % Cl⁻ should be detected. The detected yields of Cl⁻ are around 25 %, thus a combination of both pathways seems likely.

To provide further evidence for the postulated reaction mechanism for 4-chlorophenol, 4-bromophenol was investigated as well. It was expected that, if the postulated mechanism is indeed taking place, the excess of Cl⁻ in the case of 4-chlorophenol should resemble the bromide (Br⁻) yields in the case of the reaction of ClO₂ with 4-bromophenol. If ClOBr is formed, it may react, similar to Cl₂O, with water to form HOCl and HOBr. HOBr is known to react 2 – 3 orders of magnitude faster with primary amines than HOCl, causing the formation of *N*-bromo amines (Heeb et al., 2017; Jütte et al., 2023). In the reaction with glycine bromo-glycine (Br-Gly) is formed, which is a very reactive compound (Wajon and Morris, 1982). Additionally, Hawkins et al. gave

Chapter 3.2: Reaction mechanism of chlorine dioxide with phenolic compounds – Influence of different substituents on stoichiometric ratios and intrinsic formation of free available chlorine

evidence that *N*-bromo amines undergo decomposition (2005). Either way, the cleaved Br turns into Br⁻. This is in agreement with literature which has reported the FAC and Br⁻ formation in the reaction of ClO₂ with bromide-containing DBPs (Han et al., 2021). The summarized results in Figure 18 and detailed results in Figure AIII.9c are indeed showing that around 25 % of Br⁻ is formed per dosed ClO₂ (molar concentration). The postulated mechanism for 4-bromophenol is shown in Figure AIII.12. In the case of 2- and 3-bromophenol the Br⁻ formation was only minor since *para*-BQ formation does not require *C-Br* cleavage, which again agrees with the results of the corresponding chlorophenols indicating a preferred pathway at the unoccupied *para*-position.

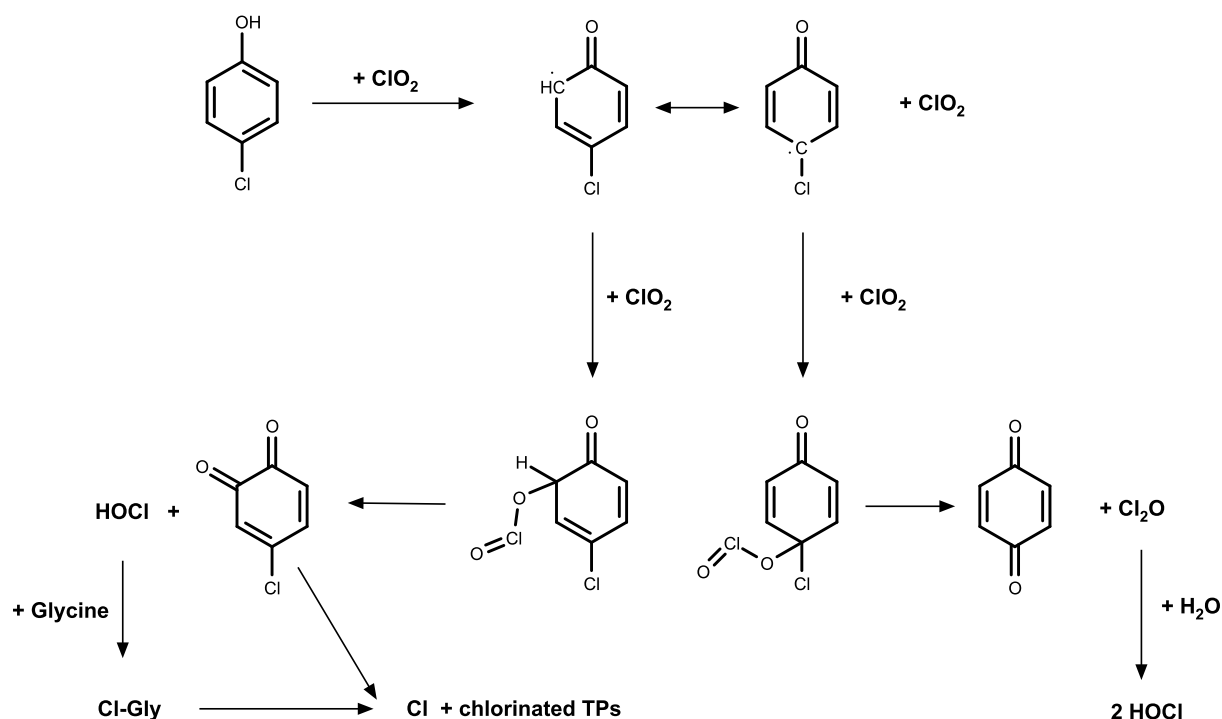


Figure 19: Postulated reaction mechanism of 4-chlorophenol with ClO₂.

3.2.3.2.2 Hydroxyphenols

In case of OH-groups as substituents for *H* in *ortho*- or *para*-position, a significant effect on FAC formation could be observed. For instance, hydroquinone and catechol show ClO_2^- yields of almost 100 % and 0 % FAC. This is in accordance with reported literature data, which shows that ClO_2^- is by far the dominant product of these compounds (Gan et al., 2019; Hupperich et al., 2020). However, resorcinol, which contains the same substituents but in *meta*-position, resulted in 50 % FAC formation. The reason for this observation is that the phenoxy radical, which is formed in the first step of this reaction, cannot localize in the *meta*-position (Figure AIII.1), where the second hydroxyl group of resorcinol is located. Thus, it can be stated that if the radical can be localized at the same *C*-atom which is connected to the second hydroxyl-substituent, the reaction mechanism changes, and no FAC formation is observed, which in turn means that *meta*-substituents do not change the reaction pathway.

Wajon et al. postulated a two-time electron transfer mechanism in the case of hydroquinone (Wajon et al., 1982). Based on this mechanism, the chlorine balance of resorcinol should also consist of 100 % ClO_2^- , since the second electron transfer should happen independently of the location of the second hydroxyl-group. However, as shown in Figure 18 50 % ClO_2^- and 50 % FAC could be detected in case of resorcinol. Thus a different pathway based on *OCIO*-addition can be postulated (Figure 20). In the first step, an electron transfer takes place, which is in accordance with unsubstituted phenol. In the second step, the *OCIO*-adduct is formed at the *C*-bonded to the second hydroxyl substituent. Afterward, the hydroxyl group cleaves *H* and forms a double bond to yield *para*-BQ. The cleaved hydrogen bonds to *OCIO* and forms HClO_2 , which dissociates at pH 7 to ClO_2^- ($\text{p}K_a = 1.97$ (Gordon et al., 1972)). It also seems that the second hydroxyl-group in *ortho*-/ or *para*-position stabilizes the carbon-centered radical in *ortho*-/ or *para*-position, respectively, which contradicts the results observed for methyl-substituents. Otherwise, yields of FAC formation should be observed in the case of hydroquinone and catechol.

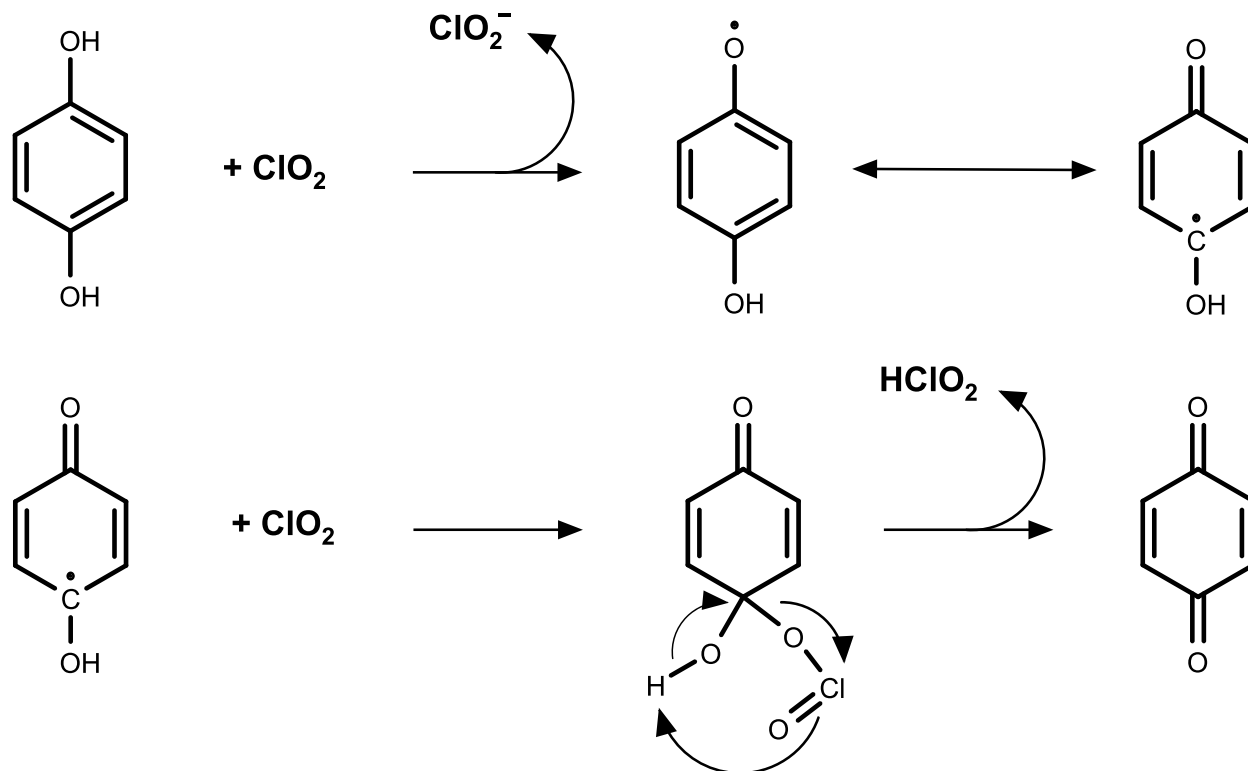


Figure 20: Postulated reaction mechanism of Hydroquinone with ClO_2 . The first attack occurs by electron abstraction. In the second step, the unstable OClO-adduct abstracts the hydrogen of the hydroxyl group and cleaves as HClO_2 .

Resorcinol is the only investigated compound in this study that showed a clear trend of decreasing FAC formation with increasing doses of ClO_2 (Figure AIII.10b). Additionally, the overall chlorine balance decreases at higher concentrations of ClO_2 . Insufficient scavenging of FAC by glycine was ruled out by an analogous experiment with a 10-fold increased concentration of glycine to 100 mM (Figure AIII.13), resulting in only slightly higher FAC yields. However, the trend of decreasing total chlorine balance remains similar in the experiments with different glycine concentrations. Thus, it seems that FAC (in the form of Cl-Gly) is escaping detection. Based on the observations above, it seems likely that the reaction of resorcinol with ClO_2 forms a transformation product with a high reactivity towards FAC and/or Cl-Gly and forms a chlorinated transformation product. This phenomenon was not observed in the case of the other hydroxyphenols since no FAC formation was detected in the case of hydroquinone and catechol.

The hydroxyphenols, hydroquinone and catechol are known to undergo autoxidation (James et al., 1938; Schüsler-Van Hees et al., 1985). It has been reported that the autoxidation of hydroquinone causes the formation of superoxide radicals ($O_2^{\bullet-}$) (Cadenas et al., 1988; Eyer, 1991). These radicals are in general reactive towards ClO_2 ($k(ClO_2 + O_2^{\bullet-}) 3 \times 10^9 M^{-1} s^{-1}$ at $pH > 6$) (Huie and Neta, 1986). Therefore, the stoichiometry might be biased by the formation of $O_2^{\bullet-}$. The results at $pH 7$ (Figure AIII.10) indeed show abnormality compared to the other compounds under study, whereby the stoichiometry increases to $\approx 1:4.5$, which means that 4.5 molecules of ClO_2 are reacting with one molecule of the model compound. It is known that autoxidation is pH-dependent and slower at low pH (La Mer and Rideal, 1924; Reinders and Dingemans, 1934), since autoxidation is controlled by the twice deprotonated hydroquinone species (James et al., 1938). Thus, to confirm that the increased ClO_2 demand is caused by the autoxidation a pH-dependent stoichiometry was determined for these compounds. Note that the stoichiometry could only be measured at pH values ≤ 7 , due to the too-fast autoxidation at higher pH values (Figure AIII.14). The results (Figure AIII.15) confirm that a pH-dependent stoichiometry for hydroquinone and catechol. Hydroquinone has a stoichiometry of 2:1 at $pH \leq 6$ and catechol shows a stoichiometry of 3:1 at $pH \leq 5$. Note that for resorcinol no pH-dependent autoxidation (Figure AIII.14) and stoichiometry were detected (Figure AIII.15).

The observed pH-dependent ClO_2 demand can be explained by the Hydroquinone cycle (Figure 21). Hydroquinone can be autoxidized by O_2 and form semiquinone (SQ) and $O_2^{\bullet-}$ ($K = 10^{-14}$ (Eyer, 1991)) (Step 1). SQ can further react with O_2 (Step 2) to form *para*-BQ and another $O_2^{\bullet-}$ ($k_{app}(SQ + O_2) = 5 \times 10^4 M^{-1} s^{-1}$ at $pH 7$ (Eyer, 1991)). If hydroquinone is present in excess, it can react with *para*-BQ ($k_{app}(\text{Hydroquinone} + \text{BQ}) = 58 M^{-1} s^{-1}$ at $pH 7$ (Rodríguez and von Gunten, 2020; Yamazaki and Ohnishi, 1966)) to reform SQ (Step 3). SQ can either be autoxidized back to *para*-BQ (Step 2) or may react with an electron donating compound (e.g., glycine) and reform hydroquinone (postulation) (Step 4) and react again as described in Step 1. The generation of $O_2^{\bullet-}$ might be the reason for the high ClO_2 demand at pH levels above 6. $O_2^{\bullet-}$ reacts fast with ClO_2 and forms ClO_2^- (Huie and Neta, 1986). Thus, hydroquinone and $O_2^{\bullet-}$ are competing for ClO_2 , which causes higher observed ClO_2 demand per hydroquinone degradation. This is further underlined by the fact that high ClO_2 demands are only observed at pH values that favor autoxidation (compare Figure AIII.14 and Figure AIII.15). Thus, without autoxidation at low pH, no $O_2^{\bullet-}$ are formed, and excessive ClO_2 consumption does not take place. The reaction of hydroquinone with *para*-BQ is

also reported to be pH-dependent (Yamazaki and Ohnishi, 1966). Therefore, step 3 also does not take place at lower pH. Additionally, autoxidation is reported to be accelerated by increased *para*-BQ concentrations (Eyer, 1991; Ishii and Fridovich, 1990; Roginsky et al., 1999). The determined chlorine balance did not show any significant change at pH 4 (Figure AIII.16), which also indicates that the high ClO₂ demand occurred by side reactions and not from the main reaction pathway with hydroxyphenols.

The 3:1 stoichiometry of catechol at low pH values can be explained by the formation of *ortho*-BQ, which has been confirmed as unstable and reactive compound. Therefore, it seems very likely that *ortho*-BQ also reacts with ClO₂ in a similar reaction rate as catechol at pH ≤ 6 and thus increases the observed stoichiometry.

Note that the experiments for determining the stoichiometric ratios of hydroquinone and catechol at pH 7 were also carried out in the absence of glycine (no FAC-scavenger was needed since no FAC was formed). In the case of hydroquinone, the stoichiometry changes from 1:4 (with glycine) to 1:3 (without glycine) (Figure AIII.17). On the other hand, the stoichiometry of catechol does not change in the presence or absence of glycine at pH 7 (Figure AIII.17). The change in stoichiometry can be explained again by the instability of hydroquinone (Figure AIII.14). The concentration of hydroquinone in the sample without any ClO₂ addition already shows a loss 20 % of the expected concentration. This drop in concentration may decrease the slope of the hydroquinone degradation vs. ClO₂ dose mimicking a lower ClO₂ consumption. The reason for this observation is the autoxidation of hydroquinone by O₂ (Eyer, 1991; Reinders and Dingemans, 1934). It seems that glycine has a stabilizing effect on the unstable model compound hydroquinone. In the presence of glycine, the autoxidation of this compound is slower compared to the absence of glycine (data not shown). This phenomenon is not fully understood yet and needs further investigation.

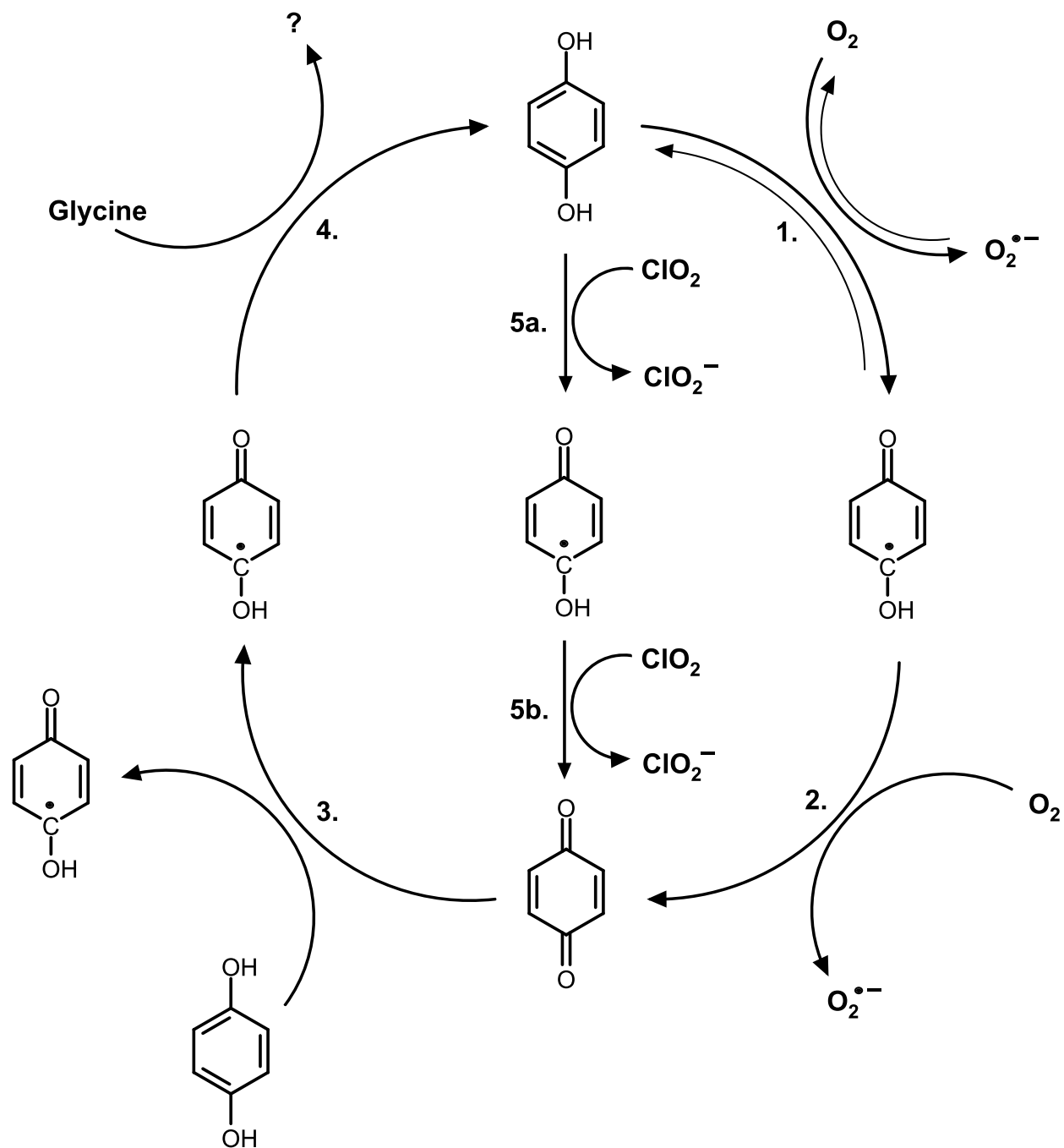


Figure 21: Hydroquinone cycle. Hydroquinone is autoxidized by O₂ to form *para*-BQ and O₂^{•-}. BQ can react with hydroquinone to form SQ, which again can be turned into hydroquinone. This cycle can be cut by adding an excess of ClO₂ over hydroquinone.

3.2.3.3.3 Aminophenols

The same reaction behavior of hydroxyphenols was observed for the group of aminophenols. In the case of *ortho*- and *para*-aminophenol, nearly 100 % ClO_2^- was detected, and for *meta*-aminophenol, 50 % FAC was measured. Based on the results, it can be postulated that the reaction mechanism of aminophenols is similar to hydroxyphenols, as shown in Figure 20. As a result, the formation of quinone imines is likely. In the case of aminophenols, the electron transfer reaction (first reaction step) may happen at the amine or hydroxyl group. Thereby the attack at the amines seems to be more likely, due to the higher reaction kinetics of aniline towards ClO_2 compared to phenol at pH 7 (Neta et al., 1988). However, the first point of attack would not affect FAC formation since the reaction mechanism of aniline and phenol with ClO_2 is also postulated to be similar (Aguilar et al., 2014, 2013).

In the case of aminophenols, the slope of the aminophenol degradation over dosed ClO_2 concentration is non-linear (Figure AIII.11). It seems that competing reactions are taking place, whereby a transformation product from the first reaction step is as reactive as the aminophenol itself. In fact, it has been reported that the reaction of aminophenols can form iminoquinones, which are highly reactive toward primary amines (Barry et al., 1988; Bruins et al., 2018). Similar to hydroxyphenols, aminophenols also undergo autoxidation, which increases at elevated pH and temperature (Oancea and Puiu, 2003). It seems reasonable that occurring side reactions biased the observed stoichiometry and no general statements on stoichiometric ratios can be made.

Table 11 summarizes all the achieved data obtained in this study and compares it with known literature data for the same model compounds. It can be stated that the data on FAC formation is quite limited or not investigated in most cases. However, the results are in accordance with most of the data regarding the ClO_2^- yields.

Chapter 3.2: Reaction mechanism of chlorine dioxide with phenolic compounds – Influence of different substituents on stoichiometric ratios and intrinsic formation of free available chlorine

Table 11: Different yields of chlorine species and reaction stoichiometry achieved in this study compared with literature data.

| Compound | Yield [%] | | | | Sum [%] | Stoichiometry ClO ₂ :Compound | Ref |
|------------------------------|-----------|-------------------------------|-----------------|-------------------------------|---------|---|------------|
| | FAC | ClO ₂ ⁻ | Cl ⁻ | ClO ₃ ⁻ | | | |
| Phenol | 42 ± 3 | 62 ± 4 | – | – | 104 | 2:1 | a) |
| | ≈ 50 | ≈ 50 | – | – | 100 | n.d. | b) |
| | – | 50 | – | – | 50 | 2.4:1 | c) |
| 4-Methylphenol | 37 ± 2 | 55 ± 2 | 2 ± 1 | 2 ± 0 | 96 | 2.44 (± 0.01) :1 | This study |
| 2,4-Dimethylphenol | 45 ± 1 | 50 ± 3 | 2 ± 0 | 1 ± 0 | 98 | 2.35 (± 0.03) :1 | This study |
| 2,6-Dimethylphenol | 53 ± 2 | 48 ± 2 | < 1 | 1 ± 1 | 103 | 2.11 (± 0.02) :1 | This study |
| 3,5-Dimethylphenol | 52 ± 4 | 48 ± 1 | < 1 | 2 ± 0 | 103 | 2.05 (± 0.02) :1 | This study |
| 2,4,6-Trimethylphenol | 48 ± 3 | 47 ± 1 | < 1 | 2 ± 0 | 97 | 1.97 (± 0.06) :1 | This study |
| Hydroquinone | – | 95 ± 1 | 1 ± 0 | < 1 | 96 | pH dependent† | This study |
| | – | 90 | – | – | 90 | 3:1 | d) |
| | – | 100 | – | – | 100 | 1.6:1 | c) |
| Catechol | – | 96 ± 1 | 1 ± 0 | 1 ± 0 | 97 | pH dependent‡ | This study |
| | n.d. | ≈ 70 | n.d. | ≈ 5 | 75 | n.d. | e) |
| Resorcinol | 36 ± 3 | 50 ± 0 | 1 ± 0 | 1 ± 0 | 88 | 2.54 (± 0.06) :1 | This study |
| | n.d. | ≈ 46 | n.d. | < 1 | 50 | n.d. | e) |
| 2-Bromophenol | 51 ± 4 | 51 ± 2 | 1 ± 0 | < 1 | 103 | 2.44 (± 0.04) :1 | This study |
| 3-Bromophenol | 47 ± 2 | 49 ± 2 | 1 ± 0 | < 1 | 97 | 2.08 (± 0.08) :1 | This study |
| 4-Bromophenol | 38 ± 4 | 51 ± 1 | 4 ± 0 | 6 ± 1 | 99 | 2.36 (± 0.05) :1 | This study |
| 2-Chlorophenol | 51 ± 1 | 51 ± 2 | 4 ± 0 | 4 ± 1 | 108 | 2.21 (± 0.02) :1 | This study |
| 3-Chlorophenol | 49 ± 1 | 51 ± 2 | 3 ± 1 | 1 ± 0 | 103 | 2.15 (± 0.24) :1 | This study |
| 4-Chlorophenol | 43 ± 3 | 50 ± 2 | 28 ± 1 | 4 ± 1 | 125 | 2.23 (± 0.03) :1 | This study |
| 2-Methoxyphenol | 46 ± 4 | 50 ± 2 | 7 ± 0 | 1 ± 1 | 105 | 2.39 (± 0.01) :1 | This study |
| 3-Methoxyphenol | 52 ± 2 | 51 ± 2 | 2 ± 0 | < 1 | 105 | 2.18 (± 0.04) :1 | This study |
| 4-Methoxyphenol | 45 ± 1 | 54 ± 1 | 2 ± 0 | < 1 | 102 | 2.19 (± 0.01) :1 | This study |
| | n.d. | ≈ 40 | n.d. | ≈ 2 | 52 | n.d. | e) |
| 2-Aminophenol | 2 ± 1 | 92 ± 2 | < 1 | 1 ± 0 | 96 | Not linear | This study |
| 3-Aminophenol | 53 ± 1 | 50 ± 2 | 4 ± 1 | < 1 | 107 | Not linear | This study |
| 4-Aminophenol | – | 94 ± 2 | < 1 | < 1 | 96 | Not linear | This study |
| | n.d. | ≈ 85 | n.d. | ≈ 5 | 90 | n.d. | e) |
| Vanillin | 22 ± 1 | 51 ± 1 | 19 ± 1 | 4 ± 0 | 96 | n.d. | This study |
| | – | 50 ± 1 | 35 ± 1 | 3 ± 0 | 89 | 2:1 | d) |

† At pH 4 = 2.11 (± 0.06) :1 and at pH 7 = 4.35 (± 0.55) :1;

‡ At pH 4 = 3.06 (± 0.26) :1 and at pH 7 = 4.71 (± 0.04) :1;

n.d. = not determined

Reference: a) (Terhalle et al., 2018) b) (Rougé et al., 2018) c) (Wajon et al., 1982) d) (Hupperich et al., 2020) e) (Gan et al., 2019)

3.2.4. Practical implications

The present study has shown that FAC is an undoubtedly important by-product of ClO₂ reactions with phenolic moieties of NOM and micropollutants. Thereby, FAC can contribute to disinfection and pollutant degradation, which has yet, not been considered in applications of ClO₂. Furthermore, the present study indicates that monitoring of chlorinated DBPs should be emphasized. Thereby, it is important to note that due to the pre-oxidation effect of ClO₂, the set of by-products may be different compared to chlorination, which requires further investigation.

To further improve the understanding of phenol oxidation by ClO₂, more research is necessary. Most importantly, experiments should be unified to a similar procedure to ensure comparable results. Additionally, it should be ensured that the experimentally determined yields of FAC are stable and thus represent the actual FAC yields. Other functional groups attached to phenol should be investigated to look for FAC precursors. Thereby, either faster reacting (i.e., more relevant) FAC forming moieties or structures with even higher yields of FAC might be discovered. The combination of different functional groups attached to one phenolic moiety could provide an insight into which functional group has a more substantial effect on hampering FAC formation (e.g. 4-methylcatechol).

Investigation of methionine as a selective scavenger for free available chlorine in chlorine dioxide-based reactions

Mischa Jütte, Josephine Heyns, Mohammad S. Abdighahroudi, Christoph Schüth, and Holger V. Lutze

This chapter has been submitted as: M. Jütte, J. Heyns, M. S. Abdighahroudi, C. Schüth, and H. V. Lutze, “Investigation of methionine as a selective scavenger for free available chlorine in chlorine dioxide-based reactions,” to *Environmental Science Water Research & Technology*, Royal Society of Chemistry, (date of submission: 29.03.2023)

3.3 Investigation of methionine as a selective scavenger for free available chlorine in chlorine dioxide-based reactions

The present study investigates the application of methionine as a selective scavenger for free available chlorine (FAC) in chlorine dioxide (ClO_2) reactions. It has been reported that ClO_2 forms chlorite and FAC in the reaction with phenolic compounds. However, for some reactive moieties like sulfur-containing compounds, no quantification of FAC could be carried out yet, due to the limitation of the current methods. Methionine reacts fast with FAC ($k_{app} = 6.8 \times 10^8 \text{ M}^{-1} \text{ s}^{-1}$ at pH 7), and the second-order reaction rate of methionine with ClO_2 is determined in this study to be very slow ($k_{app} = 10^{-2} \text{ M}^{-1} \text{ s}^{-1}$ at pH 7). Methionine sulfoxide and chloride are formed in equal parts in the reaction of methionine with FAC. Hence the yield of methionine sulfoxide and chloride can be used to quantify intrinsic FAC. While the results for phenol were in accordance with the literature (50% chlorite and 50% FAC), hydroquinone and dimethylpiperazine also resulted in methionine sulfoxide yields, even though no FAC formation has been reported for these compounds. It is possible that reactive organic species are formed, which additionally causes methionine sulfoxide formation (e.g., benzoquinone). For glutathione, the yields of chlorine species depend strongly on the added concentration of ClO_2 . The reason for this observation is the follow-up reaction of chlorite with glutathione. Based on this study, the FAC formation in the reaction of glutathione with ClO_2 can be confirmed and is expected to be 50 %. However, to corroborate the FAC yield, how and why methionine sulfoxide is formed still needs to be investigated, especially in reactions that are not expected to form FAC.

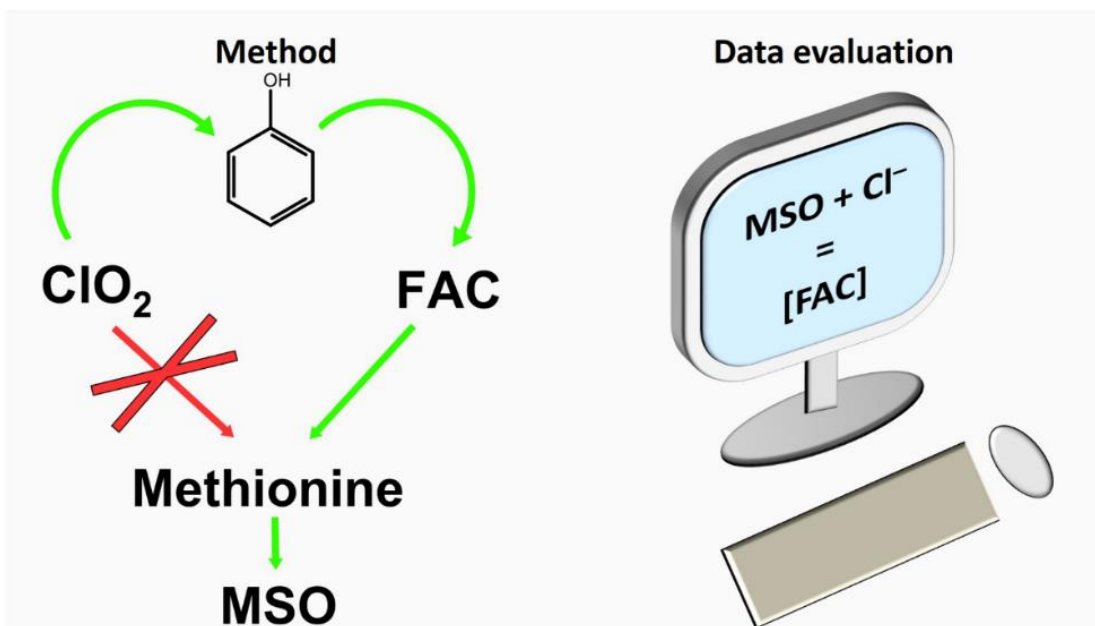


Figure 22: Graphical abstract of chapter 3.3.

3.3.1 Introduction

Chlorine dioxide (ClO_2) based oxidation is increasingly used in water treatment since it is less prone to form halogenated disinfection by-products (DBPs) compared to chlorine which forms DBPs such as trihalomethane (THM) (Gallard and von Gunten, 2002; Richardson et al., 2007). Indeed, ClO_2 shows less THM formation compared to chlorine (Zhang et al., 2000). However, it is proven that in reactions with specific reactive moieties (e.g., phenols) free available chlorine (FAC) is formed as a reaction product (Hupperich et al., 2020; Jütte et al., 2022; Rougé et al., 2018; Terhalle et al., 2018). Although the most abundant reaction product is chlorite (ClO_2^-), in the reaction with most phenolic moieties, FAC and ClO_2^- are formed in 50 % ratios each (Hupperich et al., 2020; Jütte et al., 2022; Rougé et al., 2018; Terhalle et al., 2018). In the reaction with saturated nitrogen-containing heterocycles, ClO_2 is reported to react mainly via electron transfer, and nearly 100 % ClO_2^- is formed (Abdighahroudi et al., 2022). Other studies showed that ClO_2 could react with specific amino acids and form 50% FAC and 50 % ClO_2^- (Jütte et al., 2022; Napolitano et al., 2005; Stewart et al., 2008). The fate of this intrinsically formed FAC has not been fully investigated yet. Intrinsically formed FAC may be causing the formation of harmful DBPs in ClO_2 treatment. However, this secondary oxidant might positively affect pollutant degradation and disinfection. For instance, the reaction with phenols and amines, which are reactive moieties of a broad range of micropollutants, differs strongly between ClO_2 and FAC. While phenolic compounds react fast with ClO_2 (Abdighahroudi et al., 2021), they react rather slow with FAC (Deborde and von Gunten, 2008). On the other hand, FAC reacts very fast with primary amines, while ClO_2 tends to react slow. This synergy might be used to degrade a broader spectrum of pollutants during (waste)water treatment (Abdighahroudi et al., 2021; Terhalle et al., 2018).

The challenge of determining intrinsic FAC formation is to outcompete all other reactions that FAC might undergo in the corresponding reaction system (cf. reactivities of FAC (Deborde and von Gunten, 2008)). This can only be done with a selective scavenger (for FAC reactions) which provides full scavenging of FAC without reacting with ClO_2 . Different approaches have been used so far. One reported approach is the addition of ammonia as a selective scavenger (Rougé et al., 2018). Thereby, ammonia reacts many orders of magnitude faster with FAC than ClO_2 ($k_{app}(\text{FAC} + \text{NH}_3) = 1.3 \times 10^4 \text{ M}^{-1} \text{ s}^{-1}$ at pH 7, $k_{app}(\text{ClO}_2 + \text{NH}_3) = < 10^{-6} \text{ M}^{-1} \text{ s}^{-1}$ at pH 7 (Deborde and von Gunten, 2008; Hoigné and Bader, 1994)) and forms chloramine (NH_2Cl), which can be quantitatively detected (Rougé et al., 2018). Terhalle et al., used bromide (Br^-) as FAC scavenger.

Br^- reacts fast with FAC ($k_{app}(\text{FAC} + \text{Br}^-) = 5.3 \times 10^3 \text{ M}^{-1} \text{ s}^{-1}$ at pH 7 (Deborde and von Gunten, 2008)) and forms free available bromine (FAB), which further reacts with phenol to form bromophenols. The quantification of intrinsic FAC is carried out by quantification of formed bromophenols (Terhalle et al., 2018). Glycine has also been used as a selective scavenger (Abdighahroudi et al., 2022; Hupperich et al., 2020; Jütte et al., 2022). Glycine reacts fast with FAC ($k_{app}(\text{Glycine} + \text{FAC}) = 1.5 \times 10^5 \text{ M}^{-1} \text{ s}^{-1}$ at pH 7 (Deborde and von Gunten, 2008)) and slow with ClO_2 ($k_{app}(\text{Glycine} + \text{ClO}_2) = < 10^{-5} \text{ M}^{-1} \text{ s}^{-1}$ at pH 7 (Hoigné and Bader, 1994)) and is, therefore, a suitable scavenger for intrinsic FAC. The reaction of FAC with glycine forms chloroglycine (Cl-Gly), which can be detected photometrically in the presence of iodide in excess (Houska et al., 2021) or with IC simultaneous to other chlorine species formed in the reaction (Abdighahroudi et al., 2020). The sensitivity of the glycine method can be further increased by installing post column reaction using potassium iodine as reactant and ammonium molybdate as a catalyzer (Abdighahroudi et al., 2020). However, it has been shown that Cl-Gly can undergo follow-up reactions with intrinsically formed reactive species (e.g., *ortho*-benzoquinone) (Chapter 3.2).

All methods mentioned above have the drawback that the second-order reaction rate constant of FAC with the scavenging compound is the limiting factor. Compounds that react faster with FAC than a FAC scavenger require large surpluses of the FAC scavenger. This can be limited by solubility or direct reactions of ClO_2 with the scavenger. Thus, most sulfur-containing compounds can hardly be investigated in terms of FAC formation because the reaction rate with FAC is several orders of magnitude faster compared to the aforementioned scavengers (Deborde and von Gunten, 2008). Ison et al. gave evidence that FAC might be formed in the reactions of cysteine and glutathione (GSH) with ClO_2 (2006). However, the available FAC determination methods are not capable of quantifying the FAC yields in these reactions. Thus, we used methionine as a novel scavenger for the determination of intrinsic FAC in the reaction of ClO_2 with sulfur-containing compounds. The reaction rate for methionine with FAC is $k_{app} = 6.8 \times 10^8 \text{ M}^{-1} \text{ s}^{-1}$ at pH 7 (Deborde and von Gunten, 2008). Furthermore, methionine has been reported to be unreactive toward ClO_2 ; however, no second-order reaction rate for this reaction is available. A proposed pathway for the reaction of methionine shows that the reaction stoichiometry of FAC with methionine is 1:1 and yields 1 molecule of methionine sulfoxide (MSO) and one molecule of chloride (Cl^-) (Deborde and

von Gunten, 2008). This study investigates the applicability of methionine as a scavenger for intrinsic FAC and the study of ClO₂-based reaction mechanisms.

3.3.2 Material and Methods

3.3.2.1 Chemicals, Instruments, & Methods

The chemicals used in this study and their purpose of use are listed in Table AIV.1. Table AIV.2 gives an overview of the instruments used in this study. Finally, Table AIV.3 and Table AIV.4 show the IC and LC method used for detection, respectively.

3.3.2.2 Determination of reaction kinetics

The second-order reaction constant (k_{app}) of methionine with ClO₂ has been determined by pseudo first-order kinetics by monitoring the UV absorbance over time. Therefore, a reaction solution containing different concentrations of methionine and ClO₂ was mixed in a 3 mL quartz cuvette, and the adsorption of ClO₂ at $\lambda = 359$ nm was monitored over time (data point was measured every 2 seconds for 30 minutes). Furthermore, the reaction solution contained 5 mM phosphate buffer to ensure the pH stability at 7. ClO₂ was added with three different ratios towards methionine (1:1, 1:10, and 1:100). All experiments were carried out in triplicates.

By plotting the ClO₂ degradation as $\ln([\text{ClO}_2]/[\text{ClO}_2]_0)$ over time pseudo-first-order rate constant (k_{obs}) of the reaction can be calculated. The slope of this plot (k_{obs}) needs to be divided by the initial concentration of the compounds in excess ($[A]$), which gives the second-order reaction rate constant according to equation 3.

$$k_{app} = \frac{k_{obs}}{[A]_0} \quad \text{Equation 3}$$

3.3.2.3 Formation of Chloride and MSO in methionine oxidation by FAC

The inorganic reaction products of the reaction of methionine with FAC have been determined via IC. Therefore, 100 μM methionine solution reacted with different concentrations of FAC (20-100 μM) at pH 7. After a reaction time of 10 minutes, the aliquots were transferred into IC vials (polypropylene (PP)) and measured with the IC method described in Table AIV.3. One has to take into account that the stock solution of FAC contains high impurities of Cl⁻. Therefore, the determination of Cl⁻ impurities is necessary. For this purpose, identical FAC concentrations were dosed into a 10 mM glycine solution (further containing 5 mM phosphate buffer at pH 7) to

scavenge all FAC species. The remaining Cl^- can be quantified and later subtracted from the measured Cl^- concentration in the reaction of methionine with FAC.

The formation of MSO as a reaction product was measured via LC-MSMS, described in Table AIV.4. The formation of MSO was measured as the reaction product of methionine with FAC and calibrated with the commercially available standard. For determining the reaction product of methionine and FAC, different concentrations of FAC were added to 100 μM methionine solution, buffered at pH 7. Different standard solutions of commercially available MSO have been prepared to contain the same concentration as the dosed FAC. The samples were measured, and the standard was used to quantify the MSO formed in the reaction of methionine and FAC. All experiments were carried out in triplicates.

3.3.2.4 Model compounds

To test the suitability of the developed method, four model compounds were chosen with different chlorine balances (sum of different chlorine species formed per consumed ClO_2). While phenol is reported to show 50 % FAC and 50 % ClO_2^- formation (Rougé et al., 2018; Terhalle et al., 2018), dimethylpiperazine (DMP) and hydroquinone have been observed to form 100 % ClO_2^- in ClO_2 -based reactions as inorganic by-products (Abdighahroudi et al., 2022; Hupperich et al., 2020). GSH was investigated as well as a sulfur-containing model compound.

Reaction solutions contained 100 μM of the model compound, 1 mM methionine, and 5 mM phosphate buffer adjusted to pH 7. ClO_2 was added in different concentrations (50, 100, and 200 μM). After a reaction time of 30 min, aliquots were transferred to LC (glass) and IC (PP) vials and were measured by IC and LC-MSMS described in Table AIV.3 and Table AIV.4. All chlorine balances were determined in triplicates. Additionally, FAC was dosed to an aliquot of the reaction solution as well to determine the FAC recovery.

3.3.2.5 Chlorite reactions

For investigation the follow-up reactions of GSH with ClO_2^- , different concentrations of GSH were dosed to 100 μM ClO_2^- in presence of 10 mM glycine at pH 7. The chlorine balance of these solutions were measured after 5min, 24 hours, and 48 hours.

To investigate if intrinsic formed ClO_2^- is causing MSO formation by reacting with methionine, a long-term monitoring experiment was conducted. Thereby 100 μM ClO_2^- and 100 μM methionine were mixed in the presence of 5 mM phosphate buffer at pH 7. Then ClO_2^- , Cl^- , and MSO were monitored over time. To achieve comparable results, it was ensured that IC and LC were always measuring simultaneously (same time of sample injection). The total period was set to 24 hours. Cl^- samples need to be blank corrected and the impurity of ClO_2^- solutions (purity = 80%) also contains Cl^- . Thus, the Cl^- concentration of the impurity needs to be determined as well and subtracted from the final result.

3.3.3 Results and Discussion

3.3.3.1 Reaction kinetics

To investigate if methionine is a suitable scavenger for the intrinsically formed FAC as the secondary oxidant in ClO₂-based reactions, two features are necessary. First, the second-order reaction rate with FAC should be high, which has been reported for methionine (k_{app} (methionine + FAC) = $6.8 \times 10^8 \text{ M}^{-1} \text{ s}^{-1}$ at pH 7 (Deborde and von Gunten, 2008)). Furthermore, the second-order reaction rate with ClO₂ should be several orders of magnitude lower. The second-order reaction rate constant for the reaction of methionine and ClO₂ has not been reported in the literature yet. Table 12 shows the achieved pseudo first-order reaction rates and the second-order reaction rate constants for different ratios between methionine and ClO₂.

Table 12: Results of pseudo first-order kinetic reactions of methionine with ClO₂. The reaction solution contained different concentrations of methionine (0.5, 5, and 50 mM) and 5 mM phosphate buffer. 0.5 mM ClO₂ was dosed to all samples, and all experiments were carried out in triplicates.

| Ratio methionine / ClO ₂ | $k_{obs} [\text{s}^{-1}]$ | $k_{app} [\text{M}^{-1} \text{s}^{-1}]$ |
|-------------------------------------|----------------------------------|---|
| 1:1 | $9.54 (\pm 2.65) \times 10^{-6}$ | $1.91 (\pm 0.53) \times 10^{-2}$ |
| 1:10 | $5.05 (\pm 0.02) \times 10^{-5}$ | $1.01 (\pm 0.01) \times 10^{-2}$ |
| 1:100 | $5.82 (\pm 0.02) \times 10^{-4}$ | $1.16 (\pm 0.01) \times 10^{-2}$ |

Based on the results, it can be stated that the effect of lowering the concentration of the compound in excess of the same concentration of the compound under investigation hardly affects the observed reaction order. Although the reaction should not follow pseudo first-order kinetics under these conditions, a linear ClO₂ consumption was observed and the calculated second-order reaction rate constant is in agreement with the other experimental conditions. Please note that the results were blank corrected to rule out ClO₂ evaporation over time. By increasing the excess of methionine, the method seems less error-prone, due to the lower standard deviation of the triplicate measurement. Overall, the reaction rate of methionine with ClO₂ is with $k_{app} \approx 10^{-2} \text{ M}^{-1} \text{ s}^{-1}$ at pH 7 very slow and ten orders of magnitude slower compared to the corresponding reaction kinetics of FAC. Thus, methionine can effectively and selectively scavenge FAC in the presence of ClO₂.

3.3.3.2 Formation of Chloride and MSO

It was investigated if Cl^- is the only inorganic reaction product of the reaction of methionine and FAC. In that, different concentrations of FAC were added to a 0.1 mM methionine solution and measured with IC. The relative yields based on the dosed FAC concentration are shown in Figure 23. It is visible that Cl^- is the main reaction product in this reaction, with yields ranging between 90 and 110 %. The standard deviation of the triplicate measurement is relatively high in this experiment, which can be explained by the high Cl^- background concentrations in the FAC stock solution. Despite the high Cl^- background concentrations, the determination of Cl^- seems to be fairly precise. It has to be mentioned that no other chlorine species (i.e., ClO_2^- , ClO_3^-) were detected in this experiment, indicating that the reaction of FAC with methionine forms 100 % Cl^- .

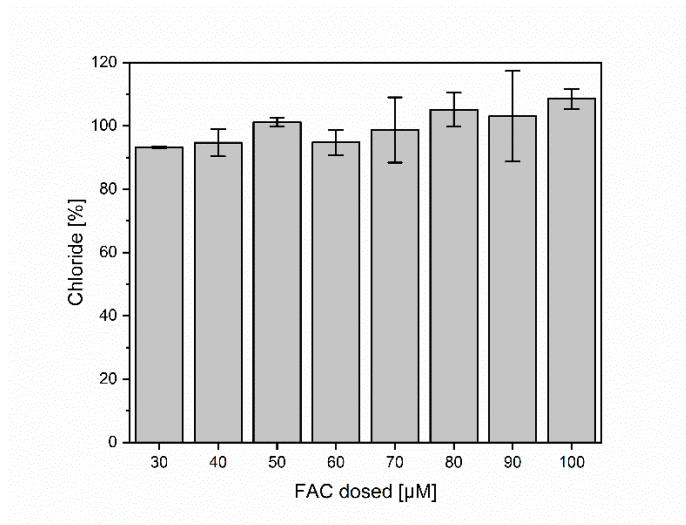


Figure 23: Relative yields of chloride based on the dosed concentration of FAC. Solutions contained 1 mM methionine and 5 mM phosphate buffer at $\text{pH} = 7$. All experiments were carried out in triplicates and the error bars represent the standard deviation of the triplicate measurement.

The formation of MSO as the reaction product of the reaction of methionine with FAC has been investigated as well. Thereby, the focus was to determine the yield of MSO per FAC consumed, which is later required to determine FAC from measured MSO yields when methionine is applied as an FAC scavenger. For this purpose, FAC was added in different concentrations to methionine. Parallel, an MSO calibration was prepared with standards having the same molar concentrations as the added FAC doses. The resulting correlation of MSO formation with FAC dose is shown in Figure 24.

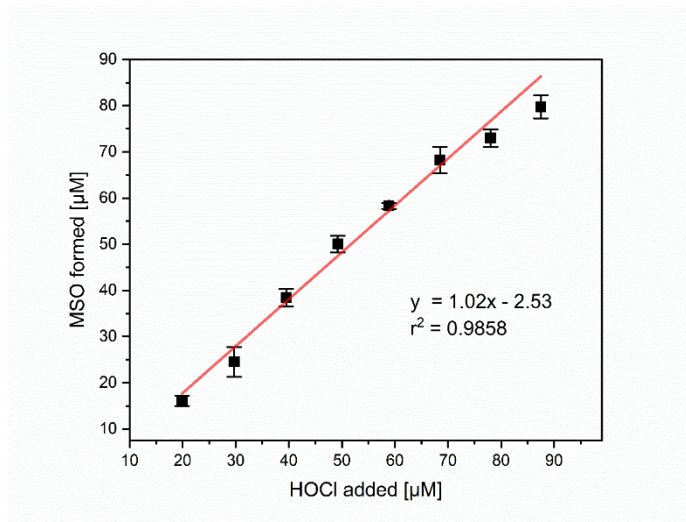


Figure 24: Correlation of MSO formation with the addition of FAC. Reaction solutions contained 1 mM methionine and 5 mM phosphate buffer (pH =7). All experiments were carried out in triplicates, and the error bars represent the standard deviation of the results.

The correlation of MSO formation with added FAC shows a linear trend. Based on the slope of the plot, which is very close to one, it can be stated that the stoichiometry of the proposed reaction mechanism is one, i.e. one molecule of MSO is formed per molecule of FAC added.

3.3.3.3 Chlorine balance of model compounds

Phenol, hydroquinone, and DMP have been chosen as model compounds since their chlorine balance is known (Table 13). This data will later be compared to the chlorine balances measured with the methionine method.

Table 13: Literature data for the chlorine balance of different model compounds.

| Compound | FAC [%] | Chlorite [%] | Chloride [%] | Reference |
|--------------------|---------|--------------|--------------|------------------------------|
| Phenol | ≈50 | ≈50 | – | (Rougé et al., 2018; |
| | 42 ± 3 | 62 ± 4 | – | Terhalle et al., 2018) |
| Hydroquinone | – | 92 ± 5 | – | (Hupperich et al., 2020) |
| Dimethylpiperazine | – | 100 ± 3 | – | (Abdighahroudi et al., 2022) |

Chapter 3.3: Investigation of methionine as a selective scavenger for free available chlorine in chlorine dioxide-based reactions

The determined chlorine balance for phenol is shown in Figure 25. In Figure 25A, all species formed and measured in this reaction (Cl^- , ClO_2^- , and MSO) are shown. Additionally, the recovery of FAC is shown, which is close to 100%. This shows that if FAC is formed in this reaction, methionine is added in sufficient concentrations to effectively scavenge FAC and form MSO.

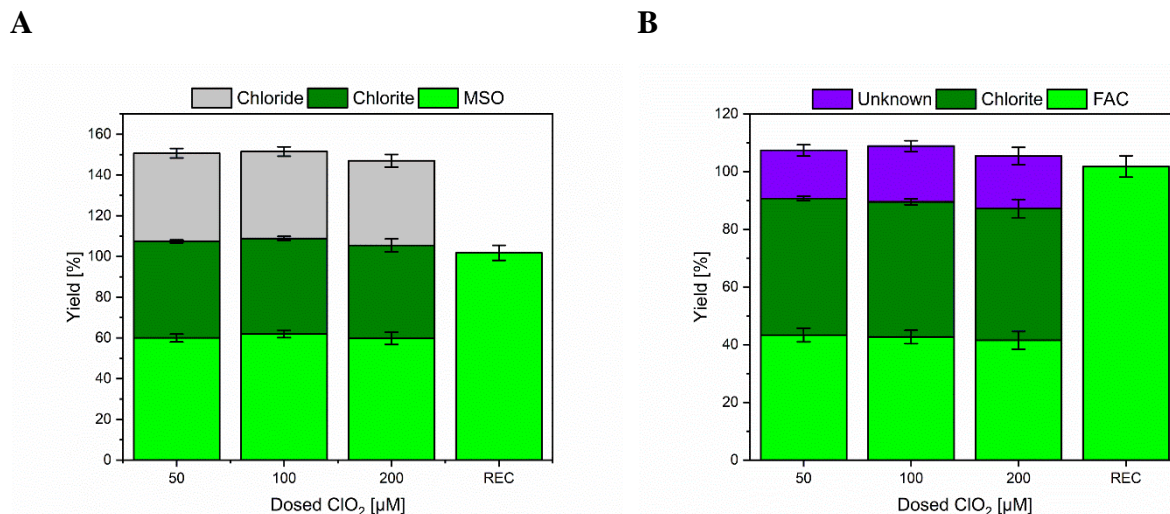


Figure 25: Measured chlorine balance of phenol by using the developed methionine method. **A** shows the yields of all compounds (please note chloride is formed in the reaction of FAC with methionine) and **B** shows the remaining MSO fraction after subtracting the chloride yields from MSO yields. All reaction solutions contained 0.1 mM phenol, 1 mM methionine, and 5 mM phosphate buffer. The buffer was used to preserve $\text{pH} = 7$. All experiments were carried out in triplicates, and the error bars represent the standard deviation of the triplicate measurement.

As demonstrated before, FAC reacts with methionine in a 1:1 stoichiometric ratio and forms 1 molecule of Cl^- and MSO. Therefore, if MSO and Cl^- are included in the mass balance, the total yield would be $> 100\%$. Hence the Cl^- yields have been corrected by the MSO yields. In this case, the formed Cl^- yields (40 – 50 %) represents the formed FAC in this reaction, which is in accordance with previously reported literature values for phenol (Rougé et al., 2018; Terhalle et al., 2018). After subtracting Cl^- yields from MSO yields, a fraction of MSO remains, labeled as unknown in Figure 25B, which is not formed from the reaction of FAC with methionine. Thus, MSO must be formed during a different reaction pathway involving different reaction partners. This could point to a reaction of ClO_2^- with methionine. However, in this experiment, ClO_2^- is formed in 50 % of the dosed ClO_2 concentration, which is in accordance with the previously reported literature (Rougé et al., 2018; Terhalle et al., 2018). Therefore, MSO might be formed by reactive organic species, which are formed during the reaction of phenol with ClO_2 . It is postulated

Chapter 3.3: Investigation of methionine as a selective scavenger for free available chlorine in chlorine dioxide-based reactions

that the reaction forms benzoquinone (Wajon et al., 1982), a weak oxidant with a standard reduction potential of 0.6992 V and might be reactive with methionine (Weiss, 2016). This would also explain the missing Cl^- yields compared to MSO.

The chlorine balances of two other compounds have been investigated as well. Hydroquinone is also a phenolic moiety with a second hydroxyl group in the *para*-position. Hydroquinone is reported to form 100 % ClO_2^- (Hupperich et al., 2020; Wajon et al., 1982). DMP is also reported to form 100 % ClO_2^- (Abdighahroudi et al., 2022); however, the reactive moieties of DMP are tertiary amines. This compound is investigated as well to discover if different functional groups have different outcomes in the chlorine balances. Figure 26 shows the chlorine balances of hydroquinone (A) and DMP (B).

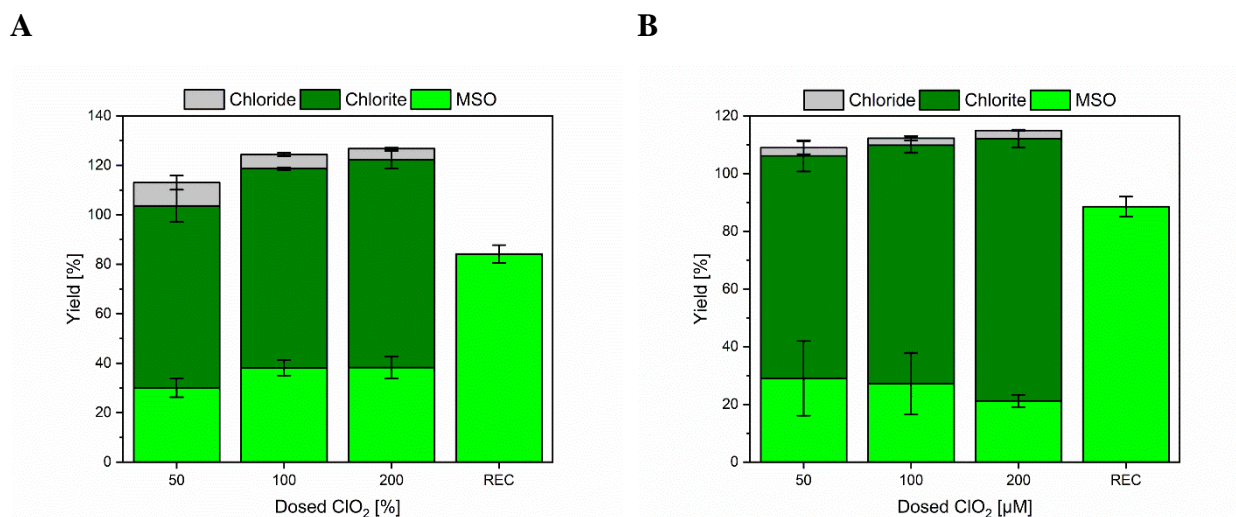


Figure 26: Estimated chlorine balance of hydroquinone (A) and DMP (B) by using the developed methionine method. All reactions contained 0.1 mM of either hydroquinone or DMP, 1 mM methionine, and 5 mM phosphate buffer at pH 7. All experiments were carried out in triplicates, and the error bars represent the standard deviation of the triplicate measurements.

In both cases, the main inorganic product is ClO_2^- , which is in accordance with the literature. However, the yields of ClO_2^- are below 100 %. Additionally, the recovery of MSO by dosing 100 μM FAC ranges between 80 – 90 %, which is lower than the results in the presence of phenol. An increase in the methionine concentration might support better results; however, due to the low solubility of methionine, the initial concentration could not be increased much further.

Based on the literature data, no FAC is formed in the reaction of hydroquinone and DMP with ClO_2 . However, in this experiment, 20 – 30 % MSO is detected. The simultaneously formed Cl^-

concentrations are much lower, which indicates, that not FAC but another reactive organic species is formed during the reaction. This reactive species can cause the oxidation of methionine to MSO similar to phenol (e.g., benzoquinone in case of hydroquinone).

Another critical aspect is the overall chlorine recovery. The sum of Cl^- and ClO_2^- is around 80 % which is lower than the dosed ClO_2 concentration. A loss in the chlorine balance typically indicates the formation of halogenated products. However, from the reaction of DMP and hydroquinone with ClO_2 , no halogenated reaction products are reported. It might be possible that the presence of methionine interferes with the reaction pathway and causes the chlorination of organic molecules. For both compounds, the overall chlorine balance shows an increasing trend with increasing ClO_2 dose, mainly due to the increasing yields of ClO_2^- . This might be caused by the fact that the effect of side reactions is reduced with a higher degree of reactant oxidation by ClO_2 . Further experiments are necessary to investigate if this effect is canceled out completely at one point, where the $[\text{ClO}_2]/[\text{reactant}]$ fold increased.

To investigate if the developed method can be applied to study sulfur-containing compounds, GSH has been chosen as a model compound. The determined chlorine balance and the FAC recovery are shown in Figure 27. The FAC recovery is with 92 % fairly complete. Thus, if FAC is formed in this reaction, it will be scavenged by methionine. For GSH, the yields of inorganic chlorine species show a strong dependency on the ClO_2 dose. If ClO_2 is dosed in a ratio of 0.5:1 to GSH, the most dominant reaction product is Cl^- . The higher the stoichiometric ratio, the more dominant ClO_2^- becomes. This might be explainable by follow-up reactions of ClO_2^- with residual GSH concentration. The reaction of ClO_2^- with GSH takes place very slowly and forms Cl^- (See Figure AIV.1). The stoichiometry of this reaction has been determined to be 2 molecules of GSH reacting with one molecule of ClO_2^- (see Figure AIV.2), which is in accordance with reported literature values (Ison et al., 2006). The principle of this reaction for the dosed ClO_2 concentrations is shown in Figure 28.

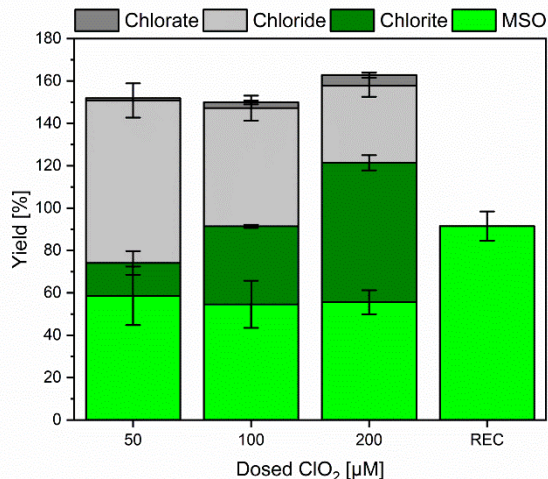


Figure 27: Chlorine balance of GSH established by using the methionine method. A reaction solution containing 0.1 mM GSH, 5 mM phosphate buffer, and 1 mM methionine at pH 7 were mixed with different concentrations of ClO₂. All experiments were carried out in triplicates and the error bars represent the standard deviation.

In case 50 µM ClO₂ is dosed to 100 µM GSH (Figure 28A), ClO₂ will be fully consumed, and 50 % of ClO₂ will be transformed to FAC (25 µM), and 50 % will be transformed to ClO₂⁻ (25 µM), which leaves a fraction of 75 µM GSH. This fraction will react with ClO₂⁻ in a 2:1 stoichiometry, eventually forming 25 µM Cl⁻ and leaves a fraction of 25 µM GSH. In this case, in total, 50 µM Cl⁻, 25 µM MSO, and 0 µM ClO₂⁻ should be formed in the final sample, which are 100, 50, and 0 % of the dosed ClO₂ concentration, respectively. This changes if the dosed ClO₂ concentration is increased (Figure 28B & C), whereby the fraction of GSH available for follow-up reaction with ClO₂⁻ is getting reduced. The theoretical values in Figure 28 are in good accordance with the measured values in Figure 27. The differences in yields of ClO₂⁻ can be explained by the different reaction times in Figure 27 and Figure AIV.2. Since the reaction of ClO₂⁻ with GSH is very slow, the reaction in Figure 27 did not fully proceed. Based on the observed results, it can be concluded that FAC is formed in the reaction of ClO₂ with GSH during a two-step reaction mechanism, which is shown in Figure 29.

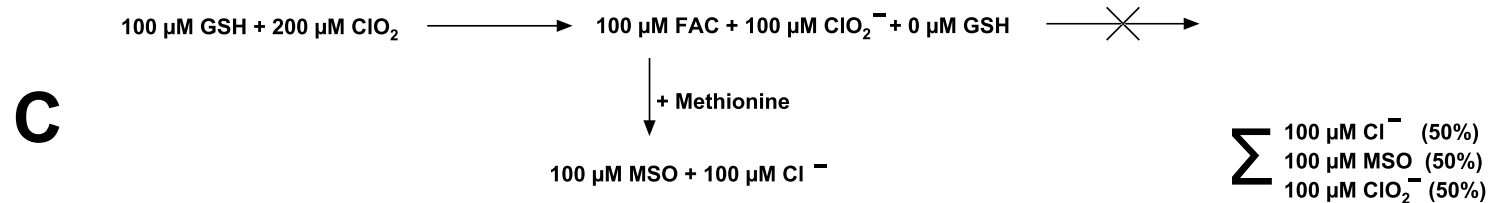
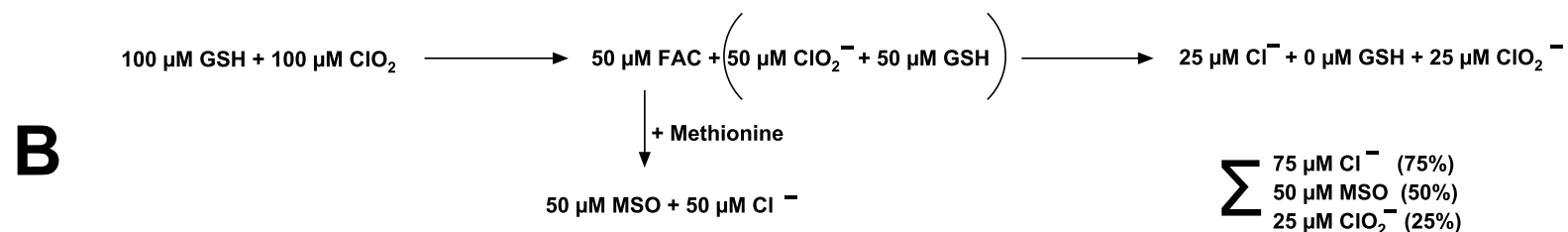
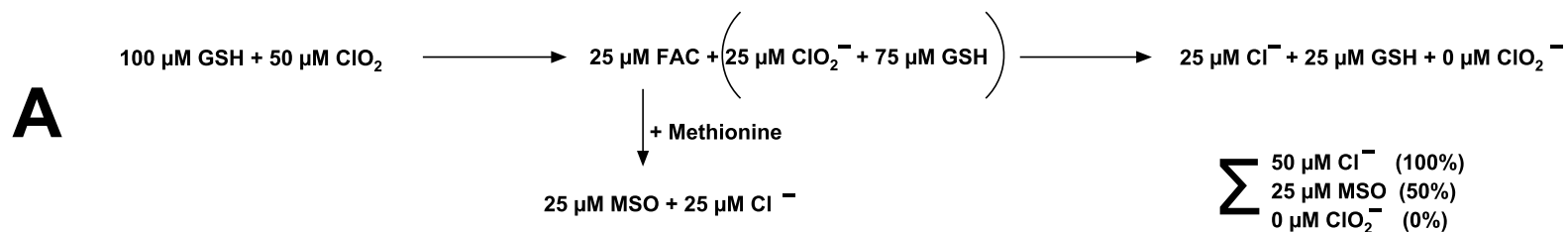


Figure 28: Postulated reaction pattern of GSH in case of different dosed ClO₂ concentrations at pH 7 in presence of 1 mM methionine.

Chapter 3.3: Development of a novel method for selective scavenging of free available chlorine in chlorine dioxide-based reactions by using methionine as a selective scavenger

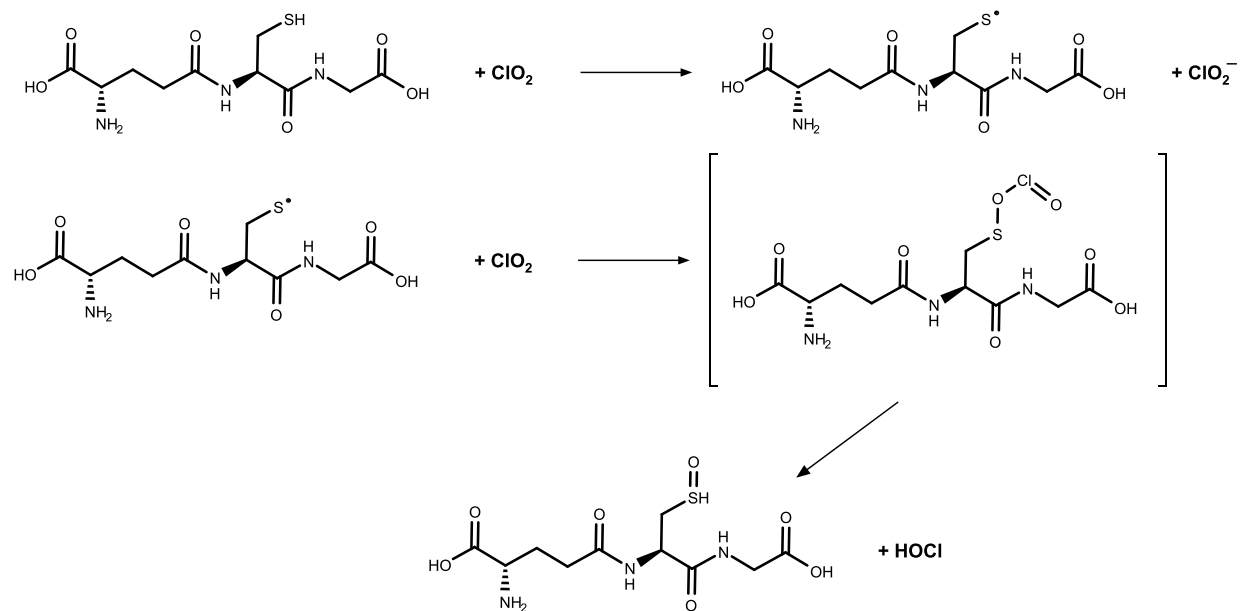


Figure 29: Proposed reaction mechanism for Glutathione with Chlorine dioxide. GSH reacts with two molecules of ClO_2 and forms ClO_2^- and HOCl (FAC).

3.3.3.4 MSO formation by chlorite

Previous results indicated a slow but possible reactivity between ClO_2^- and methionine. To investigate this theory, ClO_2^- and methionine were mixed 1:1, and the degradation of ClO_2^- and formation of MSO was observed for 24 h every 40 min. The results are shown in Figure 30.

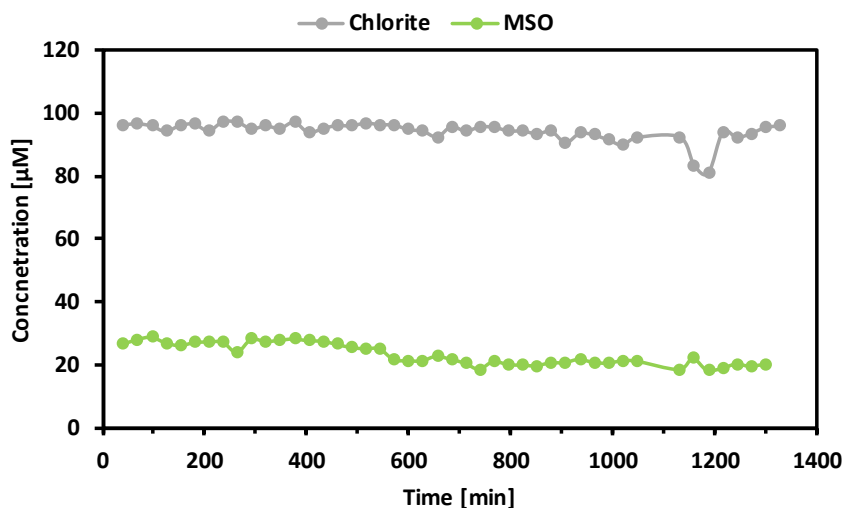


Figure 30: Monitoring of ClO_2^- and MSO over 24 hours. The reaction solution contained 0.1 mM methionine and 5 mM phosphate buffer at pH 7. 0.1 mM ClO_2^- was added and was measured with IC and LC-MSMS simultaneously.

It can be stated that ClO_2^- is not significantly degraded during the investigated time frame. On the other hand, MSO is formed by around 30 % but shows a slightly decreasing trend during the investigated period. Cl^- was also monitored in this experiment. However, after subtracting the Cl^- concentration of the blank samples and the impurities of the ClO_2^- solution, the remaining value for Cl^- was below zero. It has to be noted that the sensitivity of the Cl^- measurement is strongly reduced due to the high Cl^- background concentration in the ClO_2^- solution. Based on these results, it can be stated that ClO_2^- does not react with methionine. However, MSO is formed from an unknown source. So far, it cannot be explained why MSO is formed in the presence of ClO_2^- and is not formed in the absence of ClO_2^- , although no ClO_2^- degradation can be observed. One possibility might be the presence of 20 % impurities in ClO_2^- stock solutions. Although the impurities are mainly Cl^- , it might be possible that some fraction shows high reactivity towards methionine.

The slow degradation of MSO over time might be explainable by the formation of methionine sulfone. It is reported that sulfoxides might be further oxidized to sulfones (Lopez et al., 1994). However, the formation of methionine sulfone was not observed in this study.

3.3.4 Conclusion and Outlook

Based on the results of this study, it can be concluded that methionine can be a suitable scavenger for FAC in ClO_2 -based reaction mechanisms; however, further investigations are necessary for quantification. Even though the reaction of methionine and FAC leads to the formation of MSO and Cl^- in a 1:1 ratio, the formation of MSO from an unknown source might bias the final results. It seems that this unknown reaction with methionine does not form Cl^- therefore it is possible to quantify the MSO yields caused by the reaction with FAC. However, if the chlorine balance is not known many assumptions have to be done, which makes quantification of FAC yields difficult. Especially, in the case of GSH, where a stoichiometry-dependent chlorine balance was observed, it is hard to predict exactly which fraction of MSO is caused by FAC. One possible option to solve this problem is combining this method with an existing method. It would be for example possible to quantify the ClO_2^- yields of the reaction of GSH with ClO_2 by using glycine as FAC scavenger (Abdighahroudi et al., 2020). Then only the FAC yields are not known and could be determined by using the methionine method, since MSO is stable compared to Cl-Gly (Chapter 3.2). Additionally, it still needs to be investigated which other reactive species or generally which factors may contribute in to MSO formation. Even though the methionine method does not seem suitable for FAC yields quantifying, it can be used to make qualitative statements about FAC formation. For instance, GSH seems to form FAC, however, precise FAC yields are yet unclear and their determination requires further investigations.

Participation of free available chlorine as secondary oxidant during chlorine dioxide-based disinfection mechanisms of *Escherichia coli* – Effect of extracellularly formed FAC

Mischa Jütte, Britta Schubert, Mohammad S. Abdighahroudi, Torsten Waldminghaus, and Holger V. Lutze

3.4 Participation of free available chlorine as secondary oxidant during chlorine dioxide-based disinfection of *Escherichia coli* – Effect of extracellularly formed FAC

In the recent years, chlorine dioxide (ClO_2) has been in the focus of research and application of oxidative water treatment. The main application is as a suitable substitute for chlorine in drinking water disinfection to lower the formation of harmful halogenated DBPs. One key element of ClO_2 based disinfection is the formation of free available chlorine (FAC) as secondary oxidant. It has been reported that ClO_2 reacts with the phenolic moieties of natural organic matter (NOM) and forms 25 % FAC. This study investigates the participation of FAC in ClO_2 -based disinfection of *Escherichia coli*. Therefore, ClO_2 was added to NOM containing solutions to induce intrinsic FAC and the disinfection effect was measured by a novel approach based on lag phase extension. After the addition of ClO_2 the lag phase of *E. coli* growth was ≈ 40 % longer compared to control samples, which were not treated with ClO_2 . In the presence of 100 μM methionine, a selective FAC scavenger (fast reaction with FAC, no reaction with ClO_2), the inactivation effect on *E. coli* was barely observable indicating that the intrinsic FAC formation is the major contributor in ClO_2 based disinfection. Furthermore, the inactivation became weaker with increasing pH. This is due to speciation of intrinsic FAC (i.e., HOCl/OCl^- , $\text{p}K_a = 7.54$ (Deborde and von Gunten, 2008)), since OCl^- is a much weaker disinfectant than HOCl . Additionally, the speciation of the phenolic moieties of NOM (phenol/phenolate $\text{p}K_a: 10$) results in decreased disinfection strength of ClO_2 by increased pH ($6.5 > 7.5 > 8.5$). In that, phenolate reacts many orders of magnitudes faster with ClO_2 compared to phenol, which means that higher abundance of phenolate causes stronger scavenging of ClO_2 by NOM. Thus, NOM is of major importance in ClO_2 based disinfection.

3.4.1 Introduction

Disinfection is one of the major achievements in human history. It is applied in many fields, for example, in medicine, food industry, and sanitation. One of the most important fields is water disinfection. Since it was found out that water that is polluted by pathogens is the cause of the spread of lethal diseases, drinking water disinfection became mandatory. The most frequently used disinfecting agent worldwide is chlorine (free available chlorine (FAC)). However, it has been shown that the application of FAC causes formation of undesired harmful halogenated disinfection by-products (DBPs) (Gallard and von Gunten, 2002; Richardson et al., 2007; Rook, 1974). Therefore, FAC is substituted by other chemical oxidants like ozone (O_3) and chlorine dioxide (ClO_2).

The disinfection strength of ClO_2 has been shown in several studies (Cho et al., 2010; Ofori et al., 2017; Taylor et al., 2000; Vicuña-Reyes et al., 2008). The reported inactivation kinetics can range from $10^2 \text{ M}^{-1} \text{ s}^{-1}$ for *Mycobacterium avium* (Vicuña-Reyes et al., 2008) to $10^5 \text{ M}^{-1} \text{ s}^{-1}$ for *E. coli* (Ofori et al., 2017). This makes ClO_2 a more potent disinfectant than FAC ($\approx 10^4 \text{ M}^{-1} \text{ s}^{-1}$ for *E. coli* (Cho et al., 2010; Mwatondo and Silverman, 2021)) but weaker than O_3 ($\approx 10^6 \text{ M}^{-1} \text{ s}^{-1}$ for *E. coli* (Hunt and Mariñas, 1997)). While it has been observed that O_3 mainly causes damage to the bacterial membrane and FAC causes mainly inner cell damage, the observation for ClO_2 was a combination of both, membrane and inner cell damage (Cho et al., 2010). O_3 is a broadband oxidant which reacts with many functional groups, including double bonds (von Sonntag and von Gunten, 2012). These double bonds are present in the lipid double layer of the bacterial membrane. The reaction with O_3 causes a loss in the membrane integrity, cell lysis, and eventually a lethal event (McNair Scott and Leshner, 1963). FAC is a more selective oxidant than O_3 , and thus reacts with less functional groups (Deborde and von Gunten, 2008). Due to the observed mainly inner cell damage it seems likely that FAC is not interacting with the lipid layer and diffuses inside the cell and causing lethal events from inside (Cho et al., 2010). The observed inactivation behavior of ClO_2 might be explainable by the reaction of ClO_2 with membrane proteins. The reactivity of ClO_2 with a large range of different amino acids sidechains, which are the building blocks of proteins, is known (Jütte et al., 2023). Thus, simultaneous reactions with membrane proteins and inner cell proteins are the possible disinfection mechanism of ClO_2 .

Recent attention has been brought to the intrinsic formation of secondary oxidants (Jütte et al., 2023). Secondary oxidants are formed in reactions of the primary oxidants with specific reaction partners and can further oxidize recalcitrant compounds. For example, the formation of hydroxyl radicals ($\cdot\text{OH}$) in reactions of O_3 has been widely studied (von Sonntag and von Gunten, 2012). The reactivity of $\cdot\text{OH}$ is very high with a broad range of different compounds and $\cdot\text{OH}$ is therefore one of the most unselective known oxidants (Buxton et al., 1988). It has been reported that in the presence of *t*-BuOH as selective scavenger for $\cdot\text{OH}$, the inactivation of *Bacillus subtilis* was hampered (Cho et al., 2004). Recently it has been shown that ClO_2 reacts with e.g., phenolic compounds and forms FAC as a secondary oxidant (Rougé et al., 2018; Terhalle et al., 2018). Since FAC is a disinfectant as well, it might be interesting to investigate how strong the formation influences the disinfection process. While the participation of $\cdot\text{OH}$ in O_3 reaction mechanism has been studied, the participation of FAC in ClO_2 based mechanisms is still barely investigated. Lately, it has been proven that ClO_2 forms FAC also in the reaction with specific amino acids (i.e., tyrosine and tryptophan (Jütte et al., 2022)). Therefore, it might be possible that the FAC formation also occurs in the reaction of ClO_2 with (membrane)proteins inside the cell. The intrinsically formed FAC might cause further damage to the microbial cells. To this end no study is available, which investigated the intrinsic FAC formation during ClO_2 based disinfection of bacterial cells.

The aim of this study is to investigate the influence of intrinsic FAC in ClO_2 based disinfection of *E. coli*. Thereby, *E. coli* will be inactivated by ClO_2 in the presence and absence of methionine as selective FAC scavenger to investigate the influence on inactivation.

3.4.2 Materials and Methods

3.4.2.1 Chemicals, Instruments, and Analytical Methods

The lists of used chemicals and instruments can be found in Table AV.1 and Table AV.2, respectively. The preparation of the NOM solution has been carried out as described by Hupperich et al. (2020).

3.4.2.2 Bacterial Strains

Wild-type *E. coli* strain MG1655 was inoculated in 5 mL lysogeny broth (LB) media. The solution was incubated for 16 hours at 37°C in the incubator shaker (180 rpm). For the experiments the inoculated solution was centrifuged for 5 minutes at 4200 rpm. The supernatant was discarded and the remaining *E. coli* pellet was resuspended in 5 mL of phosphate buffered saline (PBS) by using the vortex. This process was repeated two times to remove all remaining media solution from the cells. Afterward, the optical density was determined at 600nm (OD₆₀₀).

3.4.2.3 Production of ClO₂ and FAC

Since ClO₂ and FAC are unstable oxidants, new stock solutions were prepared on a regular basis. The production and maintenance have been described in Jütte et al. (2022). In brief: ClO₂ was produced by the persulfate-chlorite method and was used until the concentration dropped below 80% of the production concentration. The ClO₂ concentration was quantified immediately after the production of the stock solution and prior to each experiment by measuring adsorption at $\lambda = 359$ nm ($\epsilon_{359\text{nm}} = 1250 \text{ M}^{-1} \text{ s}^{-1}$ (Gates et al., 2009)). FAC solution was prepared daily before every experiment. An aliquot from a 15 % FAC stock solution was diluted (125 μL in 50 mL of pure water), and the resulting FAC concentration was determined by direct UV adsorption at $\lambda = 292$ nm ($\epsilon_{292\text{nm}} = 350 \text{ M}^{-1} \text{ s}^{-1}$ (Abdighahroudi et al., 2020)).

3.4.2.4 Inactivation kinetics

To determine the inactivation rate of *E. coli* with ClO₂, the indigo-method was used in combination with the plate counting method. 7 μM ClO₂ was dosed to *E. coli* suspension (OD₆₀₀ = 0.1) in PBS. The indigo-method was used to determine the exposure of ClO₂ by monitoring [ClO₂] over time. After the addition of ClO₂ to the suspension, aliquots were taken each 10 seconds (first sample at 20 seconds after addition), and the reaction was quenched by indigotrisulfonate (indigo) (30 μM), which was present in excess over ClO₂. Note that the reaction stoichiometry of the ClO₂ indigo reaction is approximately 2:1. The adsorption coefficient which includes the reaction stoichiometry is $\varepsilon_{600\text{nm}} = 9955 \text{ cm}^{-1} \text{ s}^{-1}$ (Terhalle et al., 2018). By calculating the difference in adsorption at 600 nm compared to a reference sample (taken before ClO₂ dosage), the remaining [ClO₂] and the corresponding ClO₂ exposure can be calculated (Hoigne and Bader, 1980). This experiment was repeated, and at the same time slots, 0.1 mL samples were taken and added to 0.9 mL 1.5 % (w/w) sodium thiosulfate to scavenge all excess oxidants and the samples were stored on ice until the experiment was finished (≤ 10 min). Afterward, a dilution series were prepared ($10^{-1} - 10^{-8}$), and 50 μL of each solution was spotted on agar plates and incubated at 37 °C for 24 h. The quantification of *E. coli* was carried out by counting the colony-forming units (CFU).

3.4.2.5 Novel approach to determine inactivation

A novel methodology to determine different levels of inactivation was developed. ClO₂ was added to different *E. coli* suspension with different characteristics (e.g., pH). After a reaction time of 20 minutes an aliquot of 100 μL was transferred to one well of the 96 well plate. Note that ≈ 90 % of ClO₂ is depleted after 20 minutes (Figure AV.1). After all plates are filled with samples of different *E. coli* suspensions 100 μL of 2:1 LB media is added to all wells and mixed intensively. Note that some plates contain untreated *E. coli* suspension as an experimental reference and some plates contain PBS solution as an instrumental reference. Afterwards the 96 well plate is measured by the plate reader described in Table AV.2. The OD at 600 nm at (37°C) is measured every five minutes for 16 hours. The inactivation was determined by comparing the length of the lag phase and the doubling time, which is the necessary time for the bacterial population to double in size. The lag phase was determined as the time required for the sample to reach an OD₆₀₀ > 0.1, and doubling time (t_d) was calculated according to equation 4, whereby k can be taken as slope from OD₆₀₀ over time.

$$\ln(2) = k \times t_d$$

Equation 4

This method has the advantage over the cell counting method of CFU is less time and material-consuming.

3.4.2.6 Participation of FAC in ClO₂ based disinfection

To determine the participation of FAC in ClO₂ based disinfection processes, *E. coli* inactivation was monitored in the presence of NOM and selective scavengers for FAC. NOM solution has been prepared as described in Hupperich et al. (2020), and the DOC of the stock solution was determined by a TOC analyzer ($c(\text{NOM})_{\text{stock}} = 18 \text{ mg L}^{-1}$). The reaction of NOM with ClO₂ has been reported to form 25 % FAC (Hupperich et al., 2020; Rougé et al., 2018). In the inactivation experiments, *E. coli* suspensions with 5 mg L⁻¹ DOC were treated by adding different concentrations of ClO₂ to determine the optimal dosage to observe an inactivation effect in the monitored time range of 16 hours. Then this concentration was added to samples that contain different concentrations of methionine. Methionine reacts very fast with FAC (Deborde and von Gunten, 2008) but is reported to react slowly with ClO₂ (Noss et al., 1986).

3.4.3 Results and Discussion

3.4.3.1 Inactivation kinetics

The inactivation kinetic (k) of a bacterium by a specific oxidant can strongly differ depending on the strain and if the strain was cultivated from a culture collection or from environmental samples (Mwatondo and Silverman, 2021). For instance, the inactivation of *E. coli* by ClO_2 can differ from 10^3 to $10^5 \text{ M}^{-1} \text{ s}^{-1}$ (Jütte et al., 2023). To incorporate the investigated *E. coli* strain MG1655 the inactivation kinetics was determined as well. To determine the inactivation kinetics, Equation 5 can be used.

$$\ln\left(\frac{N_t}{N_0}\right) = -k \int [\text{ClO}_2] dt \quad \text{Equation 5}$$

Whereby, N_t / N_0 is the inactivation of *E. coli* based on the number of CFU at a specific time t , and the integral of the remaining ClO_2 over time represents the exposure. By plotting the inactivation vs. oxidant exposure, the slope of the linear fit equals the corresponding inactivation kinetic. The results are shown in Figure 31.

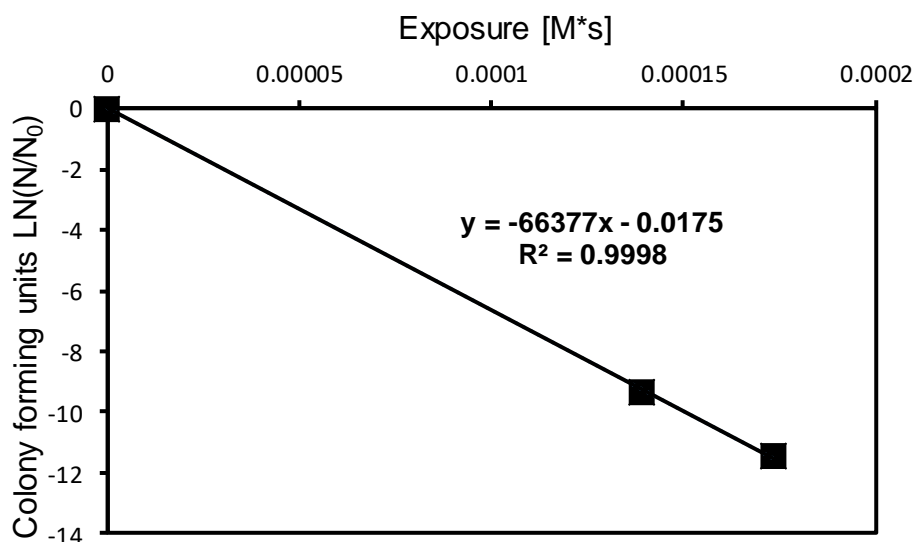


Figure 31: Inactivation of *E. coli* by adding $7 \mu\text{M}$ of ClO_2 (0.5 mg L^{-1}). ClO_2 was added to *E. coli* suspension in PBS at pH 7 and 25°C . The figure shows the counted CFU at a specific time as a function of determined ClO_2 exposure. Cell count was determined by plating a dilution series on agar plates and incubating at 37°C for 24 hours.

The determined inactivation rate of Strain MG1655 ($k = 6.6 \times 10^4 \text{ M}^{-1} \text{ s}^{-1}$) is in accordance with the reported literature values for other *E. coli* strains (Jütte et al., 2023). However, due to the fast consumption of ClO_2 and strong inactivation of *E. coli*, only a short time window can be used to

determine the inactivation kinetics. ClO_2 is fully consumed after 30 seconds (Figure AV.2) and an increase in initial ClO_2 dose to 1 mg L^{-1} resulted in the complete inactivation of *E. coli* only after 10 seconds. Therefore, a new concept was developed, which allows statements about the inactivation even at low initial ClO_2 concentrations, which cannot be detected by the exposure measurement. Figure 32 shows the growth curves of untreated *E. coli* and *E. coli* treated with $7 \text{ }\mu\text{M ClO}_2$, whereby the reaction was stopped after 10, 20, and 30 seconds.

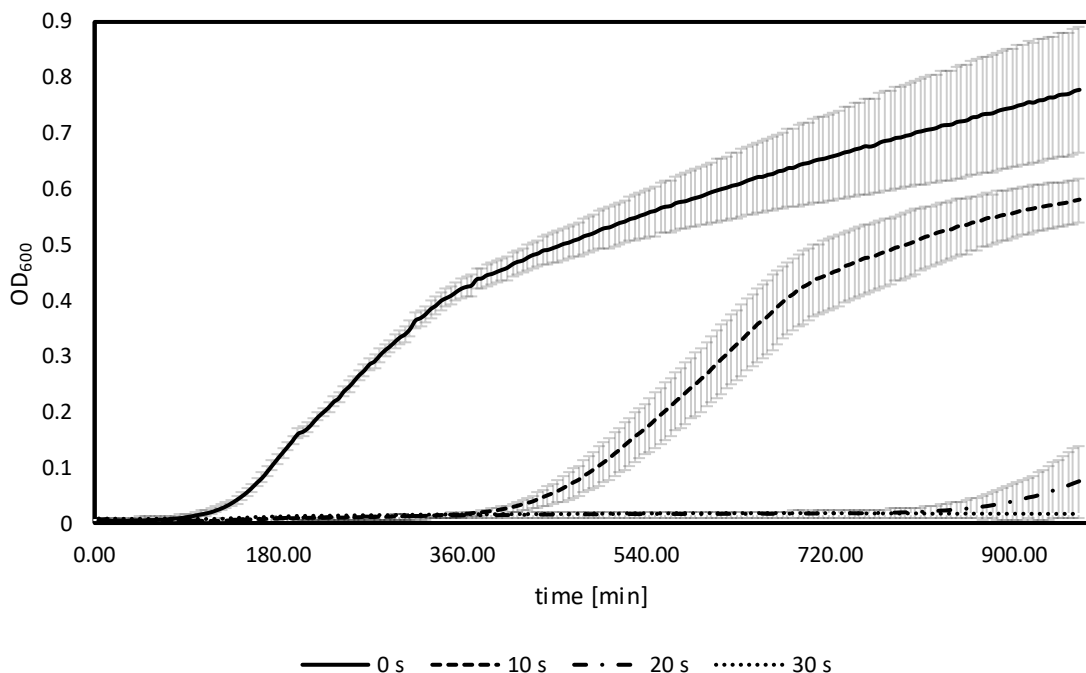


Figure 32: Growth curve of *E. coli* after different time exposures of ClO_2 determined by a plate reader. OD at 600 nm was determined for 16 hours every 5 min at 37°C . Experimental condition: $7 \text{ }\mu\text{M ClO}_2$ was dosed to *E. coli* suspension at pH 7.8 and 25°C . Samples were taken at specific times, and the reaction was stopped by using thiosulfate. Aliquots were transferred to a 96-well plate and mixed with 2:1 LB media. Each sample was measured 8 times in different wells, thus, the data points show the mean values of the eightfold determination, and the error bars represent the standard deviation.

The results show that a longer reaction time (higher oxidant exposure) of ClO_2 leads to a shift in the growth curve, and increased lag phase. Due to the increasing oxidant exposure, the remaining *E. coli* requires more time to reach an $\text{OD}_{600} \geq 0.1$ to enter the exponential phase. The start of the exponential growth is summarized in Table 14. Even a short reaction time of 10 seconds can cause a nearly threefold delay of the log phase compared to the untreated sample, and after 30 seconds, no bacterial growth can be observed in the monitored range of 16 hours.

Table 14: Delay of exponential *E. coli* growth after different time of ClO₂ exposure in PBS. Initial ClO₂ concentration = 7 μM.

| Time of ClO ₂ exposure [s] | lag phase [min] | Delay [%] |
|---------------------------------------|------------------------|-----------|
| 0 | 174 | 0 |
| 10 | 494 | 284 |
| 20 | 993 | 570 |
| 30 | Out of monitored range | – |

Since the time for an observed effect is very short, the sample was modified by adding NOM (5 mg L⁻¹ DOC). Due to the addition of NOM, higher concentrations of ClO₂ can be added due to the depletion of ClO₂ by the phenolic moieties in NOM. To evaluate the optimal concentration and to observe an effect within the monitored time different initial concentrations of ClO₂ were added (2 – 200 μM). The results shown in Figure 33 indicate that an initial ClO₂ concentration of 100 μM displays a suitable lag phase increase compared to the reference sample without addition of ClO₂. This enables to observe possible decrease in the lag phase in the presence of methionine. At higher concentrations (e.g., 200 μM ClO₂), no growth can be observed in the monitored time range.

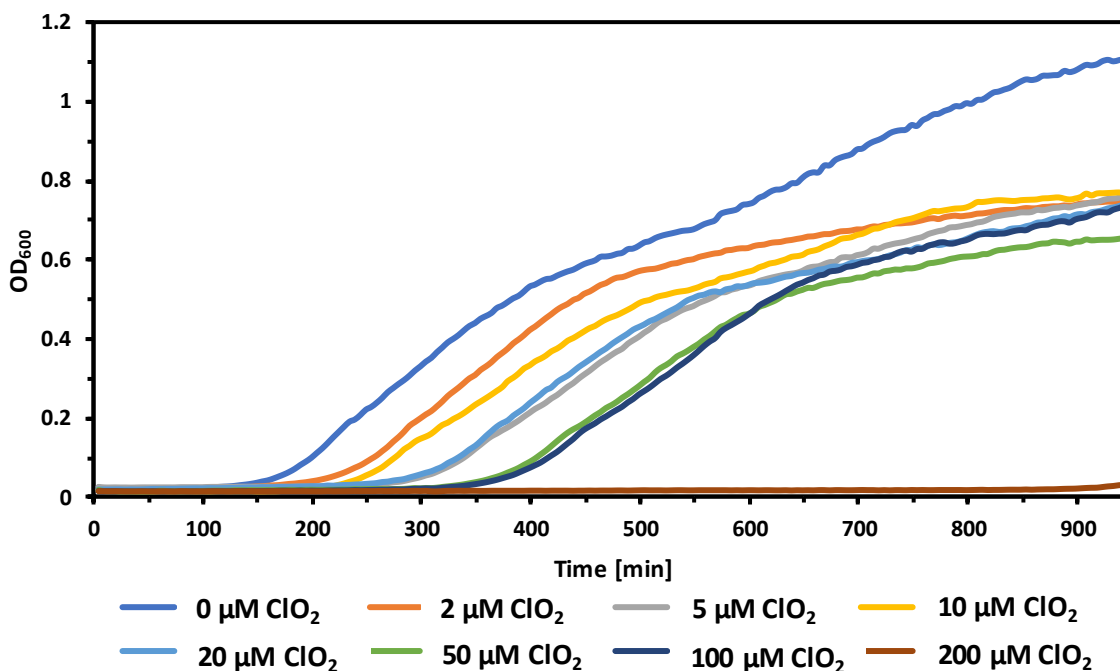


Figure 33: Dose dependent inactivation of *E. coli* by ClO₂. ClO₂ was added in different concentrations to *E. coli* suspension containing NOM (DOC: 5 mg L⁻¹) in PBS pH = 7.8. All experiments were carried out in quadruple determinations and the lines represent the mean values. To increase the clarity, the standard deviations of the results have been removed.

3.4.3.2 Participation of FAC in ClO₂ based inactivation

To investigate if intrinsically formed FAC is indeed playing a role in ClO₂ application, the inactivation of *E. coli* in the presence of NOM and a selective FAC scavenger has been carried out. NOM was added to initiate FAC formation (reported yields $\approx 25\%$) (Hupperich et al., 2020; Rougé et al., 2018). The same dosage was investigated for FAC as well (Figure AV.3). The results show that the FAC concentration, which is needed to observe full inactivation is lower compared to ClO₂ (i.e., full inactivation can be achieved with 100 μM FAC). The reason for this observation is the lower reactivity between FAC and the phenolic moieties in NOM (Deborde and von Gunten, 2008). To show that FAC can be successfully scavenged by methionine and prevent disinfection 50 μM FAC was dosed to different *E. coli* suspensions containing different concentrations of methionine. The results (Figure AV.4) show that the increasing methionine concentrations causes significant reduction in the disinfection efficiency. Note that the amino acid methionine had no effect in the growth curve of *E. coli* (Figure AV.5).

Thus, 100 μM ClO₂ and 50 μM FAC were applied to samples which contained different concentrations of methionine. Methionine reacts very fast with FAC ($k_{app} = 6.8 \times 10^8 \text{ M}^{-1} \text{ s}^{-1}$ at pH 7 (Deborde and von Gunten, 2008)) and very slowly with ClO₂ ($k_{app} = 10^{-2} \text{ M}^{-1} \text{ s}^{-1}$ at pH 7 (Chapter 3.3)) (Noss et al., 1986). Thus, hampered inactivation in the presence of methionine indicates FAC participation in ClO₂ disinfection. The results in Table 15 show that the lag-time of *E. coli* without the addition of an oxidant is ranging between 190 – 198 minutes. After adding ClO₂, the lag phase was increased by 38 % in the absence of methionine. If methionine is added in low concentrations (5 – 50 μM), no significant effect on the lag phase can be observed. However, if methionine is added in higher concentration (100 μM) the lag phase is getting reduced to a level similar to lag phase were no ClO₂ was added. This can be explained by the fact that ClO₂ probably has been fully consumed by the phenolic moieties of NOM, and the observed effect in lag phase increase is caused by FAC rather than ClO₂. This agrees with the results from experiments were FAC was added directly to the solution and a very strong lag phase delay can be observed (Table 15).

Table 15: Inactivation of *E. coli* by ClO₂ and FAC in presence of different methionine concentrations. Oxidants were added to *E. coli* suspensions which contain NOM (DOC = 5 mg L⁻¹). The initial dose of *E. coli* was OD₆₀₀ = 0.1. Growth was monitored by 96 well plates for 16 hours every five minutes at 37 °C. All samples were measured in quadruple determination. The percentage value represents the relative lag phase increase compared to growth curves which were not treated with any oxidant.

| c(Methionine) | No oxidant | 100 µM ClO ₂ | 50 µM FAC |
|---------------|-----------------|-------------------------|------------------------|
| | lag phase [Min] | | |
| 0 | 190.3 ± 2.3 | 262.3 ± 11.5 (+38 %) | Out of monitored range |
| 5 | 191.5 ± 10.9 | 274.0 ± 5.0 (+43 %) | 811.5 ± 42.5 (+324 %) |
| 10 | 190.3 ± 7.4 | 262.8 ± 9.6 (+38 %) | 387.8 ± 8.9 (+104 %) |
| 20 | 194.0 ± 3.5 | 291.5 ± 11.5 (+50 %) | 566.5 ± 4.2 (+192 %) |
| 50 | 195.3 ± 4.1 | 285 ± 2.2 (+46 %) | 195.25 ± 4.1 (+0 %) |
| 100 | 197.8 ± 4.1 | 185.3 ± 4.1 (-4 %) | 305.25 ± 18.15 (+54 %) |

Figure 34 shows the growth curves of *E. coli* in the presence and absence of 100 µM methionine after ClO₂ addition compared to the growth curve without any oxidant. It can be seen that the growth curve in the presence of 100 µM methionine follows a similar trend to the sample without ClO₂ addition. Thus, it can be assumed that FAC is fully scavenged. The growth curves of all experiments are shown in Figure AV.6.

Based on the results, it is not possible to calculate the fraction of FAC, which is formed intrinsically and responsible for *E. coli* inactivation. One reason is that lag phase extension does not show a linear trend with increasing FAC dosage (Figure AV.3). Therefore, the 50 % lag phase extension observed in Table 15 cannot be transferred to a corresponding FAC dosage. Additionally, ClO₂ inactivation in the presence of different levels of methionine also does not follow linear trends. Which makes precise estimation impractical.

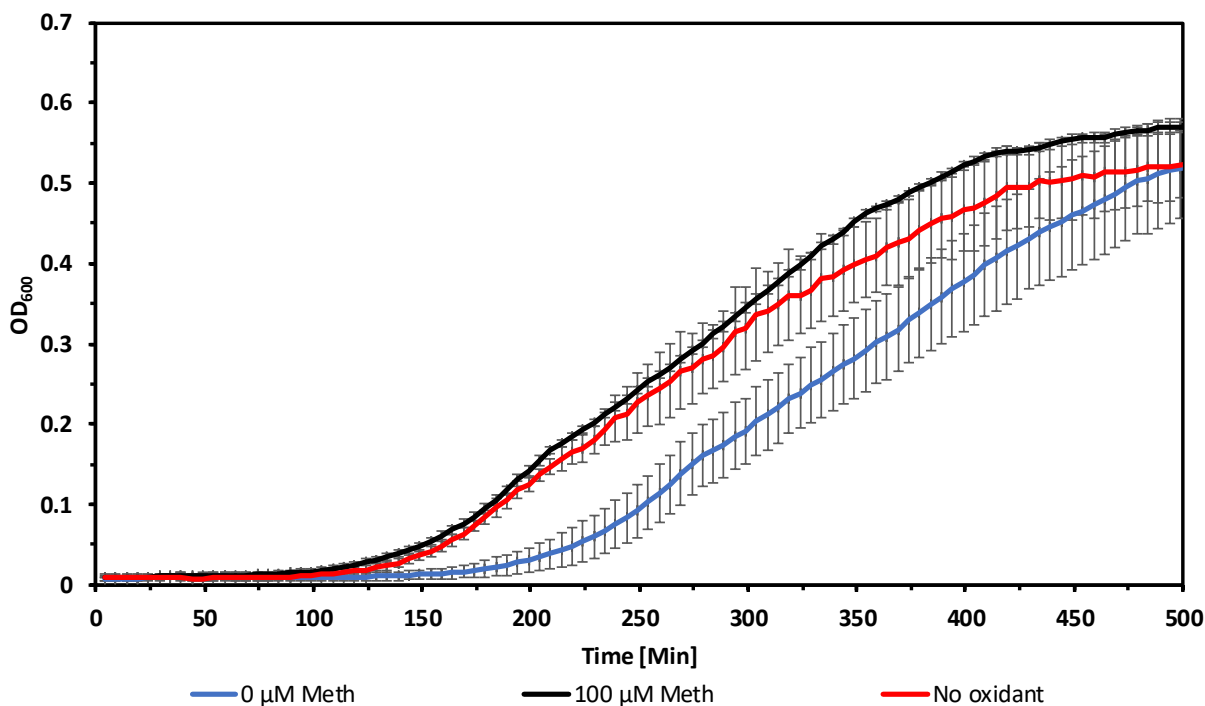


Figure 34: Inactivation of *E. coli* in the presence (black line) and absence (blue line) of 100 μM methionine. The black line represents a control sample of *E. coli* with no addition of ClO_2 . Samples contained *E. coli* ($\text{OD}_{600} = 0.1$) and NOM ($\text{DOC} = 5 \text{ mg L}^{-1}$). All samples were measured in quadruple determination and the error bars represent the standard deviation of the results.

3.4.3.3 pH dependent inactivation

To investigate the pH dependent inactivation of *E. coli*, the experiment was also carried out at different pH values, and compared with literature data. Ofori et al. showed that at pH 6.55, an inactivation of only 0.5 log units was achieved after the addition of $1 \text{ mg L}^{-1} \text{ ClO}_2$. The inactivation improved by increasing the pH under the same reaction conditions. At pH 7.4 and 8.5, an inactivation of 3 and 4 log could be observed, respectively (2017). The results of this experiment are shown in Table 16. Please note that the length of the lag phase shows a pH-dependent trend even without ClO_2 addition ($\text{pH } 6.5 < \text{pH } 7.5 < \text{pH } 8.5$). Therefore, for comparability, the lag time extension has to be presented relative to the lag time of the corresponding pH. The results show that at pH 6.5, no growth of *E. coli* was observed after ClO_2 addition. At pH 7.5 and 8.5, the lag phase extension was 197 % and 175 %, respectively. These results contradict the reported values by Ofori et al. (2017) regarding the pH trend. However, the experiments carried out by Ofori et al. (2017) is in the absence of NOM. NOM consists of phenolic moieties which are reactive toward ClO_2 (Hoigné and Bader, 1994). The reaction rates are pH-dependent due to the speciation of the

phenolic compounds (e.g., pK_a of phenol: 10 (Hoigné and Bader, 1994)). Therefore, at lower pH values ClO_2 shows less interactions with NOM, which results in higher ClO_2 exposure and causes stronger inactivation of *E. coli*. If the pH increases the reaction of ClO_2 with NOM becomes faster and the disinfection strength decreases. Furthermore, the speciation of the secondary oxidant FAC may be responsible for this observation (pK_a (HOCl/OCl^-): 7.54 (Deborde and von Gunten, 2008)), since HOCl is a stronger disinfectant compared to OCl^- . The doubling time was extended compared to 36.1 min at pH 7.5 and 8.5, which shows that ClO_2 caused some cell damage which hampered the regrowth rate of *E. coli*.

Table 16: pH-dependent growth of *E. coli* after addition of 0 and 100 μM ClO_2 . Initial samples contained *E. coli* ($\text{OD}_{600} = 0.1$) and NOM ($\text{DOC} = 5 \text{ mg L}^{-1}$). ClO_2 was added and after 5 min of reaction time 100 μL of the reaction solution was transferred to a 96-well plate and 100 μL 2:1 LB-media was added. OD_{600} was measured every 5 min for 16 hours at 37 °C. All experiments were carried out in triplicate and each sample was measured four times. In parentheses the relative extension of the lag phase is given.

| pH | lag phase [Min] | | Doubling time [Min] | |
|------------|--------------------------------|----------------------------------|--------------------------------|----------------------------------|
| | 0 μM ClO_2 | 100 μM ClO_2 | 0 μM ClO_2 | 100 μM ClO_2 |
| 6.5 | 107.8 \pm 2.5 | Out of monitored range | 26.4 \pm 3.2 | Out of monitored range |
| 7.5 | 120.7 \pm 5.8 | 237.8 \pm 30.1 (+97 %) | 26.3 \pm 2.9 | 36.1 \pm 1.3 |
| 8.5 | 151.1 \pm 5.0 | 265.9 \pm 4.4 (+75 %) | 30.4 \pm 0.2 | 36.1 \pm 2.9 |

3.4.4 Conclusion and Outlook

Based on the achieved results in this study it can be concluded that FAC is indeed playing a major role in ClO₂-based disinfection mechanisms, especially in presence of NOM. FAC, formed in the reaction with NOM seems to be the major oxidant in scenarios of fast ClO₂ depletion, such as ClO₂-based preoxidation. This may also explain the pH-dependent inactivation, which showed that stronger inactivation of *E. coli* can be achieved at lower pH since HOCl is a 100-fold stronger disinfectant than OCl⁻ (pK_a = 7.54 (Deborde and von Gunten, 2008)) and the pH-dependent disinfection of chlorination applies, even though the primary oxidant is ClO₂. Additionally, the scavenging of ClO₂ by NOM might be increased at higher pH. In the case of secondary disinfection in the distribution system where excess ClO₂ is applied to very clean water matrices the situation may be different and has to be assessed in future studies.

Further investigations regarding the participation of FAC can be carried out by investigating the differences in observed cell damage in the presence and absence of methionine. For instance, membrane damage (permeability) or protein alteration might differ if FAC is scavenged. Finally, the differences in DNA degradation should be investigated, which might be relevant for antibiotic-resistant gene removal.

Chapter 4

General conclusion and further perspective

4. General conclusion and further perspective

The present study investigated the fundamental reactions of ClO_2 during disinfection and pollutant control. It can be concluded that the reactions of ClO_2 are even more complex than previously reported. The formation of FAC as a secondary oxidant of ClO_2 could be shown in various reactions (e.g., amino acids, phenolic compounds, antioxidants), which shows that FAC is indeed a very important secondary oxidant of ClO_2 . Additionally, a method for scavenging intrinsic FAC could be developed, which allows FAC scavenging even for fast reactions between FAC and the compound under study. Finally, the important role of intrinsic FAC in ClO_2 -based disinfection could be shown.

By reviewing the current literature regarding the formation of secondary oxidants and their participation in primary oxidants disinfection mechanisms, it could be observed that this is a very complex research field, and a lot of additional research is necessary to understand the overall mechanisms. The importance of this research is given by the field of ARGs removal, which might be improvable by secondary oxidants. Additionally, it might help to improve the overall disinfection process, e.g., by more precise dosages, which might cause a reduction of undesired by-product formation. The fact that bacterial strains which are isolated from places which are exposed to chemical oxidants (e.g., oxidative wastewater treatment) are more resistant to chemical oxidants compared to their laboratory-cultivated analogs should be very concerning. It seems that bacteria are able to develop some kind of resistance/resilience against chemical oxidants over time. Thus, higher concentrations of chemical oxidants might be necessary in future to successfully inactivate bacteria during water treatment. This will be aggravated by increasing length and intensity of heatwaves, resulting in elevated source water temperatures ($> 20^\circ\text{C}$), which may allow pathogens to grow in e.g., distribution networks and thus, favor their adaption to chemical disinfection.

Due to the fast second-order reaction rate of ClO_2 towards specific amino acids, it seems very likely that the reaction of ClO_2 with vital proteins is part of the disinfection process. In the presented study, it could be shown that in the reactions of ClO_2 with tyrosine and tryptophan, present as peptides, 50 % FAC is formed intrinsically. Due to the high abundance of these amino acids in proteins, it is very likely that this reaction also occurs under real conditions inside bacterial cells. The intracellular-formed FAC might be responsible for additional cell damage. However, to investigate how strong the influence of FAC is and if FAC might be responsible for causing lethal

events, further research needs to be carried out. This can be done by genetically modifying bacterial cells, which produce proteins with designed amino acid abundance at different locations (e.g., membrane and cytoplasm). For instance, proteins that contain an even higher abundance of FAC-forming amino acids or proteins that contain selective FAC-scavenging amino acids (e.g., methionine). An intensified FAC formation should cause stronger inactivation due to the additional cell damage. On the other hand, the modified cells with high abundance of FAC-scavenging amino acids should show some resistance towards ClO₂.

Besides the direct interaction of ClO₂ with bacterial cells during water treatment, the reaction with the water matrix also strongly influences the overall reaction mechanism. The main component of the water matrix is NOM, which consists mostly of phenolic moieties. Due to the high reactivity of ClO₂ with phenols, NOM can be considered a strong ClO₂ scavenger. The reported FAC yields in the literature need to be handled carefully since follow-up reactions might be responsible for lower detected FAC yields. This study showed that if FAC is formed, it is always 50 % of the initially dosed ClO₂ concentration. Since most investigated phenolic compounds formed 50 % FAC, regardless of the number and location of different groups attached to the aromatic ring (e.g., methyl, methoxy, bromine/chlorine) groups, it can be concluded that intrinsic FAC is indeed a very important contributor in ClO₂-based disinfection. The observed rather low formation of these DBPs might be caused by the ClO₂ pre-oxidation of NOM, since ClO₂ has to react with NOM before FAC can be formed. Only specific functional groups attached to specific locations of the phenolic ring are preventing FAC formation (i.e., -OH and -NH₂), whereby the reason for this observation needs further investigations. The proposed formation of HClO₂ instead of HOCl might be investigated by isotopic analysis.

By using methionine as a selective scavenger for FAC, a new branch of compounds can be investigated regarding the intrinsic formation of FAC in ClO₂-based reactions. So far, the high reaction kinetics of sulfur-containing compounds with FAC has impeded the detection of FAC by the existing methods. The problem is the consumption of FAC in the follow-up reaction of FAC with the compound under study. An increase in the scavenger concentration would lead to an increase in the fraction of ClO₂, which reacts with the scavenger. By using methionine which also reacts very fast with FAC ($k_{app} = 6.8 \times 10^8 \text{ M}^{-1} \text{ s}^{-1}$ at pH 7 (Deborde and von Gunten, 2008)), the formation of FAC in the reaction of ClO₂ with thiol containing GSH could be shown for the first

time. Since GSH is an antioxidant produced by bacteria to prevent oxidative damage, the formation of FAC is a very interesting observation, which might be responsible for enhanced inactivation by ClO_2 . However, it still needs to be investigated if the transformation product of GSH also scavenges FAC.

The reaction of ClO_2 with NOM during water disinfection is crucial. However, the reported formation of FAC in this reaction might be beneficial for disinfection purposes. It has been shown that intrinsic FAC may play an important role in the disinfection process of ClO_2 . The inactivation of the model bacterium *E. coli* was hampered in the presence of methionine, which was added to scavenge intrinsic FAC. This implies that ClO_2 reacts mainly with NOM and forms FAC which in turn fully drives the disinfection process if ClO_2 is dosed in substoichiometric ratios compared to NOM. Further research might investigate the different cell damage that occurs in the absence and presence of methionine, indicating which cell damage is caused by ClO_2 itself and which is caused by intrinsically formed FAC.

Literature

5. Literature

- Abdighahroudi, M.S., Jütte, M., Hupperich, K., Mutke, X.A.M., Schmidt, T.C., Lutze, H. V., 2021. Mechanisms and byproduct formation in the application of chlorine dioxide, in: *Comprehensive Analytical Chemistry*. pp. 51–83. <https://doi.org/10.1016/bs.coac.2021.01.003>
- Abdighahroudi, M.S., Mutke, X.A.M., Jütte, M., Klein, K., Schmidt, T.C., Lutze, H. V., 2022. Reaction of Chlorine Dioxide with Saturated Nitrogen-Containing Heterocycles and Comparison with the Micropollutant Behavior in a Real Water Matrix. *Environ. Sci. Technol.* 56, 11589–11601. <https://doi.org/10.1021/acs.est.1c08381>
- Abdighahroudi, M.S., Schmidt, T.C., Lutze, H. V., 2020. Determination of free chlorine based on ion chromatography—application of glycine as a selective scavenger. *Anal. Bioanal. Chem.* 412, 7713–7722. <https://doi.org/10.1007/s00216-020-02885-1>
- Aguilar, C.A.H., Narayanan, J., Manoharan, M., Singh, N., Thangarasu, P., 2013. A much-needed mechanism and reaction rate for the oxidation of phenols with ClO₂: A joint experimental and computational study. *Aust. J. Chem.* 66, 814–824. <https://doi.org/10.1071/CH13101>
- Aguilar, C.A.H., Narayanan, J., Singh, N., Thangarasu, P., 2014. Kinetics and mechanism for the oxidation of anilines by ClO₂: A combined experimental and computational study. *J. Phys. Org. Chem.* 27, 440–449. <https://doi.org/10.1002/poc.3281>
- Al-Otoum, F., Al-Ghouti, M.A., Ahmed, T.A., Abu-Dieyeh, M., Ali, M., 2016. Disinfection by-products of chlorine dioxide (chlorite, chlorate, and trihalomethanes): Occurrence in drinking water in Qatar. *Chemosphere* 164, 649–656. <https://doi.org/10.1016/j.chemosphere.2016.09.008>
- Alcaide, E., Garay, E., 1984. R-plasmid transfer in *Salmonella* spp. isolated from wastewater and sewage-contaminated surface waters. *Appl. Environ. Microbiol.* 48, 435–438. <https://doi.org/10.1128/aem.48.2.435-438.1984>
- Alfassi, Z.B., Huie, R.E., Neta, P., 1986. Substituent effects on rates of one-electron oxidation of phenols by the radicals ClO₂, NO₂, and SO₃⁻. *J. Phys. Chem.* 90, 4156–4158. <https://doi.org/10.1021/j100408a063>
- Andrzejewski, P., Kasprzyk-Hordern, B., Nawrocki, J., 2008. *N*-nitrosodimethylamine (NDMA) formation during ozonation of dimethylamine-containing waters. *Water Res.* 42, 863–870. <https://doi.org/10.1016/j.watres.2007.08.032>
- Antibiotic resistance [WWW Document], 2018. World Heal. Organ. URL <https://www.who.int/news-room/fact-sheets/detail/antibiotic-resistance> (accessed 6.6.20).
- Arnhold, J., Hammerschmidt, S., Arnold, K., 1991. Role of functional groups of human plasma and luminol in scavenging of NaOCl and neutrophil-derived hypochlorous acid. *BBA - Mol. Basis Dis.* 1097, 145–151. [https://doi.org/10.1016/0925-4439\(91\)90099-U](https://doi.org/10.1016/0925-4439(91)90099-U)
- Awofeso, N., Aldabk, K., 2018. Cholera, Migration, and Global Health – A Critical Review. *Int. J. Travel Med. Glob. Heal.* 6, 92–99. <https://doi.org/10.15171/ijtmgh.2018.19>

- Barry, C.E., Nayar, P.G., Begley, T.P., 1988. Phenoxazinone synthase: Enzymatic catalysis of an aminophenol oxidative cascade. *J. Am. Chem. Soc.* 110, 3333–3334. <https://doi.org/10.1021/ja00218a072>
- Benarde, M.A., Israel, B.M., Olivieri, V.P., Granstrom, M.L., 1965. Efficiency of Chlorine Dioxide as a Bactericide. *Appl. Microbiol.* 13, 776–780.
- Bennett, B.D., Kimball, E.H., Gao, M., Osterhout, R., Van Dien, S.J., Rabinowitz, J.D., 2009. Absolute metabolite concentrations and implied enzyme active site occupancy in *Escherichia coli*. *Nat. Chem. Biol.* 5, 593–599. <https://doi.org/10.1038/nchembio.186>
- Bergeron, S., Boopathy, R., Nathaniel, R., Corbin, A., LaFleur, G., 2015. Presence of antibiotic resistant bacteria and antibiotic resistance genes in raw source water and treated drinking water. *Int. Biodeterior. Biodegrad.* 102, 370–374. <https://doi.org/10.1016/j.ibiod.2015.04.017>
- Berliner, J.F.T., 1931. The chemistry of Chloramines. *Am. Water Work. Assoc.* 23, 1320–1333.
- Bichsel, Y., von Gunten, U., 1999. Oxidation of iodide and hypiodous acid in the disinfection of natural waters. *Environ. Sci. Technol.* 33, 4040–4045. <https://doi.org/10.1021/es990336c>
- Bougnom, B.P., Thiele-Bruhn, S., Ricci, V., Zongo, C., Piddock, L.J.V., 2020. Raw wastewater irrigation for urban agriculture in three African cities increases the abundance of transferable antibiotic resistance genes in soil, including those encoding extended spectrum β -lactamases (ESBLs). *Sci. Total Environ.* 698. <https://doi.org/10.1016/j.scitotenv.2019.134201>
- Bruins, J.J., Albada, B., van Delft, F., 2018. *ortho*-Quinones and Analogues Thereof: Highly Reactive Intermediates for Fast and Selective Biofunctionalization. *Chem. - A Eur. J.* 24, 4749–4756. <https://doi.org/10.1002/chem.201703919>
- Buxton, G. V., Greenstock, C.L., Helman, W.P., Ross, A.B., 1988. Critical Review of rate constants for reactions of hydrated electrons, hydrogen atoms and hydroxyl radicals ($\cdot\text{OH}/\cdot\text{O}^-$) in Aqueous Solution. *J. Phys. Chem. Ref. Data* 17, 513–886. <https://doi.org/10.1063/1.555805>
- Cadenas, E., Mira, D., Brunmark, A., Lind, C., Segura-Aguilar, J., Ernster, L., 1988. Effect of superoxide dismutase on the autoxidation of various hydroquinones-A possible role of superoxide dismutase as a superoxide: Semiquinone oxidoreductase. *Free Radic. Biol. Med.* 5, 71–79. [https://doi.org/10.1016/0891-5849\(88\)90032-9](https://doi.org/10.1016/0891-5849(88)90032-9)
- Carmel-Harel, O., Storz, G., 2000. Roles of the Glutathione- and Thioredoxin-Dependent Reduction Systems in the *Escherichia Coli* and *Saccharomyces Cerevisiae* Responses to Oxidative Stress. *Annu. Rev. Microbiol.* 54, 439–461. <https://doi.org/10.1146/annurev.micro.54.1.439>
- Cataldo, F., 2006. Ozone degradation of biological macromolecules: Proteins, hemoglobin, RNA, and DNA. *Ozone Sci. Eng.* 28, 317–328. <https://doi.org/10.1080/01919510600900290>
- Chen, B., Yang, Y., Liang, X., Yu, K., Zhang, T., Li, X., 2013. Metagenomic profiles of antibiotic resistance genes (ARGs) between human impacted estuary and deep ocean sediments. *Environ. Sci. Technol.* 47, 12753–12760. <https://doi.org/10.1021/es403818e>

- Chen, Q., An, X., Li, H., Su, J., Ma, Y., Zhu, Y.G., 2016. Long-term field application of sewage sludge increases the abundance of antibiotic resistance genes in soil. *Environ. Int.* 92–93, 1–10. <https://doi.org/10.1016/j.envint.2016.03.026>
- Cho, M., Chung, H., Yoon, J., 2003. Disinfection of water containing natural organic matter by using ozone-initiated radical reactions. *Appl. Environ. Microbiol.* 69, 2284–2291. <https://doi.org/10.1128/AEM.69.4.2284-2291.2003>
- Cho, M., Kim, J., Kim, J.Y., Yoon, J., Kim, J.H., 2010. Mechanisms of *Escherichia coli* inactivation by several disinfectants. *Water Res.* 44, 3410–3418. <https://doi.org/10.1016/j.watres.2010.03.017>
- Cho, M., Lee, Y., Chung, H., Yoon, J., 2004. Inactivation of *Escherichia coli* by Photochemical Reaction of Ferrioxalate at Slightly Acidic and Near-Neutral pHs. *Appl. Environ. Microbiol.* 70, 1129–1134. <https://doi.org/10.1128/AEM.70.2.1129-1134.2004>
- Choi, Y., He, H., Dodd, M.C., Lee, Y., 2021. Degradation Kinetics of Antibiotic Resistance Gene *mecA* of Methicillin-Resistant *Staphylococcus aureus* (MRSA) during Water Disinfection with Chlorine, Ozone, and Ultraviolet Light. *Environ. Sci. Technol.* 55, 2541–2552. <https://doi.org/10.1021/acs.est.0c05274>
- Choudhury, B., Portugal, S., Mastanaiah, N., Johnson, J.A., Roy, S., 2018. Inactivation of *Pseudomonas aeruginosa* and Methicillin-resistant *Staphylococcus aureus* in an open water system with ozone generated by a compact, atmospheric DBD plasma reactor. *Sci. Rep.* 8, 1–11. <https://doi.org/10.1038/s41598-018-36003-0>
- Christensen, E., Giese, A.C., 1954. Changes in absorption spectra of nucleic acids and their derivatives following exposure to ozone and ultraviolet radiations. *Arch. Biochem. Biophys.* 51, 208–216. [https://doi.org/10.1016/0003-9861\(54\)90468-3](https://doi.org/10.1016/0003-9861(54)90468-3)
- Couri, D., Abdel-Rahman, M.S., Bull, R.J., 1982. Controlled clinical evaluations of chlorine dioxide, chlorite and chlorate in man. *Environ. Health Perspect.* 46, 57–62. <https://doi.org/10.1289/ehp.824657>
- Criquet, J., Allard, S., 2021. Influence of bromide and iodide on the formation of disinfection by-products in drinking water treatment. *Compr. Anal. Chem.* 92, 113–134. <https://doi.org/10.1016/bs.coac.2021.01.004>
- Czekalski, N., Gascón Díez, E., Bürgmann, H., 2014. Wastewater as a point source of antibiotic-resistance genes in the sediment of a freshwater lake. *ISME J.* 8, 1381–1390. <https://doi.org/10.1038/ismej.2014.8>
- Czekalski, N., Imminger, S., Salhi, E., Veljkovic, M., Kleffel, K., Drissner, D., Hammes, F., Bürgmann, H., Von Gunten, U., 2016. Inactivation of Antibiotic Resistant Bacteria and Resistance Genes by Ozone: From Laboratory Experiments to Full-Scale Wastewater Treatment. *Environ. Sci. Technol.* 50, 11862–11871. <https://doi.org/10.1021/acs.est.6b02640>
- Czekalski, N., Sigdel, R., Birtel, J., Matthews, B., Bürgmann, H., 2015. Does human activity impact the natural antibiotic resistance background? Abundance of antibiotic resistance genes in 21 Swiss lakes. *Environ. Int.* 81, 45–55. <https://doi.org/10.1016/j.envint.2015.04.005>

- Daiber, E.J., DeMarini, D.M., Ravuri, S.A., Liberatore, H.K., Cuthbertson, A.A., Thompson-Klemish, A., Byer, J.D., Schmid, J.E., Afifi, M.Z., Blatchley, E.R., Richardson, S.D., 2016. Progressive Increase in Disinfection Byproducts and Mutagenicity from Source to Tap to Swimming Pool and Spa Water: Impact of Human Inputs. *Environ. Sci. Technol.* 50, 6652–6662. <https://doi.org/10.1021/acs.est.6b00808>
- Davies, J., Davies, D., 2010. Origins and evolution of antibiotic resistance. *Microbiol. Mol. Biol. Rev.* 74, 417–433. <https://doi.org/10.1128/MMBR.00016-10>
- De Beer, D., Srinivasan, R., Stewart, P.S., 1994. Direct measurement of chlorine penetration into biofilms during disinfection. *Appl. Environ. Microbiol.* 60, 4339–4344. <https://doi.org/10.1128/aem.60.12.4339-4344.1994>
- Deborde, M., von Gunten, U., 2008. Reactions of chlorine with inorganic and organic compounds during water treatment-Kinetics and mechanisms: A critical review. *Water Res.* 42, 13–51. <https://doi.org/10.1016/j.watres.2007.07.025>
- Destiani, R., Templeton, M.R., 2019. The antibiotic resistance of heterotrophic bacteria in tap waters in London. *Water Supply* 19, 179–190. <https://doi.org/10.2166/ws.2018.065>
- Dodd, M.C., 2012. Potential impacts of disinfection processes on elimination and deactivation of antibiotic resistance genes during water and wastewater treatment. *J. Environ. Monit.* 14, 1754–1771. <https://doi.org/10.1039/c2em00006g>
- Dodd, M.C., Huang, C.H., 2004. Transformation of the antibacterial agent sulfamethoxazole in reactions with chlorine: Kinetics, mechanisms, and pathways. *Environ. Sci. Technol.* 38, 5607–5615. <https://doi.org/10.1021/es035225z>
- Dong, S., Masalha, N., Plewa, M.J., Nguyen, T.H., 2017. Toxicity of Wastewater with Elevated Bromide and Iodide after Chlorination, Chloramination, or Ozonation Disinfection. *Environ. Sci. Technol.* 51, 9297–9304. <https://doi.org/10.1021/acs.est.7b02345>
- Engelbrecht, R.S., Weber, M.J., Salter, B.L., Schmidt, C.A., 1980. Comparative inactivation of viruses by chlorine. *Appl. Environ. Microbiol.* 40, 249–256. <https://doi.org/10.1128/aem.40.2.249-256.1980>
- European environment agency, 2020. Global and European temperatures [WWW Document]. URL <https://www.eea.europa.eu/data-and-maps/indicators/global-and-european-temperature-10/assessment> (accessed 7.15.21).
- Eyer, P., 1991. Effects of superoxide dismutase on the autoxidation of 1,4-hydroquinone. *Chem. Biol. Interact.* 80, 159–176. [https://doi.org/10.1016/0009-2797\(91\)90022-Y](https://doi.org/10.1016/0009-2797(91)90022-Y)
- Farkas, L., Lewin, M., Bloch, R., 1949. The Reaction between Hypochlorite and Bromides. *J. Am. Chem. Soc.* 71, 1988–1991. <https://doi.org/10.1021/ja01174a025>
- Fayyad, M.K., Al-Sheikh, A.M., 2001. Determination of *N*-chloramines in As-Samra chlorinated wastewater and their effect on the disinfection process. *Water Res.* 35, 1304–1310. [https://doi.org/10.1016/S0043-1354\(00\)00393-6](https://doi.org/10.1016/S0043-1354(00)00393-6)

- Filali, B.K., Taoufik, J., Zeroual, Y., Dzairi, F.Z., Talbi, M., Blaghen, M., 2000. Waste Water Bacterial Isolates Resistant to Heavy Metals and Antibiotics. *Curr. Microbiol.* 41, 0151–0156. <https://doi.org/10.1007/s002840010109>
- Fischbacher, A., Löppenber, K., Von Sonntag, C., Schmidt, T.C., 2015. A New Reaction Pathway for Bromite to Bromate in the Ozonation of Bromide. *Environ. Sci. Technol.* 49, 11714–11720. <https://doi.org/10.1021/acs.est.5b02634>
- Floyd, R., Sharp, D.G., Johnson, J.D., 1979. Inactivation by Chlorine of Single Poliovirus Particles in Water. *Environ. Sci. Technol.* 13, 438–442. <https://doi.org/10.1021/es60152a005>
- Forman, H.J., Zhang, H., Rinna, A., 2009. Glutathione: Overview of its protective roles, measurement, and biosynthesis. *Mol. Aspects Med.* 30, 1–12. <https://doi.org/10.1016/j.mam.2008.08.006>
- Friedberg, E.C., Walker, G.C., Siede, W., Wood, R.D., Schultz, R.A., Ellenberger, T., 2005. DNA Repair and Mutagenesis. ASM Press, Washington, DC, USA. <https://doi.org/10.1128/9781555816704>
- Fu, X., Mueller, D.M., Heinecke, J.W., 2002. Generation of intramolecular and intermolecular sulfenamides, sulfinamides, and sulfonamides by hypochlorous acid: A potential pathway for oxidative cross-linking of low-density lipoprotein by myeloperoxidase. *Biochemistry* 41, 1293–1301. <https://doi.org/10.1021/bi015777z>
- Gallard, H., von Gunten, U., 2002. Chlorination of natural organic matter: Kinetics of chlorination and of THM formation. *Water Res.* 36, 65–74. [https://doi.org/10.1016/S0043-1354\(01\)00187-7](https://doi.org/10.1016/S0043-1354(01)00187-7)
- Gan, W., Huang, S., Ge, Y., Bond, T., Westerhoff, P., Zhai, J., Yang, X., 2019. Chlorite formation during ClO₂ oxidation of model compounds having various functional groups and humic substances. *Water Res.* 159, 348–357. <https://doi.org/10.1016/j.watres.2019.05.020>
- Gates, D.J., Ziglio, G., Ozekin, K., 2009. State of the science of chlorine dioxide in drinking water. *Water Res. Found. AMGA.*
- Ge, Y., Lei, Y., Lei, X., Gan, W., Shu, L., Yang, X., 2020. Exploration of reaction rates of chlorine dioxide with tryptophan residue in oligopeptides and proteins. *J. Environ. Sci. (China)* 93, 129–136. <https://doi.org/10.1016/j.jes.2020.03.059>
- Girgin Ersoy, Z., Barisci, S., Dinc, O., 2019. Mechanisms of the *Escherichia coli* and *Enterococcus faecalis* inactivation by ozone. *LWT* 100, 306–313. <https://doi.org/10.1016/j.lwt.2018.10.095>
- Glaze, W.H., Kang, J.W., Chapin, D.H., 1987. The chemistry of water treatment processes involving ozone, hydrogen peroxide and ultraviolet radiation. *Ozone Sci. Eng.* 9, 335–352. <https://doi.org/10.1080/01919518708552148>
- Glaze, W.H., Schep, R., Chauncey, W., Ruth, E.C., Zarnoch, J.J., Aieta, E.M., Tate, C.H., McGuire, M.J., 1990. Evaluating oxidants for the removal of model taste and odor compounds from a municipal water supply. *J. / Am. Water Work. Assoc.* 82, 79–84. <https://doi.org/10.1002/j.1551-8833.1990.tb06967.x>

- Gordon, G., Kieffer, R.G., Rosenblatt, D.H., 1972. The Chemistry of chlorine dioxide. *Prog. Inorg. Chem.* 15, 200–286. <https://doi.org/10.1093/litimag/imq040>
- Gordon, G., Slootmaekers, B., Tachiyashiki, S., Wood, D.W., 1990. Minimizing chlorite ion and chlorate ion in water treated with chlorine dioxide. *J. / Am. Water Work. Assoc.* 82, 160–165. <https://doi.org/10.1002/j.1551-8833.1990.tb06947.x>
- Grguric, G., Trefry, J.H., Keaffaber, J.J., 1994. Ozonation products of bromine and chlorine in seawater aquaria. *Water Res.* 28, 1087–1094. [https://doi.org/10.1016/0043-1354\(94\)90194-5](https://doi.org/10.1016/0043-1354(94)90194-5)
- Gruchlik, Y., Tan, J., Allard, S., Heitz, A., Bowman, M., Halliwell, D., Criquet, J., Joll, C., 2014. Impact of bromide and iodine during drinking disinfection and potential treatment processes for their removal or mitigation. A study to evaluate distributed water from two Western Australian drinking water sources. *Water* 41, 38–43.
- Guidelines for Drinking-water Quality, 4th ed, 2011. . World Health Organization.
- Guo, M.T., Yuan, Q. Bin, Yang, J., 2015. Distinguishing effects of ultraviolet exposure and chlorination on the horizontal transfer of antibiotic resistance genes in municipal wastewater. *Environ. Sci. Technol.* 49, 5771–5778. <https://doi.org/10.1021/acs.est.5b00644>
- Guo, Y., Xu, J., Bai, X., Lin, Y., Zhou, W., Li, J., 2022. Free chlorine formation in the process of the chlorine dioxide oxidation of aliphatic amines. *Water Res.* 217, 118399. <https://doi.org/10.1016/j.watres.2022.118399>
- Gyürék, L.L., Finch, G.R., 1998. Modeling Water Treatment Chemical Disinfection Kinetics. *J. Environ. Eng.* 124, 783–793. [https://doi.org/10.1061/\(ASCE\)0733-9372\(1998\)124:9\(783\)](https://doi.org/10.1061/(ASCE)0733-9372(1998)124:9(783))
- Haag, W.R., Holgné, J., 1983. Ozonation of Bromide-Containing Waters: Kinetics of Formation of Hypobromous Acid and Brómate. *Environ. Sci. Technol.* 17, 261–267. <https://doi.org/10.1021/es00111a004>
- Han, J., Zhang, X., Li, W., Jiang, J., 2021. Low chlorine impurity might be beneficial in chlorine dioxide disinfection. *Water Res.* 188, 116520. <https://doi.org/10.1016/j.watres.2020.116520>
- Hao, H., Cheng, G., Iqbal, Z., Ai, X., Hussain, H.I., Huang, L., Dai, M., Wang, Y., Liu, Z., Yuan, Z., 2014. Benefits and risks of antimicrobial use in food-producing animals. *Front. Microbiol.* 5, 1–11. <https://doi.org/10.3389/fmicb.2014.00288>
- Hao, J., Qiu, S., Li, H., Chen, T., Liu, H., Li, L., 2012. Roles of hydroxyl radicals in electrolyzed oxidizing water (EOW) for the inactivation of *Escherichia coli*. *Int. J. Food Microbiol.* 155, 99–104. <https://doi.org/10.1016/j.ijfoodmicro.2011.12.031>
- Hawkins, C.L., Davies, M.J., 2005. The role of reactive *N*-bromo species and radical intermediates in hypobromous acid-induced protein oxidation. *Free Radic. Biol. Med.* 39, 900–912. <https://doi.org/10.1016/j.freeradbiomed.2005.05.011>
- Hawkins, C.L., Davies, M.J., 1999. Hypochlorite-induced oxidation of proteins in plasma: formation of chloramines and nitrogen-centred radicals and their role in protein fragmentation. *Biochem. J.* 340, 539. <https://doi.org/10.1042/0264-6021:3400539>

- Hawkins, C.L., Davies, M.J., 1998a. Hypochlorite-induced damage to proteins: Formation of nitrogen-centred radicals from lysine residues and their role in protein fragmentation. *Biochem. J.* 332, 617–625. <https://doi.org/10.1042/bj3320617>
- Hawkins, C.L., Davies, M.J., 1998b. Reaction of HOCl with amino acids and peptides: EPR evidence for rapid rearrangement and fragmentation reactions of nitrogen-centred radicals. *J. Chem. Soc. Perkin Trans. 2* 1937–1945. <https://doi.org/10.1039/a802949k>
- Hazell, L.J., Stocker, R., 1993. Oxidation of low-density lipoprotein with hypochlorite causes transformation of the lipoprotein into a high-uptake form for macrophages. *Biochem. J.* 290, 165–172. <https://doi.org/10.1042/bj2900165>
- He, H., Zhou, P., Shimabuku, K.K., Fang, X., Li, S., Lee, Y., Dodd, M.C., 2019. Degradation and Deactivation of Bacterial Antibiotic Resistance Genes during Exposure to Free Chlorine, Monochloramine, Chlorine Dioxide, Ozone, Ultraviolet Light, and Hydroxyl Radical. *Environ. Sci. Technol.* 53, 2013–2026. <https://doi.org/10.1021/acs.est.8b04393>
- Heeb, M.B., Criquet, J., Zimmermann-Steffens, S.G., von Gunten, U., 2014. Oxidative treatment of bromide-containing waters: Formation of bromine and its reactions with inorganic and organic compounds - A critical review. *Water Res.* 48, 15–42. <https://doi.org/10.1016/j.watres.2013.08.030>
- Heeb, M.B., Kristiana, I., Trogolo, D., Arey, J.S., von Gunten, U., 2017. Formation and reactivity of inorganic and organic chloramines and bromamines during oxidative water treatment. *Water Res.* 110, 91–101. <https://doi.org/10.1016/j.watres.2016.11.065>
- Hoigne, J., Bader, H., 1980. Bestimmung von Ozon und Chlordioxid in Wasser mit der Indigomethode.
- Hoigné, J., Bader, H., 1994. Kinetics of reactions of chlorine dioxide (OCIO) in water—I. Rate constants for inorganic and organic compounds. *Water Res.* 28, 45–55. [https://doi.org/10.1016/0043-1354\(94\)90118-X](https://doi.org/10.1016/0043-1354(94)90118-X)
- Hoigné, J., Bader, H., 1983. Rate constants of reactions of ozone with organic and inorganic compounds in water—I Non-dissociating organic compounds. *Water Res.* 17, 173–183. [https://doi.org/10.1016/0043-1354\(83\)90098-2](https://doi.org/10.1016/0043-1354(83)90098-2)
- Hoigné, J., Bader, H., Haag, W.R., Staehelin, J., 1983. Rate constants of reactions of ozone with organic and inorganic compounds in water-II. Dissociating organic compounds. *Water Res.* 17, 185–194. [https://doi.org/10.1016/0043-1354\(85\)90368-9](https://doi.org/10.1016/0043-1354(85)90368-9)
- Houska, J., Salhi, E., Walpen, N., von Gunten, U., 2021. Oxidant-reactive carbonous moieties in dissolved organic matter: Selective quantification by oxidative titration using chlorine dioxide and ozone. *Water Res.* 207, 117790. <https://doi.org/10.1016/j.watres.2021.117790>
- How, Z.T., Linge, K.L., Busetti, F., Joll, C.A., 2017. Chlorination of Amino Acids: Reaction Pathways and Reaction Rates. *Environ. Sci. Technol.* 51, 4870–4876. <https://doi.org/10.1021/acs.est.6b04440>
- Hua, G., Reckhow, D.A., 2013. Effect of pre-ozonation on the formation and speciation of DBPs. *Water Res.* 47, 4322–4330. <https://doi.org/10.1016/j.watres.2013.04.057>

- Huber, M.M., Korhonen, S., Ternes, T.A., von Gunten, U., 2005. Oxidation of pharmaceuticals during water treatment with chlorine dioxide. *Water Res.* 39, 3607–3617. <https://doi.org/10.1016/j.watres.2005.05.040>
- Huie, R.E., Neta, P., 1986. Kinetics of one-electron transfer reactions involving ClO₂ and NO₂. *J. Phys. Chem.* 90, 1193–1198. <https://doi.org/10.1021/j100278a046>
- Hunt, N.K., Mariñas, B.J., 1999. Inactivation of *Escherichia coli* with ozone: Chemical and inactivation kinetics. *Water Res.* 33, 2633–2641. [https://doi.org/10.1016/S0043-1354\(99\)00115-3](https://doi.org/10.1016/S0043-1354(99)00115-3)
- Hunt, N.K., Mariñas, B.J., 1997. Kinetics of *Escherichia coli* inactivation with ozone. *Water Res.* 31, 1355–1362. [https://doi.org/10.1016/S0043-1354\(96\)00394-6](https://doi.org/10.1016/S0043-1354(96)00394-6)
- Hupperich, K., Mutke, X.A.M., Abdighahroudi, M.S., Jütte, M., Schmidt, T.C., Lutze, H.V., 2020. Reaction of chlorine dioxide with organic matter – formation of inorganic products. *Environ. Sci. Water Res. Technol.* 6, 2597–2606. <https://doi.org/10.1039/D0EW00408A>
- Hureiki, L., Croué, J.P., Legube, B., 1994. Chlorination studies of free and combined amino acids. *Water Res.* 28, 2521–2531. [https://doi.org/10.1016/0043-1354\(94\)90070-1](https://doi.org/10.1016/0043-1354(94)90070-1)
- Ishii, T., Fridovich, I., 1990. Dual effects of superoxide dismutase on the autoxidation of 1,4-naphthohydroquinone. *Free Radic. Biol. Med.* 8, 21–24. [https://doi.org/10.1016/0891-5849\(90\)90140-E](https://doi.org/10.1016/0891-5849(90)90140-E)
- Ishizaki, K., Sawadaishi, K., Miura, K., Shinriki, N., 1987. Effect of ozone on plasmid DNA of *Escherichia coli in situ*. *Water Res.* 21, 823–827. [https://doi.org/10.1016/0043-1354\(87\)90158-8](https://doi.org/10.1016/0043-1354(87)90158-8)
- Ison, A., Odeh, I.N., Margerum, D.W., 2006. Kinetics and mechanisms of chlorine dioxide and chlorite oxidations of cysteine and glutathione. *Inorg. Chem.* 45, 8768–8775. <https://doi.org/10.1021/ic0609554>
- Jacoby, G.A., 2009. AmpC B-Lactamases. *Clin. Microbiol. Rev.* 22, 161–182. <https://doi.org/10.1128/CMR.00036-08>
- Jäger, T., Hembach, N., Elpers, C., Wieland, A., Alexander, J., Hiller, C., Krauter, G., Schwartz, T., 2018. Reduction of Antibiotic Resistant Bacteria During Conventional and Advanced Wastewater Treatment, and the Disseminated Loads Released to the Environment. *Front. Microbiol.* 9, 1–16. <https://doi.org/10.3389/fmicb.2018.02599>
- James, T.H., Snell, J.M., Weissberger, A., 1938. Oxidation Processes. XII. 1 The Autoxidation of Hydroquinone and of the Mono-, Di- and Trimethylhydroquinones. *J. Am. Chem. Soc.* 60, 2084–2093. <https://doi.org/10.1021/ja01276a020>
- Jamil, A., Farooq, S., Hashmi, I., 2017. Ozone Disinfection Efficiency for Indicator Microorganisms at Different pH Values and Temperatures. *Ozone Sci. Eng.* 39, 407–416. <https://doi.org/10.1080/01919512.2017.1322489>
- Jensen, J.N., 2010. Disinfection Model Based on Excess Inactivation Sites: Implications for Linear Disinfection Curves and the Chick-Watson Dilution Coefficient. *Environ. Sci. Technol.* 44, 8162–8168. <https://doi.org/10.1021/es101818z>

- Jensen, J.S., Lam, Y.F., Helz, G.R., 1999. Role of amide nitrogen in water chlorination: Proton NMR evidence. *Environ. Sci. Technol.* 33, 3568–3573. <https://doi.org/10.1021/es980878e>
- Jin, M., Liu, L., Wang, D. ning, Yang, D., Liu, W. li, Yin, J., Yang, Z. wei, Wang, H. ran, Qiu, Z. gang, Shen, Z. qiang, Shi, D. yang, Li, H. bei, Guo, J. hua, Li, J. wen, 2020. Chlorine disinfection promotes the exchange of antibiotic resistance genes across bacterial genera by natural transformation. *ISME J.* 14, 1847–1856. <https://doi.org/10.1038/s41396-020-0656-9>
- Judd, S.J., Jeffrey, J.A., 1995. Trihalomethane formation during swimming pool water disinfection using hypobromous and hypochlorous acids. *Water Res.* 29, 1203–1206. [https://doi.org/10.1016/0043-1354\(94\)00230-5](https://doi.org/10.1016/0043-1354(94)00230-5)
- Jung, Y., Hong, E., Kwon, M., Kang, J.W., 2017. A kinetic study of ozone decay and bromine formation in saltwater ozonation: Effect of O₃ dose, salinity, pH, and temperature. *Chem. Eng. J.* 312, 30–38. <https://doi.org/10.1016/j.cej.2016.11.113>
- Junli, H., Li, W., Nanqi, R., Fang, M., Juli, 1997. Disinfection effect of chlorine dioxide on bacteria in water. *Water Res.* 31, 607–613. [https://doi.org/10.1016/S0043-1354\(96\)00275-8](https://doi.org/10.1016/S0043-1354(96)00275-8)
- Jütte, M., Abdighahroudi, M.S., Waldminghaus, T., Lackner, S., V. Lutze, H., 2023. Bacterial inactivation processes in water disinfection – mechanistic aspects of primary and secondary oxidants – A critical review. *Water Res.* 231, 119626. <https://doi.org/10.1016/j.watres.2023.119626>
- Jütte, M., Große, J.V., Abdighahroudi, M.S., Schüth, C., Lutze, H.V., 2022. Novel insights into chlorine dioxide based disinfection mechanisms – investigation of the reaction with amino acids. *Environ. Sci. Water Res. Technol.* 8, 630–639. <https://doi.org/10.1039/D1EW00812A>
- Karkman, A., Do, T.T., Walsh, F., Virta, M.P.J., 2018. Antibiotic-Resistance Genes in Waste Water. *Trends Microbiol.* 26, 220–228. <https://doi.org/10.1016/j.tim.2017.09.005>
- Katz, A., Narkis, N., 2001. Removal of chlorine dioxide disinfection by-products by ferrous salts. *Water Res.* 35, 101–108. [https://doi.org/10.1016/S0043-1354\(00\)00250-5](https://doi.org/10.1016/S0043-1354(00)00250-5)
- Knapp, C.W., Dolfing, J., Ehlert, P.A.I., Graham, D.W., 2010. Evidence of increasing antibiotic resistance gene abundances in archived soils since 1940. *Environ. Sci. Technol.* 44, 580–587. <https://doi.org/10.1021/es901221x>
- Korn, C., Andrews, R.C., Escobar, M.D., 2002. Development of chlorine dioxide-related by-product models for drinking water treatment. *Water Res.* 36, 330–342. [https://doi.org/10.1016/S0043-1354\(01\)00194-4](https://doi.org/10.1016/S0043-1354(01)00194-4)
- La Mer, V.K., Rideal, E.K., 1924. The influence of hydrogen concentration on the auto-oxidation of hydroquinone. A note on the stability of the quinhydrone electrode. *J. Am. Chem. Soc.* 46, 223–231. <https://doi.org/10.1021/ja01666a030>
- Lawrence, J., Cappelli, F.P., 1977. Ozone in drinking water treatment: A review. *Sci. Total Environ.* 7, 99–108. [https://doi.org/10.1016/0048-9697\(77\)90001-8](https://doi.org/10.1016/0048-9697(77)90001-8)
- Le Dantec, C., Duguet, J.P., Montiel, A., Dumoutier, N., Dubrou, S., Vincent, V., 2002. Chlorine disinfection of atypical mycobacteria isolated from a water distribution system. *Appl. Environ. Microbiol.* 68, 1025–1032. <https://doi.org/10.1128/AEM.68.3.1025-1032.2002>

- Lee, Y., von Gunten, U., 2012. Quantitative structure-activity relationships (QSARs) for the transformation of organic micropollutants during oxidative water treatment. *Water Res.* 46, 6177–6195. <https://doi.org/10.1016/j.watres.2012.06.006>
- Lee, Y., von Gunten, U., 2010. Oxidative transformation of micropollutants during municipal wastewater treatment: Comparison of kinetic aspects of selective (chlorine, chlorine dioxide, ferrate^{VI}, and ozone) and non-selective oxidants (hydroxyl radical). *Water Res.* 44, 555–566. <https://doi.org/10.1016/j.watres.2009.11.045>
- Lee, Y.J., Kim, H.T., Lee, U.G., 2004. Formation of chlorite and chlorate from chlorine dioxide with Han river water. *Korean J. Chem. Eng.* 21, 647–653. <https://doi.org/10.1007/BF02705500>
- Levanov, A. V., Isaikina, O.Y., Gasanova, R.B., Lunin, V. V., 2018. Solubility of Ozone and Kinetics of Its Decomposition in Aqueous Chloride Solutions. *Ind. Eng. Chem. Res.* 57, 14355–14364. <https://doi.org/10.1021/acs.iecr.8b03371>
- Lezcano, I., Pérez Rey, R., Baluja, C., Sánchez, E., 1999. Ozone inactivation of *Pseudomonas aeruginosa*, *Escherichia coli*, *Shigella sonnei* and *Salmonella typhimurium* in water. *Ozone Sci. Eng.* 21, 293–300. <https://doi.org/10.1080/01919519908547242>
- Li, J., Jiang, J., Pang, S., Cao, Y., Zhou, Y., Guan, C., 2020. Oxidation of iodide and hypiodous acid by non-chlorinated water treatment oxidants and formation of iodinated organic compounds: A review. *Chem. Eng. J.* 386. <https://doi.org/10.1016/j.cej.2019.123822>
- Lopez, A., Mascolo, G., Tiravanti, G., Santori, M., Passino, R., 1994. Oxidation of Sulfur-containing s-Triazines during groundwater hypochlorination. *Water Sci. Technol.* 30, 53–59. <https://doi.org/doi.org/10.2166/wst.1994.0304>
- Lu, J., Zhang, T., Ma, J., Chen, Z., 2009. Evaluation of disinfection by-products formation during chlorination and chloramination of dissolved natural organic matter fractions isolated from a filtered river water. *J. Hazard. Mater.* 162, 140–145. <https://doi.org/10.1016/j.jhazmat.2008.05.058>
- Magazinovic, R.S., Nicholson, B.C., Mulcahy, D.E., Davey, D.E., 2004. Bromide levels in natural waters: Its relationship to levels of both chloride and total dissolved solids and the implications for water treatment. *Chemosphere* 57, 329–335. <https://doi.org/10.1016/j.chemosphere.2004.04.056>
- Mao, D., Luo, Y., Mathieu, J., Wang, Q., Feng, L., Mu, Q., Feng, C., Alvarez, P.J.J., 2014. Persistence of extracellular DNA in river sediment facilitates antibiotic resistance gene propagation. *Environ. Sci. Technol.* 48, 71–78. <https://doi.org/10.1021/es404280v>
- Marti, R., Scott, A., Tien, Y.C., Murray, R., Sabourin, L., Zhang, Y., Topp, E., 2013. Impact of manure fertilization on the abundance of antibiotic-resistant bacteria and frequency of detection of antibiotic resistance genes in soil and on vegetables at harvest. *Appl. Environ. Microbiol.* 79, 5701–5709. <https://doi.org/10.1128/AEM.01682-13>
- Martínez-Carballo, E., González-Barreiro, C., Scharf, S., Gans, O., 2007. Environmental monitoring study of selected veterinary antibiotics in animal manure and soils in Austria. *Environ. Pollut.* 148, 570–579. <https://doi.org/10.1016/j.envpol.2006.11.035>

- Masson-Delmotte, V., Zhai, P., Pirani, A., Connors, S.L., Péan, P., Berger, S., Caud, N., Chen, Y., Goldfarb, L., Gomis, M.I., Huang, M., Leitzell, K., Lonnoy, E., Matthews, J.B.R., Maycock, T.K., Waterfield, T., Yelekci, O., Yu, R., Zhou, B., 2021. Technical Summary. Contribution of Working Group I to the Sixth Assessment Report of the Intergovernmental Panel on Climate Change, Climate Change 2021: The Physical Science Basis.
- Mayberry, W.E., Rall, J.E., Berman, M., Bertoli, D., 1965. Kinetics of Iodination. III. Iodination of N-Acetyl-L-tyrosine and N-Acetyl-3-iodo-L-tyrosine Studied in a pH-Stat System. *Biochemistry* 4, 1965–1972.
- Mazza, S., Danishefsky, S., McCurry, P., 1974. Diels-Alder reactions of o-benzoquinones. *J. Org. Chem.* 39, 3610–3611. <https://doi.org/10.1021/jo00938a043>
- McNair Scott, D.B., Leshner, E.C., 1963. Effect of Ozone on Survival and Permeability of *Escherichia Coli*. *J. Bacteriol.* 85, 567–576. <https://doi.org/10.1128/jb.85.3.567-576.1963>
- Morrison, C.M., Hogard, S., Pearce, R., Gerrity, D., von Gunten, U., Wert, E.C., 2022. Ozone disinfection of waterborne pathogens and their surrogates: A critical review. *Water Res.* 214. <https://doi.org/10.1016/j.watres.2022.118206>
- Mwatondo, M.H., Silverman, A.I., 2021. *Escherichia coli* and *Enterococcus spp.* Indigenous to Wastewater Have Slower Free Chlorine Disinfection Rates than Their Laboratory-Cultured Counterparts. *Environ. Sci. Technol. Lett.* 8, 1091–1097. <https://doi.org/10.1021/acs.estlett.1c00732>
- Na, C., Olson, T.M., 2007. Relative reactivity of amino acids with chlorine in mixtures. *Environ. Sci. Technol.* 41, 3220–3225. <https://doi.org/10.1021/es061999e>
- Nakagawara, S., Goto, T., Nara, M., Ozawa, Y., Hotta, K., Arata, Y., 1998. Spectroscopic Characterization and the pH Dependence of Bactericidal Activity of the Aqueous Chlorine Solution. *Anal. Sci.* 14, 691–698. <https://doi.org/10.2116/analsci.14.691>
- Napolitano, M.J., Green, B.J., Nicoson, J.S., Margerum, D.W., 2005. Chlorine dioxide oxidations of tyrosine, N-acetyltyrosine, and dopa. *Chem. Res. Toxicol.* 18, 501–508. <https://doi.org/10.1021/tx049697i>
- Neta, P., Huie, R.E., Ross, A.B., 1988. Rate Constants for Reactions of Inorganic Radicals in Aqueous Solution. *J. Phys. Chem. Ref. Data* 17, 1027–1284. <https://doi.org/10.1063/1.555808>
- Nihemaiti, M., Yoon, Y., He, H., Dodd, M.C., Croué, J.P., Lee, Y., 2020. Degradation and deactivation of a plasmid-encoded extracellular antibiotic resistance gene during separate and combined exposures to UV₂₅₄ and radicals. *Water Res.* 182. <https://doi.org/10.1016/j.watres.2020.115921>
- Noss, C.I., Hauchman, F.S., Olivieri, V.P., 1986. Chlorine dioxide reactivity with proteins. *Water Res.* 20, 351–356. [https://doi.org/10.1016/0043-1354\(86\)90083-7](https://doi.org/10.1016/0043-1354(86)90083-7)
- Nöthe, T., Fahlenkamp, H., von Sonntag, C., 2009. Ozonation of wastewater: Rate of ozone consumption and hydroxyl radical yield. *Environ. Sci. Technol.* 43, 5990–5995. <https://doi.org/10.1021/es900825f>

- Nuanualsuwan, S., Cliver, D.O., 2003. Capsid functions of inactivated human picornaviruses and feline calicivirus. *Appl. Environ. Microbiol.* 69, 350–357. <https://doi.org/10.1128/AEM.69.1.350-357.2003>
- Oancea, D., Puiu, M., 2003. Temperature and pH Effects on the kinetics of 2-aminophenol auto-oxidation in aqueous solution. *Open Chem.* 1, 233–241. <https://doi.org/10.2478/bf02476226>
- Ofori, I., Maddila, S., Lin, J., Jonnalagadda, S.B., 2017. Chlorine dioxide oxidation of *Escherichia coli* in water—A study of the disinfection kinetics and mechanism. *J. Environ. Sci. Heal. - Part A Toxic/Hazardous Subst. Environ. Eng.* 52, 598–606. <https://doi.org/10.1080/10934529.2017.1293993>
- Ogata, N., 2007. Denaturation of protein by chlorine dioxide: Oxidative modification of tryptophan and tyrosine residues. *Biochemistry* 46, 4898–4911. <https://doi.org/10.1021/bi061827u>
- Oki, T., Kanae, S., 2006. Global hydrological cycles and world water resources. *Science* (80-.). 313, 1068–1072. <https://doi.org/10.1126/science.1128845>
- Okusu, H., Ma, D., Nikaido, H., 1996. AcrAB efflux pump plays a major role in the antibiotic resistance phenotype of *Escherichia coli* multiple-antibiotic-resistance (Mar) mutants. *J. Bacteriol.* 178, 306–308. <https://doi.org/10.1128/jb.178.1.306-308.1996>
- Ooi, B.G., Branning, S.A., 2017. Correlation of Conformational Changes and Protein Degradation with Loss of Lysozyme Activity Due to Chlorine Dioxide Treatment. *Appl. Biochem. Biotechnol.* 182, 782–791. <https://doi.org/10.1007/s12010-016-2361-8>
- Padan, E., Zilberstein, D., Schuldiner, S., 1981. pH homeostasis in bacteria. *Biochim. Biophys. Acta - Rev. Biomembr.* 650, 151–166. [https://doi.org/10.1016/0304-4157\(81\)90004-6](https://doi.org/10.1016/0304-4157(81)90004-6)
- Page, M.A., Shisler, J.L., Mariñas, B.J., 2010. Mechanistic Aspects of Adenovirus Serotype 2 Inactivation with Free Chlorine. *Appl. Environ. Microbiol.* 76, 2946–2954. <https://doi.org/10.1128/AEM.02267-09>
- Pal, M., Ayele, Y., Hadush, A., Panigrahi, S., Jadhav, V.J., 2018. Public Health Hazards Due to Unsafe Drinking Water. *Air Water Borne Dis.* 7, 1–6. <https://doi.org/10.4172/2167-7719.1000138>
- Pan, S., An, W., Li, H., Su, M., Zhang, J., Yang, M., 2014. Cancer risk assessment on trihalomethanes and haloacetic acids in drinking water of China using disability-adjusted life years. *J. Hazard. Mater.* 280, 288–294. <https://doi.org/10.1016/j.jhazmat.2014.07.080>
- Panasenko, O.M., Briviba, K., Klotz, L.O., Sies, H., 1997. Oxidative modification and nitration of human low-density lipoproteins by the reaction of hypochlorous acid with nitrite. *Arch. Biochem. Biophys.* 343, 254–259. <https://doi.org/10.1006/abbi.1997.0171>
- Pattison, D.I., Davies, M.J., 2004. Kinetic Analysis of the Reactions of Hypobromous Acid with Protein Components: Implications for Cellular Damage and Use of 3-Bromotyrosine as a Marker of Oxidative Stress. *Biochemistry* 43, 4799–4809. <https://doi.org/10.1021/bi035946a>
- Pattison, D.I., Davies, M.J., 2001. Absolute rate constants for the reaction of hypochlorous acid with protein side chains and peptide bonds. *Chem. Res. Toxicol.* 14, 1453–1464. <https://doi.org/10.1021/tx0155451>

- Pattison, D.I., Hawkins, C.L., Davies, M.J., 2007. Hypochlorous acid-mediated protein oxidation: How important are chloramine transfer reactions and protein tertiary structure? *Biochemistry* 46, 9853–9864. <https://doi.org/10.1021/bi7008294>
- Pattison, D.I., Hawkins, C.L., Davies, M.J., 2003. Hypochlorous acid-mediated oxidation of lipid components and antioxidants present in low-density lipoproteins: Absolute rate constants, product analysis, and computational modeling. *Chem. Res. Toxicol.* 16, 439–449. <https://doi.org/10.1021/tx025670s>
- Pazda, M., Kumirska, J., Stepnowski, P., Mulkiewicz, E., 2019. Antibiotic resistance genes identified in wastewater treatment plant systems – A review. *Sci. Total Environ.* 697. <https://doi.org/10.1016/j.scitotenv.2019.134023>
- Peskin, A. V., Winterbourn, C.C., 2001. Kinetics of the reactions of hypochlorous acid and amino acid chloramines with thiols, methionine, and ascorbate. *Free Radic. Biol. Med.* 30, 572–579. [https://doi.org/10.1016/S0891-5849\(00\)00506-2](https://doi.org/10.1016/S0891-5849(00)00506-2)
- Porcelli, A.M., Ghelli, A., Zanna, C., Pinton, P., Rizzuto, R., Rugolo, M., 2005. pH difference across the outer mitochondrial membrane measured with a green fluorescent protein mutant. *Biochem. Biophys. Res. Commun.* 326, 799–804. <https://doi.org/10.1016/j.bbrc.2004.11.105>
- Pruden, A., Pei, R., Storteboom, H., Carlson, K.H., 2006. Antibiotic resistance genes as emerging contaminants: Studies in northern Colorado. *Environ. Sci. Technol.* 40, 7445–7450. <https://doi.org/10.1021/es060413l>
- Pryor, W.A., Das, B., Church, D.F., 1991. The Ozonation of Unsaturated Fatty Acids: Aldehydes and Hydrogen Peroxide as Products and Possible Mediators of Ozone Toxicity. *Chem. Res. Toxicol.* 4, 341–348. <https://doi.org/10.1021/tx00021a014>
- Pryor, W.A., Giamalva, D.H., Church, D.F., 1984. Kinetics of Ozonation. 2. Amino Acids and Model Compounds in Water and Comparisons to Rates in Nonpolar Solvents. *J. Am. Chem. Soc.* 106, 7094–7100. <https://doi.org/10.1021/ja00335a038>
- Ratkowsky, D.A., Olley, J., McMeekin, T.A., Ball, A., 1982. Relationship between temperature and growth rate of bacterial cultures. *J. Bacteriol.* 149, 1–5. <https://doi.org/10.1128/jb.149.1.1-5.1982>
- Reinders, W., Dingemans, P., 1934. Die Oxydationsgeschwindigkeit von Hydrochinon mit Luftsauerstoff. I. *Recl. des Trav. Chim. des Pays-Bas* 53, 209–230. <https://doi.org/10.1002/recl.19340530304>
- Renard, J.J., Bolker, H.I., 1976. The Chemistry of Chlorine Monoxide (Dichlorine Monoxide). *Chem. Rev.* 76, 487–508. <https://doi.org/10.1021/cr60302a004>
- Richardson, S.D., Plewa, M.J., Wagner, E.D., Schoeny, R., DeMarini, D.M., 2007. Occurrence, genotoxicity, and carcinogenicity of regulated and emerging disinfection by-products in drinking water: A review and roadmap for research. *Mutat. Res. - Rev. Mutat. Res.* 636, 178–242. <https://doi.org/10.1016/j.mrrev.2007.09.001>
- Ridenour, G.M., Ingols, R.S., 1947. Bactericidal Properties of Chlorine Dioxide. *Am. Water Work. Assoc.* 39, 561–567.

- Roberts, S.C., Zembower, T.R., 2020. Global increases in antibiotic consumption: a concerning trend for WHO targets. *Lancet Infect. Dis.* 3099, 2019–2020. [https://doi.org/10.1016/S1473-3099\(20\)30456-4](https://doi.org/10.1016/S1473-3099(20)30456-4)
- Rodríguez, E.M., von Gunten, U., 2020. Generation of hydroxyl radical during chlorination of hydroxyphenols and natural organic matter extracts. *Water Res.* 177. <https://doi.org/10.1016/j.watres.2020.115691>
- Roginsky, V.A., Pisarenko, L.M., Bors, W., Michel, C., 1999. The kinetics and thermodynamics of quinone-semiquinone-hydroquinone systems under physiological conditions. *J. Chem. Soc. Perkin Trans. 2* 871–876. <https://doi.org/10.1039/a807650b>
- Roller, S.D., Olivieri, V.P., Kawata, K., 1980. Mode of bacterial inactivation by chlorine dioxide. *Water Res.* 14, 635–641. [https://doi.org/10.1016/0043-1354\(80\)90121-9](https://doi.org/10.1016/0043-1354(80)90121-9)
- Rook, J.J., 1976. Haloforms in drinking water. *Am. Water Work. Assoc.* 68, 168–172. <https://doi.org/10.1002/j.1551-8833.1976.tb02376.x>
- Rook, J.J., 1974. Formation of haloforms during chlorination of natural waters. *Water Treat. Exam.* 23, 234–243.
- Rosenblatt, D.H., Hull, L.A., De Luca, D.C., Davis, G.T., Weglein, R.C., Williams, H.K.R., 1967. Oxidations of Amines. II. Substituent Effects in Chlorine Dioxide Oxidations. *J. Am. Chem. Soc.* 89, 1158–1163. <https://doi.org/10.1021/ja00981a022>
- Rossi-Fedele, G., Guastalli, A.R., Dođramaci, E.J., Steier, L., de Figueiredo, J.A.P., 2011. Influence of pH changes on chlorine-containing endodontic irrigating solutions. *Int. Endod. J.* 44, 792–799. <https://doi.org/10.1111/j.1365-2591.2011.01911.x>
- Rougé, V., Allard, S., Croué, J.P., Von Gunten, U., 2018. In Situ Formation of Free Chlorine during ClO₂ Treatment: Implications on the Formation of Disinfection Byproducts. *Environ. Sci. Technol.* 52, 13421–13429. <https://doi.org/10.1021/acs.est.8b04415>
- Sanganyado, E., Gwenzu, W., 2019. Antibiotic resistance in drinking water systems: Occurrence, removal, and human health risks. *Sci. Total Environ.* 669, 785–797. <https://doi.org/10.1016/j.scitotenv.2019.03.162>
- Sanitation [WWW Document], 2019. World Heal. Organ. URL <https://www.who.int/en/news-room/fact-sheets/detail/sanitation> (accessed 6.15.20).
- Sawadaishi, K., Miura, K., Ohtsuka, E., Ueda, T., Ishizaki, K., Shinriki, N., 1985. Ozonolysis of supercoiled pBR322 DNA resulting in strand scission to open circular DNA. *Nucleic Acids Res.* 13, 7183–7194. <https://doi.org/10.1093/nar/13.20.7183>
- Schüsler-Van Hees, M.T.I.W., Beijersbergen Van Henegouwen, G.M.J., Stoutenberg, P., 1985. Autoxidation of catechol(amine)s. *Pharm. Weekbl. Sci. Ed.* 7, 245–251. <https://doi.org/10.1007/BF01959197>
- Schwartz, T., Kohnen, W., Jansen, B., Obst, U., 2003. Detection of antibiotic-resistant bacteria and their resistance genes in wastewater, surface water, and drinking water biofilms. *FEMS Microbiol. Ecol.* 43, 325–335. [https://doi.org/10.1016/S0168-6496\(02\)00444-0](https://doi.org/10.1016/S0168-6496(02)00444-0)

- Semenza, J.C., 2020. Cascading risks of waterborne diseases from climate change. *Nat. Immunol.* 21, 479–483. <https://doi.org/10.1038/s41590-020-0648-y>
- Sharma, V.K., Graham, N.J.D., 2010. Oxidation of Amino Acids, Peptides and Proteins by Ozone: A Review. *Ozone Sci. Eng.* 32, 81–90. <https://doi.org/10.1080/01919510903510507>
- Sharma, V.K., Sohn, M., 2012. Reactivity of chlorine dioxide with amino acids, peptides, and proteins. *Environ. Chem. Lett.* 10, 255–264. <https://doi.org/10.1007/s10311-012-0355-5>
- Shiklomanov, I.A., Rodda, J.C., 2003. *World Water Resources at the Beginning of the Twenty-First Century*. Cambridge University Press.
- Sivey, J.D., McCullough, C.E., Roberts, A.L., 2010. Chlorine monoxide (Cl₂O) and molecular chlorine (Cl₂) as active chlorinating agents in reaction of dimethenamid with aqueous free chlorine. *Environ. Sci. Technol.* 44, 3357–3362. <https://doi.org/10.1021/es9038903>
- Smol, J.P., 2012. A planet in flux How is life on Earth reacting to climate change? *Nat.* 483, 12–15.
- Sorlini, S., Collivignarelli, C., 2005. Trihalomethane formation during chemical oxidation with chlorine, chlorine dioxide and ozone of ten Italian natural waters. *Desalination* 176, 103–111. <https://doi.org/10.1016/j.desal.2004.10.022>
- Stewart, D.J., Napolitano, M.J., Bakhmutova-Albert, E. V., Margerum, D.W., 2008. Kinetics and mechanisms of chlorine dioxide oxidation of tryptophan. *Inorg. Chem.* 47, 1639–1647. <https://doi.org/10.1021/ic701761p>
- Storkey, C., Davies, M.J., Pattison, D.I., 2014. Reevaluation of the rate constants for the reaction of hypochlorous acid (HOCl) with cysteine, methionine, and peptide derivatives using a new competition kinetic approach. *Free Radic. Biol. Med.* 73, 60–66. <https://doi.org/10.1016/j.freeradbiomed.2014.04.024>
- Su, S., Li, C., Yang, J., Xu, Q., Qiu, Z., Xue, B., Wang, S., Zhao, C., Xiao, Z., Wang, J., Shen, Z., 2020. Distribution of antibiotic resistance genes in three different natural water bodies—a lake, river and sea. *Int. J. Environ. Res. Public Health* 17, 1–12. <https://doi.org/10.3390/ijerph17020552>
- Su, W.-F., 2013. Characterization of Polymer, in: *Principles of Polymer Design and Synthesis. Lecture Notes in Chemistry*. Springer, pp. 89–110. https://doi.org/10.1007/978-3-642-38730-2_5
- Suquet, C., Warren, J.J., Seth, N., Hurst, J.K., 2010. Comparative study of HOCl-inflicted damage to bacterial DNA *ex vivo* and within cells. *Arch. Biochem. Biophys.* 493, 135–142. <https://doi.org/10.1016/j.abb.2009.10.006>
- Świetlik, J., Dąbrowska, A., Raczyk-Stanisławiak, U., Nawrocki, J., 2004. Reactivity of natural organic matter fractions with chlorine dioxide and ozone. *Water Res.* 38, 547–558. <https://doi.org/10.1016/j.watres.2003.10.034>
- Szattmári, D., Sárkány, P., Kocsis, B., Nagy, T., Miseta, A., Barkó, S., Longauer, B., Robinson, R.C., Nyitrai, M., 2020. Intracellular ion concentrations and cation-dependent remodelling of bacterial MreB assemblies. *Sci. Rep.* 10, 1–13. <https://doi.org/10.1038/s41598-020-68960-w>

- Szczuka, A., Horton, J., Evans, K.J., Dipietri, V.T., Sivey, J.D., Wigginton, K.R., 2022. Chloride Enhances DNA Reactivity with Chlorine under Conditions Relevant to Water Treatment. *Environ. Sci. Technol.* 13347–13356. <https://doi.org/10.1021/acs.est.2c03267>
- Tan, H., Sen, A.C., Wheeler, W.B., Cornell, J.A., Wei, C.I., 1987a. A Kinetic Study of the Reaction of Aqueous Chlorine and Chlorine Dioxide with Amino Acids, Peptides and Proteins. *J. Food Sci.* 52, 1706–1711. <https://doi.org/10.1111/j.1365-2621.1987.tb05910.x>
- Tan, H., Wheeler, W.B., Wei, C. i., 1987b. Reaction of chlorine dioxide with amino acids and peptides: Kinetics and mutagenicity studies. *Mutat. Res. Toxicol.* 188, 259–266. [https://doi.org/10.1016/0165-1218\(87\)90002-4](https://doi.org/10.1016/0165-1218(87)90002-4)
- Taylor, R.H., Falkinham, J.O., Norton, C.D., LeChevallier, M.W., 2000. Chlorine, chloramine, chlorine dioxide, and ozone susceptibility of *Mycobacterium avium*. *Appl. Environ. Microbiol.* 66, 1702–1705. <https://doi.org/10.1128/AEM.66.4.1702-1705.2000>
- Terhalle, J., Kaiser, P., Jütte, M., Buss, J., Yasar, S., Marks, R., Uhlmann, H., Schmidt, T.C., Lutze, H. V., 2018. Chlorine Dioxide—Pollutant Transformation and Formation of Hypochlorous Acid as a Secondary Oxidant. *Environ. Sci. Technol.* 52, 9964–9971. <https://doi.org/10.1021/acs.est.8b01099>
- Thevenon, F., Adatte, T., Wildi, W., Poté, J., 2012. Antibiotic resistant bacteria/genes dissemination in lacustrine sediments highly increased following cultural eutrophication of Lake Geneva (Switzerland). *Chemosphere* 86, 468–476. <https://doi.org/10.1016/j.chemosphere.2011.09.048>
- Tratnyek, P.G., Hoigné, J., 1994. Kinetics of reactions of chlorine dioxide (OCIO) in water-II. Quantitative structure-activity relationships for phenolic compounds. *Water Res.* 28, 57–66. [https://doi.org/10.1016/0043-1354\(94\)90119-8](https://doi.org/10.1016/0043-1354(94)90119-8)
- Ulmschneider, M.B., Sansom, M.S.P., 2001. Amino acid distributions in integral membrane protein structures. *Biochim. Biophys. Acta - Biomembr.* 1512, 1–14. [https://doi.org/10.1016/S0005-2736\(01\)00299-1](https://doi.org/10.1016/S0005-2736(01)00299-1)
- Van Wijk, D.J., Kroon, S.G.M., Gattener-Arends, I.C.M., 1998. Toxicity of chlorate and chlorite to selected species of algae, bacteria, and fungi. *Ecotoxicol. Environ. Saf.* 40, 206–211. <https://doi.org/10.1006/eesa.1998.1685>
- Venkobachar, C., Iyengar, L., Prabhakara Rao, A.V.S., 1977. Mechanism of disinfection: Effect of chlorine on cell membrane functions. *Water Res.* 11, 727–729. [https://doi.org/10.1016/0043-1354\(77\)90114-2](https://doi.org/10.1016/0043-1354(77)90114-2)
- Vicuña-Reyes, J.P., Luh, J., Mariñas, B.J., 2008. Inactivation of *Mycobacterium avium* with chlorine dioxide. *Water Res.* 42, 1531–1538. <https://doi.org/10.1016/j.watres.2007.10.035>
- Vikesland, P.J., Ozekin, K., Valentine, R.L., 1998. Effect of natural organic matter on monochloramine decomposition: Pathway elucidation through the use of mass and redox balances. *Environ. Sci. Technol.* 32, 1409–1416. <https://doi.org/10.1021/es970589a>

- Visser, M.C.M., Winterbourn, C.C., 1991. Oxidative damage to fibronectin. I. The effects of the neutrophil myeloperoxidase system and HOCl. *Arch. Biochem. Biophys.* 285, 53–59. [https://doi.org/10.1016/0003-9861\(91\)90327-F](https://doi.org/10.1016/0003-9861(91)90327-F)
- von Gunten, U., 2018. Oxidation Processes in Water Treatment: Are We on Track? *Environ. Sci. Technol.* 52, 5062–5075. <https://doi.org/10.1021/acs.est.8b00586>
- von Gunten, U., 2003a. Ozonation of drinking water: Part II. Disinfection and by-product formation in presence of bromide, iodide or chlorine. *Water Res.* 37, 1469–1487. [https://doi.org/10.1016/S0043-1354\(02\)00458-X](https://doi.org/10.1016/S0043-1354(02)00458-X)
- von Gunten, U., 2003b. Ozonation of drinking water: Part I. Oxidation kinetics and product formation. *Water Res.* 37, 1443–1467. [https://doi.org/10.1016/S0043-1354\(02\)00457-8](https://doi.org/10.1016/S0043-1354(02)00457-8)
- von Gunten, U., Hoigne, J., 1994. Bromate Formation during Ozonation of Bromide-Containing Waters: Interaction of Ozone and Hydroxyl Radical Reactions. *Environ. Sci. Technol.* 28, 1234–1242. <https://doi.org/10.1021/es00056a009>
- von Sonntag, C., 2006. Free-Radical-Induced DNA Damage and Its Repair, Free-Radical-Induced DNA Damage and Its Repair. <https://doi.org/10.1007/3-540-30592-0>
- von Sonntag, C., von Gunten, U., 2012. Chemistry of Ozone in Water and Wastewater Treatment: From Basic Principles to Applications. <https://doi.org/10.2166/9781780400839>
- Wajon, J.E., Morris, J.C., 1982. Rates of Formation of N-Bromo Amines in Aqueous Solution. *Inorg. Chem.* 21, 4258–4263. <https://doi.org/10.1021/ic00142a030>
- Wajon, J.E., Rosenblatt, D.H., Burrows, E.P., 1982. Oxidation of Phenol and Hydroquinone by Chlorine Dioxide. *Environ. Sci. Technol.* 16, 396–402. <https://doi.org/10.1021/es00101a006>
- Walker, J.T., 2018. The influence of climate change on waterborne disease and *Legionella*: a review. *Perspect. Public Health* 138, 282–286. <https://doi.org/10.1177/1757913918791198>
- Wang, F.H., Qiao, M., Su, J.Q., Chen, Z., Zhou, X., Zhu, Y.G., 2014. High throughput profiling of antibiotic resistance genes in urban park soils with reclaimed water irrigation. *Environ. Sci. Technol.* 48, 9079–9085. <https://doi.org/10.1021/es502615e>
- Wang, G.S., Deng, Y.C., Lin, T.F., 2007. Cancer risk assessment from trihalomethanes in drinking water. *Sci. Total Environ.* 387, 86–95. <https://doi.org/10.1016/j.scitotenv.2007.07.029>
- Wang, P., He, Y.L., Huang, C.H., 2011. Reactions of tetracycline antibiotics with chlorine dioxide and free chlorine. *Water Res.* 45, 1838–1846. <https://doi.org/10.1016/j.watres.2010.11.039>
- Wang, P., He, Y.L., Huang, C.H., 2010. Oxidation of fluoroquinolone antibiotics and structurally related amines by chlorine dioxide: Reaction kinetics, product and pathway evaluation. *Water Res.* 44, 5989–5998. <https://doi.org/10.1016/j.watres.2010.07.053>
- Watson, K., Shaw, G., Leusch, F.D.L., Knight, N.L., 2012. Chlorine disinfection by-products in wastewater effluent: Bioassay-based assessment of toxicological impact. *Water Res.* 46, 6069–6083. <https://doi.org/10.1016/j.watres.2012.08.026>

- Weiss, J., 2016. Handbook of Ion Chromatography. Wiley-VCH Verlag GmbH & Co. KGaA, Weinheim, Germany. <https://doi.org/10.1002/9783527651610>
- Wenk, J., Aeschbacher, M., Salhi, E., Canonica, S., Von Gunten, U., Sander, M., 2013. Chemical oxidation of dissolved organic matter by chlorine dioxide, chlorine, and ozone: Effects on its optical and antioxidant properties. *Environ. Sci. Technol.* 47, 11147–11156. <https://doi.org/10.1021/es402516b>
- Werdehoff, K.S., Singer, P.C., 1987. Chlorine Dioxide Effects on Thmfp, Toxfp, and the Formation of Inorganic By-Products. *J. / Am. Water Work. Assoc.* 79, 107–113. <https://doi.org/10.1002/j.1551-8833.1987.tb02908.x>
- Westerhoff, P., Chao, P., Mash, H., 2004. Reactivity of natural organic matter with aqueous chlorine and bromine. *Water Res.* 38, 1502–1513. <https://doi.org/10.1016/j.watres.2003.12.014>
- Wigginton, K.R., Pecson, B.M., Sigstam, T., Bosshard, F., Kohn, T., 2012. Virus inactivation mechanisms: Impact of disinfectants on virus function and structural integrity. *Environ. Sci. Technol.* 46, 12069–12078. <https://doi.org/10.1021/es3029473>
- Winterbourn, C.C., 1985. Comparative reactivities of various biological compounds with myeloperoxidase-hydrogen peroxide-chloride, and similarity of oxidant to hypochlorite. *Biochim. Biophys. Acta - Gen. Subj.* 840, 204–210. [https://doi.org/10.1016/0304-4165\(85\)90120-5](https://doi.org/10.1016/0304-4165(85)90120-5)
- Wirzberger, V., Klein, M., Woermann, M., Lutze, H. V., Sures, B., Schmidt, T.C., 2021. Matrix composition during ozonation of *N*-containing substances may influence the acute toxicity towards *Daphnia magna*. *Sci. Total Environ.* 765, 142727. <https://doi.org/10.1016/j.scitotenv.2020.142727>
- Wojtowicz, J.A., 2004. Sanitizer and oxidizer product information summaries. *J. Swim. Pool Spa Ind.* 5, 20–38.
- Xue, Z., Hessler, C.M., Panmanee, W., Hassett, D.J., Seo, Y., 2013. *Pseudomonas aeruginosa* inactivation mechanism is affected by capsular extracellular polymeric substances reactivity with chlorine and monochloramine. *FEMS Microbiol. Ecol.* 83, 101–111. <https://doi.org/10.1111/j.1574-6941.2012.01453.x>
- Yamazaki, I., Ohnishi, T., 1966. One-electron-transfer reactions in biochemical systems I. Kinetic analysis of the oxidation-reduction equilibrium between quinol-quinone and ferroferricytochrome c. *Biochim. Biophys. Acta - Biophys. Incl. Photosynth.* 112, 469–481. [https://doi.org/10.1016/0926-6585\(66\)90249-4](https://doi.org/10.1016/0926-6585(66)90249-4)
- Yang, X., Guo, W., Lee, W., 2013. Formation of disinfection byproducts upon chlorine dioxide preoxidation followed by chlorination or chloramination of natural organic matter. *Chemosphere* 91, 1477–1485. <https://doi.org/10.1016/j.chemosphere.2012.12.014>
- Yoon, Y., Chung, H.J., Wen Di, D.Y., Dodd, M.C., Hur, H.G., Lee, Y., 2017. Inactivation efficiency of plasmid-encoded antibiotic resistance genes during water treatment with chlorine, UV, and UV/H₂O₂. *Water Res.* 123, 783–793. <https://doi.org/10.1016/j.watres.2017.06.056>

- Yoon, Y., He, H., Dodd, M.C., Lee, Y., 2021. Degradation and deactivation of plasmid-encoded antibiotic resistance genes during exposure to ozone and chlorine. *Water Res.* 202. <https://doi.org/10.1016/j.watres.2021.117408>
- Yu, Q., Feng, T., Yang, J., Su, W., Zhou, R., Wang, Y., Zhang, H., Li, H., 2022. Seasonal distribution of antibiotic resistance genes in the Yellow River water and tap water, and their potential transmission from water to human. *Environ. Pollut.* 292. <https://doi.org/10.1016/j.envpol.2021.118304>
- Zhang, H., Zhang, Y., Shi, Q., Hu, J., Chu, M., Yu, J., Yang, M., 2012. Study on transformation of natural organic matter in source water during chlorination and its chlorinated products using ultrahigh resolution mass spectrometry. *Environ. Sci. Technol.* 46, 4396–4402. <https://doi.org/10.1021/es203587q>
- Zhang, M., Chen, S., Yu, X., Vikesland, P., Pruden, A., 2019. Degradation of extracellular genomic, plasmid DNA and specific antibiotic resistance genes by chlorination. *Front. Environ. Sci. Eng.* 13. <https://doi.org/10.1007/s11783-019-1124-5>
- Zhang, T., Zhang, M., Zhang, X., Fang, H.H., 2009. Tetracycline resistance genes and tetracycline resistant lactose-fermenting *Enterobacteriaceae* in activated sludge of sewage treatment plants. *Environ. Sci. Technol.* 43, 3455–3460. <https://doi.org/10.1021/es803309m>
- Zhang, X., Echigo, S., Minear, R.A., Plewa, M.J., 2000. Characterization and comparison of disinfection by-products of four major disinfectants. *ACS Symp. Ser.* 761, 299–314. <https://doi.org/10.1021/bk-2000-0761.ch019>
- Zhang, Y. qing, Wu, Q. ping, Zhang, J. mei, Yang, X. hua, 2015. Effects of ozone on the cytomembrane and ultrastructure of *Pseudomonas aeruginosa*. *Food Sci. Biotechnol.* 24, 987–993. <https://doi.org/10.1007/s10068-015-0126-8>
- Zhao, B., Xu, J., Zhang, G., Lu, S., Liu, X., Li, L., Li, M., 2020. Occurrence of antibiotics and antibiotic resistance genes in the Fuxian Lake and antibiotic source analysis based on principal component analysis-multiple linear regression model. *Chemosphere* 262, 127741. <https://doi.org/10.1016/j.chemosphere.2020.127741>
- Zhao, X., Lan, W., Yang, X., Xie, J., 2022. Inactivation effect and protective barriers damage caused to *Shewanella putrefaciens* by stable chlorine dioxide combined with slightly acidic electrolyzed water. *J. Food Process. Preserv.* 46, 1–10. <https://doi.org/10.1111/jfpp.16775>
- Zhu, Y.G., Johnson, T.A., Su, J.Q., Qiao, M., Guo, G.X., Stedtfeld, R.D., Hashsham, S.A., Tiedje, J.M., 2013. Diverse and abundant antibiotic resistance genes in Chinese swine farms. *Proc. Natl. Acad. Sci. U. S. A.* 110, 3435–3440. <https://doi.org/10.1073/pnas.1222743110>
- Zilberstein, D., Agmon, V., Schuldiner, S., Padan, E., 1984. *Escherichia coli* intracellular pH, membrane potential, and cell growth. *J. Bacteriol.* 158, 246–252. <https://doi.org/10.1128/jb.158.1.246-252.1984>
- Zimmer, H., Lankin, D.C., Horgan, S.W., 1971. Oxidations with potassium nitrosodisulfonate (fremy's radical). The teuber reaction. *Chem. Rev.* 71, 229–246. <https://doi.org/10.1021/cr60270a005>

Zuma, F.N., Lin, J., Jonnalagadda, S.B., 2009. Kinetics of inactivation of *Pseudomonas aeruginosa* in aqueous solutions by ozone aeration. J. Environ. Sci. Heal. Part A 44, 929–935. <https://doi.org/10.1080/10934520902996807>

List of Figures

- Figure 1: Graphical abstract of chapter 1.2 – Bacterial inactivation processes in water disinfection – mechanistic aspects of primary and secondary oxidants – a critical review _____ 8
- Figure 2: Available inactivation rates of different bacteria with different chemical oxidants from literature. Datasets are separated by laboratory-cultivated strains (full symbol) and wastewater isolates (half full symbols). _____ 12
- Figure 3: Schematic representation of a cell with different points of attack for inactivation. The possible target structures are a) the double bonds of the lipid bilayer, b) the amino acids of the membrane proteins, c) intracellular proteins, and d) the DNA nucleotides (chromosomal DNA and plasmids). _____ 19
- Figure 4: Range of reaction rates of different oxidants towards functional groups present in the side groups of amino acids at pH 7. _____ 20
- Figure 5: Reaction of FAC with the primary amine of lysine side chains leads to the formation of N-centered radicals and causes protein fragmentation. Pathway adapted from (Hawkins and Davies, 1998a). _____ 26
- Figure 6: Overview of all possible secondary oxidants formed during FAC, ClO₂, and O₃ disinfection. _____ 40
- Figure 7: Graphical overview of the thesis content and different chapters. _____ 45
- Figure 8: Graphical abstract of Chapter 3.1 – Novel insights in chlorine dioxide-based disinfection mechanisms - investigation of the reaction with amino acids. _____ 51
- Figure 9: pH-dependent reaction kinetics of NAL-tyrosine (A) and NAL-tryptophan (B) with ClO₂. Experimental conditions: 100 μM of NAL-amino acid, 100 μM competitor, 5 mM phosphate buffer, and 10 mM glycine. A: The grey and the black line represent the speciation of NAL-tyrosine (pK_a = 10.22) (Mayberry et al., 1965), grey and black represent the protonated and the deprotonated phenolic moiety, respectively. The black dots show the determined second-order reaction rate constants, and the dashed line is the kinetic model (cf. material and methods). B: NAL-tryptophan has no dissociation center, therefore the black line is representing the neutral species, which is constant over the full pH range. Black dots are representing the measured second-order reaction rates measured by using indole as a competitor, the star represents the second-order reaction rate measured with phenol as a competitor. Measurements have been done in triplicates, the relative standard deviation was < 7%). _____ 60
- Figure 10: pH-dependent reaction rate of (A) NAL-tyrosine and (B) NAL-tryptophan with HOCl. Experimental conditions: 100 μM of NAL-amino acid, 100 μM competitors, and 5 mM phosphate buffer. (A): The black and grey line represents the speciation of NAL-tyrosine (pK_a = 10.22) (Mayberry et al., 1965), whereby grey and black are representing the protonated and the deprotonated phenolic moiety, respectively. The red and green line represents the speciation of HOCl (red = HOCl; green = OCl⁻). The black squares are the measured second-order reaction rate constants, and the dashed line shows the kinetic model. (B): NAL-tryptophan does not dissociate, therefore the black line is representing the neutral species, which is constant over the entire pH range. The red and green line represents the speciation of HOCl (red = HOCl; green = OCl⁻). Black

triangles are representing the second-order reaction rate constants measured by competition kinetics using SMX as a competitor, and the black squares represent the second-order reaction rate constants measured with phenol as a competitor. _____ 62

Figure 11: Chlorine balance of N-Acetyl-L-tyrosine (A) and N-Acetyl-L-tryptophan (B). Both balances were determined at pH 7. The reaction solution contained 10 mM glycine, 5 mM phosphate buffer, and 0.1 mM of the corresponding N-acetylated amino acid. All experiments were measured in triplicates. The error bars represent the standard deviation of the results. If the yield of a species was below 2.5 %, it is not shown in the chart. A complete overview of the detected yields of inorganic chlorine species is given in Table 10. _____ 66

Figure 12: Proposed reaction pathway of the reaction of NAL-tryptophan with ClO₂. _____ 69

Figure 13: Graphical abstract of chapter 3.2 – Reaction mechanisms of chlorine dioxide with phenolic compounds – Influence of different substituents on stoichiometric ratios and intrinsic formation of free available chlorine _____ 74

Figure 14: Phenolic model compounds investigated in this study. Besides different different methylphenols, chlorophenol, bromophenol, methoxyphenol, hydroxyphenol, and aminophenol were investigated as well. _____ 77

Figure 15: Chlorine balance of methyl-substituted compounds. The reaction solution contained 0.1 mM of the compound under study, 5 mM phosphate buffer to retain the pH at 7, and 10 mM glycine to scavenge intrinsically formed FAC. ClO₂ was dosed in six different ratios to the model compounds (4-MP: 4-Methylphenol, 2,4-DMP: 2,4-dimethylphenol, 2,6-DMP: 2,6-dimethylphenol, 3,5-DMP: 3,5-dimethylphenol, 2,4,6-TMP: 2,4,6-trimethylphenol, and vanillin), and each ratio was carried out in triplicates. This figure shows the mean values of all 18 measurements, and the error bars represent the standard deviation of those. _____ 81

Figure 16: Repetitive measurement of the same sample of 2,4-dimethylphenol (left) and 2,6-dimethylphenol (right) after dosing 200 μM ClO₂. The samples contained 200 μM compound under study, 10 mM glycine, and 5 mM phosphate buffer at pH 7. The first sample was treated identically to the previous experiments. After each injection, the sample remained in the autosampler at 5 °C and was measured five times in a row. The time between every injection was 40 minutes. ____ 82

Figure 17: Postulated pathway of *para*-unsubstituted phenolic moieties (e.g., 2,6-dimethylphenol) compared to *para*-substituted phenolic compounds (e.g., 2,4-dimethylphenol) reacting with ClO₂. _____ 84

Figure 18: Chlorine balances of the phenolic compounds which contain an amino-, hydroxyl, methoxy, bromo-, or chloro-substituent. The reaction solution contained 0.1 mM of the compound under study, 5 mM phosphate buffer to keep a constant pH of 7, and 10 mM glycine to scavenge intrinsically formed FAC. ClO₂ was dosed in six different ratios to the model compounds and each ratio was carried out in triplicates (see Figure AIII.7 – Figure AIII.11). Here the mean values of all 18 measurements are shown and the error bars represent the standard deviation. Note that due to the dose-dependent results of resorcinol (see Figure AIII.10), the results in the case of resorcinol shown in this figure display the results for the lowest dose of ClO₂ (0.02 mM). _____ 86

Figure 19: Postulated reaction mechanism of 4-chlorophenol with ClO₂. _____ 88

List of Figures

-
- Figure 20: Postulated reaction mechanism of Hydroquinone with ClO_2 . The first attack occurs by electron abstraction. In the second step, the unstable OCIO -adduct abstracts the hydrogen of the hydroxyl group and cleaves as HClO_2 . _____ 90
- Figure 21: Hydroquinone cycle. Hydroquinone is autoxidized by O_2 to form para-BQ and $\text{O}_2^{\cdot-}$. BQ can react with hydroquinone to form SQ, which again can be turned into hydroquinone. This cycle can be cut by adding an excess of ClO_2 over hydroquinone. _____ 93
- Figure 22: Graphical abstract of chapter 3.3. _____ 100
- Figure 23: Relative yields of chloride based on the dosed concentration of FAC. Solutions contained 1 mM methionine and 5 mM phosphate buffer at $\text{pH} = 7$. All experiments were carried out in triplicates and the error bars represent the standard deviation of the triplicate measurement. _____ 107
- Figure 24: Correlation of MSO formation with the addition of FAC. Reaction solutions contained 1 mM methionine and 5 mM phosphate buffer ($\text{pH} = 7$). All experiments were carried out in triplicates, and the error bars represent the standard deviation of the results. _____ 108
- Figure 25: Measured chlorine balance of phenol by using the developed methionine method. **A** shows the yields of all compounds (please note chloride is formed in the reaction of FAC with methionine) and **B** shows the remaining MSO fraction after subtracting the chloride yields from MSO yields. All reaction solutions contained 0.1 mM phenol, 1 mM methionine, and 5 mM phosphate buffer. The buffer was used to preserve $\text{pH} = 7$. All experiments were carried out in triplicates, and the error bars represent the standard deviation of the triplicate measurement. _____ 109
- Figure 26: Estimated chlorine balance of hydroquinone (A) and DMP (B) by using the developed methionine method. All reactions contained 0.1 mM of either hydroquinone or DMP, 1 mM methionine, and 5 mM phosphate buffer at $\text{pH} 7$. All experiments were carried out in triplicates, and the error bars represent the standard deviation of the triplicate measurements. _____ 110
- Figure 27: Chlorine balance of GSH established by using the methionine method. A reaction solution containing 0.1 mM GSH, 5 mM phosphate buffer, and 1 mM methionine at $\text{pH} 7$ were mixed with different concentrations of ClO_2 . All experiments were carried out in triplicates and the error bars represent the standard deviation. _____ 112
- Figure 28: Postulated reaction pattern of GSH in case of different dosed ClO_2 concentrations at $\text{pH} 7$ in presence of 1 mM methionine. _____ 113
- Figure 29: Proposed reaction mechanism for Glutathione with Chlorine dioxide. GSH reacts with two molecules of ClO_2 and forms ClO_2^- and HOCl (FAC). _____ 114
- Figure 30: Monitoring of ClO_2^- and MSO over 24 hours. The reaction solution contained 0.1 mM methionine and 5 mM phosphate buffer at $\text{pH} 7$. 0.1 mM ClO_2^- was added and was measured with IC and LC-MSMS simultaneously. _____ 114
- Figure 30: Inactivation of *E. coli* by adding 7 μM of ClO_2 (0.5 mg/L). ClO_2 was added to *E. coli* suspension in PBS at $\text{pH} 7$ and 25°C . The figure shows the counted CFU at a specific time as a function of determined ClO_2 exposure. Cell count was determined by plating a dilution series on agar plates and incubating at 37°C for 24 hours. _____ 125

List of Figures

Figure 31: Growth curve of *E. coli* after different time exposures of ClO₂ determined by a plate reader. OD at 600 nm was determined for 16 hours every 5 min at 37°C. Experimental condition: 7 μM ClO₂ was dosed to *E. coli* suspension at pH 7.8 and 25 °C. Samples were taken at specific times, and the reaction was stopped by using thiosulfate. Aliquots were transferred to a 96-well plate and mixed with 2:1 LB media. Each sample was measured 8 times in different wells, thus, the data points show the mean values of the eightfold determination, and the error bars represent the standard deviation. _____ 126

Figure 32: Dose dependent inactivation of *E. coli* by ClO₂. ClO₂ was added in different concentrations to *E. coli* suspension containing NOM (DOC: 5 mg/L) in PBS pH = 7.8. All experiments were carried out in quadruple determinations and the lines represent the mean values. To increase the clarity, the standard deviations of the results have been removed. _____ 127

Figure 33: Inactivation of *E. coli* in the presence (black line) and absence (blue line) of 100 μM methionine. The black line represents a control sample of *E. coli* with no addition of ClO₂. Samples contained *E. coli* (OD₆₀₀ = 0.1) and NOM (DOC = 5 mg/L). All samples were measured in quadruple determination and the error bars represent the standard deviation of the results. ____ 130

List of Tables

| | |
|---|-----|
| Table 1: Comparison of inactivation kinetics of different bacteria with ozone. _____ | 13 |
| Table 2: Comparison of inactivation kinetics of different bacteria with chlorine dioxide. _____ | 13 |
| Table 3: Comparison of inactivation kinetics of different bacteria with free available chlorine. _ | 14 |
| Table 4: Range of inactivation efficiency in wastewater of the oxidants ozone, chlorine dioxide, and chlorine. The exposures of the different oxidants have been determined for the same wastewater and were obtained from Lee and von Gunten (2010). _____ | 15 |
| Table 5: Known and conceivable secondary oxidants for different primary oxidants. _____ | 17 |
| Table 6: Summary of the known reaction rates of GSH towards different oxidative species ____ | 36 |
| Table 7: pH range of competitors used to determine the second-order reaction rate constants for NAL-tyrosine & NAL-tryptophan. _____ | 56 |
| Table 8: Species-specific reaction kinetics of competitors taken from literature. Reaction rates are given for protonated (HB) and deprotonated (B ⁻) species. _____ | 57 |
| Table 9: Kinetic results for amino acids reaction with ClO ₂ and HOCl and comparison of second-order reaction rate constants with literature data. Reaction rate constants are given for protonated (HB) and deprotonated (B ⁻) amino acids (AA). As mentioned above, the reaction kinetics of OCl ⁻ is neglected. _____ | 63 |
| Table 10: Quantification of chlorine species during the reaction of both amino acids and ClO ₂ . _____ | 67 |
| Table 11: Different yields of chlorine species and reaction stoichiometry achieved in this study compared with literature data. _____ | 95 |
| Table 12: Results of pseudofirst-order kinetic reactions of methionine with ClO ₂ . The reaction solution contained different concentrations of methionine (0.5, 5, and 50 mM) and 5 mM phosphate buffer. 0.5 mM ClO ₂ was dosed to all samples, and all experiments were carried out in triplicates. _____ | 106 |
| Table 13: Literature data for the chlorine balance of different model compounds. _____ | 108 |
| Table 14: Delay of exponential <i>E. coli</i> growth after different time of ClO ₂ exposure in PBS. Initial ClO ₂ concentration = 7 μM. _____ | 127 |
| Table 15: Inactivation of <i>E. coli</i> by ClO ₂ and FAC in presence of different methionine concentrations. Oxidants were added to <i>E. coli</i> suspensions which contain NOM (DOC = 5 mg/L). The initial dose of <i>E. coli</i> was OD ₆₀₀ = 0.1. Growth was monitored by 96 well plates for 16 hours every five minutes at 37 °C. All samples were measured in quadruple determination. The percentage value represents the relative lag phase increase compared to growth curves which were not treated with any oxidant. _____ | 129 |
| Table 16: pH-dependent growth of <i>E. coli</i> after addition of 0 and 100 μM ClO ₂ . Initial samples contained <i>E. coli</i> (OD ₆₀₀ = 0.1) and 5 mg/L NOM. ClO ₂ was added and after 5 min of reaction time 100 μL of the reaction solution was transferred to a 96-well plate and 100 μL 2:1 LB-media was added. OD ₆₀₀ was measured every 5 min for 16 hours at 37 °C. All experiments were carried out in triplicate and each sample was measured four times. In pretenses the relative extension of the lag phase is given. _____ | 131 |

Appendix I

Appendix I

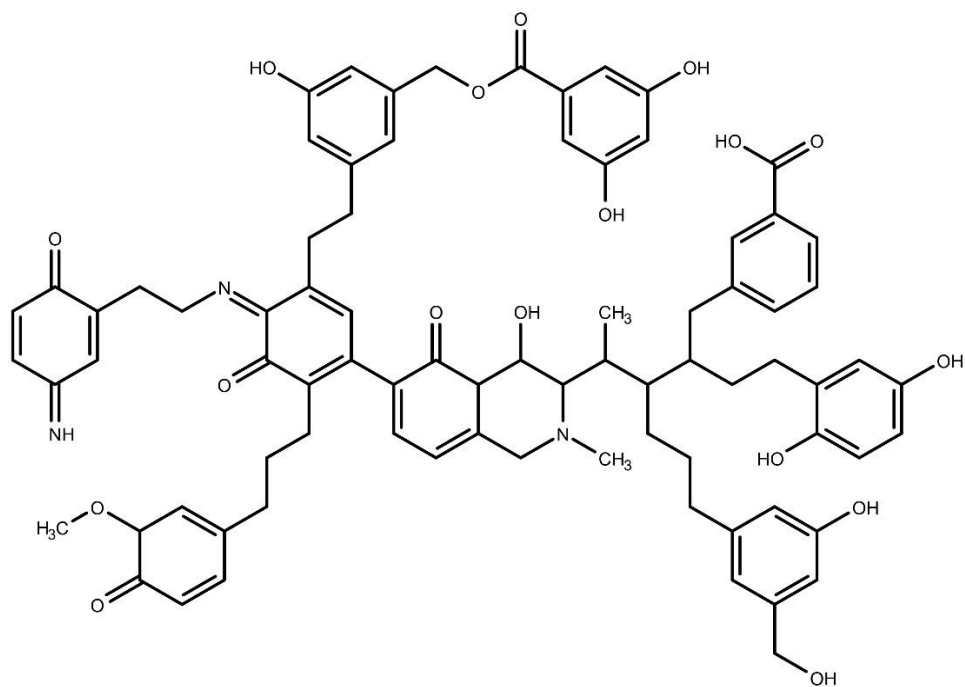


Figure AI.1: Example structure of natural organic matter.

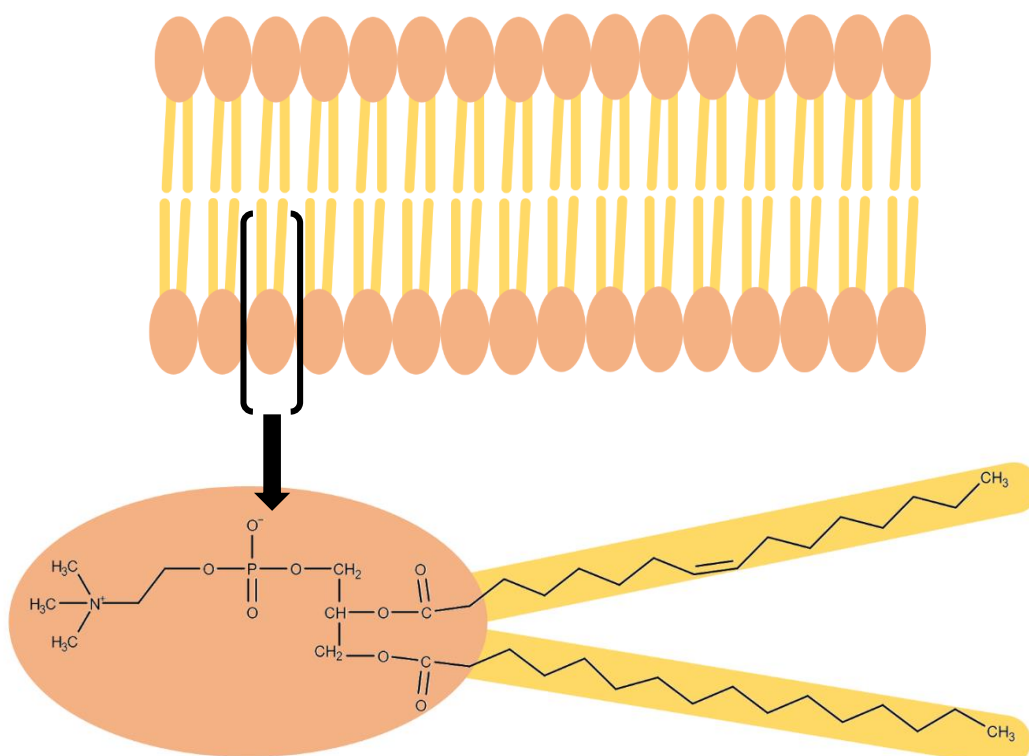


Figure AI.2: Systematic scheme of a double lipid layer of microbial cells.

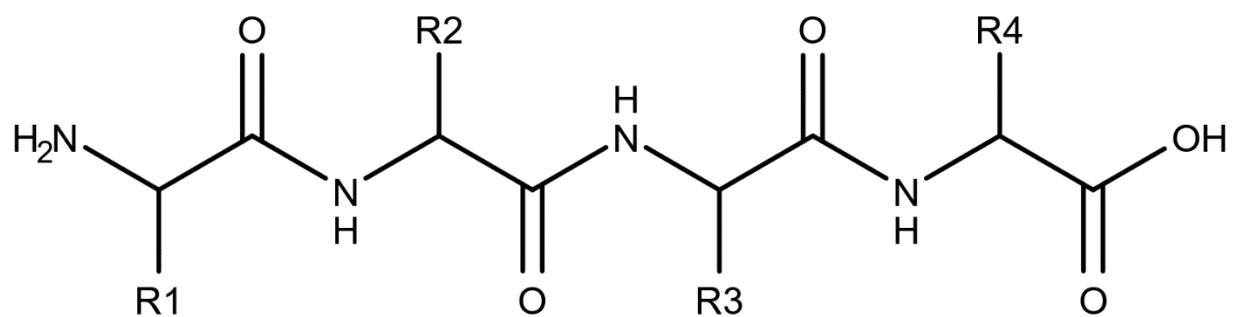
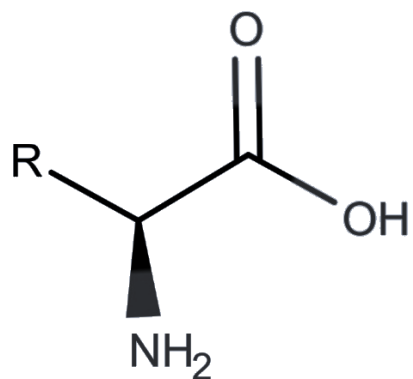


Figure AI.3: Schematic structure of free amino acids and a peptide with four amino acids. R denominates the functional side group.

Appendix I

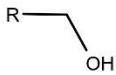
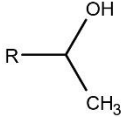
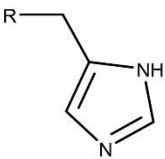
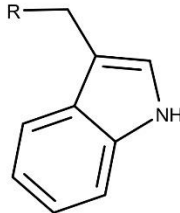
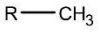
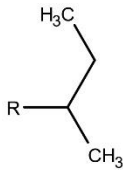
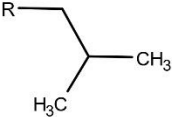
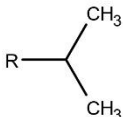
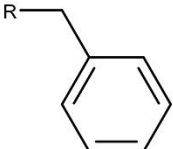
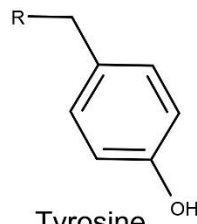
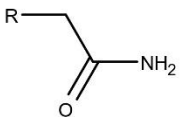
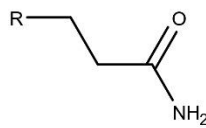
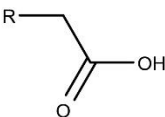
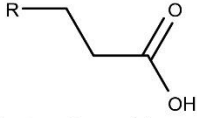
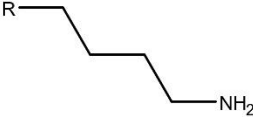
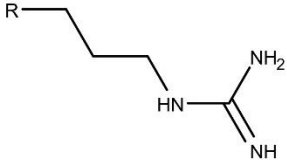
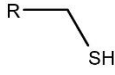
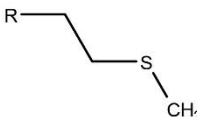
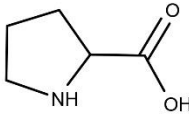
| | | |
|--|--|--|
| <p style="text-align: center;">Alcohol</p> <div style="display: flex; justify-content: space-around;"> <div style="text-align: center;">  <p>Serine</p> </div> <div style="text-align: center;">  <p>Threonine</p> </div> </div> | <p style="text-align: center;">Aromatic amine</p> <div style="display: flex; justify-content: space-around;"> <div style="text-align: center;">  <p>Histidine</p> </div> <div style="text-align: center;">  <p>Tryptophan</p> </div> </div> | |
| <p style="text-align: center;">Alkane</p> <div style="display: flex; justify-content: space-around;"> <div style="text-align: center;">  <p>Alanine</p> </div> <div style="text-align: center;">  <p>Isoleucine</p> </div> </div> <div style="display: flex; justify-content: space-around; margin-top: 20px;"> <div style="text-align: center;">  <p>Leucine</p> </div> <div style="text-align: center;">  <p>Valine</p> </div> </div> | <p style="text-align: center;">Aromatic systems</p> <div style="display: flex; justify-content: space-around;"> <div style="text-align: center;">  <p>Phenylalanine</p> </div> <div style="text-align: center;">  <p>Tyrosine</p> </div> </div> | |
| <p style="text-align: center;">Amide</p> <div style="display: flex; justify-content: space-around;"> <div style="text-align: center;">  <p>Asparagine</p> </div> <div style="text-align: center;">  <p>Glutamine</p> </div> </div> | <p style="text-align: center;">Carboxylic acids</p> <div style="display: flex; justify-content: space-around;"> <div style="text-align: center;">  <p>Aspartic acid</p> </div> <div style="text-align: center;">  <p>Glutamic acid</p> </div> </div> | |
| <p style="text-align: center;">Amine</p> <div style="display: flex; justify-content: space-around;"> <div style="text-align: center;">  <p>Lysine (1°)</p> </div> <div style="text-align: center;">  <p>Arginine (1° & 2°)</p> </div> </div> | <p style="text-align: center;">Hydrogen</p> <p style="text-align: center;">R-H</p> <p style="text-align: center;">Glycine</p> | <p style="text-align: center;">Thiol</p> <div style="text-align: center;">  <p>Cysteine</p> </div> |
| | <p style="text-align: center;">Sulfide</p> <div style="text-align: center;">  <p>Methionine</p> </div> | <p style="text-align: center;">Pyrrolidin</p> <div style="text-align: center;">  <p>Proline</p> </div> |

Figure AI.4: Categorization of the 20 canonical amino acids.

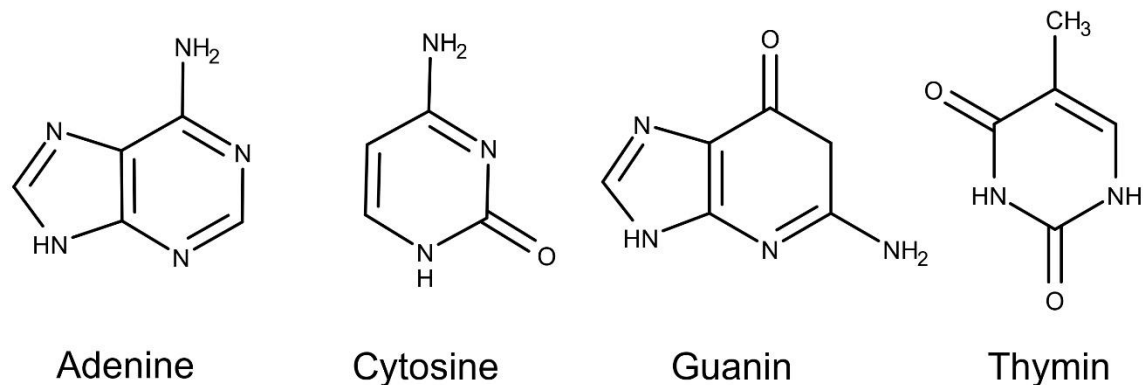


Figure AI.5: Chemical structures of the DNA nucleobases.

Text AI.1: Antibiotic resistance mechanism

Bacteria can survive exposure to antibiotic substances based on two basic principles. First, random mutations that normally occur to their genetic information can lead to mutations of structures that are the target of the specific antibiotic. If such a mutation renders the target structure to become a non-target, the respective cell would be resistant to the respective antibiotics. The exposure to the antibiotic substance will select those bacterial cells with the resistance-forming mutation, which could further grow and multiply. The described phenomenon usually confers resistance to low doses of antibiotics only. In contrast, the second principle of antibiotic resistance is based on dedicated mechanisms to escape antibiotic activity. One example is the chemical inactivation by specific enzymes, such as β -lactamases, which results in hydrolysis of the β -lactam-ring in antibiotics (Jacoby, 2009). Another example is the selective transport out of the microbial cell by specified efflux pumps targeting the antibacterial agent, omitting the toxic action within the microbial cell (Okusu et al., 1996). (c.f. further information in Pazda (2019) and references within.) (Pazda et al., 2019) The parts of DNA that encode a protein like the β -lactamase or the efflux pump are defined as antibiotic-resistant genes (ARG). Bacteria have evolved such specified resistance genes over millions of years because antibiotics also occur in nature, for example, produced by fungi, long before humanity used them to treat infectious diseases.

Text AI.2: Basic information about genetic material

The genetic material consists of the nucleobases adenine, cytosine, guanine, and thymine shown in Figure AI.5. These nucleobases are connected via a phosphate-deoxyribose-backbone, building a strand. DNA consists of two strands in a double-helix shape, whereby the nucleobases adenine/thymine and cytosine/guanine build base pairs connected by hydrogen bonds.

Appendix II

Appendix II

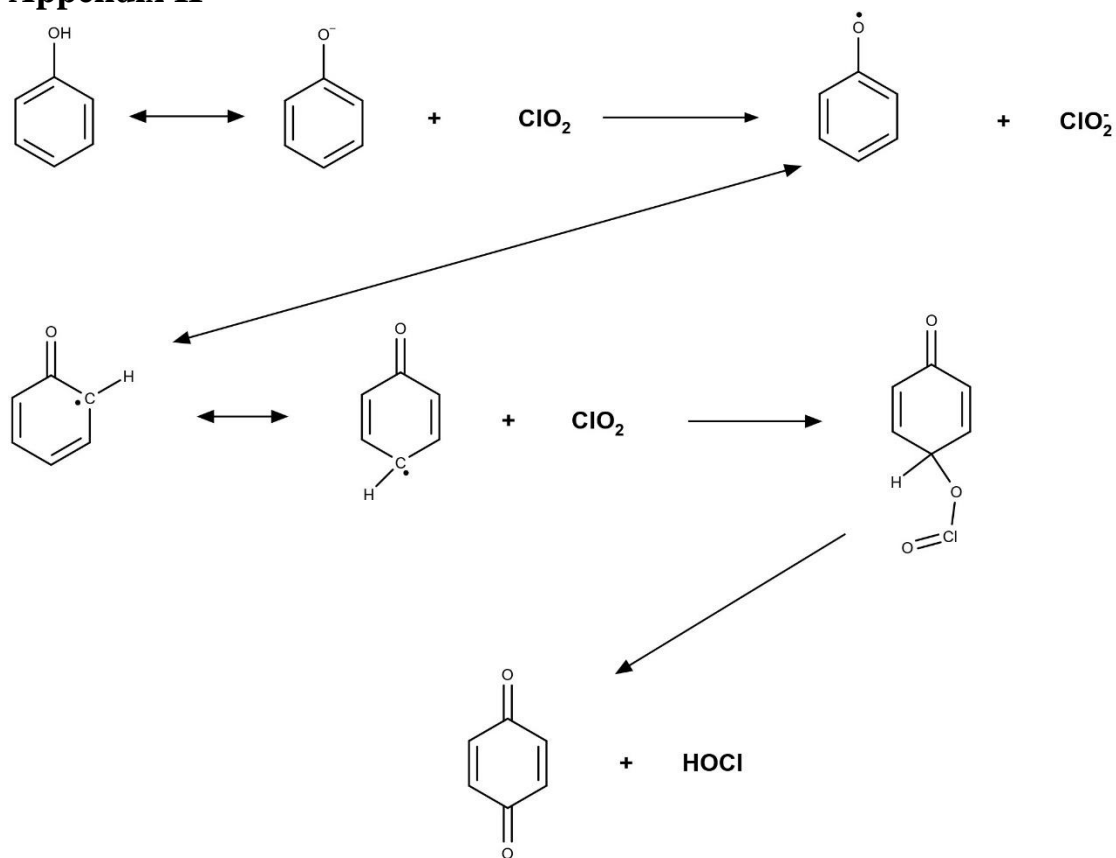


Figure AII.1: Mechanistic pathway of intrinsic formation of FAC during the reaction of phenol with ClO_2 according to Wajon et al. 1982. (Wajon et al., 1982) In the first step, phenol reacts with one molecule of ClO_2 under the formation of ClO_2^- and a phenoxy-radical. Afterward, the radical stabilizes in the *para* position. The phenoxy-radical reacts with another molecule of ClO_2 and forms an OClO-adduct in *para*-position. Eventually, the adduct disproportionates to FAC and benzoquinone.

Appendix II

Table AII.1: Chemicals used in chapter 3.1.

| Name | Purity [%] | Purpose of use | Manufacturer |
|-------------------------------------|---------------|---|---|
| Acetic acid | > 99.7 | Eluent (LC) | Alfa Aesar (Haverhill, Massachusetts, USA) |
| Acetonitrile | > 99.9 | Eluent (LC) | Honeywell Riedel-de Haen (Charlotte, North Carolina, USA) |
| Ammonium-molybdate(VI)-tetrahydrate | > 99 | Post column catalyzer | Acros Organics (Fair Lawn, New Jersey, USA) |
| Disodium phosphate | > 99 | pH buffer | Merck (Darmstadt, Germany) |
| Glycine | > 99 | HOCl Scavenger | Alfa Aesar (Haverhill, Massachusetts, USA) |
| Indol | > 99 | Competitor, model compound | Sigma-Aldrich (St. Louis, Missouri, USA) |
| Monosodium phosphate | 98 | pH buffer | Acros Organics (Fair Lawn, New Jersey, USA) |
| N-Acetyl-L-Tryptophan | ≥ 99 | Compound under study | Sigma-Aldrich (St. Louis, Missouri, USA) |
| N-Acetyl-L-Tyrosine | > 99 | Compound under study | TCI (Tokyo, Japan) |
| Nitrogen | 99.999 | ClO ₂ production | Air Liquide (Paris, France) |
| <i>Ortho</i> -phosphoric acid | 85 | pH buffer | VWR (Radnor, Pennsylvania, USA) |
| Phenol | > 99 % | Competitor | Sigma-Aldrich (St. Louis, Missouri, USA) |
| Potassium iodide | > 99 | Post column reagent | Acros Organics (Fair Lawn, New Jersey, USA) |
| Sodium acetate | > 99 | Eluent (LC) | Sigma-Aldrich (St. Louis, Missouri, USA) |
| Sodium carbonate | 99.5 | Eluent (IC) | Acros Organics (Fair Lawn, New Jersey, USA) |
| Sodium chlorate | > 99 | Calibration standard | Acros Organics (Fair Lawn, New Jersey, USA) |
| Sodium chloride | > 99.5 | Calibration standard | Honeywell Fluka (Charlotte, North Carolina, USA) |
| Sodium chlorite | 80 | Calibration standard | Honeywell Fluka (Charlotte, North Carolina, USA) |
| Sodium hypochlorite | 11 – 15 % FAC | Oxidant | Alfa Aesar (Haverhill, Massachusetts, USA) |
| Sodium persulfate | > 99 | ClO ₂ production | Carl Roth (Karlsruhe, Germany) |
| Sodium phosphate | 96 | pH buffer | Sigma-Aldrich (St. Louis, Missouri, USA) |
| Sulfamethoxazole | > 98 | Competitor | Sigma-Aldrich (St. Louis, Missouri, USA) |
| Sulfuric acid | 95 | Chemical suppressor (IC) / Post column reaction | VWR (Radnor, Pennsylvania, USA) |

Appendix II

Table AII.2: Instruments used in chapter 3.1.

| Name | Component | Description | Manufacturer |
|-----------------------|-------------------------------|--|---|
| Ion-Chromatography | Autosampler | Dionex AS-AP | Thermo scientific (Waltham, Massachusetts, USA) |
| | Column | Asupp7 – 250mm/4.0 µm | Metrohm (Herisau, Swiss) |
| | Column department | Dionex ICS-6000 DC | Thermo scientific (Waltham, Massachusetts, USA) |
| | Conductivity detector | | Thermo scientific (Waltham, Massachusetts, USA) |
| | Pump 1 (Eluent) | Dionex ICS-6000 SP | Thermo scientific (Waltham, Massachusetts, USA) |
| | Pump 2 (Suppressor) | Dionex AXP | Thermo scientific (Waltham, Massachusetts, USA) |
| | Pump 3 (Post column reaction) | Peristaltic pump | Ismatec (Wertheim, Germany) |
| | Software | Chromeleon Console | Thermo scientific (Waltham, Massachusetts, USA) |
| | Suppressor | Dionex ACRS 500 | Thermo scientific (Waltham, Massachusetts, USA) |
| | UV detector | Dionex UltiMate 3000 Diode Array Detection | Thermo scientific (Waltham, Massachusetts, USA) |
| Liquid Chromatography | Autosampler | Dionex AS-AP | Thermo scientific (Waltham, Massachusetts, USA) |
| | Column | Acclaim Trinity P1 3µm – 2.1 µm × 150 mm | Thermo scientific (Waltham, Massachusetts, USA) |
| | Column department | Dionex ICS-6000 DC | Thermo scientific (Waltham, Massachusetts, USA) |
| | Pump 1 (Eluent) | Dionex ICS-6000 SP | Thermo scientific (Waltham, Massachusetts, USA) |

Appendix II

| | | | |
|----------------|-----------------------------|---|---|
| | Software | Chromleon Console | Thermo scientific (Waltham, Massachusetts, USA) |
| | UV detector | Dionex UltiMate 3000 Diode Array Detection | Thermo scientific (Waltham, Massachusetts, USA) |
| Photometer | Photometer | Specord 200 Plus | AnalytikJena (Jena, Germany) |
| pH-meter | pH-meter | Terminal 740 | WTW Series inoLab (Weilheim, Germany) |
| Balance | Balance | SM2285Di-ION-C | VWR (Radnor, Pennsylvania, USA) |
| Reaction tubes | 15 mL CellStar® tubes | Polypropylene | Greiner bio-one (Frickenhausen, Germany) |
| HPLC Vials | 1.5 mL Short thread vial | Amber glass | VWR (Radnor, Pennsylvania, USA) |
| HPLC Vials | 1.5 mL Short thread vial | Polypropylene | VWR (Radnor, Pennsylvania, USA) |

Table AII.3: Liquid chromatography methods used in chapter 3.1. Eluent A = 20 mM sodium acetate buffer pH 5; Eluent B = ACN.

| No. Method | Total time [min] | Gradient program | | | | Compound (Ret. Time [Min]) |
|------------|---------------------|------------------|-----------|----|----|--|
| | | Time | Flow rate | %A | %B | |
| 1 | 31 | 0.000 | 0.3 | 80 | 20 | Phenol (4.0), indol (7.9), SMX (10.5), NAL-Trp (22.6) |
| | | 6.000 | 0.3 | 80 | 20 | |
| | | 10.000 | 0.4 | 40 | 60 | |
| | | 22.000 | 0.4 | 40 | 60 | |
| | | 26.000 | 0.3 | 80 | 20 | |
| 2 | 22 | 0.0 | 0.3 | 80 | 20 | Phenol (4.0), NAL-Tyr (14.6) |
| | | 6.0 | 0.3 | 80 | 20 | |
| | | 10.0 | 0.4 | 40 | 60 | |
| | | 14.0 | 0.4 | 40 | 60 | |
| | | 18.0 | 0.3 | 80 | 20 | |

Appendix II

Table AII.4: Ion chromatography methods used in chapter 3.1. Eluent A = pure H₂O; Eluent B = 4 mM Na₂CO₃. The retention times for Cl-Gly and ClO₂⁻ are given for conductivity and UV detector (CD/UV).

| No. Method | Total time [min] | Gradient program | | | | Compound (Ret. Time [Min]) |
|------------|------------------|------------------|-----------|----|-----|--|
| | | Time | Flow rate | %A | %B | |
| 1 | 40 | 0.000 | 0.75 | 70 | 30 | Cl-Gly (11.3/12.0), ClO ₂ ⁻ (12.3/12.9), Cl ⁻ (15.5), ClO ₃ ⁻ (25.3) |
| | | 16.000 | 0.75 | 70 | 30 | |
| | | 16.001 | 0.75 | 0 | 100 | |
| | | 32.000 | 0.75 | 0 | 100 | |
| | | 32.001 | 0.75 | 70 | 30 | |

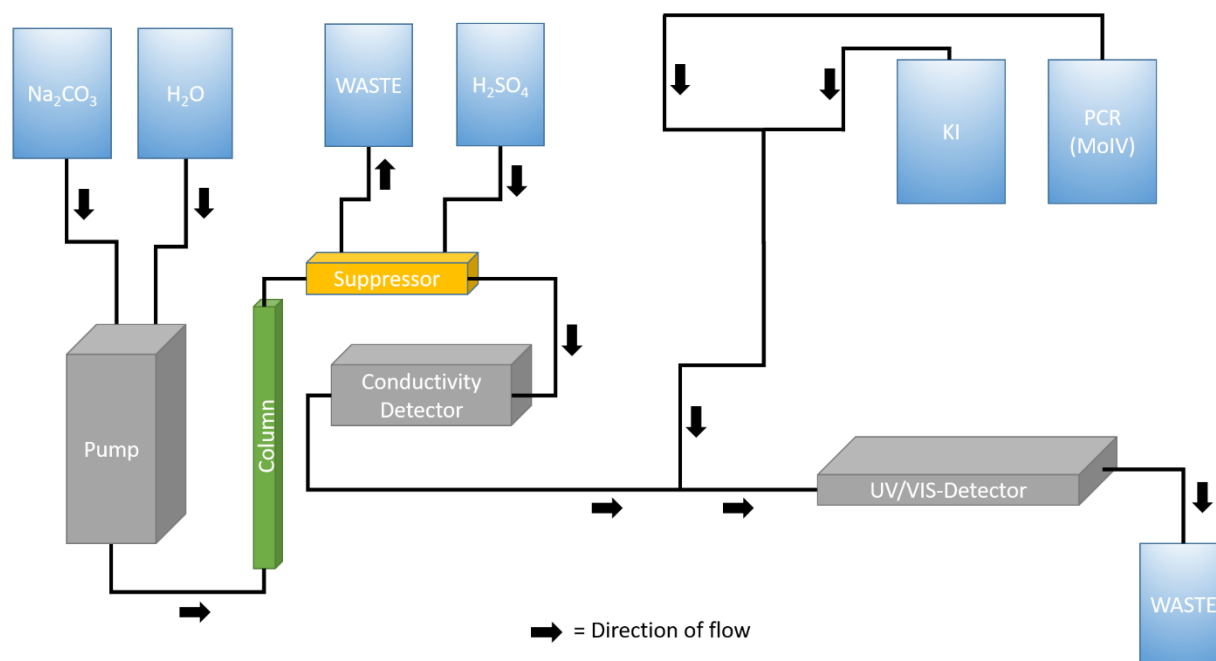


Figure AII.2: Set up of IC-CD-PCR-UV. A gradient pump is transporting the eluent A: H₂O and eluent B: 4 mM Na₂CO₃ towards the column. After the column, a chemical suppression is installed using 20 mM H₂SO₄ (1.0 mL/min). Then the analysts are detected by a conductivity detector. To increase the sensitivity for Cl-Gly and ClO₂⁻ a post column reaction is installed, whereby a 0.27 M potassium iodide (KI) and a catalyzing solution (containing 0.027 mM ammonium molybdate(VI) tetrahydrate and 0.1 M H₂SO₄) are added to the system (0.1 mL/min each solution). During this reaction Iodide is oxidized to triiodide, which has a high absorption at $\lambda = 352 \text{ nm}$ ($\epsilon_{352} = 26,000 \text{ M}^{-1} \text{ cm}^{-1}$) (Abdighahroudi et al., 2020).

Text AII.1: Calculation of necessary scavenger concentrations

In most experiments, scavengers are needed to scavenge the intrinsic formed FAC. For this purpose glycine is used ($k(\text{glycine} + \text{HOCl}) = 1.5 \times 10^5 \text{ M}^{-1} \text{ s}^{-1}$) (Deborde and von Gunten, 2008). To calculate the necessary concentration of glycine ($[\text{Scavenger}]$), Equation AII.1 is used.

$$f(\text{Scavenger} + \text{HOCl}) = \frac{k(\text{Scavenger} + \text{HOCl}) \times [\text{Scavenger}]}{\sum (k(\text{Compound} + \text{HOCl}) \times [\text{Compound}])} \quad (\text{Equation AII.1})$$

The compound under study ($[\text{Compound}]$) was always 0.0001 M, the reaction rate constants ($k(\text{compound} + \text{HOCl})$) are taken from Pattison et al. 2002 (Pattison and Davies, 2001) ($k(\text{NAL-tyrosine} + \text{HOCl}) = 4.7 \times 10^1 \text{ M}^{-1} \text{ s}^{-1}$ & $k(\text{NAL-tryptophan} + \text{HOCl}) = 7.8 \times 10^3 \text{ M}^{-1} \text{ s}^{-1}$ both at pH 7.2 – 7.4). According to Equation AII.1 it was calculated how much glycine was needed to scavenge a fraction ($f(\text{Scavenger} + \text{HOCl})$) of 99.9 % HOCl ($f = 0.999$).

Appendix II

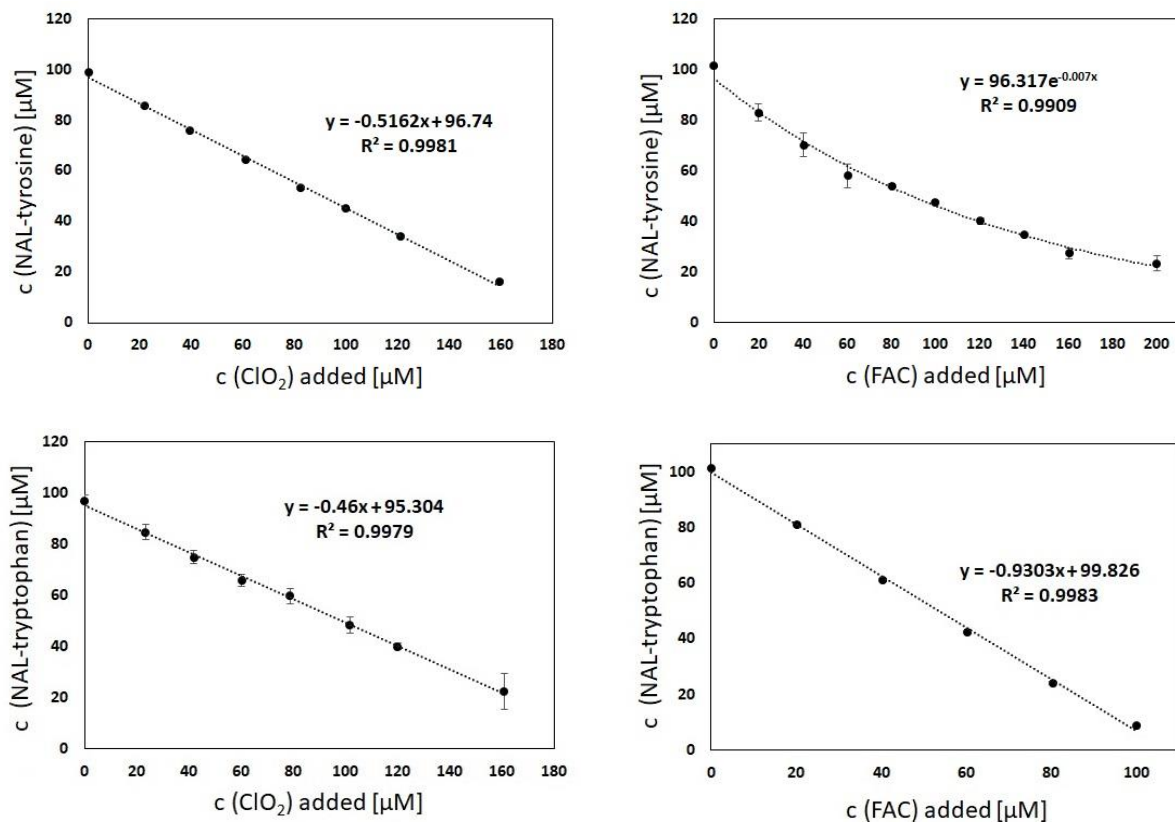


Figure AII.3: Stoichiometry results. Stoichiometry has been determined for both amino acids with oxidants at pH 7. Reaction conditions: 0.1 mM of the corresponding amino acids, 5 mM of phosphate buffer, and, in the case of determining the stoichiometry for ClO₂, 10 mM glycine was added to scavenge intrinsic formed FAC, which would bias the final results. All experiments have been carried out in triplicates, and the error bars are representing the standard deviation of the results.

Table AII.5: Measured impurities of ClO₂ stock solution. Percentage is based on the initial concentration of ClO₂, which was measured to be 17.225 mM.

| | Cl ⁻ | ClO ₂ ⁻ | ClO ₃ ⁻ | Total |
|--------------|-----------------|-------------------------------|-------------------------------|-------|
| Impurity [%] | 0.153 ± 0.002 | 0.118 ± 0.003 | 2.166 ± 0.038 | 2.438 |

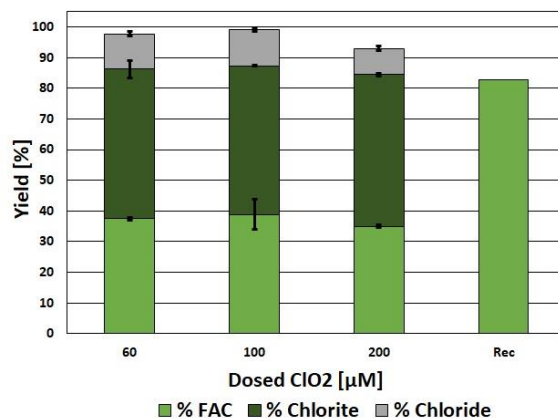


Figure AII.4: Chlorine balance of ClO₂ during the reaction with indol at pH 7. The reaction solution contained 10 mM glycine, 5 mM phosphate buffer, and 0.1 mM indol. The experiment has been carried out in triplicates, and the error bars are representing the standard deviation of the results.

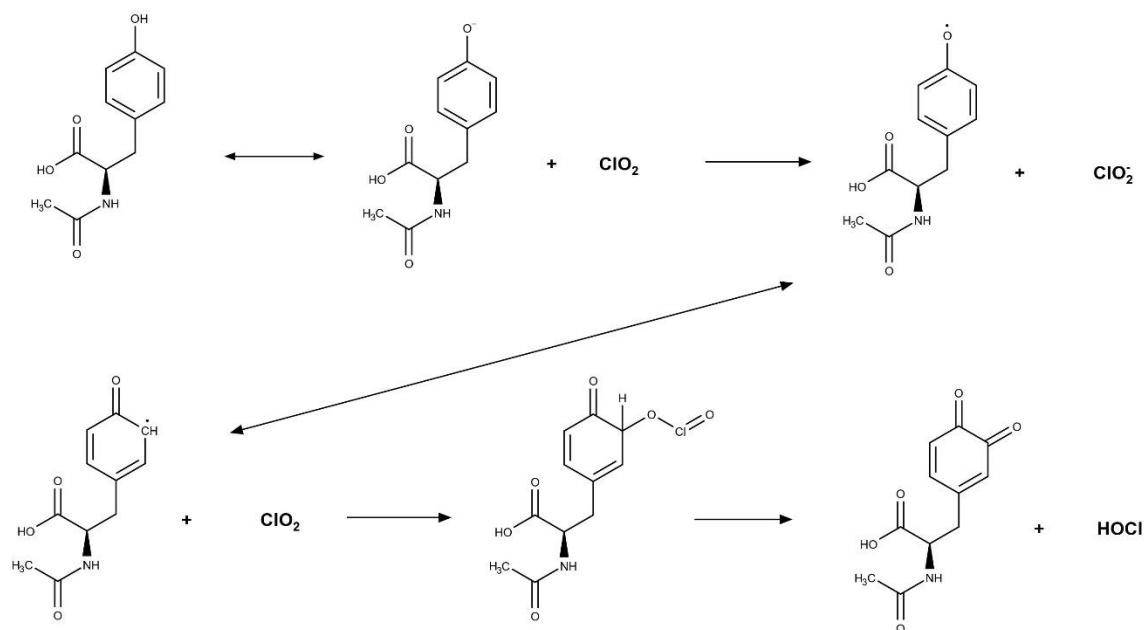


Figure AII.5: Mechanistic pathway of intrinsic formation of FAC during the reaction of phenol with ClO₂ adapted from Napolitano et al. 2005. (Napolitano et al., 2005) In the first step, NAL-tyrosine reacts with one molecule of ClO₂ under the formation of ClO₂⁻ and a phenoxy-radical. Afterwards the redistribution of the radical location to a more stable position takes place. The phenoxy-radical reacts with another molecule of ClO₂ and forms an OClO-adduct in *ortho*-position. Eventually, the adduct breaks down to a keto group and HOCl.

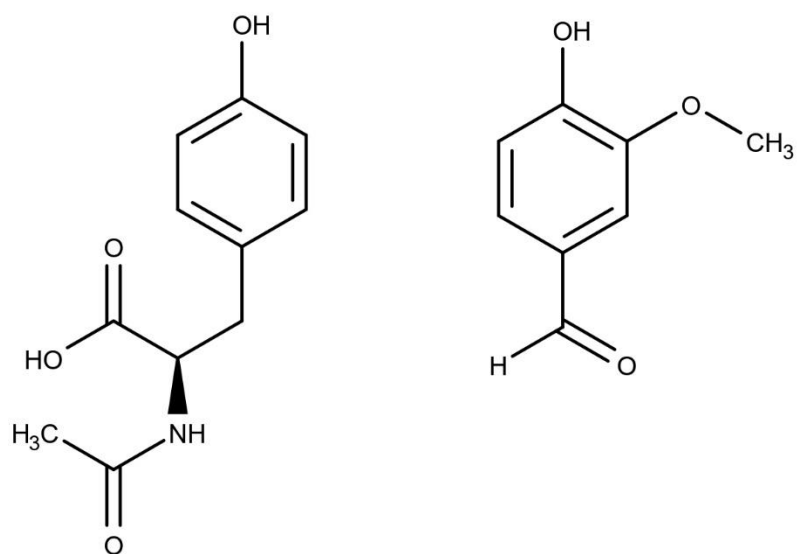


Figure AII.6: Chemical structure of NAL-tyrosine (left) and vanillin (right).

Appendix III

Appendix III

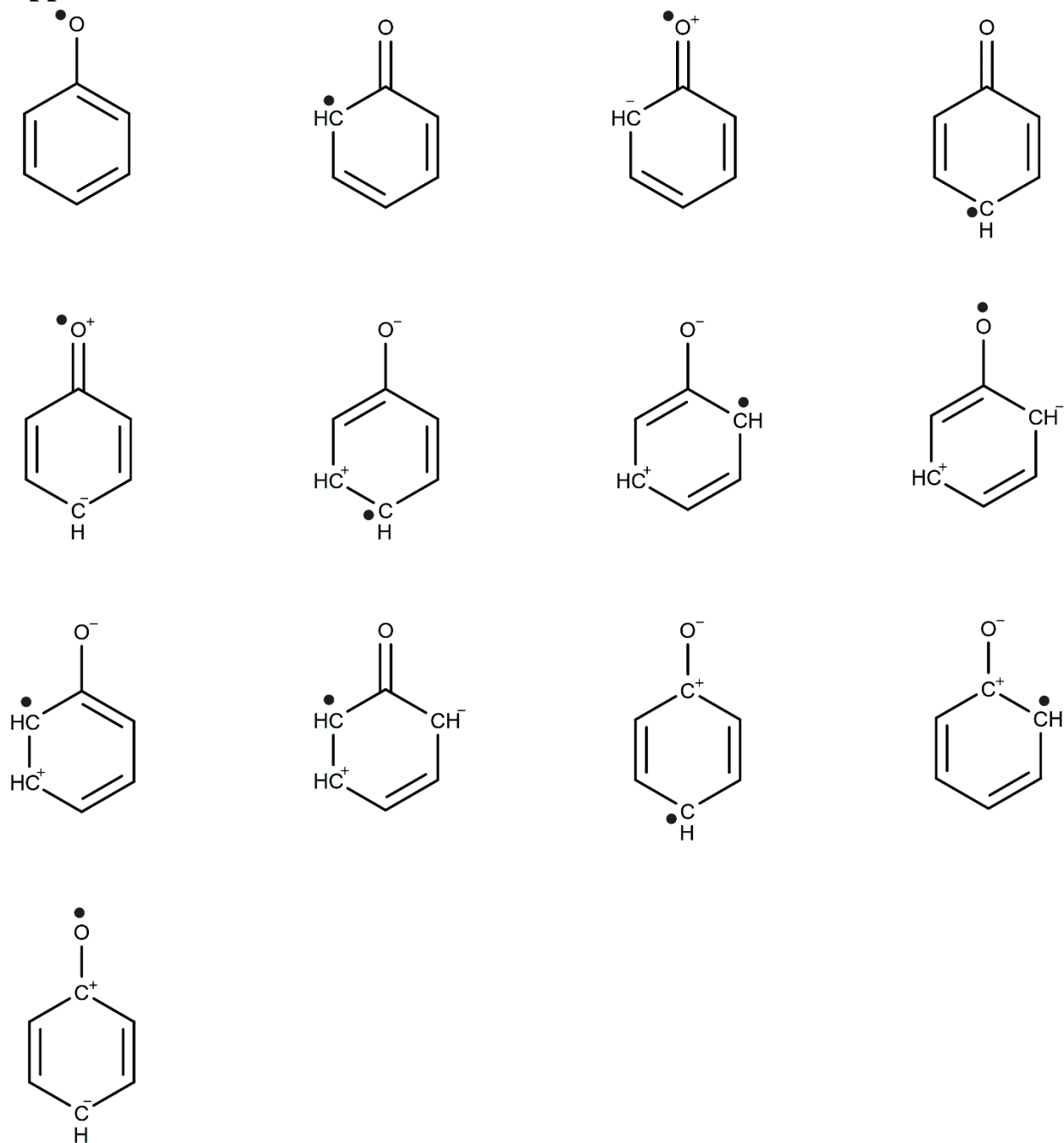


Figure AIII.1: Possible radical positions on phenolic moiety after the first attack of ClO_2 . The radical can only be in *ortho*- or *para*-position.

Appendix III

Table AIII.1: Chemicals used in chapter 3.2.

| Name | Purity [%] | Purpose of use | Manufacturer |
|--|------------|----------------------|---|
| Acetic acid | > 99.7 | Eluent (LC) | Alfa Aesar (Haverhill, Massachusetts, USA) |
| Acetonitrile | > 99.9 | Eluent (LC) | Honeywell Riedel-de Haen (Charlotte, North Carolina, USA) |
| 2-Aminophenol | 99 | Compound under study | Sigma-Aldrich (St. Louis, Missouri, USA) |
| 3-Aminophenol | 98 | Compound under study | Sigma-Aldrich (St. Louis, Missouri, USA) |
| 4-Aminophenol | ≥ 98 | Compound under study | Sigma-Aldrich (St. Louis, Missouri, USA) |
| Bromide 1 g L ⁻¹ Standard Solution | n.a. | Calibration standard | VWR (Radnor, Pennsylvania, USA) |
| 2-Bromophenol | 98 | Compound under study | Sigma-Aldrich (St. Louis, Missouri, USA) |
| 3-Bromophenol | 98 | Compound under study | Sigma-Aldrich (St. Louis, Missouri, USA) |
| 4-Bromophenol | 99 | Compound under study | Sigma-Aldrich (St. Louis, Missouri, USA) |
| Catechol (1,2-Dihydroxybenzene) | ≥ 99 | Compound under study | Sigma-Aldrich (St. Louis, Missouri, USA) |
| 2-Chlorophenol | ≥ 99 | Compound under study | Sigma-Aldrich (St. Louis, Missouri, USA) |
| 3-Chlorophenol | 98 | Compound under study | Sigma-Aldrich (St. Louis, Missouri, USA) |
| 4-Chlorophenol | ≥ 99 | Compound under study | Sigma-Aldrich (St. Louis, Missouri, USA) |
| 2,4-Dimethylphenol | 98 | Compound under study | Sigma-Aldrich (St. Louis, Missouri, USA) |
| 2,6-Dimethylphenol | 99 | Compound under study | Sigma-Aldrich (St. Louis, Missouri, USA) |
| 3,5-Dimethylphenol | ≥ 99 | Compound under study | Sigma-Aldrich (St. Louis, Missouri, USA) |
| Disodium phosphate | > 99 | pH buffer | Merck (Darmstadt, Germany) |
| Formic acid | ≥ 98 | Eluent (LC) | Merck (Darmstadt, Germany) |
| Glycine | > 99 | HOCl Scavenger | Alfa Aesar (Haverhill, Massachusetts, USA) |
| Hydroquinone (1,4-Dihydroxybenzene) | ≥ 99 | Compound under study | Sigma-Aldrich (St. Louis, Missouri, USA) |
| 2-Methoxyphenol (Guaiacol) | > 99 | Compound under study | Thermo Scientific (Waltham, Massachusetts, USA) |

Appendix III

| | | | |
|-------------------------------------|------------------|---|--|
| 3-Methoxyphenol | 96 | Compound under study | Sigma-Aldrich (St. Louis, Missouri, USA) |
| 4-Methoxyphenol | 99 | Compound under study | Sigma-Aldrich (St. Louis, Missouri, USA) |
| Monosodium phosphate | 98 | pH buffer | Acros Organics (Fair Lawn, New Jersey, USA) |
| Nitrogen | 99.999 | ClO ₂ production | Air Liquide (Paris, France) |
| <i>Ortho</i> -phosphoric acid | 85 | pH buffer | VWR (Radnor, Pennsylvania, USA) |
| p-cresol | 99 | Compound under study | Alfa Aesar (Haverhill, Massachusetts, USA) |
| Resorcinol (1,3-Dihydroxyphenol) | 99 | Compound under study | Sigma-Aldrich (St. Louis, Missouri, USA) |
| Sodium carbonate | 99.5 | Eluent (IC) | Acros Organics (Fair Lawn, New Jersey, USA) |
| Sodium chlorate | > 99 | Calibration standard | Acros Organics (Fair Lawn, New Jersey, USA) |
| Sodium chloride | > 99.5 | Calibration standard | Honeywell Fluka (Charlotte, North Carolina, USA) |
| Sodium chlorite | 80 | Calibration standard | Honeywell Fluka (Charlotte, North Carolina, USA) |
| Sodium hypochlorite | 11 – 15 % FAC | Oxidant | Alfa Aesar (Haverhill, Massachusetts, USA) |
| Sodium persulfate | > 99 | ClO ₂ production | Carl Roth (Karlsruhe, Germany) |
| Sodium phosphate | 96 | pH buffer | Sigma-Aldrich (St. Louis, Missouri, USA) |
| Sulfuric acid | 95 | Chemical suppressor (IC) / Post column reaction | VWR (Radnor, Pennsylvania, USA) |
| 2,4,6-Trimethylphenol | 97 | Compound under study | Sigma-Aldrich (St. Louis, Missouri, USA) |
| Vanillin | 99 | Compound under study | Sigma-Aldrich (St. Louis, Missouri, USA) |

Appendix III

Table AIII.2: Instruments used in chapter 3.2.

| Name | Component | Description | Manufacturer |
|-----------------------|------------------------|---|---|
| Ion-Chromatography | Autosampler | Dionex AS-AP | Thermo Scientific (Waltham, Massachusetts, USA) |
| | IC Column 1 | Asupp7 – 250mm/4.0 µm | Metrohm (Herisau, Swiss) |
| | IC Column 2 | SykroGel-Ax 300AB-A01 6µm 150 × 3 mm / Steel | Sykam (Fürstfeldbruck, Germany) |
| | Column department | Dionex ICS-6000 DC | Thermo Scientific (Waltham, Massachusetts, USA) |
| | Conductivity detector | | Thermo Scientific (Waltham, Massachusetts, USA) |
| | Pump 1 (Eluent) | Dionex ICS-6000 SP | Thermo Scientific (Waltham, Massachusetts, USA) |
| | Pump 2 (Suppressor) | Dionex AXP | Thermo Scientific (Waltham, Massachusetts, USA) |
| | Software | Chromeleon Console | Thermo Scientific (Waltham, Massachusetts, USA) |
| | Suppressor | Dionex ACRS 500 | Thermo Scientific (Waltham, Massachusetts, USA) |
| Liquid Chromatography | Autosampler | Dionex Ulimite 3000 Autosampler | Thermo Scientific (Waltham, Massachusetts, USA) |
| | LC Column 1 | Kinetex® 5 µm EVO C18 100 Å 100 × 2.1 mm | Phenomenex (Torrance, California, USA) |
| | LC Column 2 | Obelisc N 5 µm 100 Å 2.1 × 150 mm | Sielc (Wheeling, Illinois, USA) |

Appendix III

| | | | |
|--------------------|-----------------------------------|--|---|
| | Column compartment | Dionex Ultimate 3000 Column compartment | Thermo Scientific (Waltham, Massachusetts, USA) |
| | Pump 1 (Eluent) | Dionex Ultimate 3000 Pump | Thermo Scientific (Waltham, Massachusetts, USA) |
| | Software | Chromeleon Console | Thermo Scientific (Waltham, Massachusetts, USA) |
| | UV detector | Dionex UltiMate 3000 Diode Array Detection | Thermo Scientific (Waltham, Massachusetts, USA) |
| Photometer | Photometer | Specord 200 Plus | AnalytikJena (Jena, Germany) |
| pH-meter | pH-meter | Terminal 740 | WTW Series inoLab (Weilheim, Germany) |
| Analytical balance | Balance | SM2285Di-ION-C | VWR (Radnor, Pennsylvania, USA) |
| Reaction tubes | 15 mL CellStar [®] tubes | Polypropylene | Greiner bio-one (Frickenhausen, Germany) |
| HPLC Vials | 1.5 mL Short thread vial | Amber glass | VWR (Radnor, Pennsylvania, USA) |
| HPLC Vials | 1.5 mL Short thread vial | Polypropylene | VWR (Radnor, Pennsylvania, USA) |

Appendix III

Table AIII.3: Liquid chromatography methods used in chapter 3.2. Eluent A = 20 Pure water (+ 0.1 % Formic acid); Eluent B = ACN; Eluent C= 50 mM NH₄FA.

| No. Method | Column | Gradient program | | | | Compound (Ret. Time [Min]) |
|------------|--------|-------------------------------------|-----|----|----|---|
| | | Flow rate [mL × Min ⁻¹] | %A | %B | %C | |
| LC1 | 1 | 0.3 | 80 | 20 | 0 | p-cresol (5.1) 2,4-DMP (8.2) 2,6-DMP (10.6) 3,5-DMP (9.3) 2,4,6-TMP (7.8) 2-CP (6.0) 4-CP (7.3) 2-BP (6.8) 3-BP (11.6) 4-BP (10.2) |
| LC2 | 1 | 0.3 | 90 | 10 | 0 | 3-CP (15.6) 2-MOP (7.8) 3-MOP (6.7) 4-MOP (4.8) |
| LC3 | 1 | 0.3 | 100 | 0 | 0 | HQ (2.5) Cat (4.9) Res (4.4) |
| LC4 | 2 | 0.3 | 0 | 10 | 90 | 2-AP (3.8) 3-AP (3.5) 4-AP (3.2) |

Appendix III

Table AIII.4: Ion chromatography methods used in chapter 3.2. Eluent A = pure H₂O; Eluent B = 4 mM Na₂CO₃; Eluent C = 4.5 mM Na₂CO₃ + 0.5 mM NaSCN. The retention times for Cl-Gly and ClO₂⁻ are given for conductivity and UV detector (CD/UV).

| No. Method | Total time [Min] | Column | Temp. [°C] | Gradient program | | | | | Compound (Ret. Time [Min]) |
|------------|------------------|--------|------------|------------------|--------------------|----|-----|-----|---|
| | | | | Time | Flow rate [mL/min] | %A | %B | %C | |
| IC1 | 40 | 1 | 35 | 0.000 | 0.7 | 70 | 30 | 0 | Cl-Gly(11.6); ClO ₂ ⁻ (12.5); Cl ⁻ (15.2); ClO ₃ ⁻ (22.2) |
| | | | | 16.000 | 0.7 | 70 | 30 | 0 | |
| | | | | 16.001 | 0.7 | 0 | 100 | 0 | |
| | | | | 32.000 | 0.7 | 0 | 100 | 0 | |
| | | | | 32.001 | 0.7 | 70 | 30 | 0 | |
| IC2 | 17 | 2 | RT | 0.000 | 1.0 | 0 | 0 | 100 | Br ⁻ (5.6); ClO ₃ ⁻ (10.4) |
| | | | | 17.000 | 1.0 | 0 | 0 | 100 | |

Text AIII.1: Determination of impurities in ClO₂ and FAC stock solution

By using the persulfate-chlorite method ClO₂ forms during the reaction of persulfate with ClO₂⁻. The reaction took place in an air-tight gas washing bottle and the formed ClO₂ is purged out by a continuous N₂-gas stream, washed in a sodium chlorite solution for FAC removal (0.15 M), and finally trapped in ice-cooled pure water. In the ice-cooled water, ClO₂ accumulates, reaching a concentration of about 15 mM. By using this method, high purities of ClO₂ can be achieved. Additionally, by transferring ClO₂ through the gas phase, no residuals of persulfate are transferred into the final solution (indicated by hardly any carryover of ClO₂⁻), which would have affected the investigated reactions.

The 15% FAC stock solution was also investigated regarding the impurities. Therefore, diluted standards were measured by IC, and no traces of ClO₂⁻ were observed. The stock solution contained mostly Cl⁻, which did not interfere in the measuring process.

Appendix III

Table AIII.5: Calculated time necessary until > 99.9 % of the corresponding phenolic compound is degraded by ClO₂. The calculation was carried out by taking the kinetic constants available in the literature.

| Compound | pK _a | k (PhOH + ClO ₂) [M ⁻¹ s ⁻¹] | k (PHO ⁻ + ClO ₂) [M ⁻¹ s ⁻¹] | k_{app} at pH 7 [M ⁻¹ s ⁻¹] | Time necessary for > 99.9 % degradation [s] | Ref. |
|-----------------------|-----------------|---|---|--|---|-----------------------------|
| Phenol | 10 | 4×10^{-1} | 4.9×10^7 | 4.9×10^4 | 2 | (Tratnyek and Hoigné, 1994) |
| 2-Aminophenol | – | – | – | – | – | – |
| 3-Aminophenol | – | – | – | – | – | – |
| 4-Aminophenol | – | – | – | – | – | – |
| Catechol | 9.1 | 5×10^3 | 2×10^9 | 1.58×10^7 | 0.001 | (Tratnyek and Hoigné, 1994) |
| Resorcinol | 9.2 | 4×10^1 | 4.8×10^7 | 3.01×10^5 | 0.01 | (Tratnyek and Hoigné, 1994) |
| Hydroquinone | 9.8 | 3.9×10^4 | 6.5×10^9 | 1.03×10^7 | 0.001 | (Wajon et al., 1982) |
| 2-Chlorophenol | 8.5 | 1.5 | 3.5×10^7 | 1.07×10^6 | 0.01 | (Tratnyek and Hoigné, 1994) |
| 3-Chlorophenol | – | – | – | – | – | – |
| 4-Chlorophenol | 9.4 | 2 | 3.5×10^7 | 3.39×10^5 | 0.1 | (Tratnyek and Hoigné, 1994) |
| 2-Bromophenol | – | – | – | – | – | – |
| 3-Bromophenol | – | – | – | – | – | – |
| 4-Bromophenol | 9.4 | – | 2.7×10^7 | 1.07×10^5 | 0.1 | (Alfassi et al., 1986) |
| 2-Methoxyphenol | 9.9 | 1×10^3 | 1.2×10^9 | 1.51×10^6 | 0.01 | (Tratnyek and Hoigné, 1994) |
| 3-Methoxyphenol | 9.6 | – | 4.9×10^7 | 1.23×10^5 | 0.1 | (Alfassi et al., 1986) |
| 4-Methoxyphenol | 10.2 | 2.5×10^4 | 1.7×10^9 | 1.1×10^9 | 0.01 | (Tratnyek and Hoigné, 1994) |
| Vanillin | 7.7 | – | 1.8×10^8 | 2.99×10^7 | 0.01 | (Tratnyek and Hoigné, 1994) |
| 4-Methylphenol | 10.3 | 5×10^1 | 5.2×10^8 | 2.61×10^5 | 0.1 | (Tratnyek and Hoigné, 1994) |
| 2,4-Dimethylphenol | 10.6 | 9×10^2 | 2.1×10^9 | 5.28×10^5 | 0.01 | (Tratnyek and Hoigné, 1994) |
| 2,6-Dimethylphenol | – | – | – | – | – | – |
| 3,5-Dimethylphenol | – | – | – | – | – | – |
| 2,4,6-Trimethylphenol | 10.9 | 3.9×10^3 | 4×10^9 | 5.07×10^5 | 0.01 | (Tratnyek and Hoigné, 1994) |

Text AIII.2: FAC recovery rate

For a reliable quantification of intrinsic FAC, it is important to show that the intrinsic FAC is successfully and completely scavenged by glycine and that no side reactions between FAC and the compounds under study occur. For this purpose, 100 μM FAC was dosed to a sample of each compound at pH 7, and the corresponding FAC concentration was measured. The results are shown in Figure S2. It is observable that all of the investigated compounds show a good FAC recovery rate within the range of 90 – 110 %. This means that if FAC is formed intrinsically, it will be successfully scavenged by glycine and reliable statements about the yields are possible.

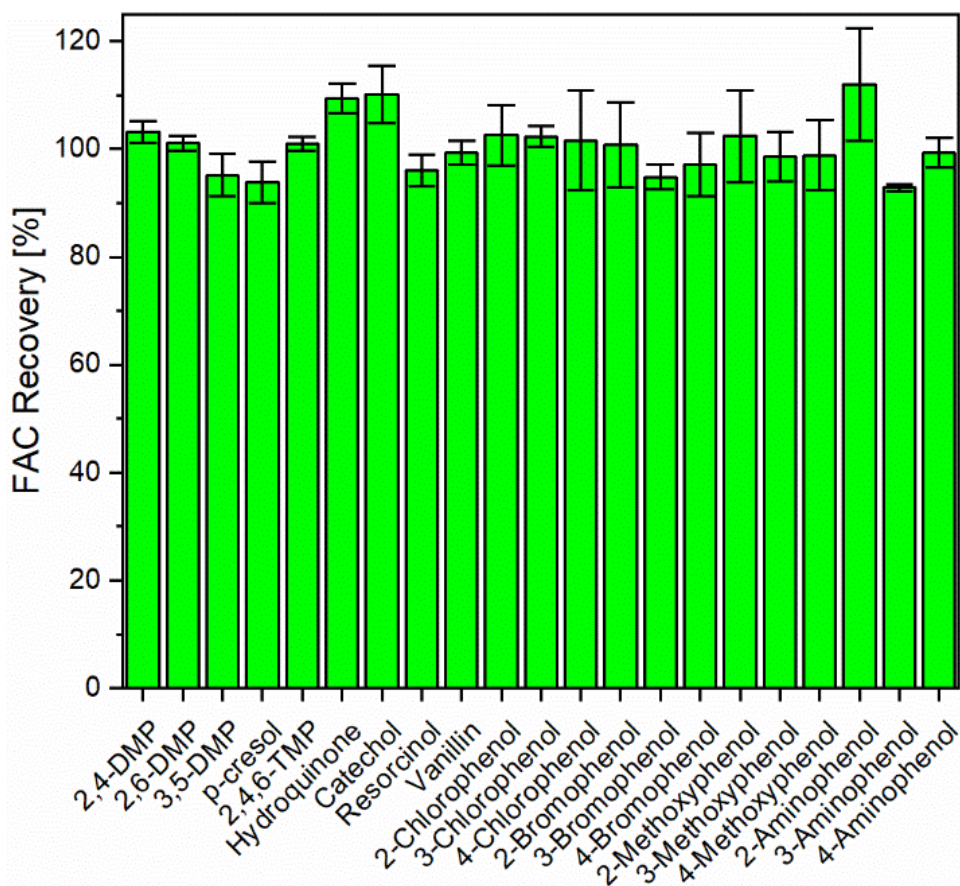


Figure AIII.2: Recoveries of FAC for all 21 compounds investigated in this study. 100 μM FAC was dosed into an aliquot of the corresponding reaction solution at pH 7. All experiments were carried out in triplicates, and the error bars represent the standard deviation of the triplicates.

Appendix III

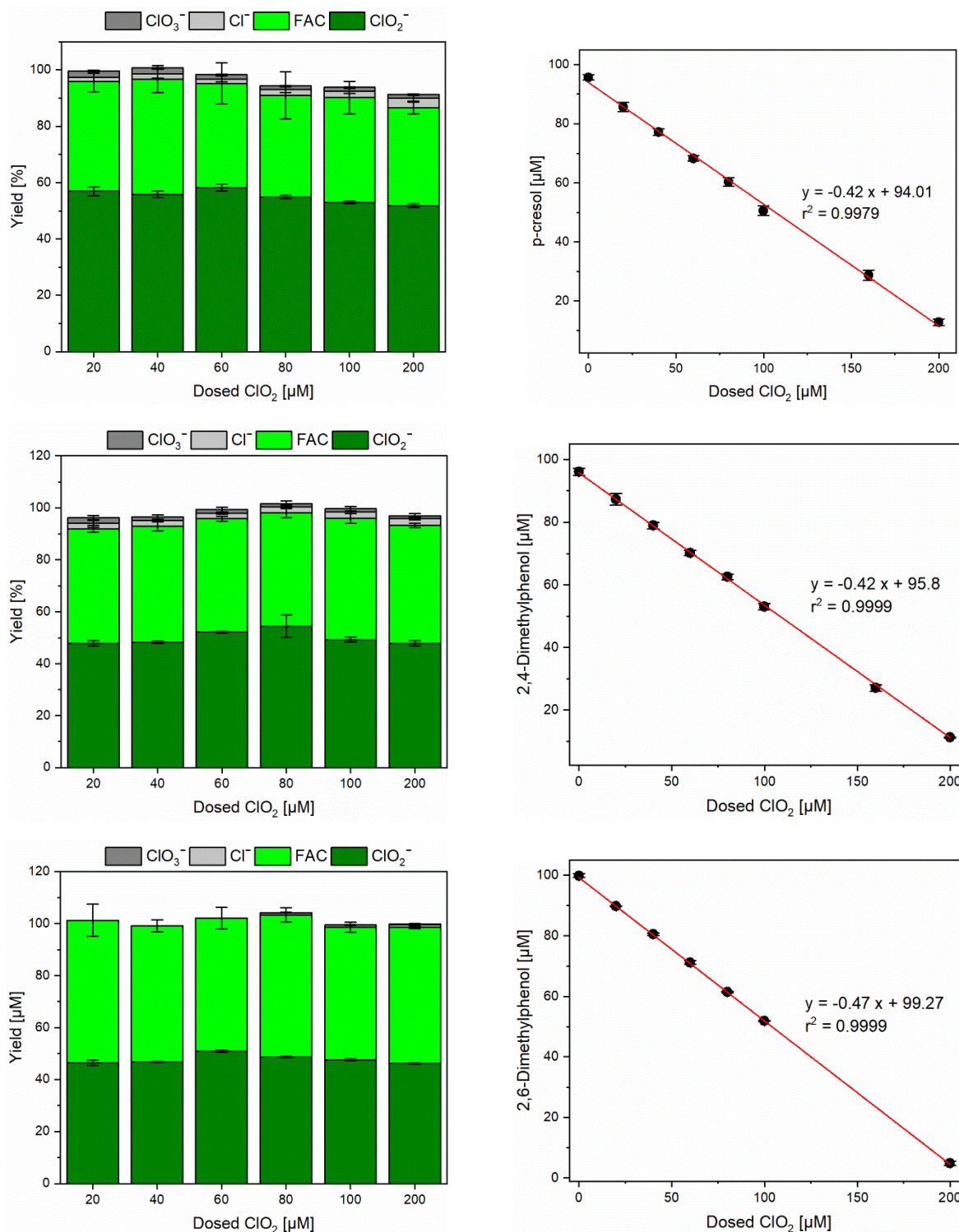


Figure AIII.3: Detailed chlorine balance (left) and stoichiometry (right) for p-cresol (top), 2,4-dimethylphenol (middle), and 2,6-dimethylphenol (bottom). All reaction solutions contained 0.1 mM compounds under study, 10 mM glycine to scavenge intrinsically formed FAC, and 5 mM phosphate buffer to stabilize the pH at 7. All experiments were carried out in triplicates, and the error bars represent the standard deviation of the triplicate measurements.

Appendix III

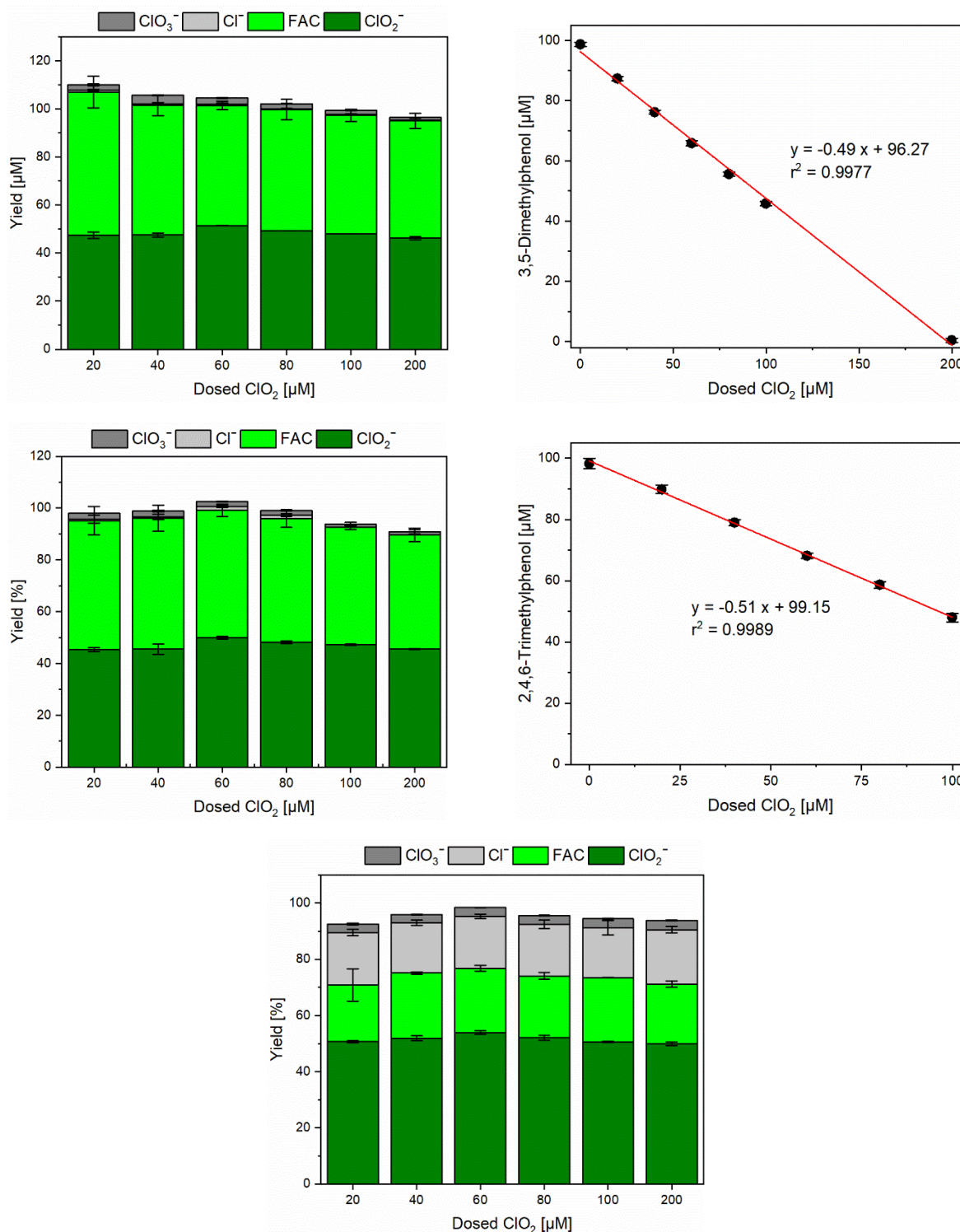


Figure AIII.4: Detailed chlorine balance (left) and stoichiometry (right) for 3,5-dimethylphenol (top), 2,4,6-trimethylphenol (middle), and vanillin (bottom). All reaction solutions contained 0.1 mM compounds under study, 10 mM glycine to scavenge intrinsically formed FAC, and 5 mM phosphate buffer to stabilize the pH at 7. All experiments were carried out in triplicates, and the error bars represent the standard deviation of the triplicate measurements.

Appendix III

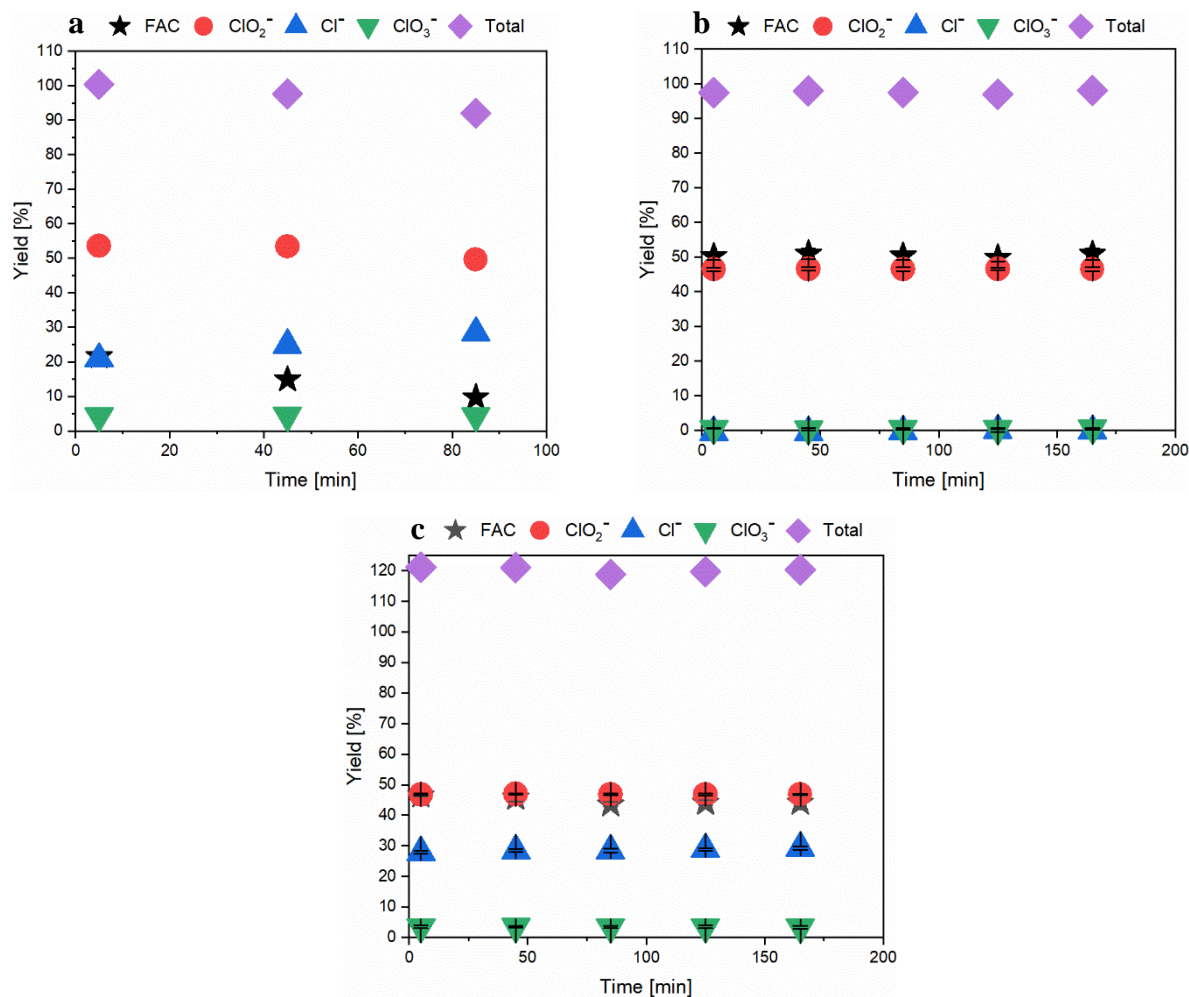


Figure AIII.5: Repetitive measurement of the same sample of vanillin (a), TMP (b), and 4-chlorophenol (c) after dosing 200 μM ClO_2 . The samples contained 100 μM compound under study, 10 mM glycine, and 5 mM phosphate buffer at pH 7. The first sample was treated identically to the previous experiments. After injection, the sample (b & c) remained in the autosampler at 5 $^\circ\text{C}$ and was measured five times in a row. The time between every injection was 40 minutes, and all experiments were determined in triplicates (error bars represent the standard deviation of the triplicate measurements). Note that the vanillin was measured only three times in a row and in single measurement.

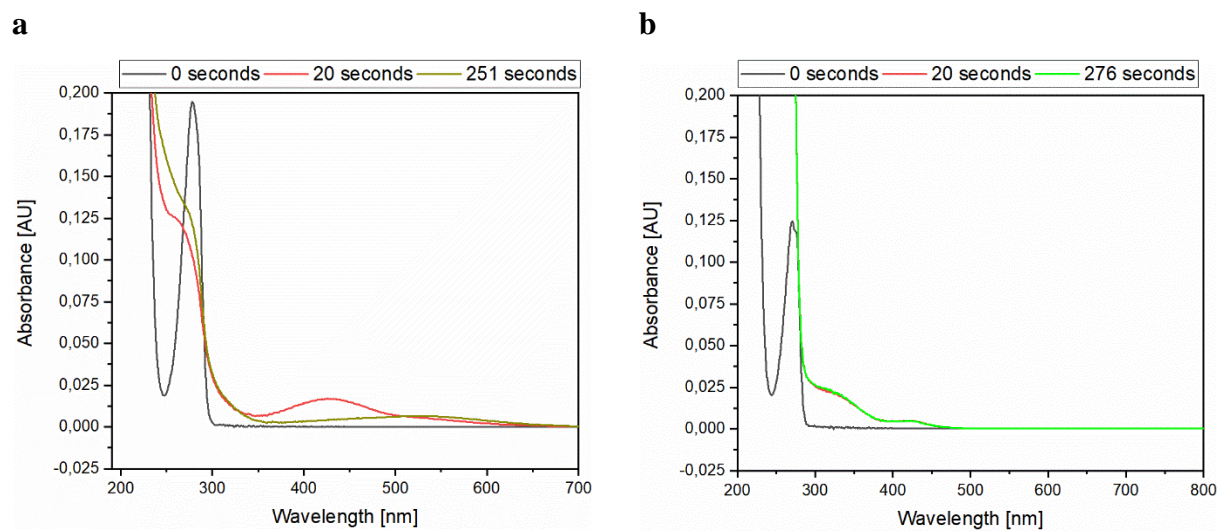


Figure AIII. 6: Change in the spectra of 2,4-dimethylphenol (a) and 2,6-dimethylphenol (b) after adding 200 μM ClO_2 . Reaction condition: 10 mM glycine, 5 mM phosphate buffer at pH 7.

Appendix III

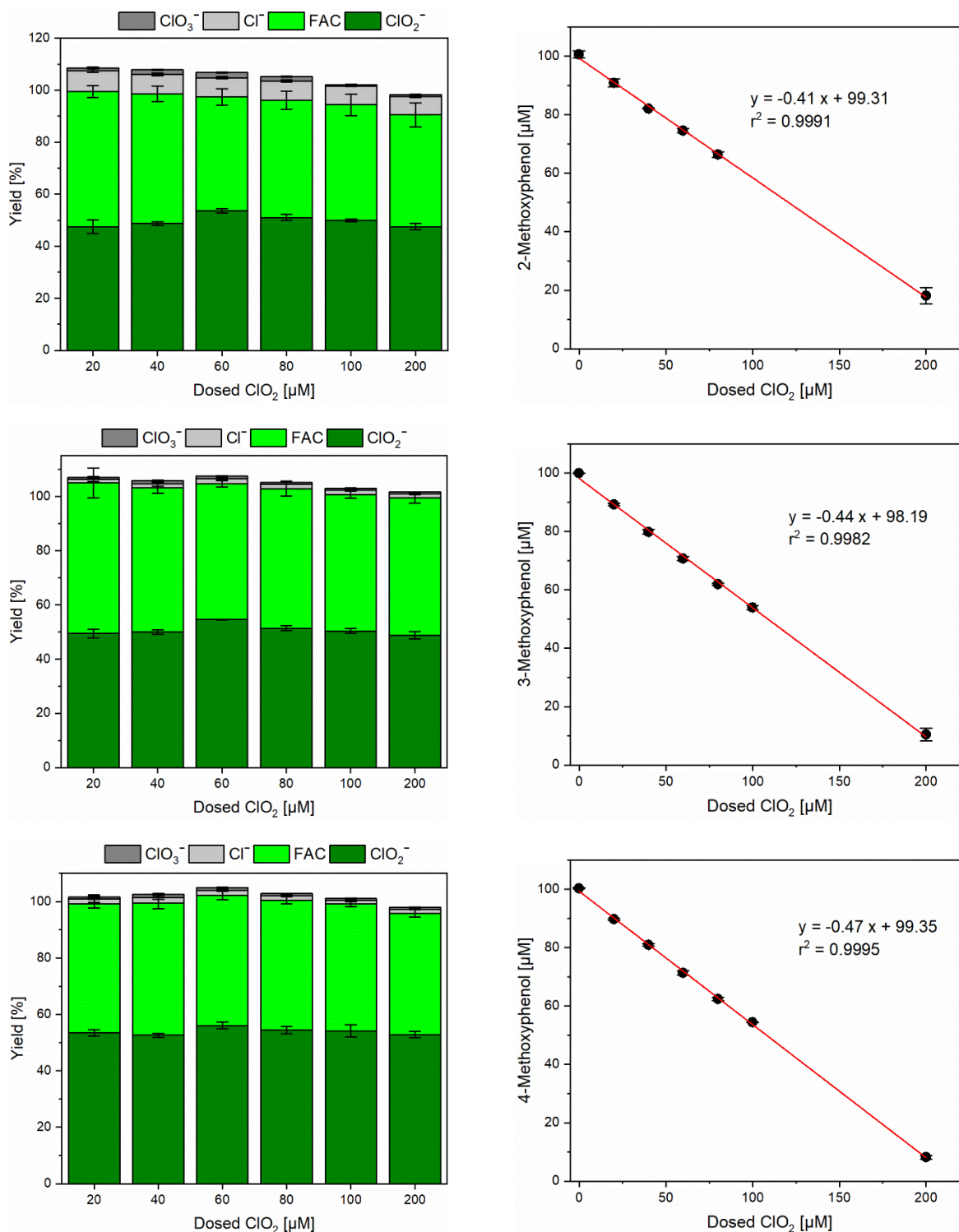


Figure AIII.7: Detailed chlorine balance (left) and stoichiometry (right) for 2-methoxyphenol (top), 3-methoxyphenol (middle), and 4-methoxyphenol (bottom). All reaction solutions contained 0.1 mM compounds under study, 10 mM glycine to scavenge intrinsically formed FAC, and 5 mM phosphate buffer to stabilize the pH at 7. All experiments were carried out in triplicates and the error bars represent the standard deviation of the triplicate measurements.

Appendix III

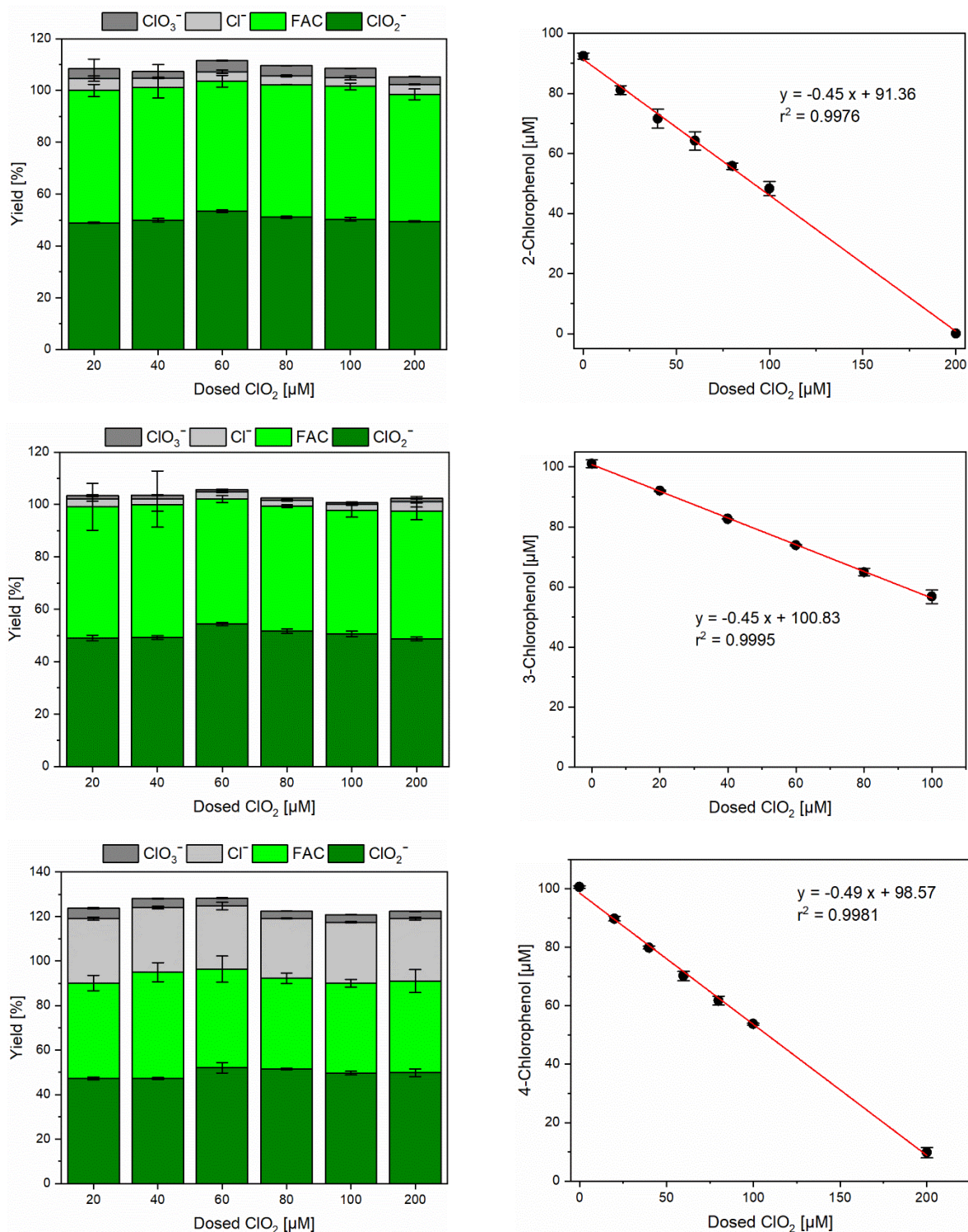


Figure AIII.8: Detailed chlorine balance (left) and stoichiometry (right) for 2-chlorophenol (top), 3-chlorophenol (middle), and 4-chlorophenol (bottom). All reaction solutions contained 0.1 mM compounds under study, 10 mM glycine to scavenge intrinsically formed FAC, and 5 mM phosphate buffer to stabilize the pH at 7. All experiments were carried out in triplicates, and the error bars represent the standard deviation of the triplicate measurements.

Appendix III

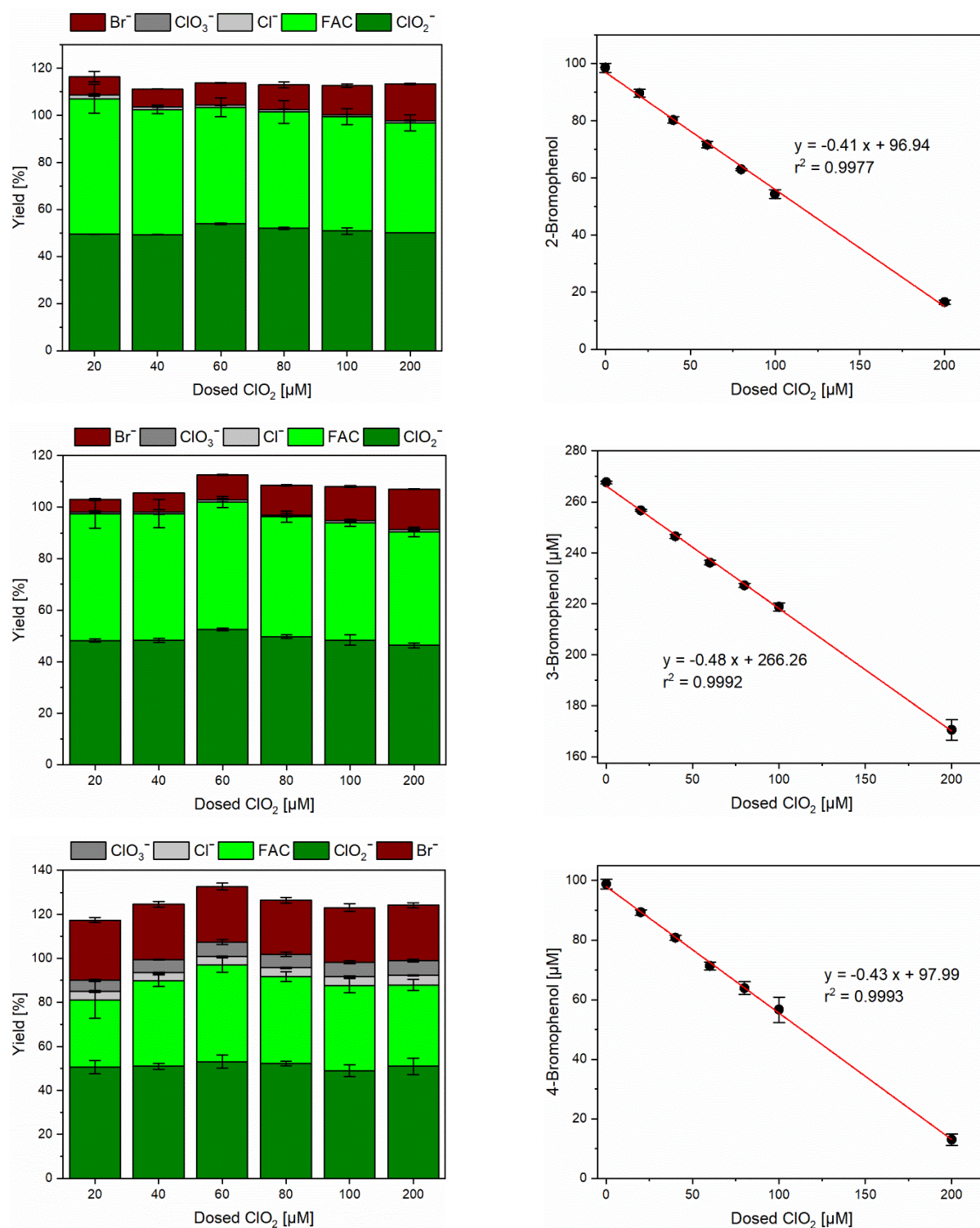


Figure AIII.9: Detailed chlorine balance (left) and stoichiometry (right) for 2-bromophenol (top), 3-bromophenol (middle), and 4-bromophenol (bottom). All reaction solutions contained 0.1 mM compounds under study, 10 mM glycine to scavenge intrinsically formed FAC, and 5 mM phosphate buffer to stabilize the pH at 7. All experiments were carried out in triplicates, and the error bars represent the standard deviation of the triplicate measurements.

Appendix III

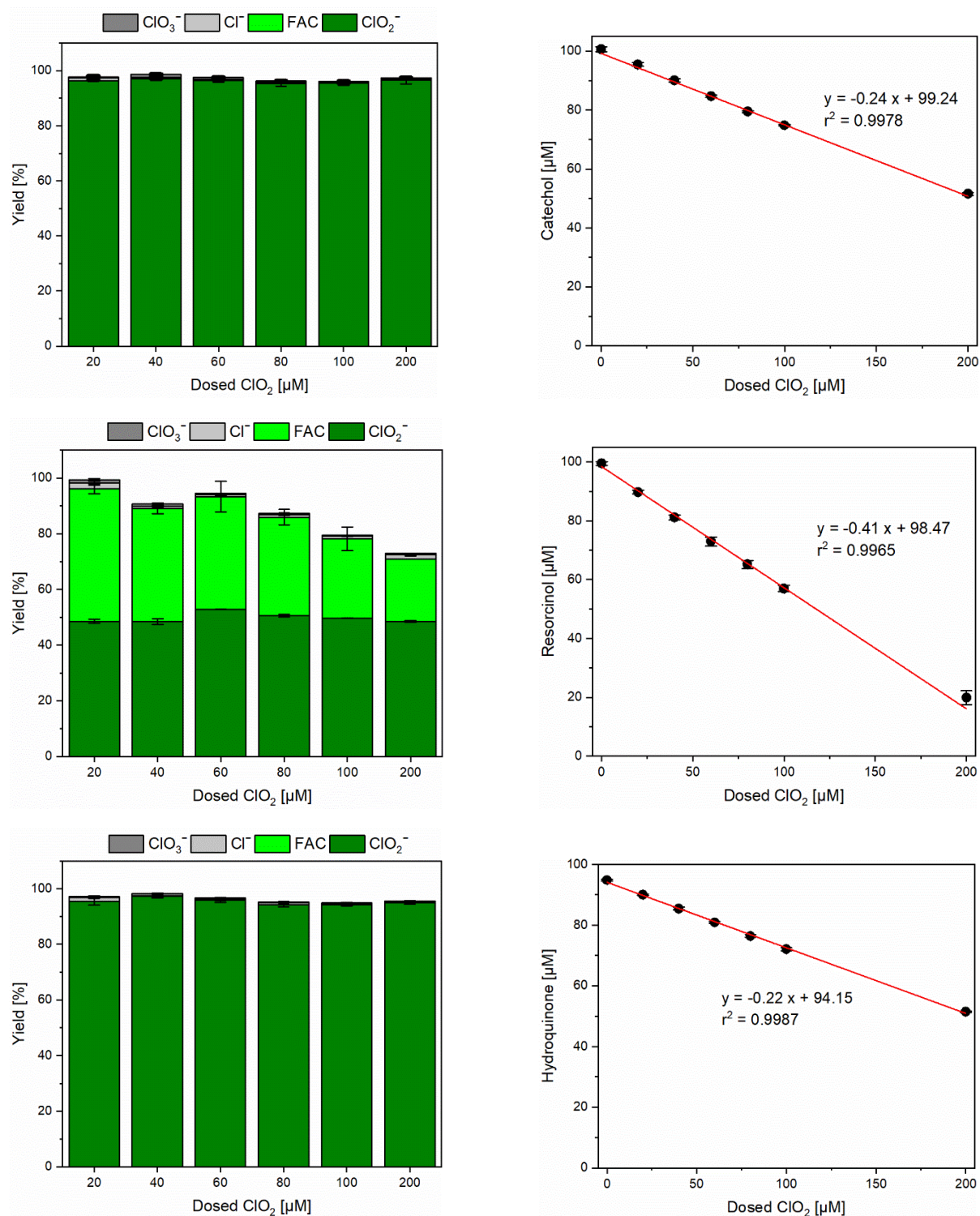


Figure AIII.10: Detailed chlorine balance (left) and stoichiometry (right) for catechol (top), resorcinol (middle), and hydroquinone (bottom). All reaction solutions contained 0.1 mM compounds under study, 10 mM glycine to scavenge intrinsically formed FAC, and 5 mM phosphate buffer to stabilize the pH at 7. All experiments were carried out in triplicates, and the error bars represent the standard deviation of the triplicate measurements.

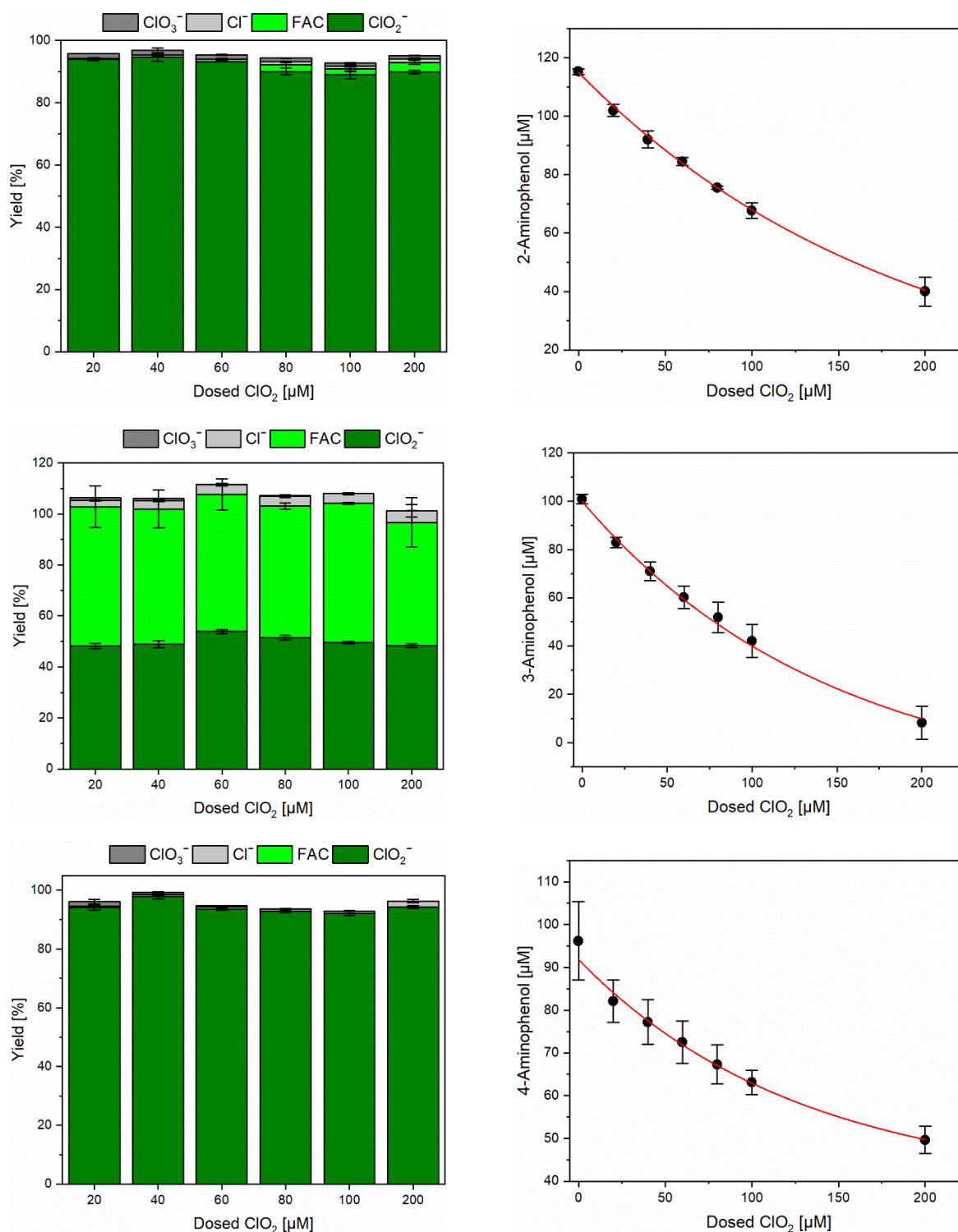


Figure AIII.11: Detailed chlorine balance (left) and stoichiometry (right) for 2-aminophenol (a), 3-aminophenol (b), and 4-aminophenol (c). All reaction solutions contained 0.1 mM compounds under study, 10 mM glycine to scavenge intrinsically formed FAC, and 5 mM phosphate buffer to stabilize the pH at 7. All experiments were carried out in triplicates, and the error bars represent the standard deviation of the triplicate measurements.

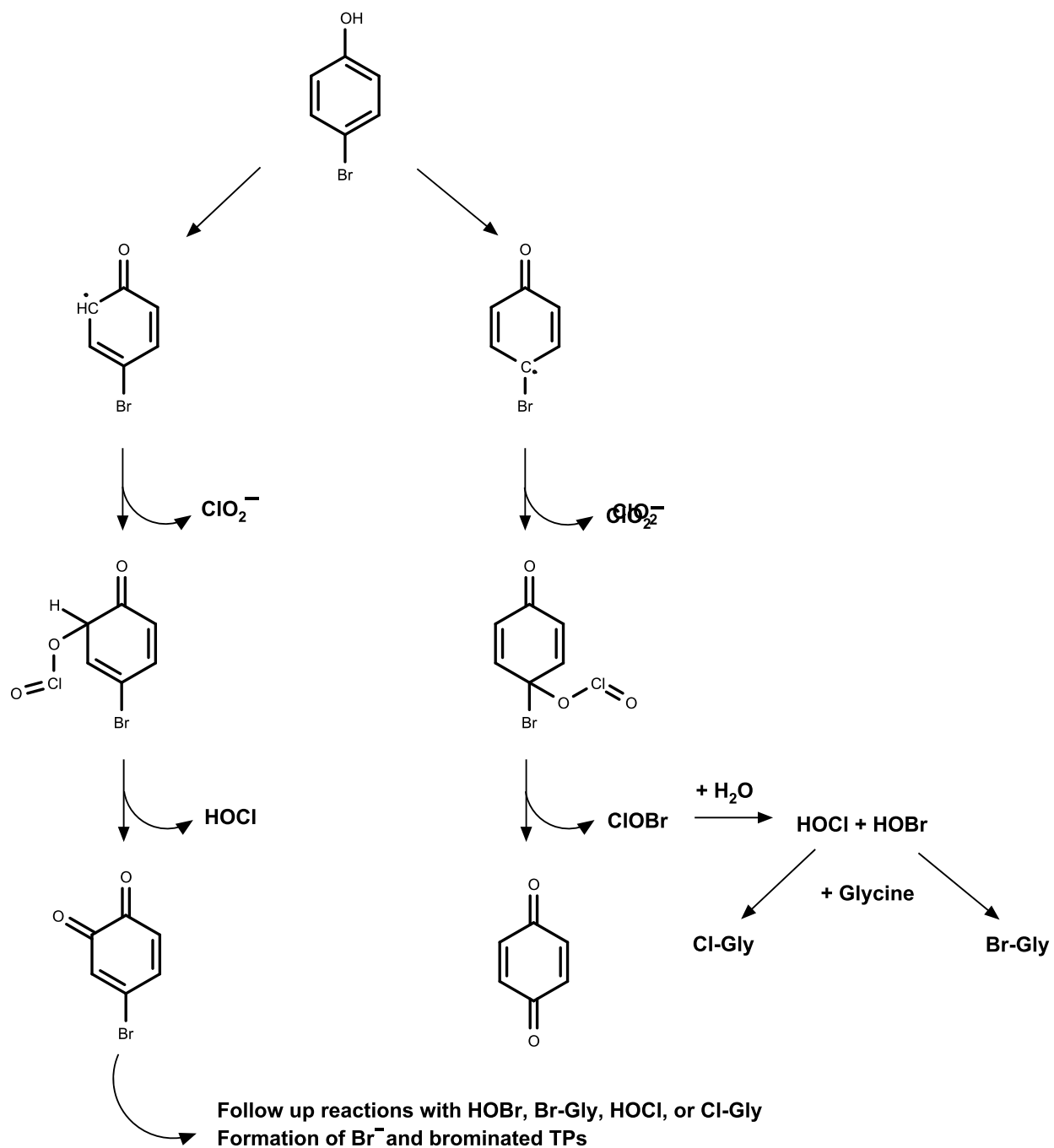


Figure AIII.12: Postulated reaction mechanism of 4-bromophenol with ClO_2 . Similar to 4-chlorophenol two different pathways may occur. ClOBr might be formed and react with water to form HOCl and HOBr . The excess of bromide might originate from decomposition of Br-Gly or the reaction of Br-Gly with *ortho*-BQ.

Appendix III

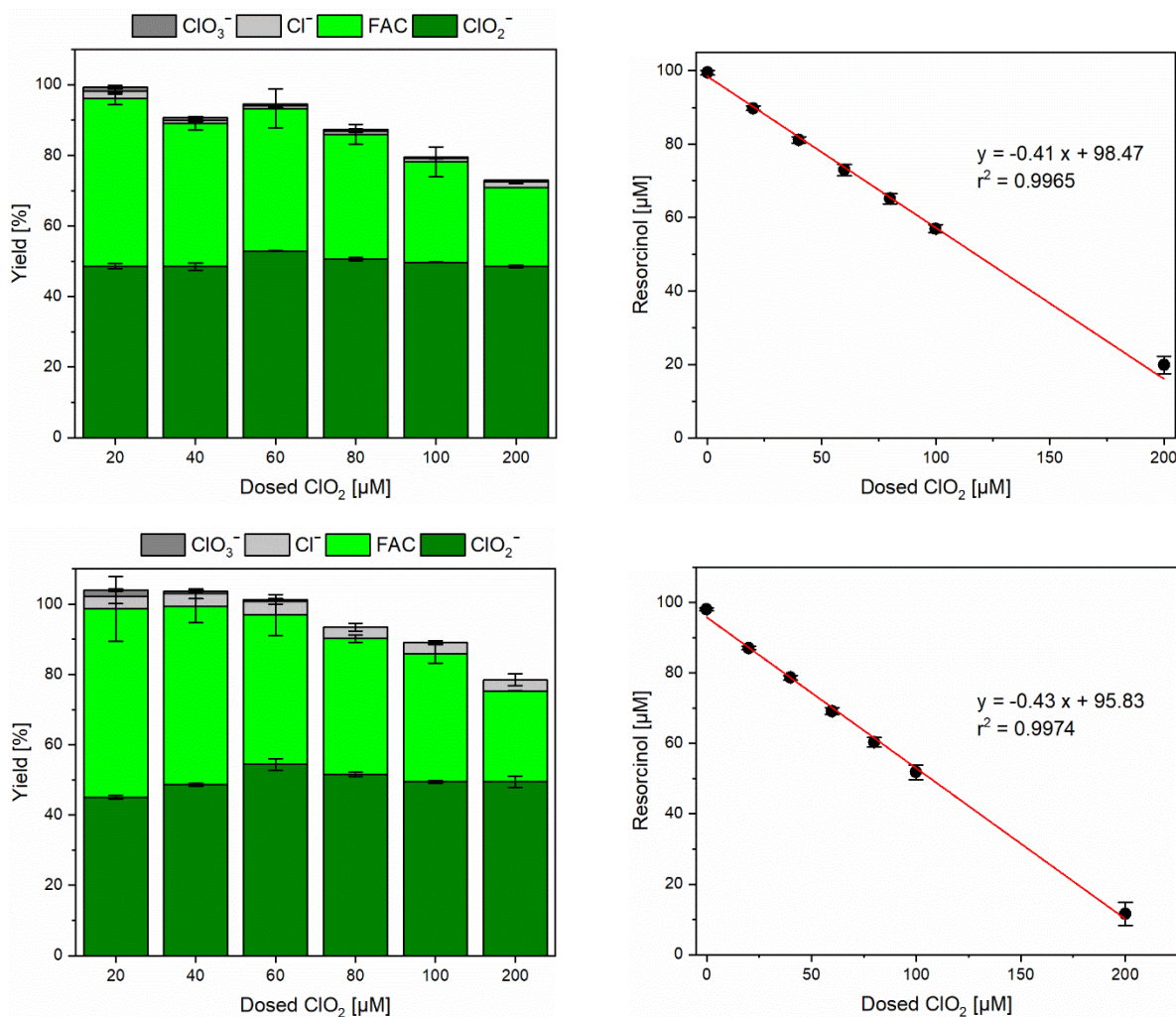


Figure AIII.13: Detailed chlorine balance (left) and stoichiometry (right) for resorcinol in the presence of 10 mM glycine (top) and in the presence of 100 mM glycine (bottom). All reaction solutions contained 0.1 mM compounds under study and 5 mM phosphate buffer to stabilize the pH at 7. All experiments were carried out in triplicates, and the error bars represent the standard deviation of the triplicate measurements.

Appendix III

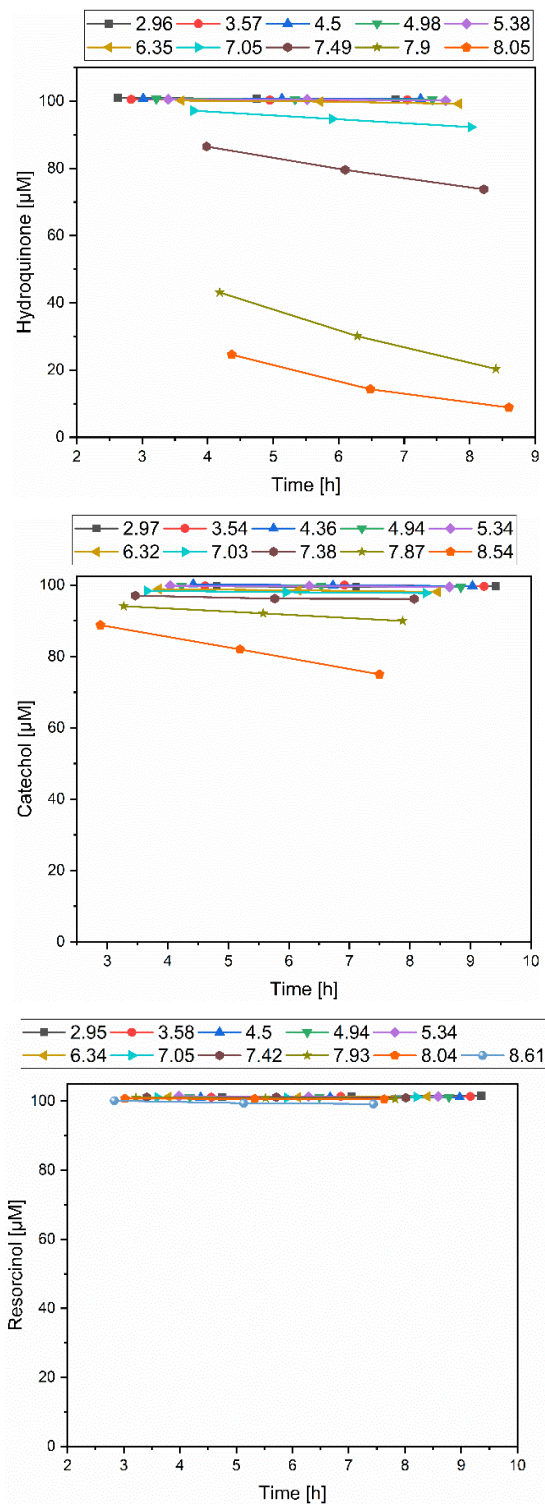


Figure AIII.14: pH-dependent stability of hydroquinone (top), catechol (middle), and resorcinol (bottom) over time. Samples contained 100 μM of the corresponding hydroxyphenol, 10 mM glycine, and 5 mM phosphate buffer. Time was measured from the point of preparing the sample solutions. Calibration was buffered at pH 4.

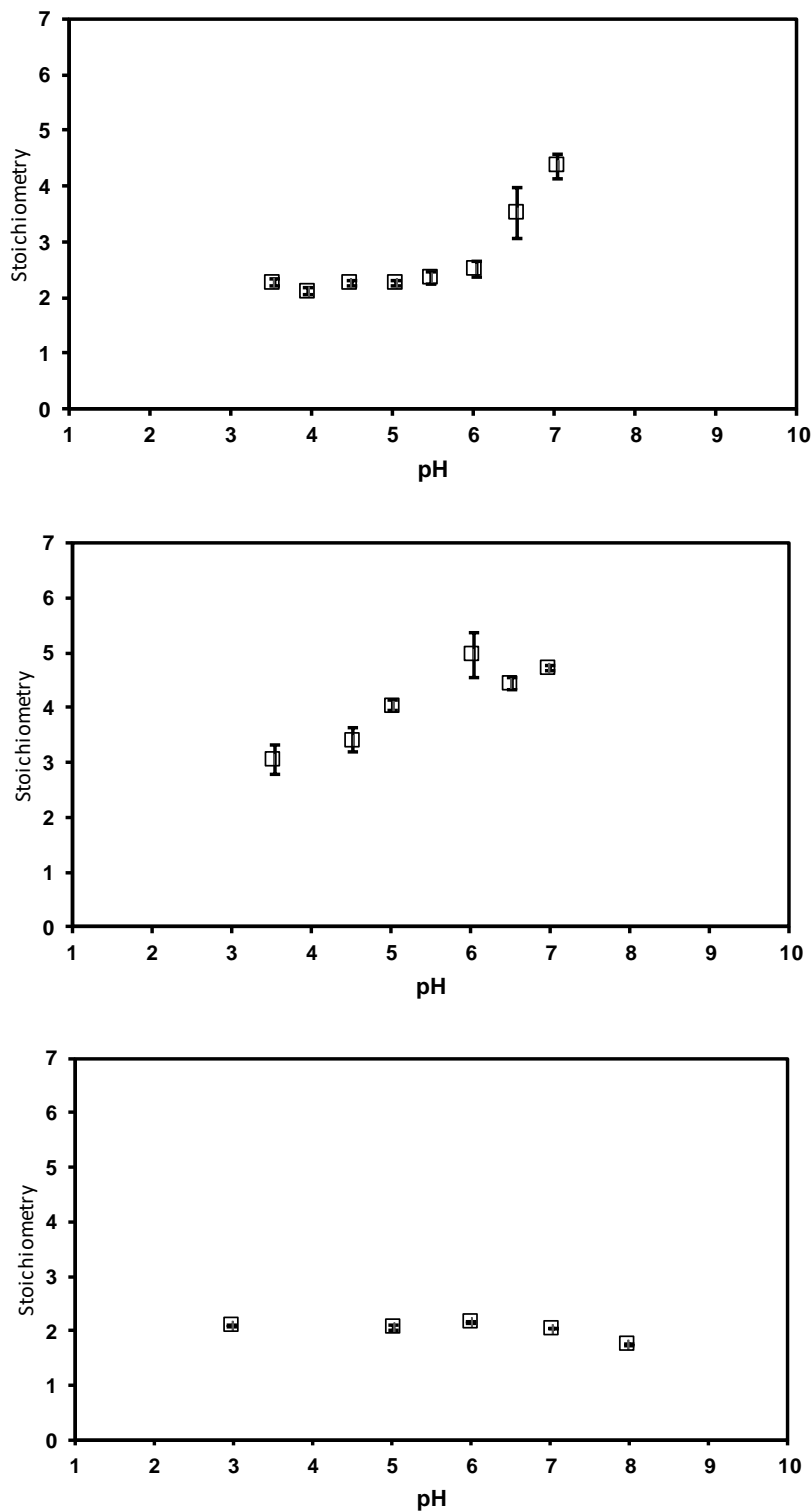


Figure AIII.15: pH-dependent stoichiometry of hydroquinone (top), catechol (middle), and resorcinol (bottom). Samples contained 100 μM of the corresponding hydroxyphenol, 10 mM glycine, and 5 mM phosphate buffer. All experiments were carried out in triplicates, and the error bars represent the standard deviation of the triplicate measurement.

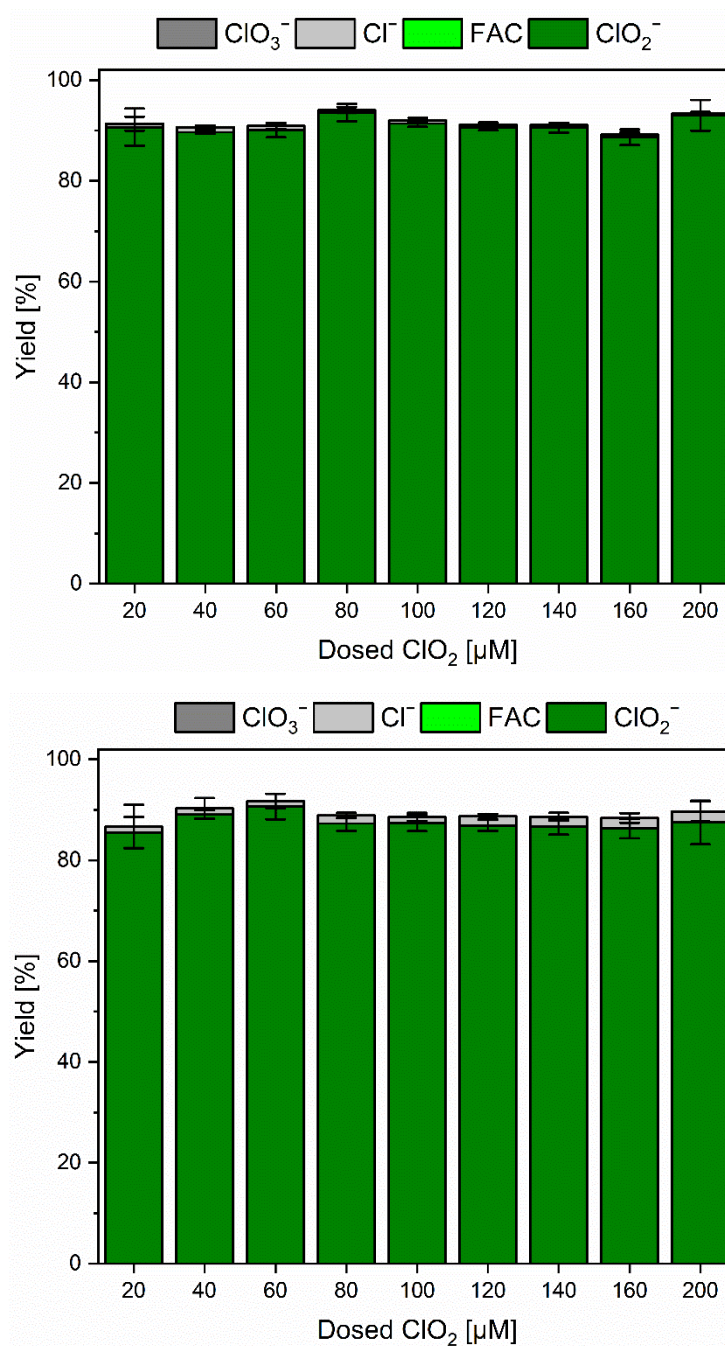


Figure AIII.16: Chlorine balance of hydroquinone (top) and catechol (bottom) at pH 4. All reaction solutions contained 100 µM of the compound under study, 10 mM glycine, and 5 mM phosphate buffer at pH 4. ClO₂ was added in different concentrations. All experiments were carried out in triplicates, and the error bars represent the standard deviation of the triplicate measurement.

Appendix III

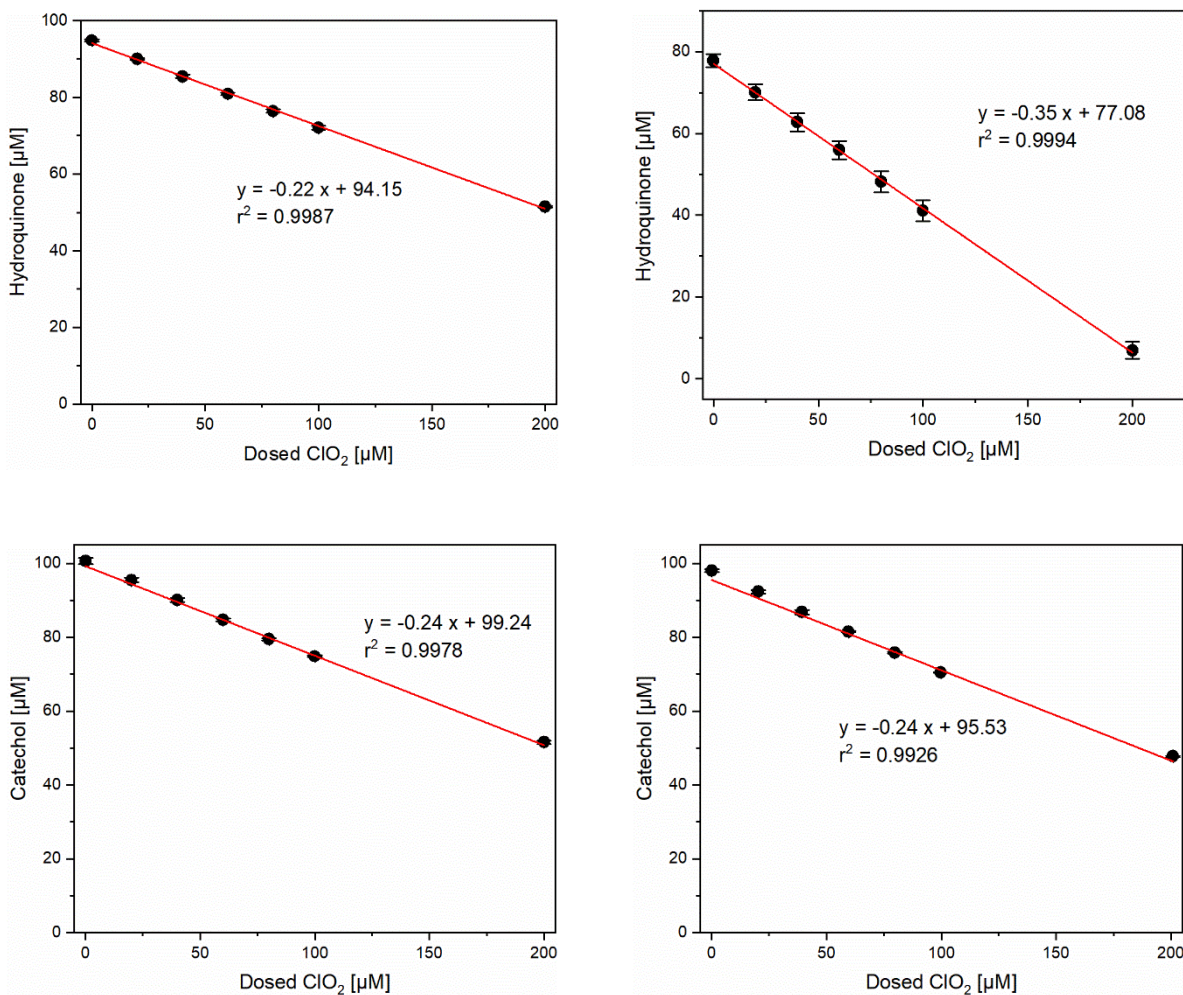


Figure AIII.17: Stoichiometry for hydroquinone (top) and catechol (bottom) in the presence and absence of 10 mM glycine, respectively. All reaction solutions contained 0.1 mM compounds under study and 5 mM phosphate buffer to stabilize the pH at 7. All experiments were carried out in triplicates, and the error bars represent the standard deviation of the triplicate measurements.

Appendix IV

Appendix IV

Appendix IV

Table AIV.1: Chemicals used in chapter 3.3.

| Name | Purity [%] | Purpose of use | Manufacturer |
|------------------------|--------------|----------------------------------|--|
| 1,4-Dimethylpiperazine | 98 | Compound under study | Alfa Aesar (Haverhill, Massachusetts, USA) |
| Acetonitrile | ≥ 99.95 | Eluent (LC) | Carl Roth (Karlsruhe, Germany) |
| Formic acid | ≥ 99 | Eluent (LC) | Sigma-Aldrich (St. Louis, Missouri, USA) |
| Ammonium acetate | ≥ 98 | Eluent | Merck (Darmstadt, Germany) |
| Disodium phosphate | > 99 | pH Buffer | Merck (Darmstadt, Germany) |
| Glutathione | ≥ 98 | Compound under study | Sigma-Aldrich (St. Louis, Missouri, USA) |
| Glycine | > 99 | HOCl Scavenger | Alfa Aesar (Haverhill, Massachusetts, USA) |
| Hydroquinone | ≥ 99 | Compound under study | Sigma-Aldrich (St. Louis, Missouri, USA) |
| L-Methionine | ≥ 98 | Scavenger / Compound under study | Sigma-Aldrich (St. Louis, Missouri, USA) |
| L-Methioninesulfoxide | | Compound under study | Alfa Aesar (Haverhill, Massachusetts, USA) |
| Sodium carbonate | 99.5 | Eluent (IC) | Sigma-Aldrich (St. Louis, Missouri, USA) |
| Sodium chlorate | > 99 | Calibration standard | Arcos organics (Fair Lawn, New Jersey, USA) |
| Sodium chlorite | 80 | Calibration standard | Honeywell Fluka (Charlotte, North Carolina, USA) |
| Sodium chloride | >99.5 | Calibration standard | Honeywell (Charlotte, North Carolina, USA) |
| Monosodium phosphate | 98 | pH Buffer | Arcos Organics (Fair Lawn, New Jersey, USA) |
| Sodium hypochlorite | 11 – 15% FAC | Oxidant | Alfa Aesar (Haverhill, Massachusetts, USA) |
| Sodium persulfate | > 99 | ClO ₂ production | Carl Roth (Karlsruhe, Germany) |
| Phenol | > 99 | Compound under study | Sigma-Aldrich (St. Louis, Missouri, USA) |

Appendix IV

Table AIV.2: Instruments used in chapter 3.3.

| Name | Component | Description | Manufacturer |
|-----------------------|--------------------------|--|---|
| Ion-Chromatography | Autosampler | Dionex AS-AP | Thermo Scientific (Waltham, Massachusetts, USA) |
| | Column | Asupp7 – 250mm/4.0 μ m | Metrohm (Herisau, Swiss) |
| | Column department | Dionex ICS-6000 DC | Thermo Scientific (Waltham, Massachusetts, USA) |
| | Conductivity detector | | Thermo Scientific (Waltham, Massachusetts, USA) |
| | Pump1 (Eluent) | Dionex ICS-6000 SP | Thermo Scientific (Waltham, Massachusetts, USA) |
| | Pump2 (Suppressor) | Dionex AXP | Thermo Scientific (Waltham, Massachusetts, USA) |
| | Software | Chromeleon Console | Thermo Scientific (Waltham, Massachusetts, USA) |
| | Suppressor | Dionex ACRS 500 | Thermo Scientific (Waltham, Massachusetts, USA) |
| Liquid Chromatography | Autosampler | 1260 Multisampler | Agilent Technologies (Santa Clara, California, USA) |
| | Column | HILIC “Luna” NH ₂ 3 μ M, 150/2 mm | Phenomenex (Torrance, California, USA) |
| | Column department | 1260 MCT | Agilent Technologies (Santa Clara, California, USA) |
| | Pump1 (Eluent) | 1260 flexible pump | Agilent Technologies (Santa Clara, California, USA) |
| | Software | Agilent MassHunter | Agilent Technologies (Santa Clara, California, USA) |
| | UV detector | 1260 DAD WR | Agilent Technologies (Santa Clara, California, USA) |
| | Mass detector | 6470 Triple Quad LC/MS | Agilent Technologies (Santa Clara, California, USA) |
| Photometer | Photometer | Specord 200 Plus | AnalytikJena (Jena, Germany) |
| pH-meter | pH-meter | Terminal 740 | WTW Series inoLab (Weilheim, Germany) |
| Balance | Balance | SM2285Di-ION-C | VWR (Radnor, Pennsylvania, USA) |
| Reaction tubes | 15 mL CellStar® tubes | Polypropylene | Greiner bio-one (Frickenhausen, Germany) |
| HPLC Vials | 1.5 mL Short thread vial | Amber glass | VWR (Radnor, Pennsylvania, USA) |
| HPLC Vials | 1.5 mL Short thread vial | Polypropylene | VWR (Radnor, Pennsylvania, USA) |

Appendix IV

Table AIV.3: Ion chromatographic method used in this study.

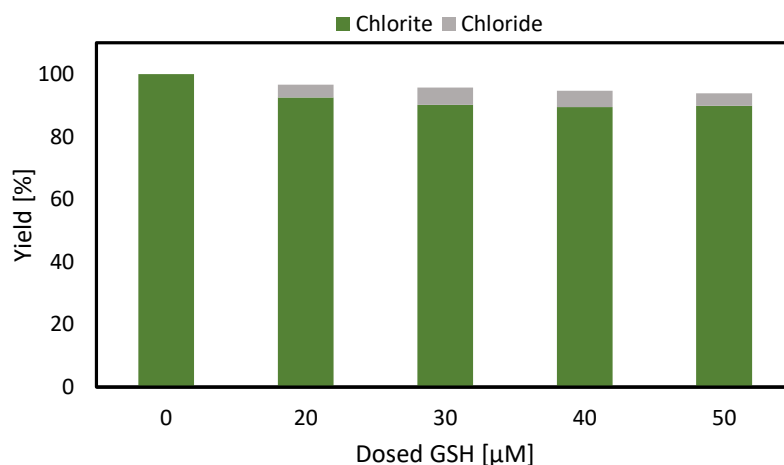
| | |
|--|--------------------------------------|
| Flow rate | 0.75 mL × Min ⁻¹ |
| Measuring time | 35 Min |
| Eluent A (4 mM Na ₂ CO ₃) | 90 % |
| Eluent B (H ₂ O) | 10 % |
| Suppressor solution | 20 mM H ₂ SO ₄ |
| Suppressor flow rate | 1 mL × Min ⁻¹ |
| Injection volume | 25 μL |
| Temperature autosampler | 5 °C |
| Temperature column oven | 45 °C |
| Retention times | |
| Cl ⁻ | 9.0 Min |
| ClO ₂ ⁻ | 7.7 Min |
| ClO ₃ ⁻ | 15.1 Min |

Table AIV.4: LC-MSMS method developed for the detection of MSO

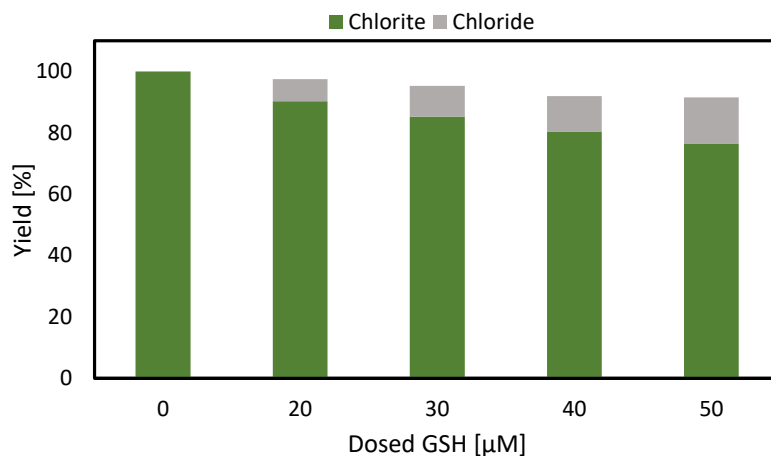
| | |
|--|----------------------------|
| Flow rate | 0.3 mL × Min ⁻¹ |
| Measuring time | 20 Min |
| Eluent A (ACN) | 80 % |
| Eluent B (H ₂ O + 0.1 % FA) | 20 % |
| Injection volume | 1 μL |
| Temperature column oven | 25 °C |
| Precursor ion | 166 Da |
| Product ion | 74.1 Da |
| Acceleration energy | 5 V |
| Collision energy | 5 V |
| Polarity | Positive |
| Retention time MSO | 10.8 Min |

Appendix IV

A



B



C

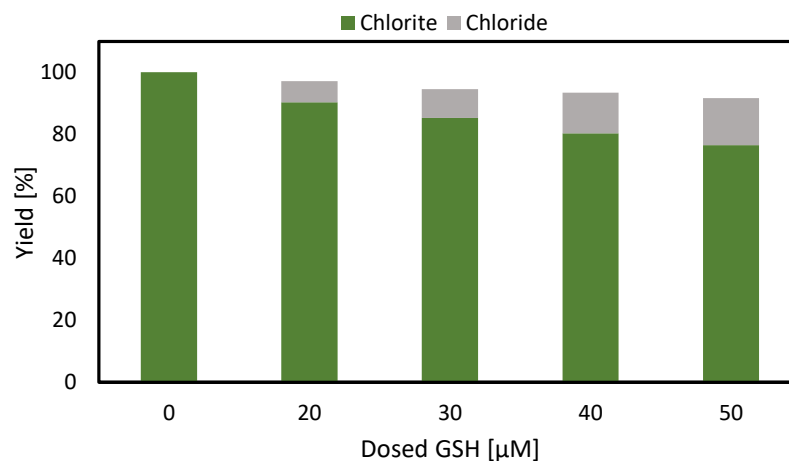


Figure AIV.1: Turnover of ClO_2^- to Cl^- in GSH reaction. Different doses of GSH (0 – 50 μM) were dosed to 100 μM ClO_2^- and chlorine species were measured by IC after different reaction times (A=5min, B = 24 hours, C = 48 hours). The reaction solution contained additionally 10 mM glycine and 5 mM phosphate buffer at pH 7.

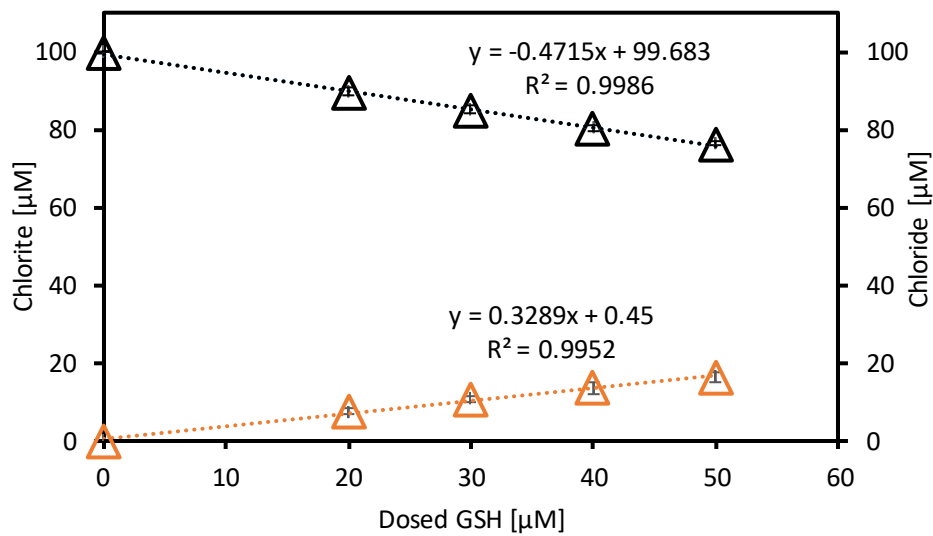


Figure AIV.2: Degradation of ClO_2^- over added GSH concentration after 24 hours of reaction time. Reaction solution contained $100 \mu\text{M}$ ClO_2^- , 10 mM glycine, and 5 mM phosphate buffer at pH 7. Experiments were carried out in triplicates and the error bars are representing the standard deviation of the results.

Appendix V

Appendix V

Table AV.1: Chemicals used in this study

| Name | Purity [%] | Purpose of use | Manufacturer |
|---|--------------------------|----------------------------------|--|
| Disodium phosphate | > 99 | pH Buffer | Merck (Darmstadt, Germany) |
| Glycine | > 99 | HOCl Scavenger | Alfa Aesar (Haverhill, Massachusetts, USA) |
| Indigo trisulfonic acid tripotassium salt | Ozone scavenging reagent | ClO ₂ scavenger | Sigma-Aldrich (St. Louis, Missouri, USA) |
| L-Methionine | ≥ 98 | Scavenger / Compound under study | Sigma-Aldrich (St. Louis, Missouri, USA) |
| Natural organic matter (Suwannee River) | RO isolate (2R101N) | Reaction matrix | International Humic Substances Society (IHSS) |
| Sodium carbonate | 99.5 | Eluent (IC) | Sigma-Aldrich (St. Louis, Missouri, USA) |
| Sodium chlorate | > 99 | Calibration standard | Arcos organics (Fair Lawn, New Jersey, USA) |
| Sodium chlorite | 80 | Calibration standard | Honeywell Fluka (Charlotte, North Carolina, USA) |
| Sodium chloride | >99.5 | Calibration standard | Honeywell (Charlotte, North Carolina, USA) |
| (Mono)sodium phosphate | 98 | pH Buffer | Arcos Organics (Fair Lawn, New Jersey, USA) |
| Sodium hypochlorite | 11 – 15% FAC | Oxidant | Alfa Aesar (Haverhill, Massachusetts, USA) |
| Sodium persulfate | > 99 | ClO ₂ production | Carl Roth (Karlsruhe, Germany) |
| Suwannee River natural organic matter (SRNOM) | RO isolate (2R101N) | Matrix | International Humic substances Society (IHSS) |

Appendix V

Table AV.2 Instruments used in this study.

| Name | Component | Description | Manufacturer |
|------------------|---------------|--------------------|--|
| Centrifuge | Centrifuge | Ecncifuge 5804 R | Eppendorf (Hamburg, Germany) |
| DOC-Analyzer | DOC-Analyzer | Vario TOC cube | Elementar (Langensfeld, Germany) |
| Incubator | Incubator | Universal oven | Memmert (Schwabach, Germany) |
| Plate Reader | Plate Reader | Synergy H1 | BioTek (Agilent Technologies (Santa Clara, California, USA)) |
| | Software | Gen5 3.10 | BioTek (Agilent Technologies (Santa Clara, California, USA)) |
| Photometer | Photometer | Navaspec Pro | Biochrom (Holliston, MA, USA) |
| pH-meter | pH-meter | Terminal 740 | WTW Series inoLab (Weilheim, Germany) |
| Incubator shaker | Heated Shaker | Multitron Standard | INFORS HT (Bottmingen, Swiss) |
| Vortex | Vortex | Vortex 2 | IKA Shakers (Staufen, Germany) |
| Well plate | Well plate | TC-Plate 96 | SARSTEDT (Nümbrecht, Germany) |

Table AV.3: Composition of LB-Medium and PBS solution.

| Solution | Compound | concentration |
|-------------------------|---------------------|----------------------|
| LB-Medium (Agar plates) | NaCl ₂ | 10 g L ⁻¹ |
| | Tryptopne | 10 g L ⁻¹ |
| | Yeast extract | 5 g L ⁻¹ |
| | Agar | 15 g L ⁻¹ |
| 2:1 LB-Medium | NaCl ₂ | 20 g L ⁻¹ |
| | Tryptopne | 20 g L ⁻¹ |
| | Yeast extract | 10 g L ⁻¹ |
| PBS Solution (pH 7.4) | Potassium phosphate | 4 mM |
| | Disodium phosphate | 16 mM |
| | Sodiumchlorid | 115 mM |

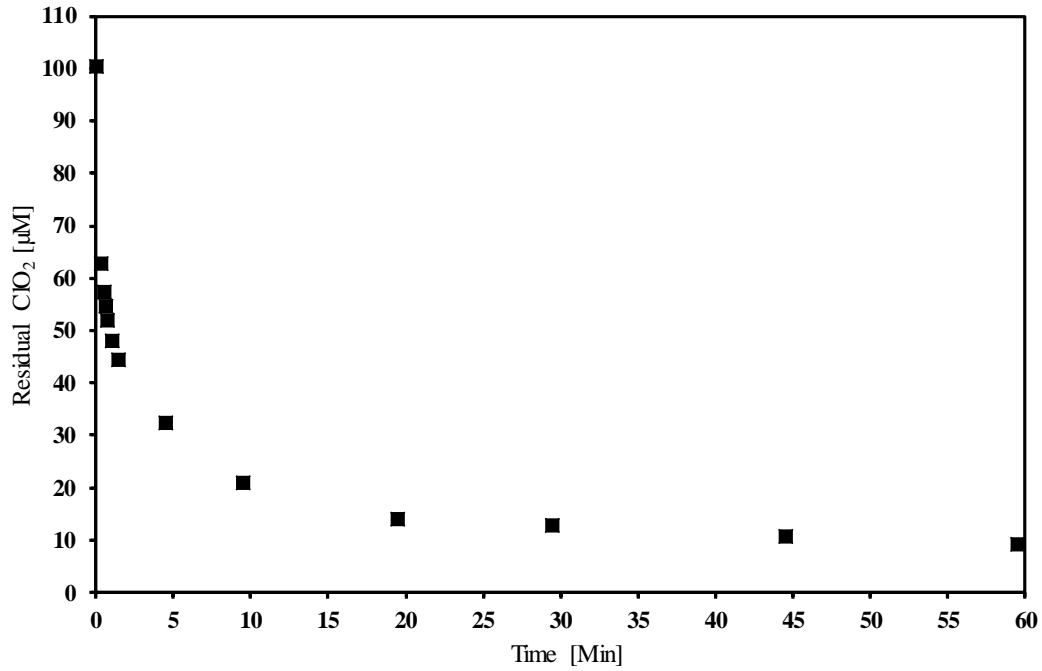


Figure AV.1: Depletion of ClO₂ in presence of NOM (DOC = 5 mg L⁻¹). 100 µM ClO₂ was dosed and after specific time intervals samples were taken and ClO₂ was scavenged by Indigo. The residual concentration of ClO₂ was calculated by the Δ Absorption at 600 nm by using an extinction coefficient of 9955 M⁻¹cm⁻¹ (Terhalle et al., 2018).

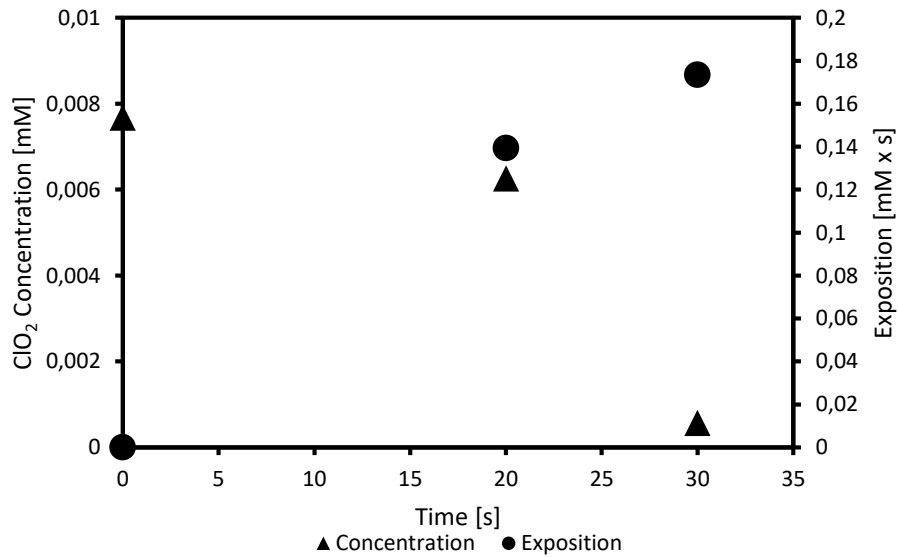


Figure AV.2: Depletion of 7 µM ClO₂ in presence of *E. coli* (initial OD₆₀₀ = 0.1) over time. Secondary y-axis shows the calculated ClO₂ exposure.

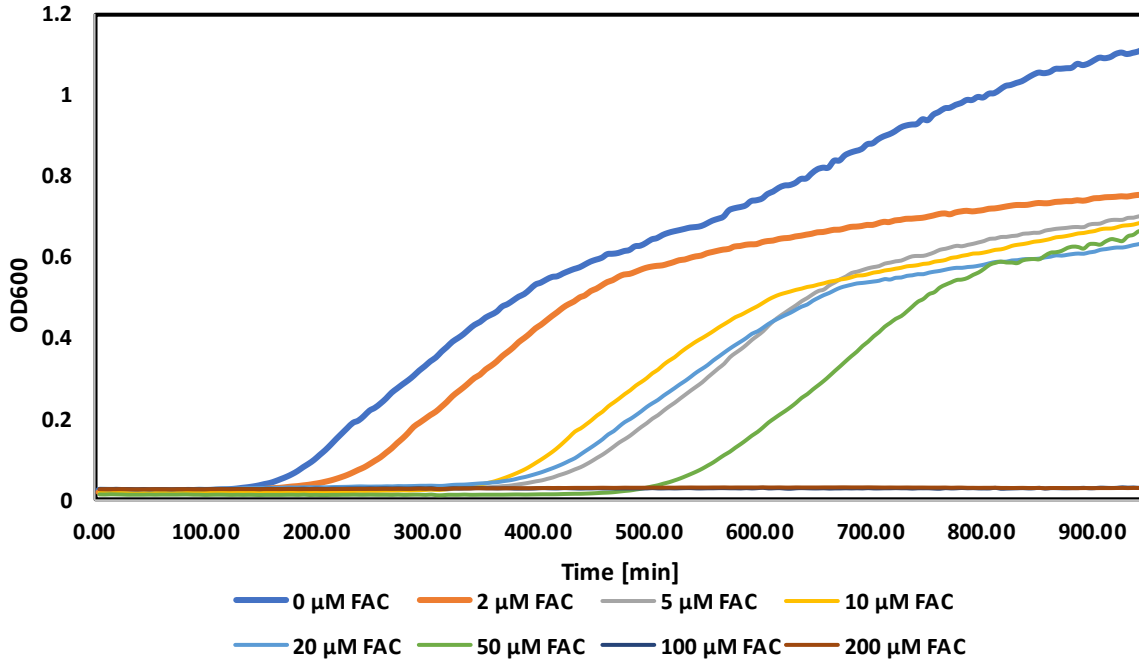


Figure AV.3: Growth curves of *E. coli* after addition of different concentrations of FAC at pH 7. Reaction solutions contained *E. coli* ($OD_{600} = 0.1$), NOM ($DOC = 5 \text{ mg L}^{-1}$). Data points were measured every 5 minutes at 37 °C for 16 hours.

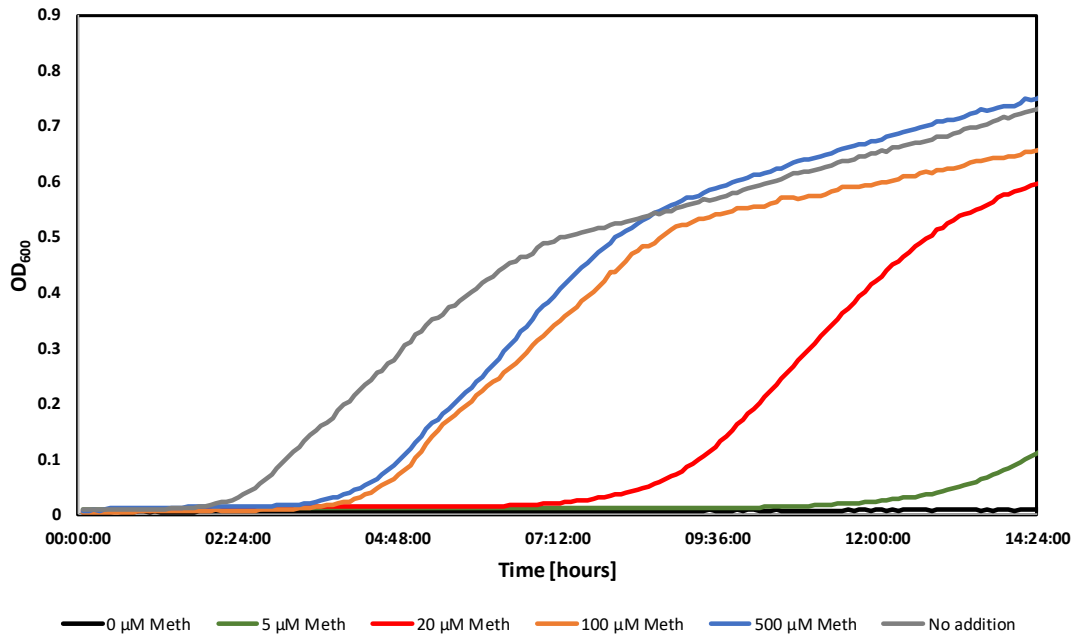


Figure AV.4: Growth curve of *E. coli* after addition of 50 μM FAC. Each sample contained different concentration of methionine. The initial OD_{600} was set to 0.1. Additionally, all samples contained NOM ($DOC = 5 \text{ mg L}^{-1}$). All experiments were carried out in quadruple determination and the line represents the

Appendix V

mean values of the measurement. To increase clarity, the standard deviation is not shown. Each sample was measured every five minutes for 16 hours and were incubated at 37 °C.

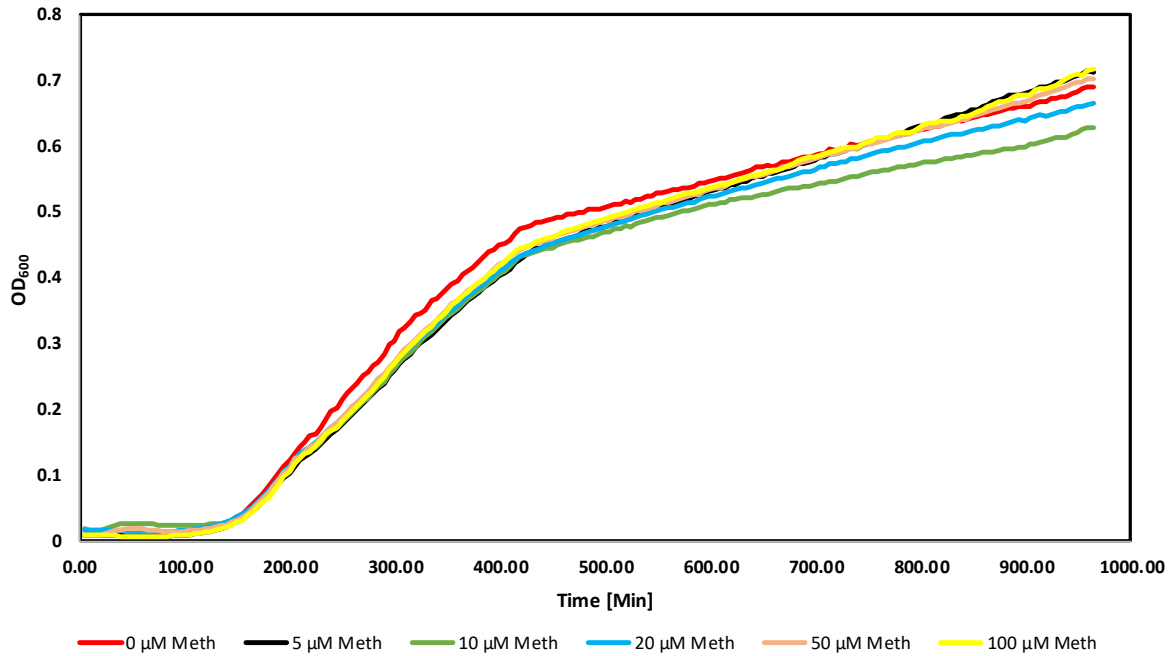


Figure AV.5: Growth curve of *E. coli* in presence of different concentrations of methionine. The initial OD₆₀₀ was set to 0.1. Additionally, all samples contained NOM (DOC = 5 mg L⁻¹). All experiments were carried out in quadruple determination and the line represents the mean values of the measurement. To increase clarity, the standard deviation is not shown. Each sample was measured every five minutes for 16 hours and were incubated at 37 °C

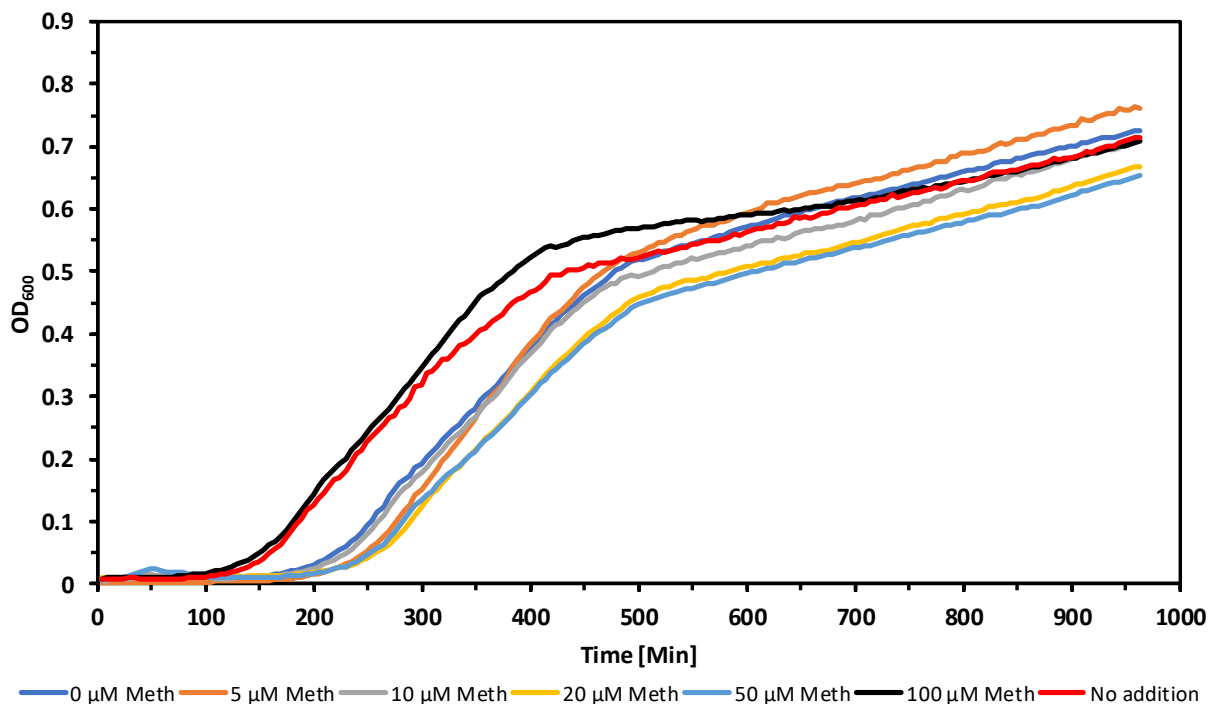


Figure AV.6: Growth curves of *E. coli* after addition of ClO_2 in presence of different concentrations of methionine. OD_{600} was monitored for 16 hours and measured every 5 minutes at 37 °C. All samples were measured in quadruples and the results show the mean values of the results.

Table AV.4: Effect on doubling time of *E. coli* after addition of ClO_2 and FAC in presence of different methionine concentrations. Oxidants were added to *E. coli* suspensions which contain NOM ($\text{DOC} = 5 \text{ mg L}^{-1}$). The initial dose of *E. coli* was $\text{OD}_{600} = 0.1$. Growth was monitored by 96 well plates for 16 hours every five minutes at 37 °C. All samples were measured in quadruple determination.

| c(Methionine) | No oxidant | 100 $\mu\text{M ClO}_2$ | 50 $\mu\text{M FAC}$ |
|---------------|---------------------|-------------------------|------------------------|
| | Doubling time [Min] | | |
| 0 | 26.5 ± 2.3 | 32.4 ± 4.0 | Out of monitored range |
| 5 | 27.3 ± 6.3 | 27.2 ± 5.0 | 44.6 ± 10.7 |
| 10 | 35.2 ± 5.1 | 21.7 ± 12.1 | 32.9 ± 5.9 |
| 20 | 30.1 ± 5.8 | 36.1 ± 4.1 | 41.6 ± 18.0 |
| 50 | 26.3 ± 2.4 | 29.9 ± 4.6 | 29.8 ± 3.5 |
| 100 | 25.3 ± 2.4 | 30.4 ± 2.1 | 30.7 ± 6.4 |

Declaration

I hereby declare that the thesis

‘Fundamental reaction mechanisms of chlorine dioxide during water treatment – Reactions with phenols and biomolecules during inactivation mechanisms’

represents my own and independent work which has been done after registration for the degree of Dr. rer. nat. at the Technical University of Darmstadt, and has not been previously included in a thesis or dissertation submitted to this or any other institution for a degree, diploma, or other qualifications. To the best of my knowledge, all external sources and auxiliary materials used in this thesis are cited completely.

Darmstadt, March 2023

Mischa Jütte



Zum Autor:

Mischa Jütte wurde 1994 in Düsseldorf geboren. Seine wissenschaftliche Karriere begann im Jahr 2014 mit dem Beginn des Studiengangs „Water Science“ an der Universität Duisburg-Essen. Seine Abschlussarbeiten absolvierte er im Fachgebiet Instrumentelle Analytische Chemie unter Leitung von Prof. Dr. Torsten Schmidt. Für seine herausragende Masterarbeit wurde er unter anderem mit dem DVGW-Studienpreis ausgezeichnet. Nach erfolgreichem Studium begann er seine Promotion im April 2020 am Institut IWAR an der Technischen Universität Darmstadt.

In dem neu gegründeten Fachgebiet Umweltanalytik und Schadstoffe unter Leitung von Prof. Dr. Holger Lutze untersuchte er die grundlegenden Reaktionsmechanismen von Chlordioxid in der Wasseraufbereitung mit starker Fokussierung auf die Desinfektion.

Zum Inhalt:

Sauberes Trinkwasser ist eines der wichtigsten Güter auf diesem Planeten. Dabei ist die Desinfektion des Wassers ein wichtiges Element um Ausbrüche von wasserbasierten Krankheiten wie Cholera zu vermeiden. Für diesen Zweck können chemische Oxidationsmitteln wie Chlor, Chlordioxid oder Ozon angewendet werden. Chlor ist das weltweit am häufigsten angewendete Desinfektionsmittel in der Trinkwasseraufbereitung. Allerdings konnte gezeigt werden, dass sich bei der Anwendung von Chlor schädliche halogenierte Desinfektionsnebenprodukte (bspw. Chloroform) bilden können. Aus diesem Grund wird Chlor sukzessive durch Alternativen wie Chlordioxid oder Ozon ersetzt.

Das Ziel der vorliegenden Dissertation war es, die grundlegenden Reaktionsmechanismen von Chlordioxid in der Trinkwasseraufbereitung zu untersuchen. Es konnte vor kurzem gezeigt werden, dass bei der Anwendung von Chlordioxid nicht nur Chlorit und Chlorat entstehen können, sondern auch freies Chlor in Form von Hypochloriger Säure gebildet wird. Die vorliegende Dissertation hat jetzt die Bildung von freiem Chlor in einer Vielzahl an Reaktionen untersucht. Dabei wurden unter anderem viele phenolische Moleküle, als Hauptbestandteil des natürlichen organischen Materials in der Wassermatrix, auf die Bildung von freiem Chlor kontrolliert. Des Weiteren wurden das Verfahren auf bestimmte Aminosäuren angewendet, um herauszufinden, ob freies Chlor in der direkten Interaktion von Chlordioxid mit Bakterien entstehen kann. Schlussendlich wurde der Einfluss des freien Chlors auf die Gesamtdesinfektion von Chlordioxid bestimmt.

ISBN 978-3-940897-75-6

